

**ARCTIC '91: Die Expedition ARK-VIII/3
mit FS „Polarstern“ 1991**

**ARCTIC '91: The Expedition ARK-VIII/3
of RV "Polarstern" in 1991**

**Edited by Dieter K. Fütterer
with contributions of the participants**

**Ber. Polarforsch. 107 (1992)
ISSN 0176 - 5027**

Cruise Report ARK-VIII/3
Inhalt / Contents

1.	INTRODUCTION	4
1.1	Cruise Itinerary	5
1.2	Weather Conditions.....	12
2.	REMOTE SENSING OF SEA-ICE.....	15
2.1	AVHRR Visible and Infrared Images	16
2.2	Line-scan Camera Observations.....	18
2.3	Surface Temperature Measurements with a KT4-radiometer.....	18
2.4	Surface Roughness Measurements.....	18
3.	SEA-ICE SAMPLING AND STUDIES.....	22
3.1	Physico-chemical Characteristics of Sea-ice and Snow	22
3.2	Sea-ice Biology	26
3.3	Sediment Inclusions in the Sea-ice	29
4.	OCEANOGRAPHIC INVESTIGATIONS.....	34
4.1	Determination of Deep Water Renewal Times Using ¹⁴ C and ³⁹ Ar Measurements.....	34
4.2	Distribution of Natural Radionuclides in the Water Column	36
5.	BIOLOGICAL INVESTIGATIONS.....	38
5.1	Bird and Mammal counts.....	38
5.2	Plankton	40
5.3	Benthos	41
6.	GEOLOGICAL INVESTIGATIONS	44
6.1	Bathymetric Surveys with HYDROSWEEP	44
6.2	PARASOUND-Sedimentechography	48
6.3	Sediment Sampling	55
6.3.1	Sampling of Near-surface Sediments	58
6.3.2	Coring of Long Sediment Cores.....	59
6.4	Sediment Descriptions and Lithostratigraphy.....	60
6.4.1	Sediments in the Nansen Basin	60
6.4.2	Sediments on the Gakkel Ridge	65
6.4.3	Sediments in the Amundsen Basin.....	69
6.4.4	Sediments on the Lomonosov Ridge.....	76
6.4.5	Sediments in the Makarov Basin.....	82
6.4.6	Sediments on the Morris Jesup Rise	86
6.4.7	Sediments on the Yermak Plateau.....	90
6.5	Physical Properties of Sediments.....	95
6.5.1	Physical Property Methods	95
6.5.2	Paleomagnetic and Mineral Magnetic Investigations.....	100
6.5.3	Electrical Resistivity in Sediment Cores.....	104
6.6	Biostratigraphy: Calcareous Nannoplankton	106

7	GEOPHYSICAL INVESTIGATIONS.....	108
7.1	Marine Geophysics.....	110
7.2	Over-ice Seismic Surveys.....	121
7.3	Magnetotelluric Measurements	124
7.4	Gravity Measurements	124
7.5	Measurements of Streamer Noise.....	125
8	REFERENCES	130
9.	ANNEX.....	133
9.1	Station List	133
9.2	Graphical Core Descriptions	143
9.3	Sample Distribution.....	260
9.3.1	Sediment Sample Distribution Policy Statement	260
9.3.2	Shipboard Sampling and Sample Distribution.....	261
9.4	List of Participating Institutions.....	264
9.5	List of Participants / Ships Crew	266

1 INTRODUCTION

Encouraged by the success and experience gained during the *Polarstern* expedition ARK-IV/3, in summer 1987, discussions and preparations of a multidisciplinary expedition into the central Arctic Ocean focussing on oceanography and geosciences started early. At the same time Swedish scientists began planning of a similar multidisciplinary but independent expedition with their new ice breaker *Oden* to the high Arctic, which was co-ordinated by the Swedish Polar Secretariat. Early contacts of the Swedish Polar Secretariat, the Alfred Wegener Institute and scientists involved, soon led to the decision to combine the two efforts. Soon after 1989, US scientists joined the discussions and introduced a third vessel to the joint venture, the US Coast Guard ice breaker *Polar Star*. Consequently, *Polarstern* ARK-VIII/3 and ODEN'91 became part of a larger international expedition: The International Arctic Ocean Expedition ARCTIC'91. Strong efforts were made during the whole planning phase to include a Soviet participation; not only to invite a larger group of Soviet scientists but to have a Soviet ice breaker joining the international effort.

At an earlier stage of planning it was hoped to carry out a major part of the research program within the Soviet Exclusive Economic Zone (EEZ) along the Eurasian continental margin and in the shallow shelf waters of the eastern Barents Sea, Kara Sea and Laptev Sea. The main target areas, however, had to be changed as unfortunately the USSR refused to give permission to do any scientific research in their EEZ covering the Eurasian Shelf.

The general planning philosophy of ARCTIC'91 was to maximize the amount of scientific research by carrying out a fully co-operative scientific program. The scientific program carried out from *Oden*, therefore, concentrated on the study of the ocean waters, sea ice, and air while *Polarstern* with her capability to handle heavy gear ran, as a first priority, the geological sampling and geophysical profiling work. The program on *Polarstern* also included the large volume sampling for tracer oceanography and the multi-disciplinary sea ice and remote sensing programs.

An important aspect of the original scientific plan was the agreement of joint operations of *Polar Star* and *Polarstern* along all transit lines between geological sampling stations to enable continuous seismic profiling. This plan became jeopardized from the very beginning when *Polar Star*, because of other obligations in the Thule area west of Greenland, was delayed about 10 days. Later on *Polar Star* experienced severe technical problems with one of her propeller shafts which finally forced *Polar Star* to cancel her further participation.

However, an essential part of the geophysical program could be carried out successfully during the second half of the expedition when *Oden* and *Polarstern* jointly in an efficient scientific operation sailed from Lomonosov Ridge via North Pole to the Yermak Plateau.

1.1 Cruise Itinerary (D.K. Fütterer)

RV *Polarstern* left Tromsø (Norway) on the evening of August 1, 1991, with 53 scientists from nine countries and 44 crew members on board. In the following days she quickly crossed the Barents Sea in a north-easterly direction, and bypassed Spitsbergen on 30° E (Figs. 1 and 2).

The Swedish icebreaker *Oden* had left Tromsø harbour a few hours earlier, and therefore officially opened ARCTIC'91. *Oden* originally had planned to pass west of Spitsbergen and then sail north on 20° E, to be in close contact with *Polarstern* while carrying out an oceanographic profile to the North, up to Gakkel Ridge. The US *Polar Star* who had been delayed due to unforeseen additional work at Thule, west of Greenland, was supposed to join the two other vessels as quickly as possible.

Already at 79° N, off Kong Karls Land, *Polarstern* passed on the night of August 4, the drift ice border. The same day, an oceanographic test station was run between Kvitøya and Nordaustlandet, and the first biological and geological material was sampled.

The scientific work program started on August 5, with a sea-ice station at 81° N, 30° 50' E, on the continental shelf. During the whole cruise hourly sea-ice observations were made from the bridge. Parallel with all geological and oceanographic stations, measurements of the ice thickness and sampling were carried out.

At the same time the first seismic profile started at 81° N, 30° 50' E, on the continental margin, and continued with 8/10 to 9/10 ice coverage until the morning of August 6, with brief interruptions. When the ice conditions got more difficult in the following night, profiling was stopped in order to avoid damage to the airguns.

On Tuesday, August 6, the first geological sampling was successfully carried out at a station on the deeper continental margin, at 81° 45' N, 29° 54' E. At the same time, *Oden* had to call at Longyearbyen on Spitsbergen due to engine troubles. She was unable to continue her cruise until August 16. For this reason, the originally planned joint advancing of *Oden* and *Polarstern* towards the Gakkel Ridge - one ship on 20° E, the other on 30° E - failed, thus creating a totally new situation for *Polarstern*. It was therefore decided that *Polarstern*, taking into account the ice conditions, should slowly cross the Nansen Basin, then continue to the Gakkel Ridge while conducting a comprehensive station program. In doing so there was a good chance that *Oden* and the delayed *Polar Star* would soon join *Polarstern*.

As ice conditions were favourable, and as the vessel's advance could not be stopped even by bad visibility and fog, *Polarstern* made good headway until August 12. The only interruptions were the daily stations for geological sampling or for geophysical and glaciological work on the ice. From August 8 to 9, at 83° 59' N, 30° 29' E in the central Nansen Basin, the first oceanographic station was established with a number of Gerard-Ewing water samplers, and *in situ* pumping. Another station followed on August 11, at 85° 27' N, 44° 29' E.

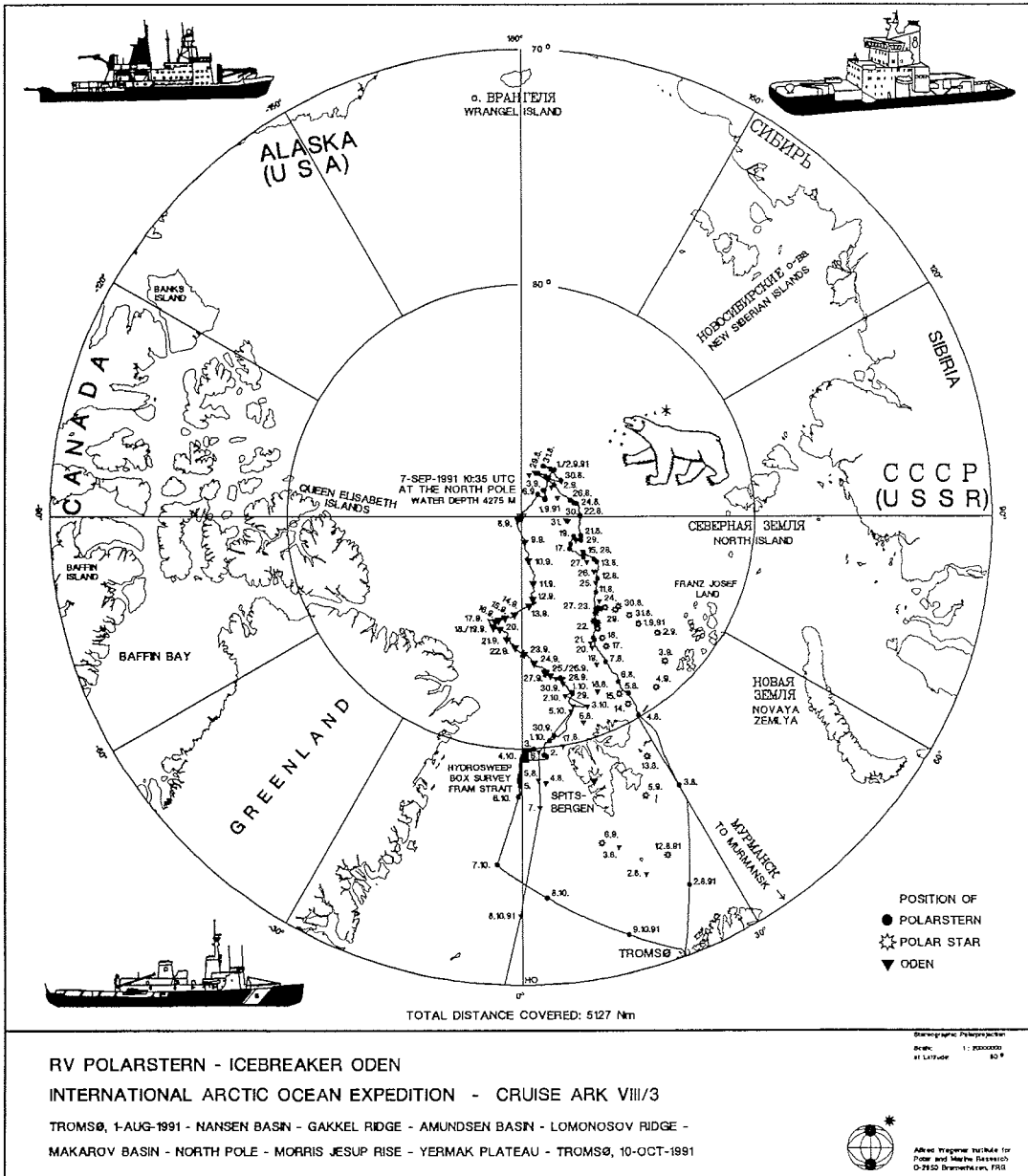


Fig. 1.1-1: General cruise track of RV *Polarstern*, icebreaker *Oden* and USCGC *Polar Star* during the International Arctic Ocean Expedition ARCTIC'91.

Abb. 1.1-1: Übersicht über die Fahrtrouten von FS *Polarstern*, Eisbrecher *Oden* und USCGC *Polar Star* während der internationalen Expedition ARCTIC'91 in den Arktischen Ozean.

On Monday, August 12, the first radio contact with *Polar Star* was established, who at that time was east of Bear Island, and who followed *Polarstern* at good speed in the ice free waters of the Barents Sea, heading north.

Gakkel Ridge was reached by *Polarstern* on the morning of August 13, at 86° N, 56° 40' E. Until August 17, on this Arctic mid-ocean ridge, several extensive stations were run, and samples were taken at different water depths. The very rough topography of the Ridge, however, made it difficult to find good coring sites.

On August 15, an ice streamer was used on an ice-floe to run a reflection and a refraction seismic profile over a part of the central valley of Gakkel Ridge. As this was the first day without fog, also a first walk on the ice was organized for everybody.

Between August 18 and 21, additional geological stations were sampled in the southern Amundsen Sea. Again, at several long-term stations, the large volume Gerard-Ewing water samplers for tracer oceanography, and *in situ* pumps for radio nucleid distribution analysis were operated in the water column. However, the search for large ice-floes (with 5-10 km of diameter) to continue refraction seismic profiling in the transition zone between Gakkel Ridge and Amundsen Basin, was in vain.

In agreement with *Oden* and *Polar Star* (who had been blocked since August 19, at 84° 10' N, 34° E due to a damage of her port shaft), *Polarstern* started alone, on August 21, to run a long profile with stations to the east along 87° 30' N, from the Amundsen Basin to the Lomonosov Ridge. As ice conditions were favourable, *Polarstern* advanced easily, and was able to establish many stations at 80°, 90° and 100° E for all disciplines.

Then, on August 24, strong winds from the south-east, which caused ice drifting and heavy ice pressure on *Polarstern*, together with a snow storm made any further advance of *Polarstern* difficult. Average speed dropped to 1 to 2 knots, and again and again *Polarstern* got caught in the sluggish ice or between large floes. On August 25, *Polarstern* was trapped for more than 31 hours and drifted 14.2 miles to the north, thus reaching her most northerly position up to that time. Due to a quickly dropping wind, the situation improved by the next day.

On August 26, again bad news arrived from *Polar Star* who once more had to interrupt her travel due to technical problems with her port shaft. Then, on August 28, a message was received from *Polar Star* saying that she had to turn back and had to cancel any further participation in ARCTIC'91. It was fortunate that *Polar Star* was still in a position to leave the pack-ice zone under her own steam. On September 4, she reached open water at 80° 38' N, 37° 55' E north-east of Svalbard, and continued to Bergen. The planned seismic program was hampered by this turn of events, as plan was to tow the streamer and airguns on *Polarstern* following *Polar Star* in her wake through the pack-ice.

As ice conditions remained quite favourable, *Polarstern* made good progress in the following days, thus reaching Lomonosov Ridge on August 27, at 88° 02' N, 135° E. After a very successful geological station on the ridge, *Polarstern* headed further east and reached the deep-sea plain of the Makarov Basin. From August 28 to 29,

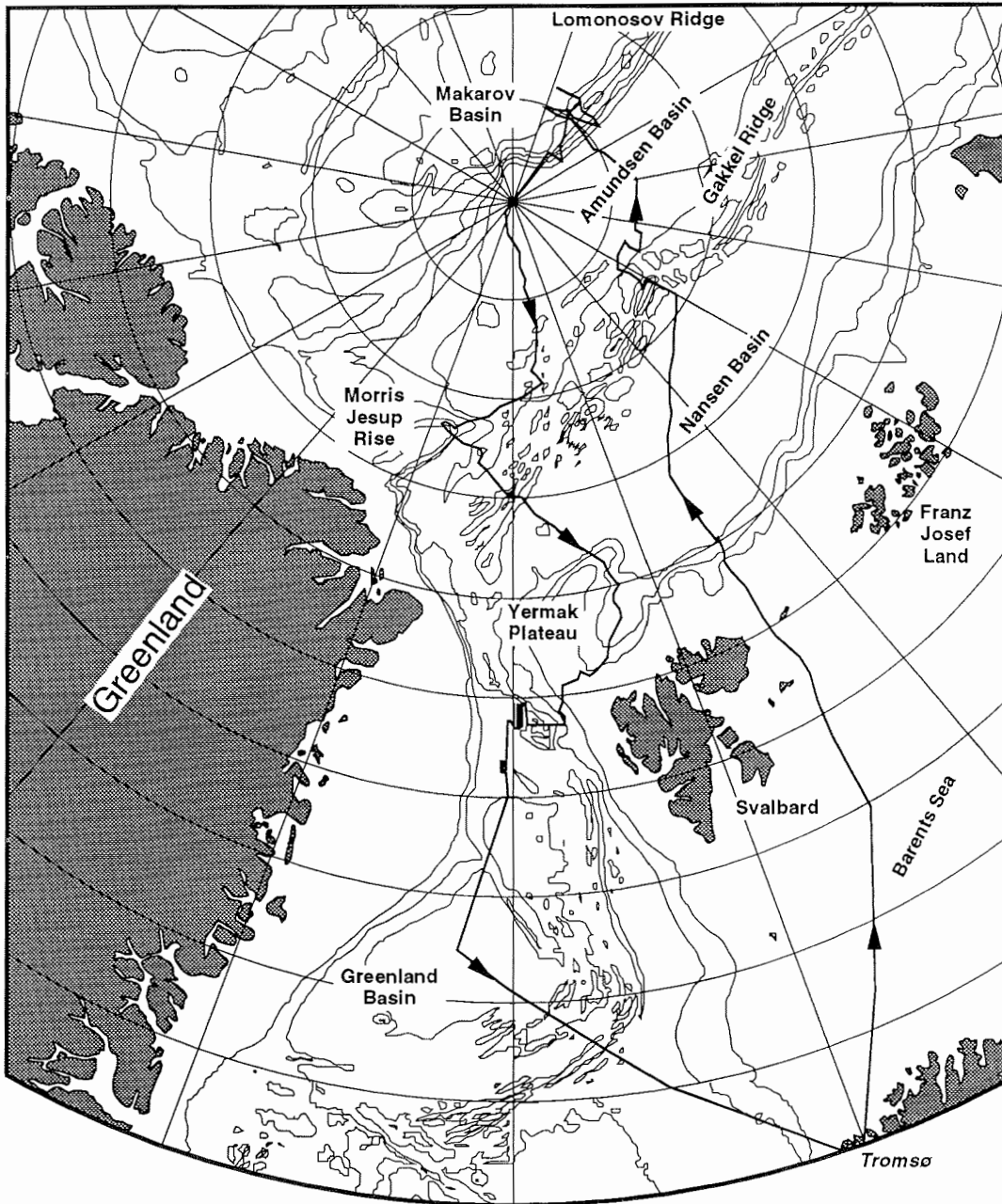


Fig. 1.1-2: Cruise track of RV *Polarstern* during Leg ARK-VIII/3 of ARCTIC'91.

Abb. 1.1-2: Fahrtroute von FS *Polarstern* während ARK-VIII/3.

at *Polarstern's* most easterly position of 88° N, 159° 20' E, full stations were carried out in oceanography and geology.

Encouraged by the relatively favourable ice conditions on August 29 and 30, a small airgun system, constructed by the ship's engineers, together with a 500 m long 12-channel streamer, were towed in order to collect seismic reflection profiles over the Lomonosov Ridge. Along two profiles between 130° E and 160° E, more than 200 km of multichannel seismic data and high resolution seismic reflection data (PARASOUND) were collected.

From August 31 to September 1, a box core transect was run from the Makarov Basin to the steep eastern slope of the Lomonosov Ridge for both geological and biological studies. Between September 1 and 2, *Polarstern* stopped for 24 hours for a geophysical station at 87° 31' N, 144° 10' E, on top of the Lomonosov Ridge (1,051 m water depth). The main experiment was the magnetotelluric measurements to explore the crustal structure, which were carried out from a large floe far enough away from the vessel so as not to interfere with the study. In addition, the visit to the drifting floe was used to collect seismic reflection and refraction data as well as to perform sea-ice studies, while *Polarstern*, in parallel, ran a full geological sampling program.

On September 3, at 87° 50' N, 146° 30' E, the first meeting with *Oden* took place to discuss the joint program for the return trip. During the previous days, *Oden* had quickly completed her stations in the Amundsen Basin, and had then went east to continue her oceanographic work in the Makarov Basin. Another meeting was envisaged for September 6, in the area of 89° N, 150° E on the northern Lomonosov Ridge, to be followed by a joint return journey of both vessels.

At the same time, *Polarstern* sailed north to take geological samples on the northern Lomonosov Ridge. A sudden gale with forces up to 50 knots and a snow storm pushed the ice so much that *Polarstern*, in the evening got caught in pressed ice pack. Although bad weather conditions continued station work was carried out on a large ice floe for all disciplines. During the following day, geological and oceanographic work continued on the northern Lomonosov Ridge; however, an attempt to deploy the seismic system into bad ice conditions failed.

After finishing station work on the northern Lomonosov Ridge at 88° 46' N, 145° E, in the afternoon of September 6, a second meeting with *Oden* took place, who in the meantime had finished her oceanographic work in the Makarov Basin. It was quickly decided to start the return journey out of the ice following a heading parallel to a great circle, and then to jointly test the ice in the North. The joint travelling of the two vessels made seismic work easier. By sailing in the wake of *Oden*, *Polarstern* was able to run the large airgun system with a total volume of 24 l and a 500 m long 12-channel streamer.

As ice conditions remained favourable, and as there appeared large areas of open water, inspite of fog and bad visibility the vessels progressed easily. On Saturday, September 7, at 10:35, *Oden* and *Polarstern* along a geophysical profile starting on the Lomonosov Ridge reached the North Pole.

Directly over the Pole, both vessels moored together at a large ice floe. On *Polarstern*, the first North Pole samples were taken from the sea bottom and the ice floe; Following this, the outstanding event was celebrated. After 24 hours at the Pole, *Polarstern* in the morning of September 8, left to continue seismic profiling in the wake of *Oden* now heading South. Regularly alternating between seismic profiling and station work, the vessels in the next few days crossed Amundsen Basin and reached approx. 86° N on September 11, travelling along 10° E.

From there, on September 12, the vessels headed for the Morris Jesup Rise off the northern tip of Greenland. Alternating again between geological, biological and oceanographic station work and seismic profiling on the other, *Polarstern* in the wake of *Oden* reached 85° 34' N, 09° 03' W the eastern slope of the Morris Jesup Rise on September 15. This activity was only interrupted on the evening of September 14, when scientists and crew members of *Polarstern* were invited by *Oden* to celebrate the close co-operation.

From September 17 to 18, seismic profiling was increasingly hampered by strong frost and therefore more difficult ice conditions over the south-eastern slope of the Morris Jesup Rise. Nevertheless it was possible to finish an E-W profile over the Rise, and another one from the Rise to the deep-sea plain of the southern Amundsen Basin. On September 18 and 19, geological sampling at different stations followed, more successful on the south-eastern edge of the Rise, and less successful on the very steep south-western slope.

In the morning of September 20, *Polarstern* left the Morris Jesup Rise heading SE to the Gakkel Ridge. Difficult ice conditions forced her to turn aside in an easterly direction before larger leads in the ice opened the way to the South. An oceanographic and geological coring station in the deep sea of the southern Amundsen Basin, which lasted until the morning of September 22, was successful for oceanography, but brought hardly any results for geology and biology. In parallel, *Oden* carried out a long-term station for meteorology.

On the morning of September 22, the air temperature increased and ice conditions improved, so that the vessels sailed easily. For the first time AVHRR images could be used to determine the routes through the ice. In large areas of open water which were only covered by thin new ice, a geological station was established on the northern slope of Gakkel Ridge, at 84° 14' N, 02° 33' W.

In the early morning of September 23, the central valley of Gakkel Ridge was reached. In close co-operation with *Oden*, the sea ice group conducted a joint ground truth experiment to calibrate radar measurements of ERS-1. Geophysicists carried out a refraction seismic experiment to determine the thickness of the crust. *Polarstern* was moving while shooting airguns, recording took place by REFTEK stations left on an ice floe. Geological station work followed on September 24, at 83° 38' N, 04° 36' E on the SE slope of Gakkel Ridge. The rough topography prevented the recovery of geological core samples.

On September 25, another geological refraction seismic experiment to determine the thickness of the crust between magnetic anomalies 6 and 13, and extensive geological station work were carried out at 83° 15' N, 08° 33' E, in the deep-sea plain of the southern Nansen Basin. With this station, the oceanographic work

program came to an end, after the large water samplers and *in situ* pumps had been applied for a last time. Favourable weather conditions with moderate winds and good visibility allowed good progress of work and, after a long interruption, the more frequent use of helicopters for laser altimeter measurements, and for sampling at a greater distance from the vessel.

In the subsequent days, strong frost led to a quick formation of new ice so that the ice conditions in general got worse. As at the same time darkness rapidly increased, sailing in ice at night became more hazardous. Furthermore, work on deck became difficult because of severe icing of sampling gears.

Nevertheless, on September 26 and 27, further geological sampling and reflection seismic profiling was carried out in the southern Nansen Basin. On the evening of September 27, at 83° 03' N, 11° 54' E, *Polarstern* and *Oden* moored alongside an ice floe. With a party on board *Polarstern*, scientists and crew took leave of *Oden*, in whose wake *Polarstern* had made, in the previous three weeks, a reflection seismic profile more than 1,500 km long.

On the next day, September 28, the last 20 nautical miles of profiling followed, then *Oden* stayed behind for an oceanographic station at 82° 50' N, 11° 54' E. In the following days, *Oden* finished the oceanographical/meteorological profile from the Morris Jesup Rise to Nordaustlandet. Both vessels remained in daily radio contact until the end of their journeys in Göteborg and Bremerhaven, respectively.

Polarstern sailed south to the Yermak Plateau, where at a geological station at 82° 39' N, 13° 04' E, a short sediment core probably of Eocene age was collected. Even after the separation from *Oden* seismic profiling continued. However, increasingly bad ice conditions on the night of September 28 to 29, forced *Polarstern* to stop reflection seismic profiling, after she was stuck several times in heavy pack-ice.

After a further very successful geological station on September 29, at 82° 01' N, 15° 41' E on the SE slope of the northern Yermak Plateau, had been completed under a bright blue sky but in a bitter cold, the vessel passed the very distinct ice edge in the morning of September 30, at 81° 23' N, 14° 41' E.

In heading south-west, the vessel speedily passed the open water and reached the same day at noon her next sampling station, at 80° 28' N, 08° 13' E on the southern Yermak Plateau. From September 30, to October 2, here as well as at 80° 16' N, 06° 38' E and at 79° 38' N, 05° 35' E, geological sampling, bathymetrical and reflection seismic profiling was carried out in areas which had been proposed as potential drill sites for the Ocean Drilling Program (ODP).

This was followed, from October 3, to the morning of October 6, in quiet seas by bathymetric surveying with HYDROSWEEP in the region of the Spitsbergen and Hovgaard fracture zones. A permanent north-easterly wind in the days before had pushed the ice edge in the Fram Strait far to the West so that large areas of Fram Strait were ice free; areas which in the preceding year had not been accessible for survey work under ARK-VII/3a.

On October 6, *Polarstern* sailed south from the Fram Strait to the central Greenland Sea, to recover a long-term mooring, at 75° N, 04° 05' E, for the international

Greenland Sea Project. Acoustic surveying by other vessels to locate the mooring had been unsuccessful so that October 7, was the last day and chance to retrieve the mooring at its original site. In spite of intensive searching between early morning and late afternoon of this day, dredging attempts were without any result. Until darkness the vessel continued cruising to eventually collect some floating fragments of the mooring system.

On October 7, at 17.30 hours, *Polarstern* left the area and sailed for Tromsø. A gale with wind speed up to 10 bft. made cruising difficult, but did not affect the travel schedule.

After 70 days at sea and a distance of approximately 5,200 miles, mostly in compact pack-ice, *Polarstern* in the morning of October 10, reached the harbour of Tromsø, thus bringing to an end the unexpectedly successful Leg ARK-VIII/3 of the ARCTIC'91 expedition.

1.2 Weather Conditions (B. Richter)

High pressure with light southwesterly winds determined the weather when *Polarstern* set course north after leaving Tromsø. When we reached the ice-edge on August 4, 1991, a High over Novaya Semlya with anticyclonic weather type and frequent formation of fog due to advection of moisture in the boundary layer interfered with helicopter activities. This lasted for more than ten days and only long-wave radiation, reflected by low stratus clouds, improved visibility from time to time.

A low, which moved from the Atlantic over Barents Sea northeastward, resulted in fresh to strong winds from southerly directions. By August 22, large-scale subsidence resulted in a few hours of sunshine, but this was quickly disrupted by advection of fog.

Although we were north of the main track of cyclones, the lows passing south of our area resulted in strong winds from southeasterly directions with temporary snowfall and white-out conditions. One of these lows formed an upper air low and became stationary. Due to high pressure over Siberia, winds reached gale-force from southwesterly directions on September 4. Pressure rise reduced wind speeds to Force 4, but resulted also in low stratus, light snowfall and fog-banks. It finally built up a high which determined the weather when we reached the Pole.

A secondary low, which formed in the vicinity of a low over the Ural mountains, crossed our area on September 10, with gale-force winds and freezing rain. Large-scale subsidence resulted in quick filling up of this low, but the probability of fog or freezing fog remained high due to radiative cooling processes in the boundary layer. Helicopter flights were not possible until September 15.

After a phase of light and variable winds, the first outbreak of cold air from Greenland occurred on September 18, with a temperature drop to minus 10.9° C, the lowest temperature until then. Backening of the wind to southeasterly directions due to a high over Scandinavia and the Barents Sea caused a rapid rise of temperature up to values of plus 0.6° C on September 22. Simultaneously,

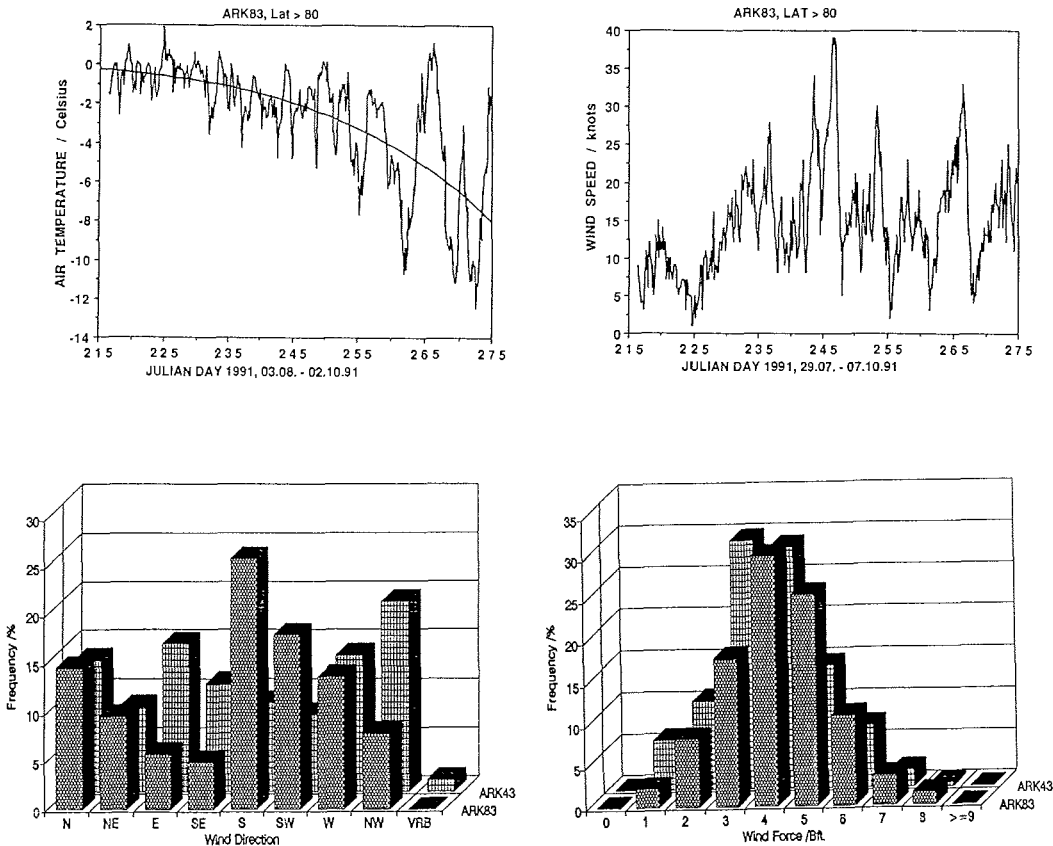


Figure 1.2-1: (a) Air temperature of the 3-hr-observations and a polynomial fit for this time series. Although there are high short-term variations, mostly due to advection and radiative processes in the boundary layer, an increased decline of temperature during mid of september can be seen. **(b)** Windspeed during ARK-VIII/3. The average windspeed was 15 knots, equivalent to Beaufort 4-5; gale events occurred more frequent during the second part of the cruise. This graph does not include the windspeed during our homebound track. **(c)** Relative frequency in percent of wind direction and **(d)** wind speed in Beaufort for both cruises. During ARK-IV/3, winds from E and SE were more frequent, mainly during high-pressure situations. This resulted in pressing of ice in 1987 and an unintended drift of *Polarstern* to the most northern position with a ship's heading of 227 degrees. During ARK-VIII/3, winds from S and SW, which opened the ice, were most frequent.

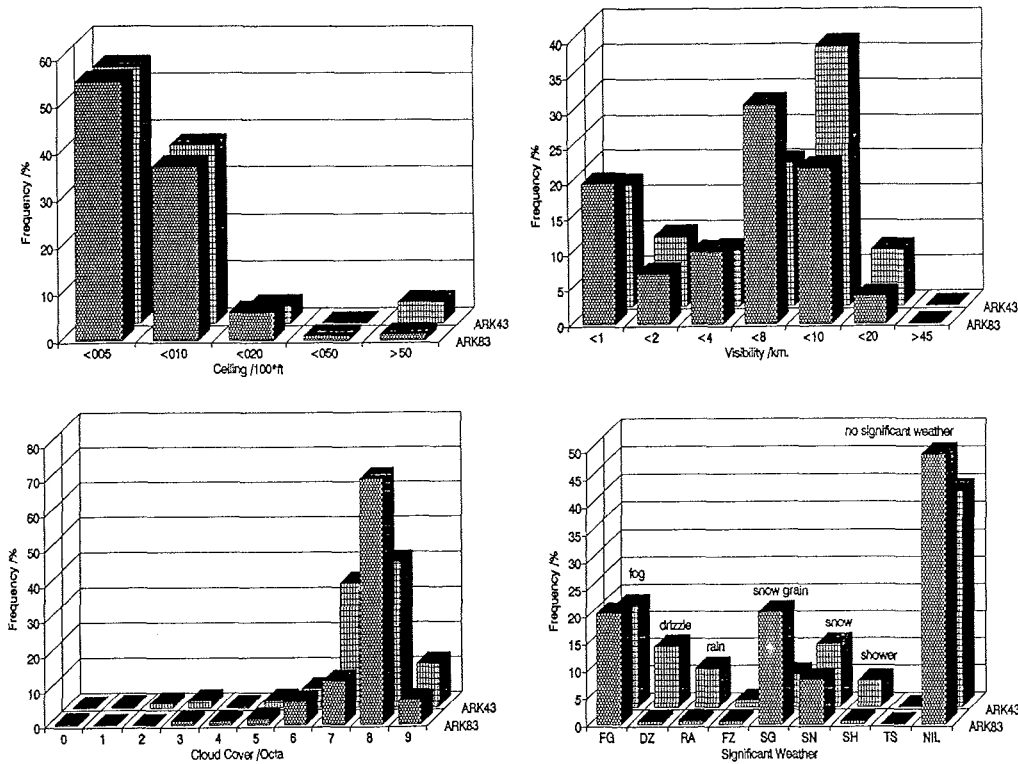


Figure 1.2-2: Frequency distribution of aviation relevant criteria (a) ceiling and (b) visibility. They were comparable during both cruises with very high probability of fog (almost 20%) and low ceiling (more than 50 percent below 500 ft). This fits to other arctic climatological observations. (c) Cloud cover in octa for both cruises. Although high cloud cover was prevailing during both cruises, we encountered even more overcast sky conditions (70%) during ARK-VIII/3. (d) Frequency of significant weather. The frequency for fog was comparable. During ARK-IV/3, more rain and drizzle were observed as that cruise was one month earlier in the year and not that far to the North. Instead, we had more snow grain during ARK-VIII/3.

increasing pressure gradients and anticyclonic curvature of isobars caused the wind to reach Force Bft.7-8.

A high north of Greenland and a low over the western Barents Sea resulted in veering of winds to northeast reaching Force 5 to 6. This opened the marginal ice zone and, after leaving the ice on September 30, we could cruise along the ice edge to a longitude of 4° W.

A gale cyclone developed in the Iceland area on October 3, with center pressure of below 957 hPa. It moved northeastward and its swell reached our area on October 5. A second low, which intensified when passing Kap Farvel northeastbound, became as well a gale cyclone of 960 hPa. It reintensified the above mentioned low

so that we encountered winds of Force 8-9 on October 7, at position 75° N, 04° E where a mooring was to be picked up.

When setting course to Tromsø the same day, winds came from northeast at Force 8. After crossing the center of the low with light and variable winds, winds became southwesterly and increased up to Force 9-10 due to intensification of the low by a short-wavelength trough and according increase of pressure gradients at the flank of a high over the Iceland area and Scandinavia. The winds did not decrease until we reached the Fjord of Tromsø.

On the last leg from Tromsø to Bremerhaven, we crossed the gale Force 8-9 windfield of a low which moved from Iceland to Jan Mayen. After passing the Lofotes, the wedge of a high over Scandinavia with prevailing southeasterly winds Force 7, decreasing later to Force 4, determined the route weather. When passing the western Skagerrak, winds increased to Force 8 temporarily due to orographic effects. During the final cruise through the North Sea, a frontal band crossed our area with moderate to fresh winds.

Climatic Review of the Cruise

As there exist only very few climatic data of the high arctic, the meteorological conditions of cruise ARK-VIII/3 will be compared to those we encountered during the cruise ARK-IV/3. The data base consists of 469 ARK-VIII/3 and 252 ARK-IV/3 observations taken every 3 hours in the area north of 80° North. It must be considered, that the ARK-IV/3 observations are from July 7, 1987, until August 17, 1987, whereas the ARK-VIII/3 data were taken between August 4, 1991 and October 1, 1991.

2. REMOTE SENSING OF SEA ICE (W. Dierking and P. Lemke)

Sea ice plays an important role in the climate system. The distribution of sea ice and open water in polar regions has a pronounced influence on the atmospheric and oceanic circulation. The most important sea ice variables relevant for climate are extent, concentration, thickness and velocity as well as the characteristics of the surface of the ice floes: albedo, surface temperature and roughness. In order to predict the time variability due to dynamic and thermodynamic processes sea ice models have been developed which treat the ice as a plastic material being deformed by winds and ocean currents and modified in size by heat and radiative fluxes. Concerning the ice extent, the results of the numerical models agree relatively well with the observations from passive microwave radiometers. Since the polar regions are hardly accessible, remote sensing of sea ice variables plays an important role for the development and verification of sea ice models. A major problem of current sea ice modelling is the lack of longer global time series of sea ice concentration, thickness, and motion required to determine the optimal values of certain model parameters.

Sea ice extent, concentration, floe-size distribution, type, motion, albedo, surface temperature, and roughness can be obtained from satellite imagery using more or

less complex algorithms. The improvement of these algorithms through comparison of satellite data with ground truth and through sensor intercomparison represents a dominant part of present remote sensing activities. In order to improve the algorithms for ice concentration, remote sensing data collected during the Winter Weddell Gyre Study 1989 aboard *Polarstern* are presently compared to SSM/I (Special Sensor Microwave Imager) observations. A major part of this research covers the verification of the AVHRR (Advanced Very High Resolution Radiometer) concentration estimates with line-scan camera observations, and the improvement of SSM/I concentration estimates using AVHRR data. Furthermore, ice motion is estimated from displacement vectors obtained from consecutive AVHRR images and from buoy tracks.

A comparison of this sensor hierarchy for the Arctic is still missing. Concentration algorithms obtained for Antarctic sea ice cannot be applied to Arctic sea ice without modification, since the physical characteristics and accordingly the radiative properties are different. Therefore, it was planned to collect a similar data set for the high Arctic during ARK-VIII/3. The remote sensing work during this expedition included the following projects:

- Estimation of sea ice concentration using NOAA-AVHRR data (visible, infrared). These data (horizontal resolution 1 km) will be used to improve the concentration algorithms applied to the low resolution (35 km) SSM/I images.
- Determination of the sea ice velocity field from displacement vectors obtained from consecutive AVHRR images and comparison with trajectories of buoys deployed from *Polar Star* by the Meteorological Institute of the University of Hamburg (H. Hoeber).
- Estimation of sea ice concentration from an airborne line-scan camera (horizontal resolution 1-3 m). The line-scan data are needed to verify AVHRR concentration algorithms.
- Measurement of the surface temperature using a KT4-radiometer. These data serve as ground truth for the AVHRR infrared data.
- Measurement of the surface roughness with an airborne laser-altimeter (large-scale roughness, ridge statistics) and with a mechanical profilometer (small-scale roughness).

2.1 AVHRR Visible and Infrared Images

During the course of the expedition 63 AVHRR images (one visible and four infrared channels) have been received from the NOAA 10 and 11 satellites. During the first six weeks of the cruise, *Polarstern* travelled in a cloudy and foggy environment. Therefore the satellite images could not be used for navigation. Nevertheless, on most of the images the area north of Svalbard and Fram Strait was cloud-free allowing a comparison to the passive microwave images from SSM/I and the tracking of individual ice floes from consecutive images to estimate the ice motion field.

The situation changed from the middle of September on, when larger areas in the vicinity of *Polarstern* were found to be relatively cloud-free. An example of the visible channel of the AVHRR after the navigation of the image and the projection onto a polarstereographic grid is given in Figure 2.1-1. Larger individual floes (>10

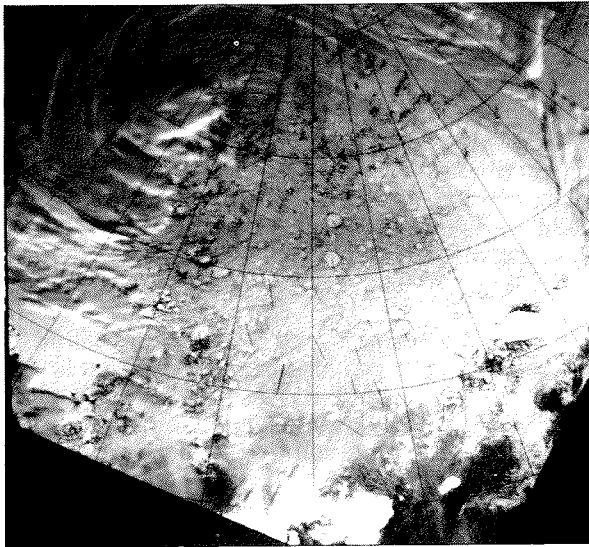


Fig. 2.1-1: Image of the sea ice obtained from channel 1 of the AVHRR aboard NOAA 11 on September 11, 1991, 8:56 UTC, projected onto a polarstereographic grid. Shown is also the displacement of the center of individual floes from September 11-17, 1991. The tip of the triangle indicates the position of *Polarstern*.

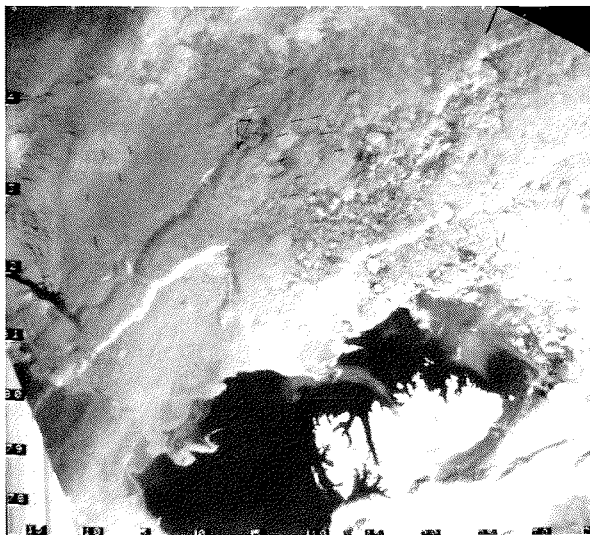


Fig. 2.1-2: Same as Fig. 2.1-1 but for September 23, 1991, 8:17 UTC, projected onto a Mercator grid. The displacement vectors indicate the drift from September 23 to 25.

nm, bright areas) and open water (dark) can clearly be identified. The tracking of several floes between the images of September 11 and 17, resulted in a southerly drift indicated by the displacement vectors in Fig 2.1-1. The drift speed amounts to some 5 nm/day and was forced by northerly winds. An example of easterly drift due to westerly winds is given in Fig. 2.1-2. The sea-ice motion generally responds on a relatively short timescale (one day) to changes in wind direction and wind speed.

2.2 Line-scan Camera Observations

The line-scan camera consists of a line of 1024 diodes which are arranged perpendicular to the flight track of the helicopter. It receives a digital image of the sea ice and ocean surface along the flight track in the visible band. The flight pattern used consists of an inner 5 nm and an outer 10 nm square. This pattern is designed to optimize the comparison with the AVHRR image. Flying at an altitude of 1,000 m the swath width is 1 km and the resolution perpendicular to the flight track is 1 m. The resolution in flight direction depends on the speed of the helicopter and the scanning rate and lies in the range of 1-3 m. For an optimal comparison between line-scan camera and AVHRR a cloud-free area larger than 10 nm x 10 nm is required at the time of a satellite overpass. This condition was only met twice during the expedition.

2.3 Surface Temperature Measurements with a KT4-radiometer

The surface temperature measurements were intended as a comparison (ground truth) for the AVHRR infrared images. Because of overcast skies during most of the expedition, the KT4-radiometer was switched on only from September 25 to October 1. An example of the surface temperature measurement is given in Figure 2.3-1. The higher temperatures around -2°C indicate that *Polarstern* sailed through open water. The lower temperatures indicate sea-ice floes.

2.4 Surface Roughness Measurements

The roughness of the sea ice surface was determined on larger spatial scales with a laser-altimeter aboard a helicopter and on a smaller scale with a mechanical profilometer.

Large Scale Roughness

Altogether 21 laser flights have been performed amounting to a total profile length of 270 nm. Two different patterns were flown: a four-leg-star with each leg being 4 nm in length, and straight lines of 10 nm. The first pattern is used to detect a specific orientation of the ridges. An example of a laser- altimeter record, i.e. the distance between the laser mounted on the helicopter and the surface, is given in Figure 2.4-1. The upper panel shows the first nine minutes of the flight on August 22, basically indicating the helicopter motion. The lower panel shows six seconds representing a blow-up of the distance between the two dashed lines in the upper curve, clearly indicating the surface topography superimposed on the helicopter motion. Since the helicopter was moving at a mean ground speed of 30 knots, one second in the

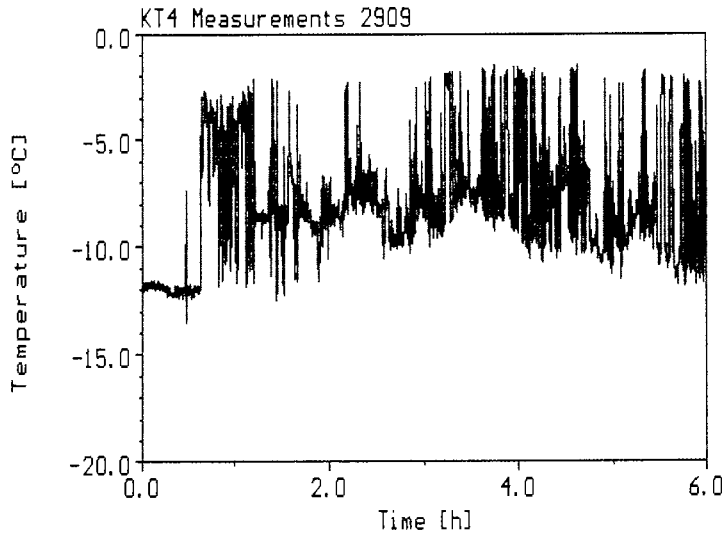


Fig. 2.3-1: Surface temperature recorded from a KT4 - radiometer on September 29, 1991.

```

LASER-Entfernungsmesser-Daten-Wiedergabe ---- L E D A R --- 01.330.87 SIC-M0e
Reg.Zeit = 37:23 22.08.91 10:00:00
Graphik von [min:sek] [Wert #] bis [min:sek] [Wert #] Fehler Kein Echo
Oben 00:00 1 09:19 55900 0 9272
Unten 03:12 19201 03:18 19759 0 142
    
```

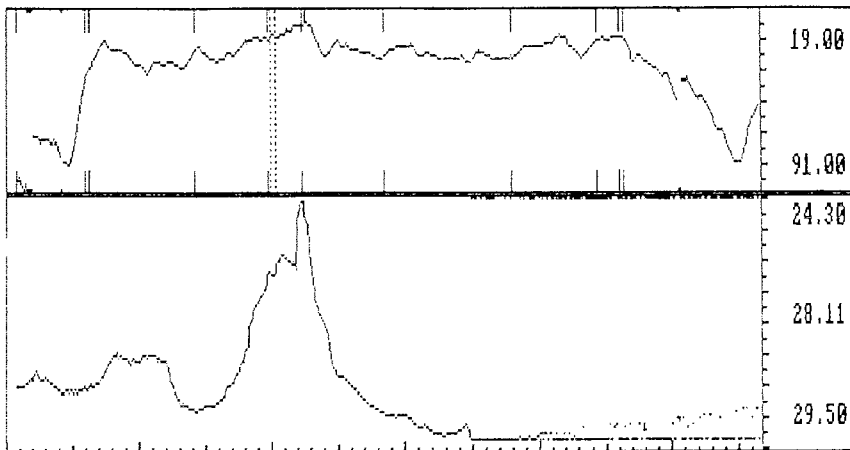


Fig. 2.4-1: Laser-altimeter record from August 22, 1991 at 87° 29' N, 91° 2' E. The upper panel shows nine minutes of the flight track. The lower panel is a blow-up of the distance between the two dashed lines in the upper graph, representing six seconds. One second amounts to about 15 m.

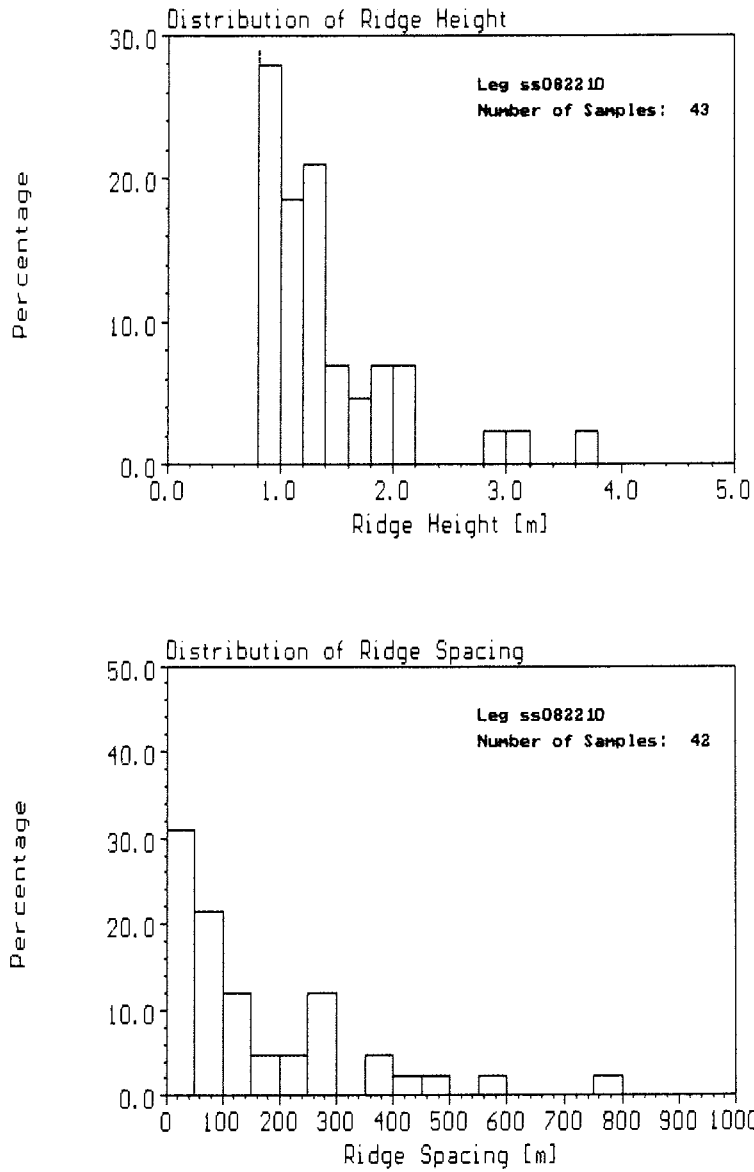


Fig. 2.4-2: (a) Distribution of ridge heights from leg ss082210 measured on August 22, 1991 at 87° 29' N, 91° 02' E. The leg was 4 nm long. **(b)** Distribution of ridge spacing from leg ss082210.

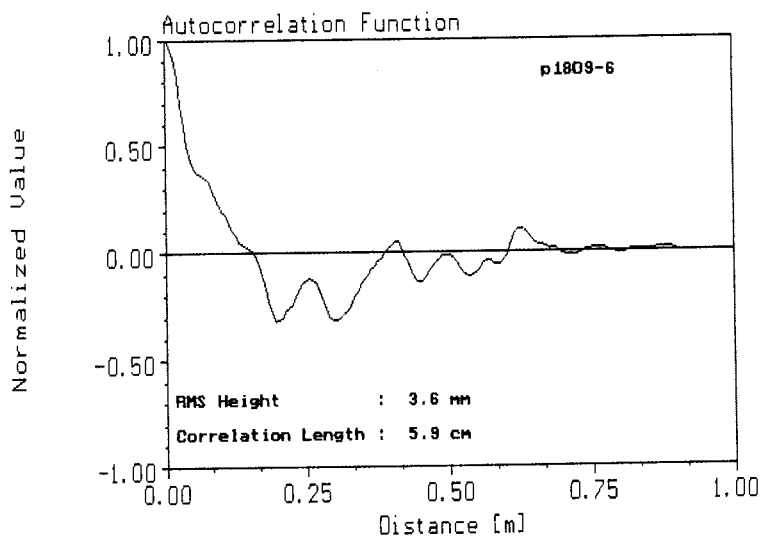
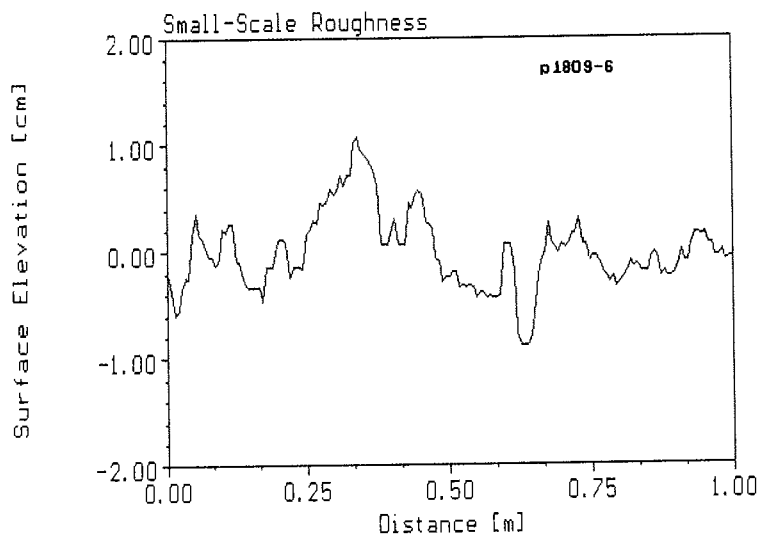


Fig. 2.4-3: (a) Small scale surface topography of sea ice measured with a mechanical profilometer. (b) Autocorrelation function of the surface profile shown in Fig.2.4-3a.

lower graph of Fig.2.4-1 represents roughly 15 m. The ridge height amounts to nearly 5 m and the width at the base to 15 m. To the right of the ridge the data sequence of an open lead can be seen which is characterized by several data gaps.

The main task of the data analysis is the removal of the helicopter motion from the original data by appropriate filtering methods and the computation of basic statistics like the distribution of the height and spacing of ridges. An example of a ridge height distribution is shown in Figure 2.4-2a. Along a 4 nm profile altogether 40 ridges above the cutoff-height of 80 cm were counted. The distribution of ridge spacing for the selected leg is given in Figure 2.4-2b.

Small Scale Roughness

The mechanical profilometer used to measure the small scale roughness consists of 6 mm square bars of equal length mounted adjacent to each other on a 1 m frame. During the measurement the frame was set up perpendicular to the surface and the bars were adjusted to sit with their lower ends on the surface. Along the upper ends of the bars the surface profile was drawn on metric graph paper. These analog-profiles were digitized and statistical properties were computed. An example of a surface profile is given in Figure 2.4-3a. The autocorrelation function of the profile is shown in Fig 2.4-3b, supplemented by the corresponding values of rms-height and correlation length. These parameters are needed for modelling the radar backscatter from the sea ice surface. Theoretical models of the interaction between radar waves and sea ice are utilized to improve the interpretation of SAR-images (SAR = Synthetic Aperture Radar), which will be obtained from the European Remote Sensing satellite ERS-1.

3. SEA ICE SAMPLING AND STUDIES

3.1 Physico-chemical Characteristics of Sea ice and Snow (H. Eicken, C. Haas and U. Wieschollek)

Sea ice Observations

In a joint effort of sea ice and remote-sensing groups, a total of 293 ice observations was conducted every two hours from the ship's bridge when underway. A report containing detailed observations including types of ice observed, concentration, thickness, floe size, surface characteristics, etc. along with meteorological parameters has been prepared separately.

Generally, ice conditions were quite favourable, with a mean ice concentration of 91 % (standard dev. 13 %) for all observations. As indicated in Fig. 3.1-1, except for the marginal ice zone which was encountered between 78° 51' N and 80° 12' N on the way in and between 81° 25' N and 80° 22' N on the way out of the ice, we encountered larger amounts of open water in three distinct zones (August 16 through 18 and 29 through 30, September 10 through 12). These took the form of

systems of leads, up to several km broad and several tens of km long. Individual leads extended for up to 20 km with a width of up to 5 km. Comparisons with mean wind direction as recorded by the ship's anemometers show that these observations of low ice concentration may be tied to veering of winds.

Floe sizes encountered during the cruise were mostly in the range of hundreds of meters to few kilometers. At 85° 47' N, 50° 45' E and 87° 35' N, 150° 14' E a marked decrease of floe sizes with a mode at 50 to 100 m could be observed. In the central Fram Strait (cf. Fig. 3.1-1) between roughly 84° N, 01° W and 82° N, 14° E, giant floes of several tens of km in size were encountered. Ridges and hummocks accounted mostly for <5 % of the floe surface area. Other than a few observations on highly ridged zones (up to 50 % of floe area up to 5 m high), prominent ridges and hummocks were more frequently observed at the westernmost locations (Morris Jesup Rise, Fig. 3.1-1) and in central Fram Strait (maximum of 30 % of floe surface ridged or hummocked up to 5 m high).

New-ice formation was observed during the entire cruise, at first only growth of dark nilas during nighttime hours at the edges of leads. After August 29, extensive new-ice sheets and accumulations of grease and pancake ice were encountered. Toward the end of the cruise (September 28/29, at roughly 82° N, 14° E), grey-white ice of 20 to 40 cm thickness covered with up to 10 cm of snow was observed.

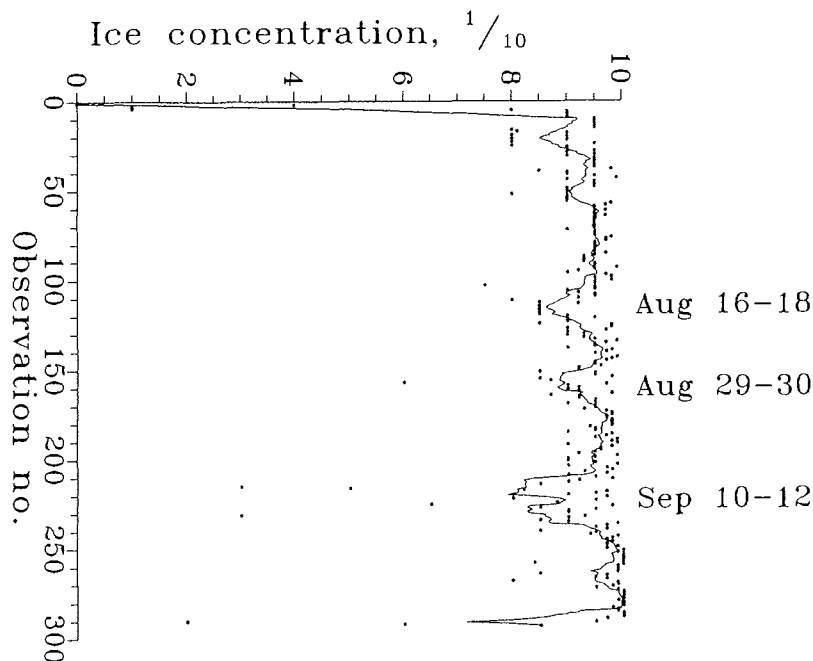


Figure 3.1-1: Ice concentration as observed from the ship's bridge during observations between August 3 and October 1 (i.e. excluding HYDROSWEEP-transect in Fram Strait). Smoothed data (5-point running-mean) are plotted as well.

The timing of the cruise allowed observations on the transition between ablation- and ice-growth-season, particularly in conjunction with detailed measurements of surface characteristics such as depth of the surface layer, density, grain size and temperature of the snow etc.. During the first two weeks of the expedition, floe surfaces were found to be covered by a layer of weathered ice. After ablation of the first new snow deposited on August 10, a stable snow cover persisted from August 25 onward. It had increased to a maximum mean thickness of 17 cm by September 23 (ice station 266).

Surface melt puddles, which had also been recorded during a total of 11 helicopter flights with a vertically mounted video camera, covered up to 50 % of floe surfaces. By August 20, the vast majority of puddles was completely covered by an ice sheet which increased to 10 cm in thickness by September 2. Warming events observed between September 8 and 10 and around September 23, caused no reopening of puddles, they induced an increase in the water content of the snow associated with a lowering of surface albedo in some spots.

During the first half of the cruise a total of 23 icebergs and ice islands have been observed. These measured mostly >100 m in diameter and rose up to 20 m above waterlevel. Further studies on surface samples and cores aim to establish origin and drift of these bergs.

Thickness and Physico-chemical Properties of Sea ice and Snow

At 48 Stations 50 m long thickness profiles were drilled at 5 m spacing in level ice, i.e. portions lacking ridges or other deformation features (see Fig. 3.1-2 for a station map). Mean and standard deviation of ice thickness, surface layer depth (i.e. weathered ice and snow) and freeboard are indicated in Table 3.1-1. Ice thicknesses exhibit a unimodal distribution with a pronounced peak at 2.2-2.4 m, tailing towards maximum values of 7 m.

For wider areal coverage, additional thickness measurements were made in level sections of 56 randomly chosen floes accessed by helicopter, several km away from the ship (10 stations, indicated by the suffix "H" in Fig. 3.1-2). These values are plotted with the means of all 50-m profiles against longitude in Figure 3.1-3. Even though some of the scatter evident in the graph might be removed once the data have been transformed into a Transpolar Drift co-ordinate system, we have difficulties in establishing any geographical trends. The variance of mean floe thickness seems to fall off with longitude (i.e. upstream in the Transpolar Drift, cf. Fig. 3.1-1). Yet, further evaluation of the data will have to include further information on the composition and evolution of the ice as well.

At 46 stations, 55 4-inch-cores were drilled through the entire thickness of the floe. All but the last two of these samples have been analysed onboard for texture, salinity and chlorophyll-a concentration (the latter for a total of ca. 45 cores). Preliminary results from the study of thick sections examined in plain light and between crossed polarizers indicate that roughly 61.9 % of the entire length of cores (130 m to date) are composed of congelation ice, which has formed through *in situ* freezing of seawater onto the ice sheet at the location of sampling. A substantial part of the total core length studied consists of ice that is in fact intro-

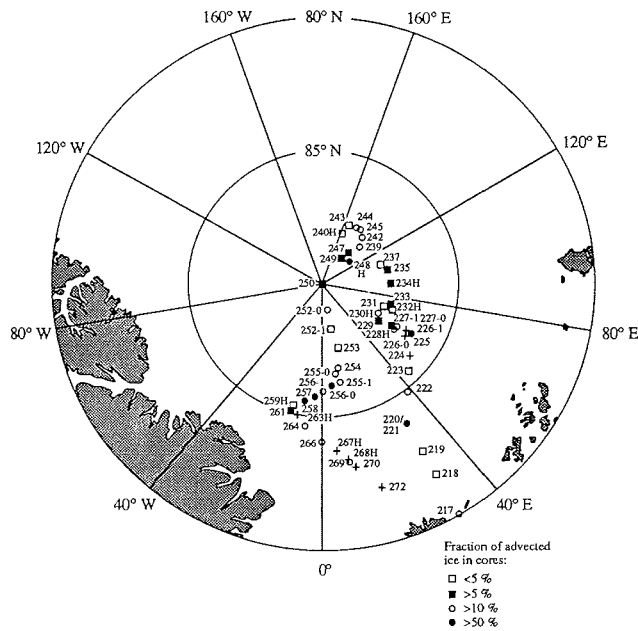


Figure 3.1-2: Map of sampling stations, with symbols denoting percentage of cores composed of advected ice (see text for detailed explanation). The suffix "H" denotes helicopter sampling stations.

	Mean (m)	Stand. dev. (m)
Ice thickness	2.86	0.99
Surface layer thickness	0.11	0.07
Freeboard	0.23	0.16

Table 3.1-1: Mean and standard deviation of thickness measurements along 50-m profiles (518 points).

duced into the ice cover as congealed fragments. This includes, e.g. rafted pieces of columnar ice or frazil ice formed in lead areas and swept underneath an existing ice cover. In all, 24.6 % of the entire core length may be attributed to such advected ice. Figure 3.1-2 indicates the percentage of advected ice within individual cores and its regional distribution. Similar to the thickness distribution of level ice, no clear trend is apparent.

At 33 sites the surface layer of snow and ice has been characterized in detail, including determinations of thickness, salinity, texture and density of surface ice and snow. A total of ca. 40 surface cores was drilled for detailed studies of the

distribution and size of pores observed in the upper layers of the ice. These studies are meant to contribute to the interpretation of remote-sensing data, in particular passive and active microwave data, from the Arctic Basin. As part of the cooperation with Scandinavian colleagues on board the icebreaker *Oden*, 12 cores were taken along 1-km profiles on two ice floes for which coverage by the European Radar Satellite (ERS-1) has been obtained. First results indicate a high variability of pore sizes and types prevailing in the upper ice layers. Yet, different classes of pores could be recognized, each of which corresponds to specific metamorphic processes occurring during ageing of the ice.

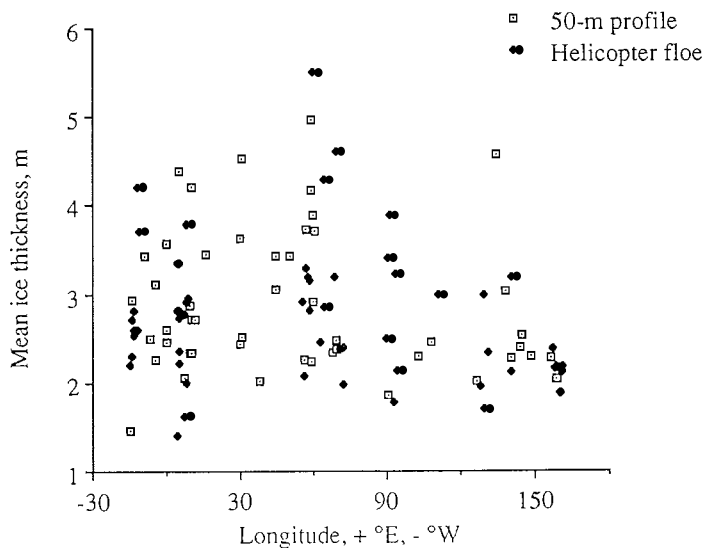


Figure 3.1-3: Longitudinal distribution of ice thickness, i.e. the means of 50-m profiles and individual measurements obtained from random-drilling flights.

3.2 Sea ice Biology (R. Gradinger and S. Härtling)

Our main aim was to study the structure of the community inhabiting the multi-year sea ice of the deep Arctic Ocean. At 25 sites a total of 36 cores were taken with a 3-inch Ruffli ice auger, sectioned into 10-20 cm long segments, which were melted in 3 l 0.2 μm filtered sea water at 1° C in the dark. After melting, 100 ml subsamples were fixed with buffered formalin (1 % final concentration) and filtered on 0.2 μm Irgalan Black stained Nuclepore filters after DAPI-staining for the determination of the abundance of bacteria, auto- and heterotrophic flagellates and diatoms by epifluorescence microscopy. For the analysis of the larger meiofauna, the rest of the melted core section was concentrated over a 10 μm screen. Organisms >60 μm were counted alive in these concentrated samples and later on fixed in various fixatives (formalin, glutaraldehyd, Bouin, Lugol) for different purposes.

In accordance with the results from earlier investigations (for reviews see HORNER 1985, 1989) the highest organism densities were always observed in the lowermost cm of the ice floes (Fig. 3.2-1), the so-called bottom community, but all habitats were

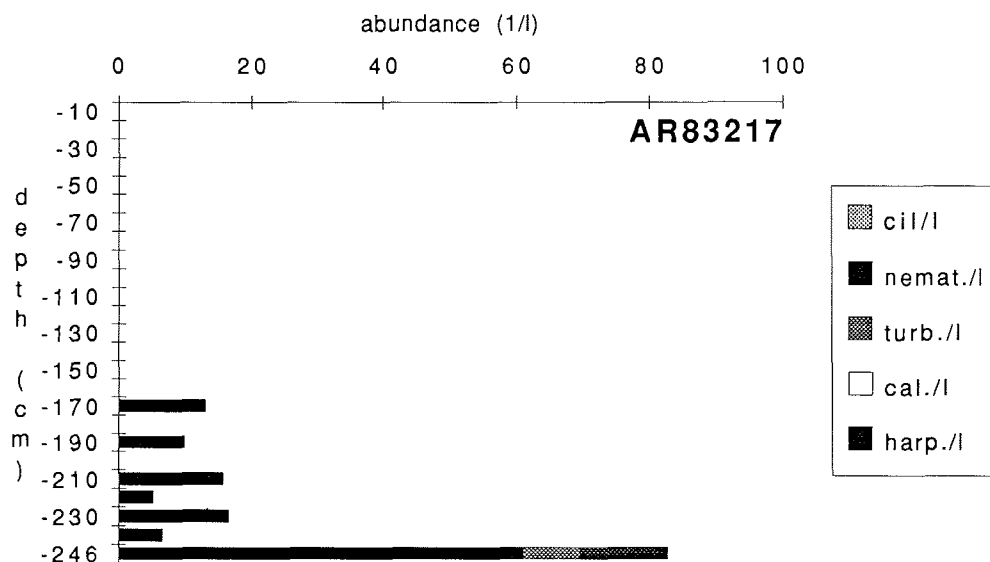


Fig. 3.2-1: Abundance of meiofauna organisms in core AR83217 (cil = ciliates; nemat. = nematodes; turb. = turbellaria; cal. = calanoid copepods; harp. = harpacticoid copepods).

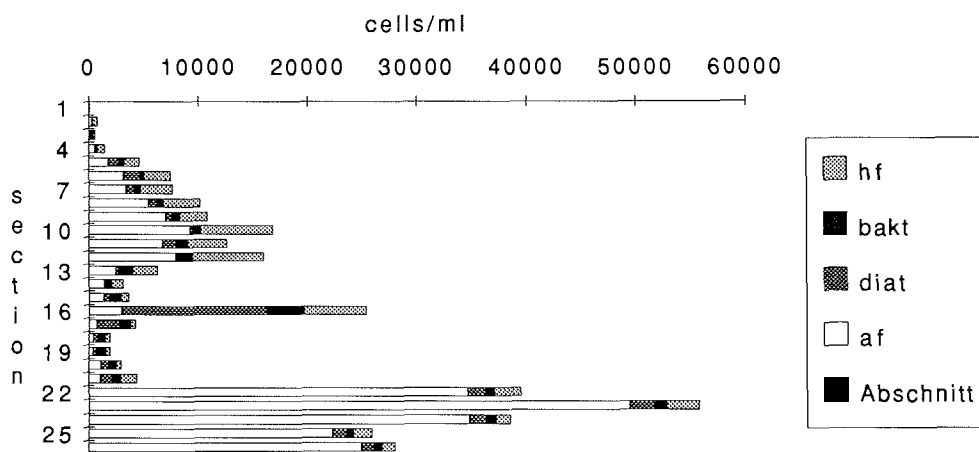


Fig. 3.2-2: Abundance of bacteria (bakt; 10^3 /ml), hetero- (hf) and autotrophic (af) flagellates and diatoms (diat) in core AR83217. The depth of the sections correspond to those in Fig. 3.2-1. Section 27 is a sea water sample.

colonized by a variety of organisms. Even red patches of snow were found on the surface of the ice, coloured by a massive development of a coccal chlorophyte.

Our finding of interior maxima in sea ice (Fig. 3.2-2) is the second report of this phenomenon from the Arctic. A comparison of our biological and physical ice data

will focus on the question of whether these internal bands are relicts from the last summer bottom community and thus tracers for the age of an ice floe, or if they are the result of ice rafting processes.

At the end of September the meiofauna spreads into the upper parts of the floes (Fig. 3.2-3). Here again, changes in the physical properties of the sea ice like, e.g. the porosity may be responsible for these changes.

The main aim of the investigation was a comparison between the sea ice community on shelves and in the deep Arctic Ocean. Earlier investigations had demonstrated that nematodes were the dominant meiofaunal group (ca. 50 % of total organism numbers) followed by copepods (30-40 %) (HORNER 1989). During ARK-VIII/3 we found this type of community restricted to stations close to the Barents shelf (e.g. Fig. 3.2-1). In all other areas, a totally different community structure was observed, characterized by ciliates and turbellaria (e.g. Fig. 3.2-3), which is, in our opinion, the typical structure of the central Arctic Ocean sea ice community. Later in the season, the abundance of copepod larvae increased, implying a biological coupling between the pelagial and the sea ice. Maybe the sea ice is serving as a "nursery ground" for the high Arctic zooplankton.

Of special interest for geological studies is our observation of empty foraminifers tests (mostly *Neogloboquadrina pachyderma*; e.g. Fig. 3.2-3) in sea ice in concentrations of up to several hundred tests/litre ice. Here further measurements of stable isotopes will be done to see if the foraminifers did grow in the sea ice or whether they have been incorporated as empty tests during sea ice formation.

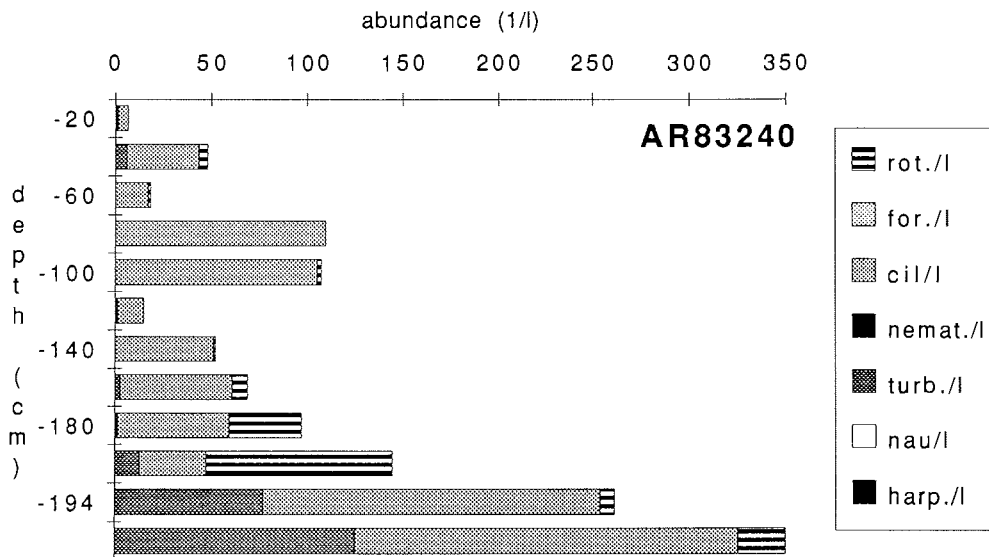


Fig. 3.2-3: Abundance of meiofauna organisms in core AR83240 (rot. = rotatoria; for. = foraminifers; cil = ciliates; nemat. = nematodes; turb. = turbellaria; naup. = nauplii; harp. = harpacticoid copepods).

Future research on our material will include taxonomical studies on diatoms, flagellates and metazoa in order to define sea ice typical organism groups which can be used as tracers for different ice origins (Beaufort Gyre sea ice or Laptev Sea ice) as well as for sedimentological studies. For the understanding of the different distribution patterns not only biological information is needed. The nutrient concentrations inside the brine, the pH and the oxygen content as well as the physical properties like pore size, temperature and salinity gradients and ice growth conditions are all important factors controlling the development of ice organisms, highlighting the need for further interdisciplinary investigations on Arctic sea ice.

3.3 Sediment Inclusions in the Seaice (D. Nürnberg)

In the line of the GEOMAR-Projekt "Global Change - Arctic sea ice and its geological and climatological importance - present and past", intensive studies on sediment inclusions in the Arctic ice cover have been performed. The Arctic sea ice cover has a large impact on the global climatic evolution. Extension, composition and thickness of the sea ice, its relation to open sea areas and the drift pattern extensively influence gas and temperature exchange between ocean and atmosphere, the global thermal balance, oceanic circulation and the ecology of marine biota. Due to its exposed position and the unequal relation between area and mean thickness (ca. 3 m), the sea ice cover is expected to react very sensitively on even small environmental changes. The importance of sedimentary inclusions on such changes is still not sufficiently known.

Main Research Objectives

Primary objectives of the "dirty ice" project during ARK-VIII/3 included:

- High-resolution sampling of sediment in sea ice and icebergs.
- Documentation of the regional distribution pattern of material-laden ice.
- Quantitative analysis of the lithogeneous and biogeneous components contained in the sea ice and the icebergs.
- Evaluation of processes by which sedimentary material is initially incorporated into the ice cover.
- Determination of processes redistributing material during melting and freezing.
- Identification of transport paths.
- Identification of probable depositional centers for the sediment transported by sea ice.

Sampling

Sampling of "dirty ice" was performed along a profile starting east of Svalbard at ca. 81° N, reaching the North Pole and ending at ca. 82° N north of Svalbard. Approximately 60 ice cores and 120 surface samples were obtained on 91 stations either directly from the ship (49 stations) or by helicopter support (42 stations). At least one 4 inch ice core covering the whole ice column was retrieved at each ship station and transferred to a 27° C freezer immediately. Core lengths range between roughly 0.5 m and 5.0 m. Downcore temperature measurements were taken every 5 to 10 cm.

In addition to the ice cores, "dirty" surfaces on the ice floes, on icebergs and sediment accumulations in cryokonites were sampled. Observations on surface characteristics including thickness of snow cover, temperature and freeboard of floes were performed routinely. Observations on the distribution of "dirty" patches on the ice surface were conducted as part of the ice watch. In addition, a video camera installed on the bridge of *Polarstern* documented the percentage of sediment in the sea ice along the ships's track from the North Pole southward.

Preliminary investigations on the sediment concentrations in ice cores and surface samples, on the grain size distribution, and on the minerogeneous and biogeneous sediment components were carried out during the cruise. Sediment concentrations were derived by vacuum filtering the ice samples and calculating the weight of sediment per litre ice. Grain size and component analyses are mainly based on smear slide analyses.

Preliminary Findings

Sedimentological investigations up to now (see THIEDE et al. 1987) show that large areas of the sea ice are covered by particulate matter. Most important mechanisms bringing sediment into the sea ice are summarized in DREWRY (1986), THIEDE et al. (1987) and REIMNITZ & SAARSO (1990).

In general, sediment accumulations of the following types could be observed:

- Sediment patches of 10-20 m in diameter with diffusely distributed sediment particles restricted to the sea ice surface. During the cruise, these patches were often covered by fresh snowfall rendering the estimation of the sediment/snow ratio difficult. Maximum averages may be as high as 50 %.
- A dirty sediment surface layer (10-15 cm) directly below the snow cover. No sediment below this layer could be observed.
- A white, sometimes dirty surface with one or more sediment layers or patches within the interior of the floe.
- Sediment within cryokonites (10-30 cm depth, 3-5 cm in diameter) located in melt water ponds. The sediment accumulations easily dispersed during sampling procedure. Mudballs as described by NANSEN (1902-1906) and THIEDE et al. (1987) were not observed. Sometimes, the surroundings of melt water ponds showed high sediment concentrations and were slightly elevated relative to the ponds.
- Sparse sediment accumulations on ridge surfaces were mostly restricted to one side of the ridge, thus implying recent eolian transport.

The continuous ice watch provided first insights into the distributional pattern of sediments on and within sea ice. Figure 3.3-1 shows locations where sediment was observed in the sea ice during the ice watch. Although the surface sediments are distributed in patches and are often not over wide areas, it is possible to recognize areas of relatively high sediment concentrations (Fig. 3.3-1). Sediment concentrations ranged from 0-20 % of the ice cover. In extremes concentrations of up to 50 % were observed. It is important to note that during the first part of the cruise (Stations AR83217 to AR83254) "dirty ice" was restricted mainly to the sea ice surface. In the southwest (Stations AR83254 to AR83264) thick and dark sediment layers were

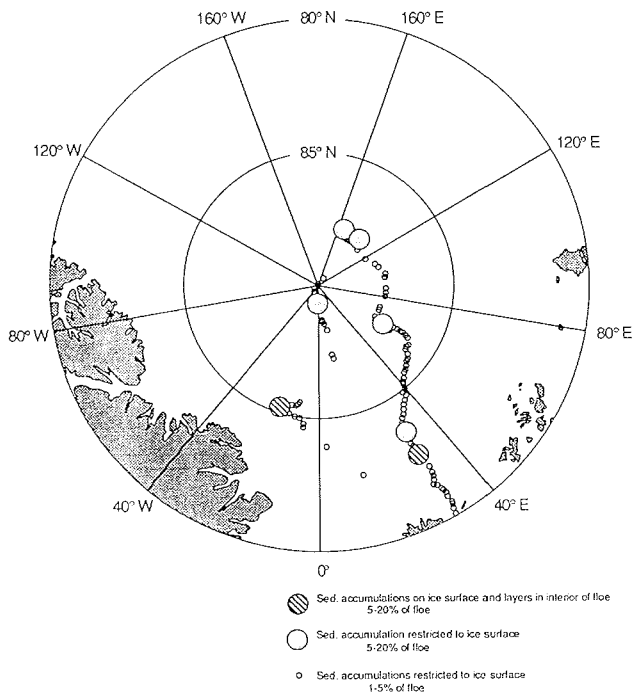


Fig. 3.3-1: Chart showing locations, where sediment inclusions in the Arctic sea ice and icebergs have been observed during ARK-VIII/3. Observations and estimations of the sediment/ice ratio were conducted as part of the ice watch. Areas of high sediment abundance are indicated.

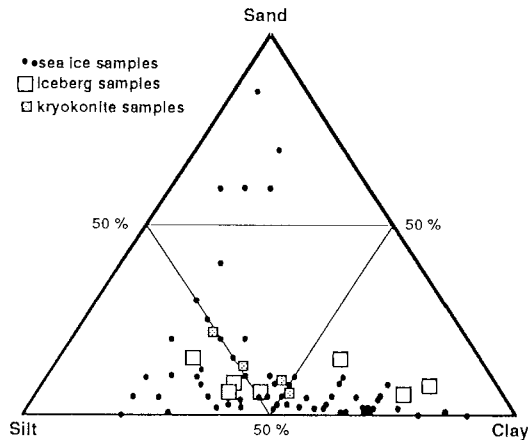


Fig. 3.3-2: Grain size investigation of ice surface samples. Sand, silt and clay fractions are presented in a triangular diagram, the peaks of which are each 100 %. Sediments are well-sorted being mainly silty clays or clayey silts. The sand fraction is underrepresented. Important to note is that iceberg surface samples and sediment accumulations in cryokonites do not differ in grain size from sea ice surface samples.

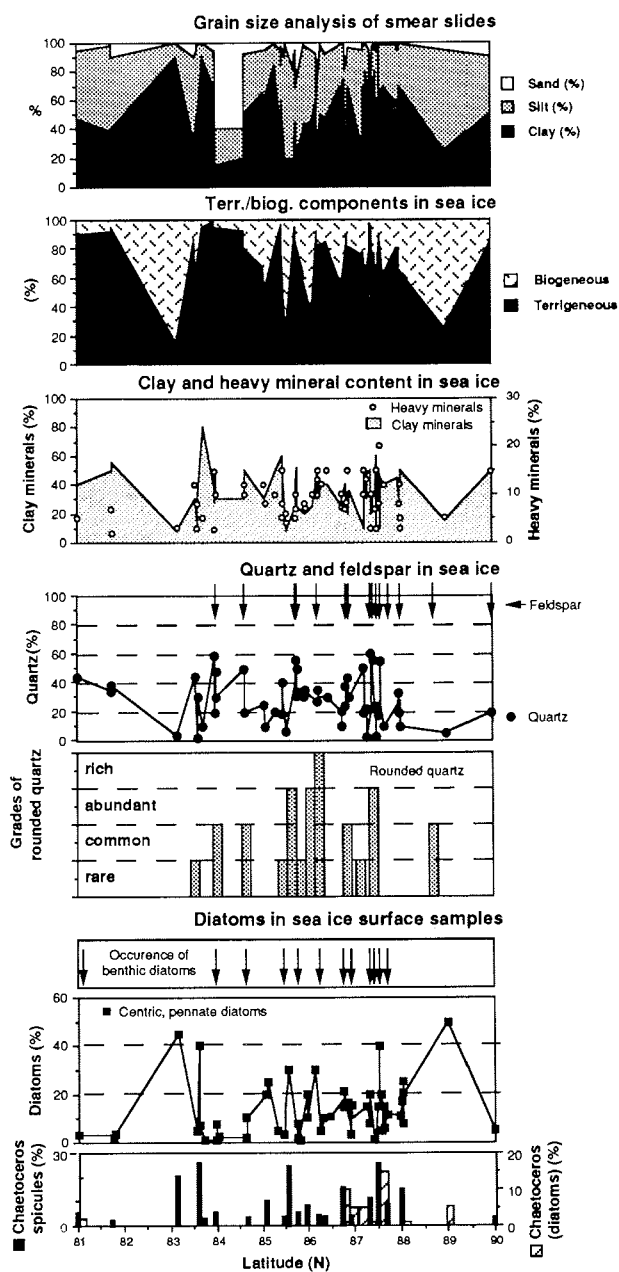


Fig. 3.3-3: Abundances of most important sediment components in sea ice surface samples as estimated from smear slides. Data are plotted against latitude.

often found in the interior of the ice floes. These differences in sediment distribution most likely result from different source areas for the southwesternmost and northeastern samples. The former may be part of the Beaufort branch of the Transpolar Drift, whereas the latter would most probably originate from Siberia .

The preliminary grain size analysis carried out by estimation from smear slides shows a dominance of clay and silt fractions (Fig. 3.3-2). Surface sediments are silty clays or clayey silts. The sand fraction, which is mainly composed of quartz, is almost negligible. These observations are consistent with the data set of WOLLENBURG (1991), who gathered "dirty ice" data between 1987 and 1991. Interesting to note is that the surface sediments from icebergs and sediment accumulations in cryokonites do not differ in grain size from sea ice surface samples.

The component analysis reveals quartz and clay minerals to be the dominant terrigenous sediment components (Fig. 3.3-3). Quartz appears often to be rounded, implying a fluvial source. Of minor importance are heavy minerals and rock fragments. Feldspar occurs only in traces. At a few stations, wood, stones of up to 5 cm in diameter (magmatites), feathers, soil patches and benthic foraminifers could be observed. Biogeneous components of sea ice sediments include planktic and benthic diatoms, ice diatoms (*Melosira arctica*), algae, spores, pollen and silicoflagellates (*Distephanus* spp.). The biogeneous components often play an important role reaching values of 10-40 % on average. Exceptional values of up to 90 % are reached in small (<2 mm), grey aggregates composed of mainly centric and pennate diatoms (*Nitzschia* spp., *Thalassionema* spp., *Chaetoceros* spp.) accreted by *Chaetoceros* spines. These aggregates were restricted to the ice and snow surface and are probably due to redistributional processes during melting and freezing. An unicellular organism (most probably *Chlamydomonas nivalis*) containing bright red to orange pigment bodies and showing a high relief - also described in THIEDE et al. (1987)- is quite common in the surface and subsurface sediments. However, it is not found in deep sea sediments (BRASS pers. com.). In contrast, still unidentified brown pollen, which are restricted to iceberg surfaces, have, at least once, been recognized in the deep sea sediment (BRASS pers. com.).

The composition of the biogeneous components (e.g. benthic foraminifers, benthic diatoms) points to a marine source area of the "dirty ice" sediments. The appearance of rounded quartz with a maximum of abundance in the core of the Transpolar Drift may raise the assumption that large parts of the sea ice sediments are fluvially transported material from large river systems in Siberia. However, the absence of larger amounts of feldspar and the restriction to fine grain sizes rather indicates reworking and redistribution processes on shelf areas near to river mouths before being incorporated into the sea ice by suspension freezing or related processes.

4. OCEANOGRAPHIC INVESTIGATIONS

4.1 Determination of Deep Water Renewal Times Using ^{14}C and ^{39}Ar Measurements (B. Kromer, A. Ludin, M. Meder and P. Schlosser)

Background

The natural component of ^{14}C (half life 5730 years) and ^{39}Ar (half life 269 years) are both produced by interaction of cosmic radiation with gas molecules in the atmosphere from where they enter the surface waters of the oceans by gas exchange. Along the pathway from the surface of the oceans through the deep basins, a certain fraction of the ^{14}C and ^{39}Ar atoms decays leading to a concentration difference between surface and deep waters. This concentration difference can be measured and converted into mean residence times of the deep waters. In the case of ^{14}C the modern surface concentrations have to be corrected because the natural ^{14}C component of waters ventilated during the past two to three decades has been changed by the so-called bomb ^{14}C . The bomb ^{14}C was produced mainly during the early 1960s by elevated neutron fluxes in the atmosphere due to surface tests of nuclear weapons. However, using pre-bomb ^{14}C measurements and tritium data, the pre-bomb oceanic ^{14}C distribution can be determined with a reasonable precision.

Being a noble gas not participating in chemical reactions, ^{39}Ar has a much simpler

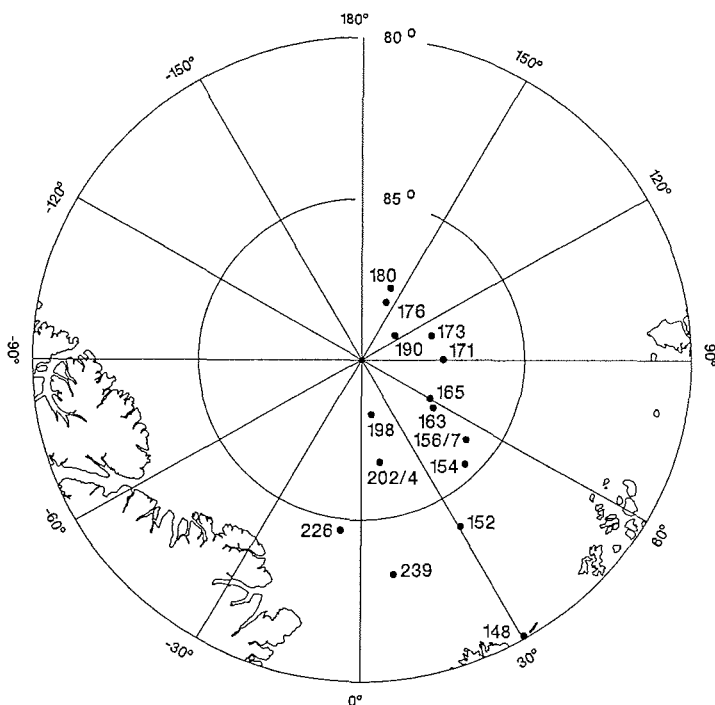


Fig. 4.1-1: Location map of large volume oceanography sampling sites.

boundary condition than ^{14}C and therefore is principally better suited for studies of deep water renewal times in the ocean. However, the extremely low concentrations of ^{39}Ar in seawater require large amounts of water and long counting times for precise measurements. Therefore, ^{39}Ar data are presently mostly used to 'calibrate' the ^{14}C data. For this purpose ^{39}Ar data are only obtained for the characteristic water masses while ^{14}C is sampled on a relatively dense grid (a typical ratio of ^{14}C to ^{39}Ar samples is of the order of 10 to 20).

The first ^{14}C samples of the Arctic Ocean were collected on drifting ice stations imposing considerable logistical constraints (OESTLUND et al. 1987). The first extensive data set for the Arctic Ocean was obtained on the 1987 *Polarstern* section across the Nansen Basin (SCHLOSSER et al. 1990). Before the ARCTIC '91 expedition, no ^{14}C data existed for the Amundsen Basin and the deep Makarov Basin was covered by only two data points (OESTLUND et al. 1987).

	Date	Latitude	Longitude	Number of Samples	Depth Range (m)
148	08-04-91	N 80-05	E 30-19	4	50-200
152/1	08-08-91	N 83-59	E 30-28	10	2260-4000
152/2	08-08-91	N 83-58	E 30-24	10	50-1900
154/1	08-11-91	N 85-27	E 44-28	10	1700-3800
154/2	08-11-91	N 85-27	E 44-23	6	50-1540
156	08-12-91	N 85-56	E 52-20	10	2500-3900
157	08-13-91	N 86-14	E 59-24	10	50-2300
163	08-17-91	N 87-20	E 55-56	10	300-4150
165/1	08-17-91	N 87-34	E 60-14	10	2400-4190
165/2	08-18-91	N 87-35	E 60-27	10	25-2200
171/1	08-22-91	N 87-30	E 90-07	10	2900-4400
171/2	08-22-91	N 87-29	E 91-49	10	50-2500
173/1	08-25-91	N 87-44	E 109-21	10	2600-4400
173/2	08-25-91	N 87-47	E 108-16	10	50-2400
173/3	08-26-91	N 87-47	E 108-08	3	1960-3740
176/1	08-28-91	N 88 -00	E 159-04	10	2500-4000
176/2	08-28-91	N 88-00	E 158-30	10	50-2200
180	08-31-91	N 87-36	E 158-25	10	1960-3040
190/1	09-05-91	N88-45	E 127-06	10	2400-3800
190/2	09-05-91	N 88-46	E 127-44	10	25-2100
198/1	09-10-91	N 88-16	E 10-07	6	2800-4300
198/2	09-10-91	N 88-15	E 08-37	10	25-2500
202	09-11-91	N 86-45	E 10-00	10	2700-4200
204	09-12-91	N 86-36	E 07-20	10	25-2400
226	09-21-91	N 84-38	W 06-44	11	3000-4000
239	09-25-91	N 83-15	E 08-36	11	2000-4000

Table 4.1-1: List of large volume sampling stations for ^{14}C and ^{39}Ar investigations

Sampling Program

During ARCTIC'91, we collected 241 ^{14}C and 14 ^{39}Ar samples on 17 stations (Tab. 4.1-1 and Fig. 4.1-1). Additionally, we collected 11 surface water samples between stations. The measurements of these samples will be part of a large integrated tracer data set collected in a joint international effort on both *Polarstern* and *Oden*. At most of the stations we obtained ^{14}C samples from 16 depth levels. We collected samples in the Nansen, Amundsen and Makarov basins with the highest spatial resolution in the Amundsen Basin (see Fig. 1.1-2). Samples from the Makarov Basin were obtained at two stations located close to the Lomonosov Ridge. We further collected 24 water samples (volume of 100 liters each) for shore based analysis of radionuclides at the University of Lund.

^{14}C samples were collected using stainless steel Gerard-Ewing water samplers (volume of 270 liters). Sample quality was checked by measuring temperature, salinity and the thermometric depth. The deepest sample at each station was usually collected about 20 meters above the sea floor (controlled by a pinger record). The water samples were acidified to pH2 and degassed in a dynamically operated vacuum extraction system (flow rate of 6 l of water per minute). During gas extraction, the water samplers were held at a slight nitrogen overpressure to avoid contamination with air. The CO_2 contained in the extracted gases was absorbed in 400 ml sodium hydroxide for shore based radiometric analysis of the ^{14}C concentration at Heidelberg. At 11 of the stations the remaining gases of some of the samples were collected in stainless steel containers for radiometric measurements of the ^{39}Ar concentration at Bern. For each ^{39}Ar sample the water of five water samplers was required. The wire length between these samplers was set to 20 m.

4.2 Distribution of Natural Radionuclides in the Water Column (J. Scholten and A. Michel)

Natural radionuclides can be used to trace geochemical pathways in the oceans. Most of the natural radionuclides are produced in the seawater by radioactive decay of the homogeneously distributed uranium. Some of these radioactive daughter products are particle reactive. They are adsorbed onto particle surfaces and removed from the water column. This scavenging process can be quantified by comparison of the production rate of a radionuclide with its concentration measured in the seawater. The resulting scavenging rate is mainly controlled by the particle flux through the water column. Low rates are observed in areas with low particle concentrations.

Another parameter which can influence the radionuclide distribution are water masses with long residence times. In combination with low scavenging rates they may cause an accumulation of particle reactive radionuclides in the water column and a transport towards areas with higher particle flux.

Since particle reactive radionuclides are incorporated into the sediments, it is possible to determine the particle flux from the radioactive ratios stored in the sediment record. This gives further informations on the paleoenvironment in the geological past.

The ARK VIII/3 cruise of *Polarstern* offered an opportunity to sample for the investigation of the distribution of dissolved and particulate natural radionuclides in the water column and sediments of the Nansen, Lomonosov and Makarov basins. From the determination of the radionuclides ^{234}Th , ^{232}Th , ^{230}Th , ^{228}Th , ^{228}Ra , ^{226}Ra , ^{210}Po , ^{210}Pb and the cosmogenic ^{10}Be in the seawater and in surface sediments we attempt to establish the present relationship between particle flux, water masses and scavenging rates. Furthermore, we want to find out, if there is an advective transport of radionuclides in the Arctic Ocean towards areas with high particle flux, e.g. Fram Strait.

In order to measure natural radionuclides in seawater, large volumes of water are required. We deployed battery powered *in situ* filtration pumps. They consist of a filter housing with a 1 μm nuclepore filter (diameter 293 mm) followed by two Mn-coated adsorbers on which the dissolved radionuclides are extracted. For the calibration of the adsorbing efficiency and for the determination of ^{234}Th , ^{210}Po and ^{210}Pb Gerard-Ewing bottles with a volume of 270 l were deployed above the *in situ* filtration pumps.

One cast consisted of six *in situ* filtration pumps in conjunction with six Gerard-Ewing bottles in depth intervals, which were previously selected by CTD data. Two casts were run in the Nansen Basin, three in the Amundsen Basin and one cast in the Makarov Basin (Tab. 4.2-1). At each station the pumping time was 2.5 hours and the filtered volumes varied between 500 liter in surface waters and 1,700 liter in mid-water depth. In total 42.3 m³ of seawater was filtered with the *in situ* pumps and 16.2 m³ were sampled with the Gerard-Ewing bottles.

On the Gakkel Ridge, a shallow cast covering the upper 300 m of the water column was run using only the Gerard-Ewing bottles. Additional surface water samples were obtained on a transect from the Nansen Basin to the Makarov Basin. For the determination of nutrients, salinity and oxygen subsamples were taken from all deployed Gerard bottles. On each station where a cast was made, sediment samples were recovered using a multicorer (MUC).

Station	Date	Latitude	Longitude	Depth Range	Remarks
19/150	6.8.91	81 47.5 N	30 12.3 E	10	GWS surface sample
19/150	6.8.91	81 45.4 N	29 57.9 E	300	ISP test
19/152	9.8.91	83 58.5 N	30 24.8 E	10-3890	GWS + ISP
19/162	16.8.91	86 50.7 N	56 48.7 E	10-300	GWS
19/165	18.8.91	87 34.4 N	60 23.1 E	10-4300	GWS + ISP
19/170	21.8.91	87 29.7 N	79 53.6 E	10	GWS surface sample
19/171	22.8.91	87 30.1 N	89 58.7 E	10	GWS surface sample
19/172	23.8.91	87 33.4 N	103 26.8 E	10	GWS surface sample
19/173	25.8.91	87 45.2 N	108 59.1 E	10-4220	GWS + ISP
19/174	26.8.91	87 47.0 N	108 08.5 E	10	GWS surface sample
19/175	27.8.91	88 02.2 N	134 55.7 E	10	GWS surface sample
19/176	28.8.91	88 00.0 N	158 51.8 E	10-3850	GWS + ISP
19/208	13.9.91	86 09.0 N	5 05.6 E	50-4180	GWS + ISP
19/239	26.9.91	83 13.9 N	8 36.4 E	50-3910	GWS + ISP

Table 4.2-1: List of radionuclide stations. GWS = Gerard-Ewing bottles ISP= *in situ* filtration pumps.

The seawater sampled with Gerard-Ewing bottles was filtrated over pre-weighed 1 µm nuclepore filter (diameter 142 mm). For determination of the dissolved radionuclides approximately 20 l of the filtrate were filled in plastic containers. The Mn-adsorbers of the *in situ* filtration pumps were leached and a further chemical purification was performed on-board using standard ion exchange procedures. Similar chemical treatment was done with the filtrate of the Gerard-Ewing bottles. Finally, Th-isotopes, ^{210}Po and ^{231}Pa were plated on silver disks, which will be counted for their radioactivities in the home lab. The particulate radionuclides on the nuclepore filters will be analysed on-shore. The ^{10}Be -analyses will be performed together with M. Segl (University of Bremen).

The water samples obtained will allow us to study the interplay among particle flux, water circulation and scavenging rates in the Arctic Ocean. Furthermore, the investigations of radionuclides in the sediments will show to what extend scavenging processes in the water column are stored in the sediments.

5. BIOLOGICAL INVESTIGATIONS

5.1. Bird and Mammal Counts (H. Eicken and R. Gradinger)

In continuation of work conducted by Joiris and coworkers during the previous two legs of the ARK-VIII expedition of *Polarstern*, birds and mammals were counted during the cruise.

Two different approaches to counting were taken. From August 2 to 26 and from September 30 to October 6, a total of 51 30-minute observations was conducted from the ship's bridge up to three times a day. In accordance with international guidelines, those birds entering into a 300-m corridor to either side of the ship were counted. Notes were taken on whether birds followed, crossed or rested in the ship's path. Wherever possible, particulars such as the ratio between juveniles and adults were recorded as well.

The occurrence of mammals was noted independent of the distance to the ship. Between August 27 and September 29 the extremely low numbers of birds and mammals encountered justified a modified counting procedure. Thus, birds or mammals observed during the ice watch conducted at two-hour-intervals while under progress (effectively 10-minute time intervals) were counted, as well as those observed during station work on the ice.

Table 5.1-1 indicates the number of birds of different species counted during the 30-minute intervals. The latitudinal distribution of the total number of birds counted during each observation is indicated in Figure 5.1-1 for the tracks going in and out of the ice. Clearly, the number of birds drops off sharply on the entering the ice. At the same time, a shift in species composition can be observed, with Auks decreasing in numbers and Ivory Gulls (*Pagophila eburnea*) particularly abundant in the marginal ice zone. The trend exhibited towards higher latitudes is representative of all observations made during the middle part of the cruise. For the entire track covered within the closed pack ice between August 5 and September 29, a total of 90 birds had been observed, with Fulmar (*Fulmarus glacialis*),

Species	Total Number Counted
<i>Rissa tridactyla</i>	Kittiwake 493
<i>Pagophila eburnea</i>	Ivory Gull 88
<i>Larus sabini</i>	Sabine's Gull 2
<i>Larus hyperboreus</i>	Glaucous Gull 3
<i>Larus glaucoides</i>	Iceland Gull 3
	Unident. Gull 15
<i>Fulmarus glacialis</i>	Fulmar 332
<i>Stercorarius longicaudus</i>	Long-tailed Skua 16
<i>Stercorarius pomarinus</i>	Pomarine Skua 15
<i>Stercorarius skua</i>	Great Skua 5
<i>Sterna paradisaea</i>	Arctic Tern 9
<i>Uria aalge</i> and	Common Guillemot and
<i>Uria lomvia</i>	Brünnich's Guillemot (total) 69
<i>Alle alle</i>	Little Auk 54
<i>Cephus grylle</i>	Black Guillemot 44
<i>Fratercula arctica</i>	Puffin 14
<i>Alca torda</i>	Razorbill 4
	unident. Auk 52
	unident. Duck 2
<i>Sylvia atricapilla</i>	Blackcap 1
Total	1221

Table 5.1-1: Total number of birds observed during 51 30-minute observations.

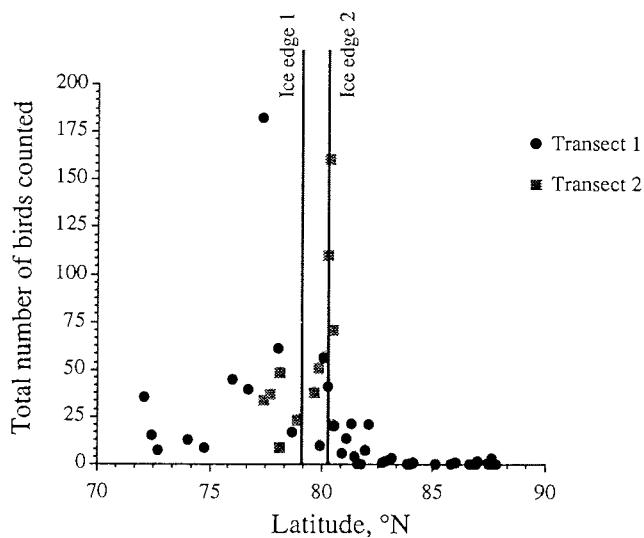


Fig. 5.1-1: Total number of birds counted during 51 30-minute intervals entering the ice on August 4 (ice edge 1 on transect 1, cf. map of cruise track) and leaving it on September 30 (ice edge 2 on transect 2).

Kittiwake (*Rissa tridactyla*) and Sabine's Gull (*Larus sabini*) accounting for 70 observations, many of which may represent duplicate countings due to birds following the ship over larger distances. This paucity in bird life contrasts with the rich fauna observed within and under the ice, most conspicuous of which are the numerous sightings of polar cod thriving in melt holes and melt puddles within the ice.

The total number of mammals observed, including counts outside of proper sampling intervals amounts to 36. This includes the sporadic sighting of 16 unidentified seals mostly in the marginal ice zone and a group of 11 humpback whales (*Megaptera novaeangliae*) encountered at 77° 23' N, 30° 19' E. A total of 9 polar bears (*Ursus maritimus*) was observed, with a sighting as far north as 88° 53' N, 144° 05' E.

5.2. Plankton (H. Eicken and R. Gradinger)

The large scale distribution of the high Arctic pico- and nanoplankton was studied using two approaches. First, the phytoplankton standing stock was continuously measured using a Turner Design fluorometer (equipped with a continuous flow cuvette), which was connected to the water pumping system of *Polarstern* (sampling depth 8 m). The *in situ* chlorophyll-a fluorescence was recorded as 15 min averages with a Li-COR Data Logger 1,100. Discrete samples were taken every day for later nutrient analysis and calibration of the fluorometer. The abundance of the pico- and nanoplankton was directly determined by means of epifluorescence microscopy.

Figure 5.2-1 shows one example of the *in situ* fluorescence readings. Along the shown track a distinctly higher algal biomass was observed south of 86° N together with high cell counts of diatoms, while in the northern part up to the North Pole, the lower biomass was nearly entirely formed by autotrophic pico- and nanoplankton. A comparison of the diatom species composition found in the ice and in the pelagial is needed to find out whether the diatoms originated from melting ice floes or if they grew in the water column.

In combination with the continuous-flow fluorometry and in continuation of a program conducted by Joiris and coworkers (Free University of Brussels, Belgium) during the previous two legs of the *Polarstern* ARK-VIII expedition to study the enrichment of pollutants within polar organisms, plankton was continuously concentrated from the surface water during the entire cruise. This was achieved by passing unfiltered seawater taken in at the ship's bow into a separator. Every three to four days the residue which had accumulated in the base retainer and the stack bowls was collected and kept frozen at -30° C for further analysis (approx. 20 samples). Similarly, surface sediment accumulations were collected for pollutant analysis as well.

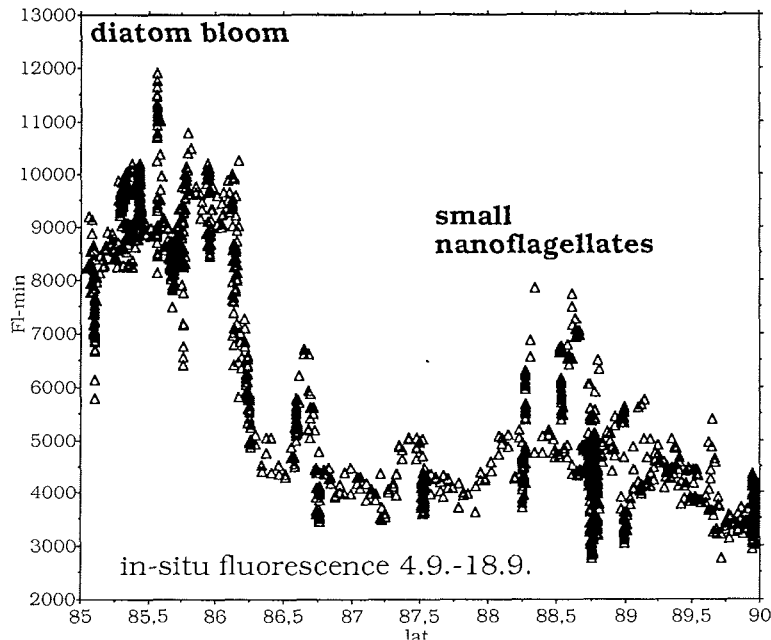


Fig. 5.2-1: *In situ* chlorophyll fluorescence (FI-min, relative units) measured during the period of September 4 through September 18, 1991.

5.3 Benthos (I. Kröncke)

The main benthological subject was to quantitatively sample the macro- and meiofauna along the continental slope and at topographic highs but especially in the deep basins of the high Arctic. Since this region has insufficiently been investigated until now we were interested in the structure and biomass distribution of the benthic communities.

Another topic was to determine how far Atlantic species have spread by submergence into the deep basins and the percentage of endemic species in the basins. The feeding structure of the communities is another interest. As food is limited in the abyssal basins under the ice, the organisms might have developed special mechanisms to survive with a minimum of food.

Sampling

In total 49 stations covering Nansen Basin (8), Gakkel Ridge (7), Amundsen Basin (13), Lomonosov Ridge (10), Makarov Basin (2), Morris Jesup Rise (6) and Yermak Plateau (5) were sampled with a 0.25 m² box core (Tab. 5.2-1). Macro-fauna samples were taken out of the box core with a subsampler of 0.02 m². Meio-fauna was sampled out of the box core using tube cores or separately with the multicorer (24 stations, Tab. 5.2-1). Sampling for pigments, ATP and biogeoche-

<u>Stat.No. - Area</u>	<u>Gear</u>	<u>Samples</u>
PS2156 - Svalbard Shelf	GKG	Macro, Meio, P, ATP, B, S
PS2157 - Nansen Basin	GKG, MUC	Macro, Meio, P, ATP, B, S
PS2158 - Nansen Basin	GKG	Macro, Meio, P, ATP, B, S
PS2160 - Nansen Basin	MUC	Meio
PS2161 - Nansen Basin	GKG, MUC	Macro, Meio, P, ATP, S
PS2162 - Nansen Basin	GKG	Macro, Meio, P, ATP, S
PS2163 - Gakkel Ridge	GKG, MUC	Macro, Meio, P, ATP, B, S
PS2164 - Gakkel Ridge	GKG, MUC	Macro, Meio, P, ATP, B, S
PS2165 - Gakkel Ridge	GKG, MUC	Macro, Meio, P, ATP, S
PS2166 - Gakkel Ridge	GKG, MUC	Macro, Meio, P, ATP, B, S
PS2168 - Gakkel Ridge	GKG, MUC	Macro, Meio, P, ATP, S
PS2170 - Amundsen Basin	GKG, MUC	Macro, Meio, P, ATP, S
PS2171 - Amundsen Basin	GKG	Macro, Meio, P, ATP, B, S
PS2172 - Amundsen Basin	GKG, MUC	Macro, Meio, P, ATP, S
PS2174 - Amundsen Basin	GKG	Macro, Meio, P, ATP, B, S
PS2175 - Amundsen Basin	GKG	Macro, Meio, P, ATP, S
PS2176 - Amundsen Basin	GKG	Macro, Meio, P, ATP, S
PS2177 - Lomonosov Ridge	GKG, MUC	Macro, Meio, P, ATP, B, S
PS2178 - Makarov Basin	GKG	Macro, Meio, P, ATP, S
PS2179 - Lomonosov Ridge	GKG	Macro, Meio, P, ATP, S
PS2180 - Makarov Basin	GKG	Macro, Meio, P, ATP, S
PS2181 - Lomonosov Ridge	GKG, MUC	Macro, Meio, P, ATP, S
PS2182 - Lomonosov Ridge	GKG, MUC	Macro, Meio, P, ATP, S
PS2183 - Lomonosov Ridge	GKG, MUC	Macro, Meio, P, ATP, S
PS2184 - Lomonosov Ridge	GKG, MUC	Macro, Meio, P, ATP, S
PS2185 - Lomonosov Ridge	GKG, MUC	Macro, Meio, P, ATP, S
PS2186 - Lomonosov Ridge	GKG, MUC	Macro, Meio, P, ATP, S
PS2187 - Lomonosov Ridge	GKG, MUC	Macro, Meio, P, ATP, S
PS2189 - Lomonosov Ridge	GKG	Macro, Meio, P, ATP, S
PS2190 - Amundsen Basin	GKG, MUC	Macro, Meio, P, ATP, S
PS2191 - Amundsen Basin	GKG	Macro
PS2192 - Amundsen Basin	GKG	Macro, Meio, P, ATP, S
PS2193 - Amundsen Basin	GKG, MUC	Macro, Meio, P, ATP, S
PS2194 - Amundsen Basin	GKG	Macro, Meio, P, ATP, S
PS2195 - Amundsen Basin	GKG	Macro, Meio, P, ATP, S
PS2196 - Amundsen Basin	GKG	Macro, Meio, P, ATP, S
PS2198 - Morris Jesup Rise	GKG	Macro, Meio, P, ATP, S
PS2199 - Morris Jesup Rise	GKG	Macro, Meio, P, ATP, S
PS2200 - Morris Jesup Rise	GKG	Macro, Meio, P, ATP, S
PS2201 - Morris Jesup Rise	GKG	Macro, Meio, P, ATP, S
PS2202 - Morris Jesup Rise	GKG	Macro, Meio, P, ATP, S
PS2205 - Morris Jesup Rise	GKG	Macro, S
PS2206 - Gakkel Ridge	MUC	Meio
PS2209 - Nansen Basin	GKG	Macro, Meio, P, ATP, S
PS2210 - Nansen Basin	GKG	Macro, Meio, P, ATP, S
PS2211 - Yermak Plateau	GKG	Macro
PS2212 - Yermak Plateau	GKG, MUC	Macro, Meio, P, ATP, S
PS2213 - Yermak Plateau	GKG, MUC	Macro, Meio, P, ATP, S
PS2214 - Yermak Plateau	GKG, MUC	Macro, Meio, P, ATP, S

mical analysis took part as well. The bacterial biomass was collected on 12 stations along the poleward transect (Tab. 5.2-1).

Preliminary Results

The macrofauna samples were partly sorted on board for 30 stations on the poleward transect. Table 5.2-2 gives a preliminary overview on the macrofauna distribution in the Arctic basins.

The Nansen and the Amundsen basins showed lowest species and individual numbers. Amphipods were the dominant species. Bioturbation was negligible. In the coarse sediments of the Gakkel Ridge the fauna was very poor, on two stations not any life at all was observed.

Area	S / 0.02 m ²	N / m ²	Taxonomic groups
Barents Shelf	17	2950	Polychaeta Ophiuroidea Amphipoda Bryozoa
Nansen Basin	1	150	Amphipoda Polychaeta Porifera
Gakkel Ridge	1	50	Amphipoda
Amundsen Basin	2	150	Amphipoda Holothuroidea
Lomonosov Ridge	3	200	Amphipoda Porifera Polychaeta Bivalvia
Makarov Basin	3	100-150	Amphipoda Porifera Anisopoda Polychaeta

Table 5.2-2: Mean species and individual numbers for the macrofauna sampled on 30 stations along the poleward transect. Samples from Morris Jesup Rise and Yermak Plateau have not been sorted so far.

Along a transect sampled from the Makarov Basin towards the Lomonosov Ridge a more diverse fauna was observed, even the abundance increased especially on shallower stations. Again the Amphipods were the dominant group, followed by Polychaetes and Sponges. Latter ones were found in very high abundance at one station (PS2186) on the slope of the Lomonosov Ridge.

Table 5.2-1: Station list for biological samples from giant box core (GKG) and multicorer (MUC) and sub-samples taken per station (Macro = Macrofauna, Meio = Meiofauna, P = Pigments, ATP, B = Bacteria, S = Sediments).

The macrofauna communities seem to be highly food limited. Most of the species from Nansen and Amundsen basins seem to be of Atlantic origin, only few endemic species were found. For species from the Makarov Basin and the Lomonosov Ridge further identification has to be done.

Samples from the Morris Jesup Rise and the Yermak Plateau have not been sorted yet. However, it can be said that the macrofauna was more diverse and abundant than in the deep basins. On the Yermak Plateau the bioturbation reached down as deep as to 30 cm.

6. GEOLOGICAL INVESTIGATIONS

6.1 Bathymetric Survey with HYDROSWEEP (T. Schöne and T. Döscher)

Continuous bathymetric survey with the multi narrow-beam sounding system HYDROSWEEP was performed during the entire expedition. Main characteristic of HYDROSWEEP is the 90° coverage angle which generates a swath width of twice the water depth underneath the ship. The fan is subdivided into 59 pre-formed beams (PFB) and provides 59 values for the water depths and the offsets. They represent a cross-profile of the sea-floor topography perpendicular to the ship's long axis. The HYDROSWEEP self-calibration process determines automatically a mean sound velocity value, necessary for the correction of the slant sonar beams.

CTD-measurements at the geological stations during the cruise provided supplementary data and information about variations of the water column. A good agreement between the mean sound velocity values from CTD and HYDROSWEEP was observed during the bathymetric survey in the Fram Strait.

The post-processing of multi-beam bathymetric data requires precise ship's positioning and heading. Satellite based systems, Global Positioning Systems (GPS) and Navy Navigation Satellite System (NNSS) TRANSIT, are used together with dead-reckoning for positioning with the integrated navigation system INDAS. Precise bathymetric charting from multi-beam sonar measurements in the deep sea requires position accuracies of ± 100 m, the heading measurements must be better than $\pm 2^\circ$. During the cruise raw navigation data from the INDAS-system was checked for satellite fix-offsets and corrected. The analysis and correction of Doppler Sonar data was very difficult and time consuming, due to large errors, which were caused by forward and backward steaming during ice-breaking. Heading measurements was adulterated by typical gyro compass errors in high latitudes. Both, speed and heading errors, led to incorrect ship's positions. North of 87° N the navigation of *Polarstern* was only possible with the GPS-receiver. Most of the heading data from the gyro compass, used for the orientation of the multi-beam sonar fan, are wrong. However, post-processing of multi-beam sonar measurements should be possible with reduced accuracy from GPS-data. The updated ship's positions were supplied as the final data set to all working groups on board.

The bathymetry program during the expedition covered in general three different types of survey:

- 1) Single multi beam sonar profiles during the transits between ship's stations.
- 2) Small box pre-site surveys for the creation of large scale maps in areas of proposed sampling points, moorings or ODP-sites.
- 3) Box surveys in the Fram Strait adjacent to multi beam surveys of previous expeditions.

Again this expedition has proved that HYDROSWEEP and PARASOUND measurements are excellent tools for the detection and selection of geological sampling stations. A multi beam pre-site survey of a mooring or sample station and their vicinity provides invaluable information about local effects of the surrounding topography. In addition, bathymetric data are essential to interpret gravity anomalies and seismic profiling data. The three-dimensional information supplied by multi-beam systems are very important for bathymetric charting and the interpolation of contour lines in areas with rare data. The first analysis of the HYDROSWEEP data indicate that more than 75% of the recorded data even under severe ice conditions can be used for the post-processing. In regions with little ice-coverage more than 85% of the measurements should be useful.

The first part of the leg crossed the Barents Sea, the continental slope northeast of Svalbard, and the Nansen Basin. The data of the continental slope were pre-processed and a digital terrain model (DTM) of the sea-floor was determined. Fig 6.1-1

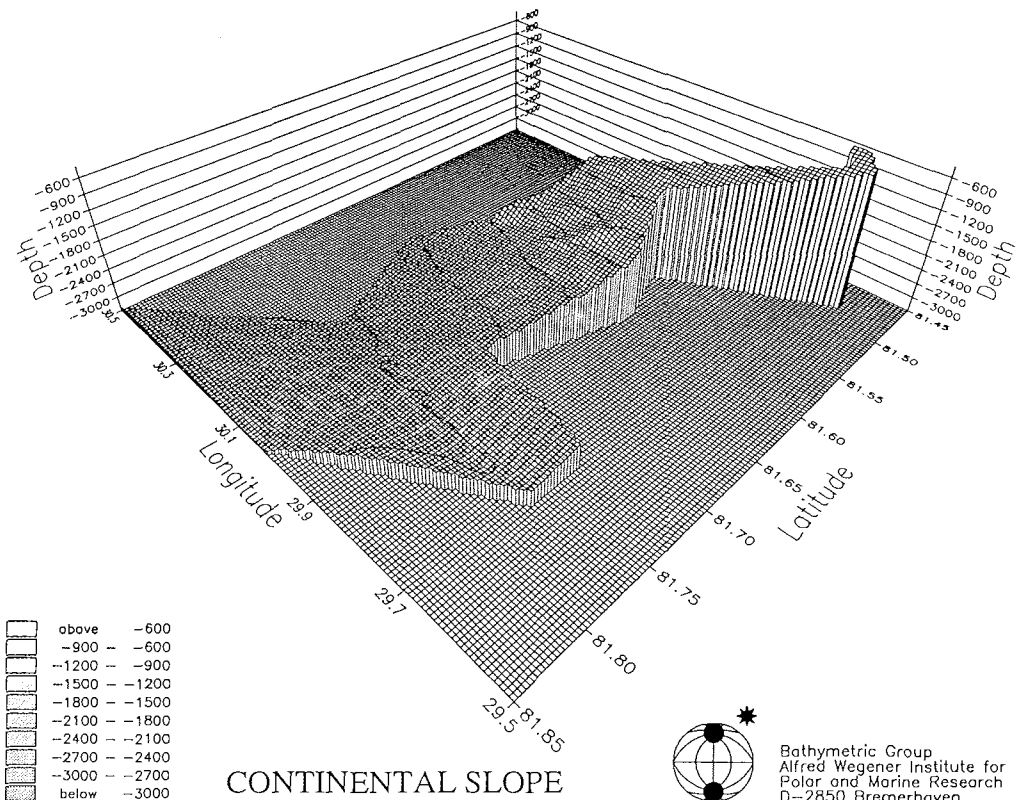


Figure 6.1-1: Continental slope northeast of Spitsbergen (from Southeast).

indicates that the slope north of Svalbard is not smooth, but shows specific topographic structures especially in the steepest area. The bathymetry of the continental slope reveals depths from 300 m to 3,100 m with an inclination of 7° in its central part and 4° in the deeper area. Then the sea bottom gently slopes into the Nansen Basin with a mean water depth of 4,000 m.

Heading north, the mid-ocean Gakkel Ridge was crossed perpendicular to its axis. The sea-floor rises here from 3,800 m to 1,100 m. The depth profile displays deep valleys striking parallel to the ridge axis. These valleys reach depths between 3,000 m and 4,500 m with maximum slopes of 11°. The central rift valley has a mean water depth of 4,700 m. The profiling perpendicular to the ridge was terminated in the abyssal plain of the Amundsen Basin at a depth of 4,400 m.

Approaching the Lomonosov Ridge at 87° 55' N, 115° E the sea-floor first rises from 4,300 m to 2,700 m, then it forms a plateau at 3,000 m. East of this plateau is a steep rise to 1,500 m, followed by a smooth rise to the ridge at top of 1,040 m. During the cruise the Lomonosov Ridge was crossed three times between 87° 35' N, 129° E and 88° 5' N, 160° E. A profile along the crest was carried out northwards up to 89°10' N. It opens a general overview of the bathymetry in this area. The ridge

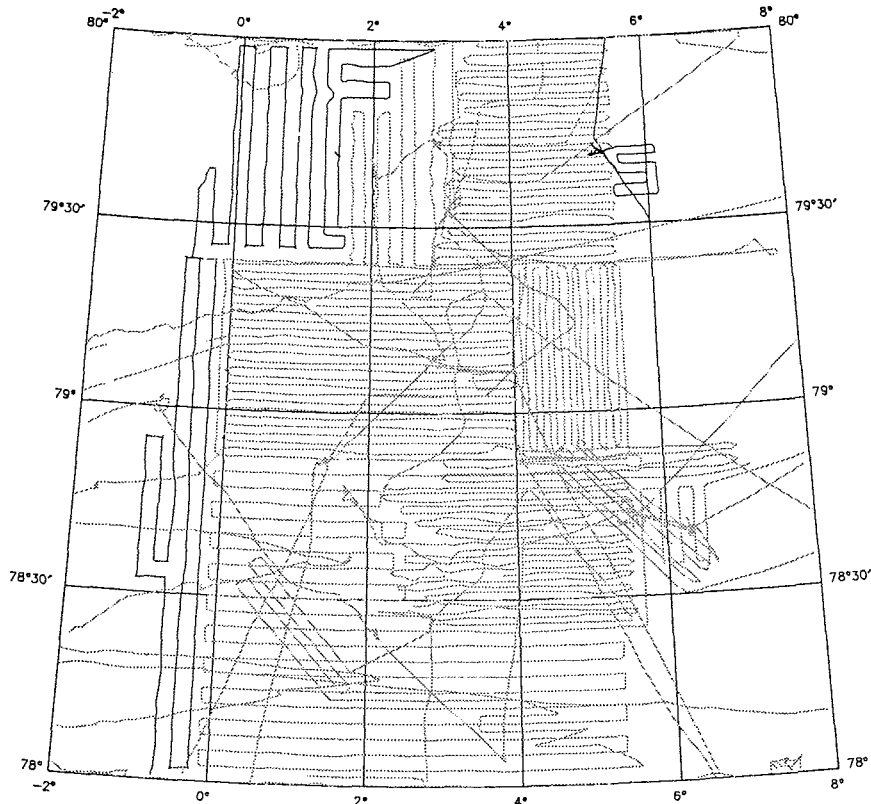


Figure 6.1-2: Bathymetric survey tracks covered by RV *Polarstern* in the Fram Strait area.

strikes north-south and decreases on its eastside towards the Makarov Basin to a depth of 4,000 m.

The northernmost profile reveals at 88° 30' N a change of the slope direction to SW-NW striking. At the eastern slope quite regularly undulating isobaths were manifested by HYDROSWEEP.

In the North Pole region the Amundsen Basin reaches a depth of about 4,300 m. No significant topographic features were observed in this region. At the positions 87° 30' N, 10° E and 87° 3' N, 10° E two topographic features at 3,500 m and 3,400 m were located. A plateau of 3,900 m striking NE-SW at 86° 52' N, 10° E was followed by a series of plateaus approaching the Gakkel Ridge from 86° 25' N, 10° E to 86° 5' N, 3° E, all with the same direction of strike and with average depth between 3,000 m and 3,500 m.

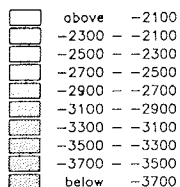
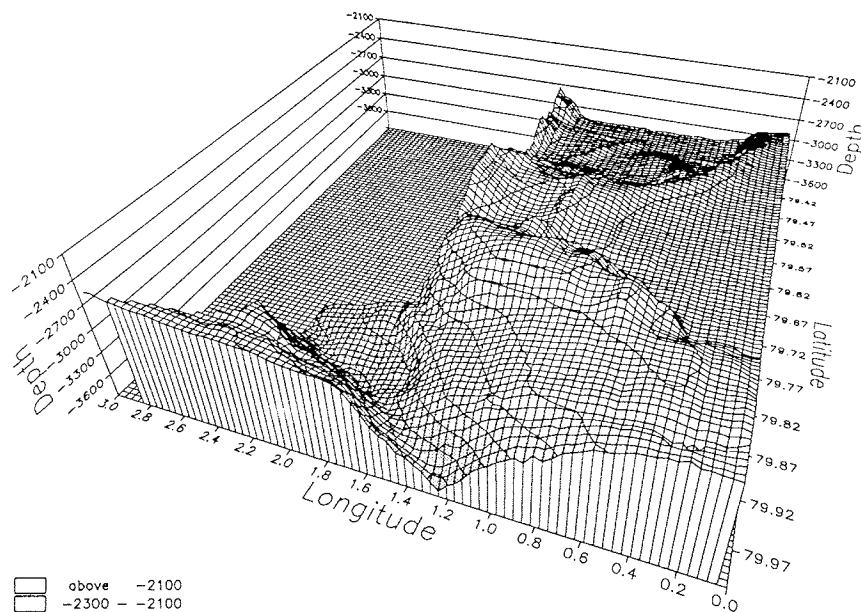
The Morris Jesup Rise was crossed twice on different profiles. This submarine plateau is characterized by a steep NE slope (inclination of 20°) from 3,900 m to 1,300 m water depth. This slope was found more to the east than charted in existing maps. Then the ridge rises slowly to 900 m at the top. The northwestern flank (inclination of 6°) only was surveyed to a depth of 2,200 m, still showing a steep sloping to the Amundsen Basin.

At the western part of the Gakkel Ridge, the shallowest point adjacent to the rift valley, was recovered at 1,800 m depth. HYDROSWEEP profiling at the 4,300 m contour line of the rift valley was performed for 15 nm in NE-SW direction. At 84° 4' N, 0° 30' E the rift valley is displaced 5 nm towards NW indicating a relatively young transform fault.

Southeast of the Gakkel Ridge the sea-floor topography also presents deep valleys, ranging between 2,800 m and 3,800 m. The ascent to the Yermak Plateau starts at a water depth of 4,000 m, is characterized by a steep slope with inclinations up to 13°, which are interrupted by larger plateaus. The minimum depth at the Yermak Plateau is 560 m.

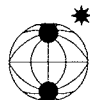
At the end of the cruise a bathymetric survey in the Fram Strait was performed (Fig. 6.1-2). Due to favourable ice conditions it was possible to cover the area between 79° 24' N, 0° E and 80° N, 3° E. One box survey comprises profiles of a total length of 390 nm which covers an area of approximately 900 nm². This area includes the central part of the Spitsbergen Fracture Zone together with its trench and southwest ridge (Fig. 6.1-3).

A second box survey consists of long profiles of 80 nm, west of previous surveys by SEABEAM and HYDROSWEEP. The total profile length of this box was 300 nm, with a covered area of about 800 nm². During this box survey it was possible to complete the mapping of the Hovgaard Fracture Zone area, which terminates at 78° 52' N, 01° 10' W. North of it, a small ridge with depths between 2,600 m and 2,400 m is located. Topographic variations were also found further to the west. The survey boxes will be linked to the sonar measurement of previous *Polarstern* cruises for the compilation of the Bathymetric Fram Strait Atlas.



PART OF SPITSBERGEN FRACTURE ZONE

ARK VIII/3
03.-04.10.1991



Bothymetric Group
Alfred Wegener Institute for
Polar and Marine Research
D-2850 Bremerhaven

Figure 6.1-3: Morphology of the Spitsbergen Fracture Zone (viewed from Northwest)

6.2 PARASOUND-Sedimentechography (U. Bergmann)

During cruise ARK-VIII/3, the PARASOUND sediment echosounder provided a continuous 24 h-record along the ship's track to document sedimentary features below the sea bottom and to indicate suitable coring locations.

In addition to the conventional black and white paper recordings of the sediment features with the survey echosounder DESO 25, the PARADIGMA data acquisition system allows for recording of digital sediment echograms onto a hard disk on a PC (V. Spieß, Universität Bremen). The DESO 25 works with a constant water velocity of 1500 m/sec and displays a vertical section of the sea sub-bottom on a monitor. This window was set to 200 m equivalent to a record length of 266 msec. The time interval between each stored digital sediment echogram was 10 sec at a sampling frequency of 40 kHz. A backup of the hard disk (143 Mb) to a 9 and 1/2 inch tape was made every 24 hours.

At the beginning of the cruise poor records of the continental slope north of Nordaustlandet were received since the slope was too steep for the PARASOUND system. This system works in a frequency range of 2.5 to 5.5 kHz with a beamwidth

of approximately 4°. The beam's footprint on the sea bottom is about 7 % of the waterdepth. Therefore, a high resolution image of the morphology and the sub-bottom can be displayed by PARASOUND only if the inclination of a slope is less than about 4°.

Heavy ice conditions also caused data deficits, i.e. air bubbles together with the ice were carried under the transmitter, so that the transmission and/or reception of the signal was interrupted. The quality of profiles across the Gakkel Ridge, Lomonosov Ridge, Morris Jesup Rise and Yermak Plateau were reduced by this effect, too. Nevertheless, it was generally possible to achieve excellent recordings most of the time.

Heading north across Nansen Basin to Gakkel Ridge, a 430 km continuous profile was recorded with an average sub-bottom penetration of the PARASOUND signal of 30 m. The Gakkel Ridge is characterized by steep slopes (maximum inclination 11) so that only poor records were achieved across this area.

The records of Amundsen Basin showed a penetration of about 40 m along a profile length of 180 km. This profile was completed near the Lomonosov Ridge at 87° 51' N, 112° 37' E. Two profiles (Fig. 6.2-1 shows the second one), each about 40 km long, were recorded of the upper part of Lomonosov Ridge. They strike the ridge axis at about 90° and were separated by a short profile of Makarov Basin near the east side of Lomonosov Ridge. In the Makarov Basin the penetration of the acoustical signal amounted to 60 m. As similar to Amundsen Basin and Nansen Basin, the records showed typical acoustically well-stratified deep sea sediment features.

Sailing from the western flank of Lomonosov Ridge over the North Pole to the western spur of Gakkel Ridge (380 km profile length), some erosion channels were observed with depths of about 20 m between 89° 52' N, 48° 30' W and 89° 31' N, 19° 26' W. Acoustically well-stratified sediments, similar to that of Lomonosov Ridge, were recorded at Morris Jesup Rise at waterdepths below 1000 m but a change to a rough bathymetry appeared in a water depth of about 950 m (Fig.6.2-2). The Yermak Plateau was crossed by various tracks and always showed stratified sediment features and a penetration between 10 m and 40 m of the PARASOUND signal in the upper part (Fig. 6.2-3).

To get a regional mapping of sediment features, a box survey was done in the Fram Strait together with the multibeam echosounder HYDROSWEEP. After the box survey in the Fram Strait and a second box survey in the Hovgaard Fracture Zone, a continuous profile in SE direction of the Norwegian continental slope was recorded. It showed gravity flows and also well-established stratifications of the sediments.

The following five figures illustrate some interesting examples of different profiles recorded in the Arctic Ocean.

Figure 6.2-1 displays a profile of Lomonosov Ridge in NE-SW direction perpendicular to the ridge axis between 88° 03' N, 135° 56' E and 88° 02' N, 144° 44' E.

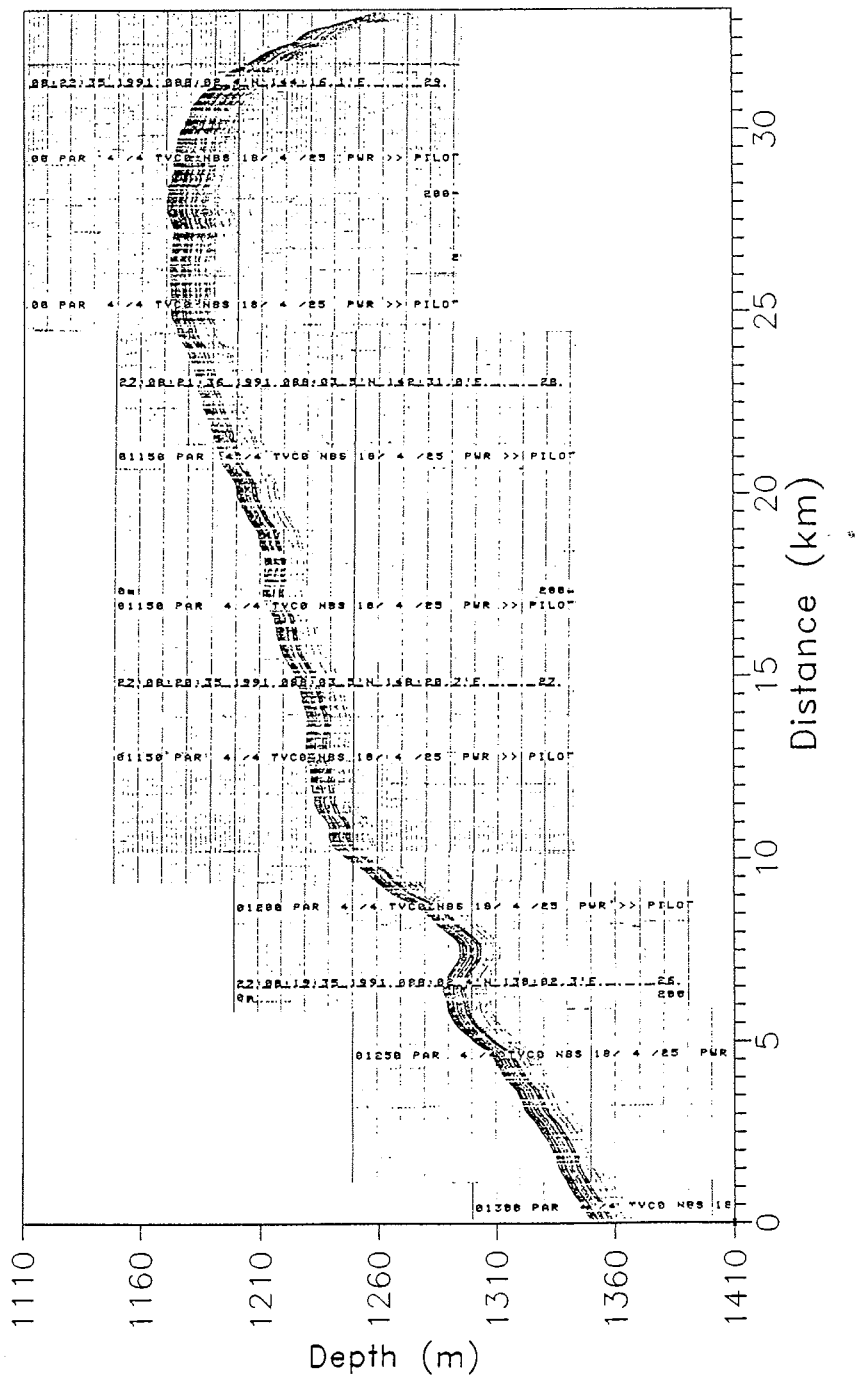


Fig. 6.2-1: Profile in crossing Lomonosov Ridge in NE-SW direction between 88° 03' N, 135° 56' E and 88° 02' N, 144° 44' E.

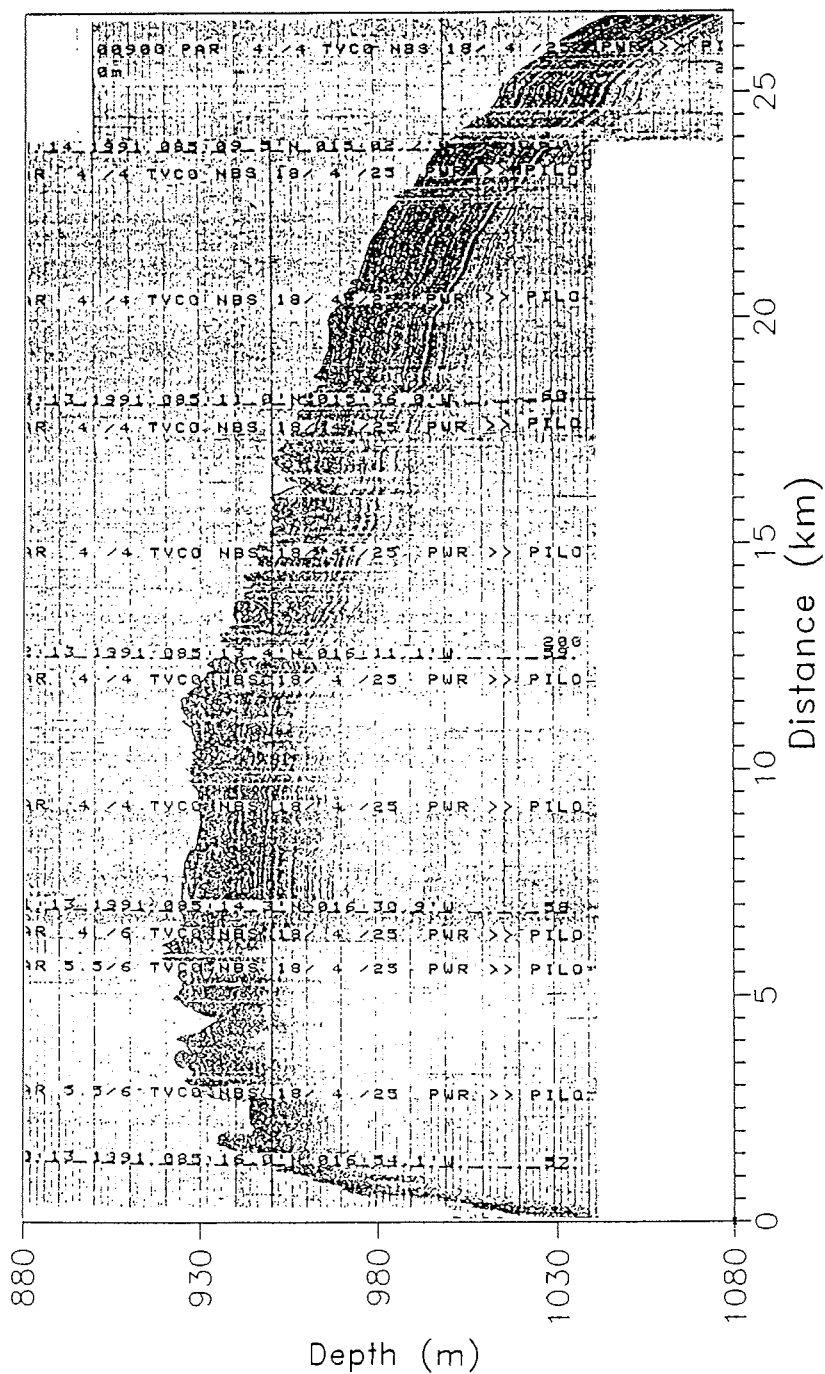


Fig. 6.2-2: Profile on top of Morris Jesup Rise, recorded in NW-SE direction between 85° 16' N, 17° 05' W and 85° 08' N, 14° 38' W.

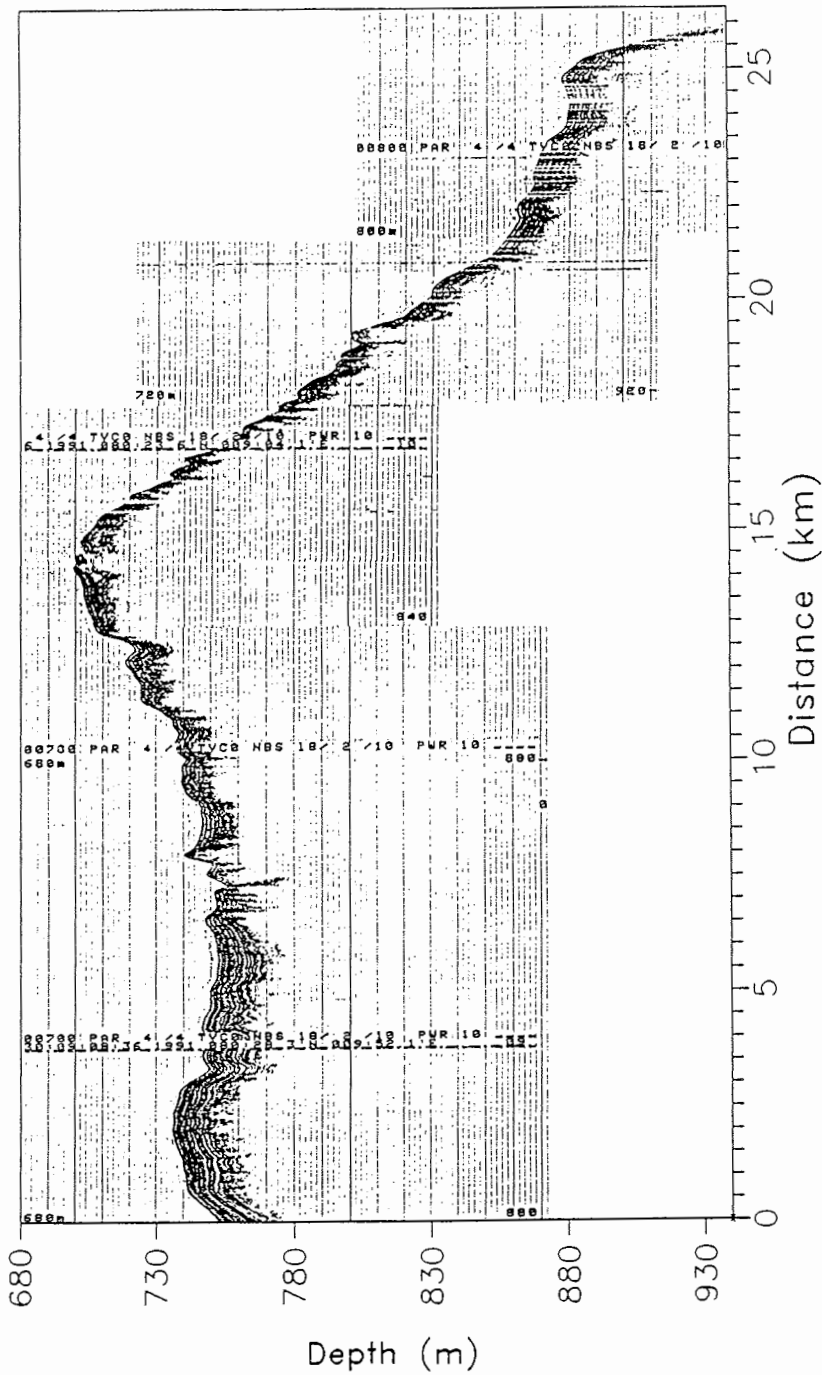


Fig. 6.2-3: Profile in NE-SW direction between 80° 30' N, 10° 07' E and 80° 26' N, 08° 44' E, recorded on top of Yermak Plateau.

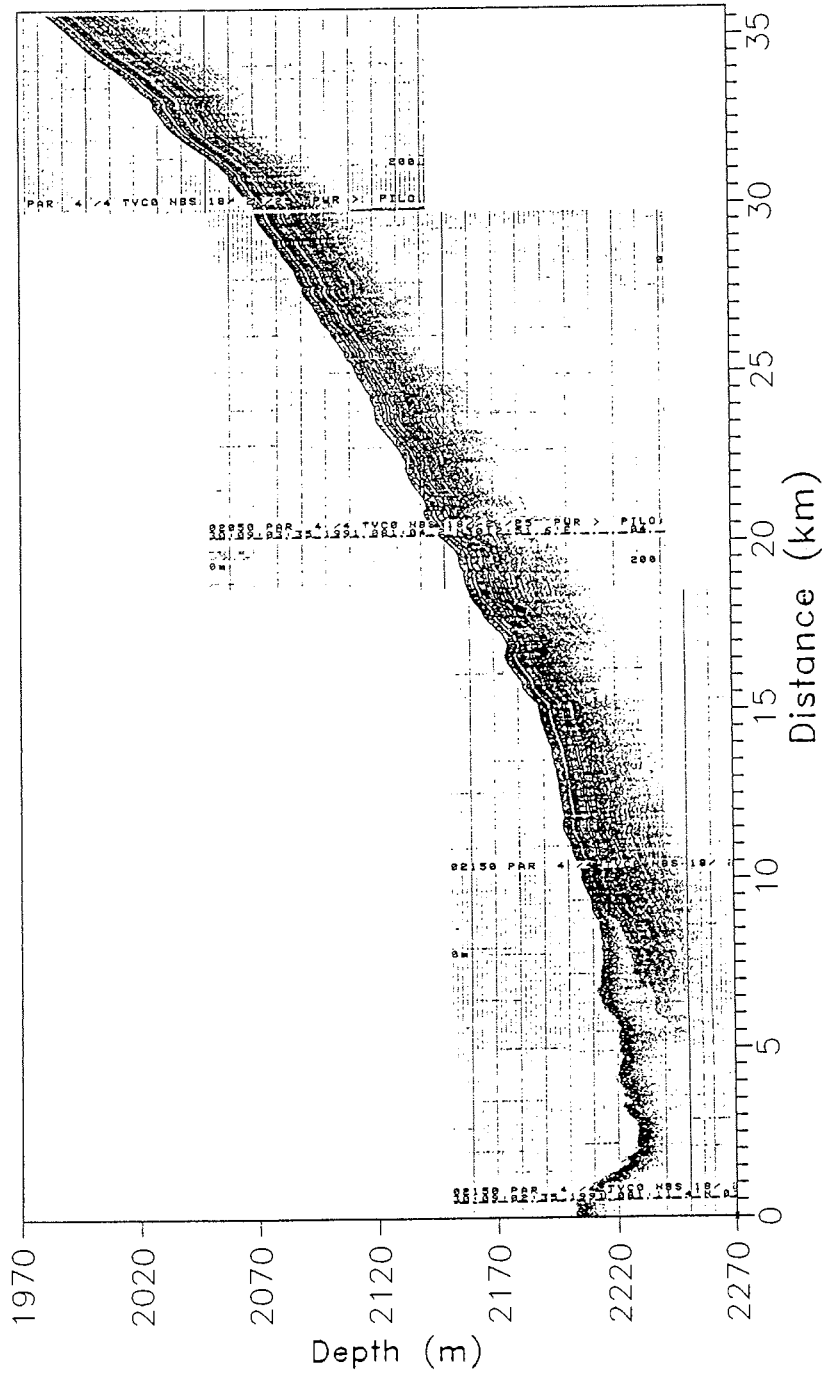


Fig. 6.2-4: Profile crossing the eastern flank of Yermak Plateau, recorded in NE-SW direction between $81^{\circ} 13' N, 13^{\circ} 04' W$ and $80^{\circ} 58' N, 12^{\circ} 16' W$.

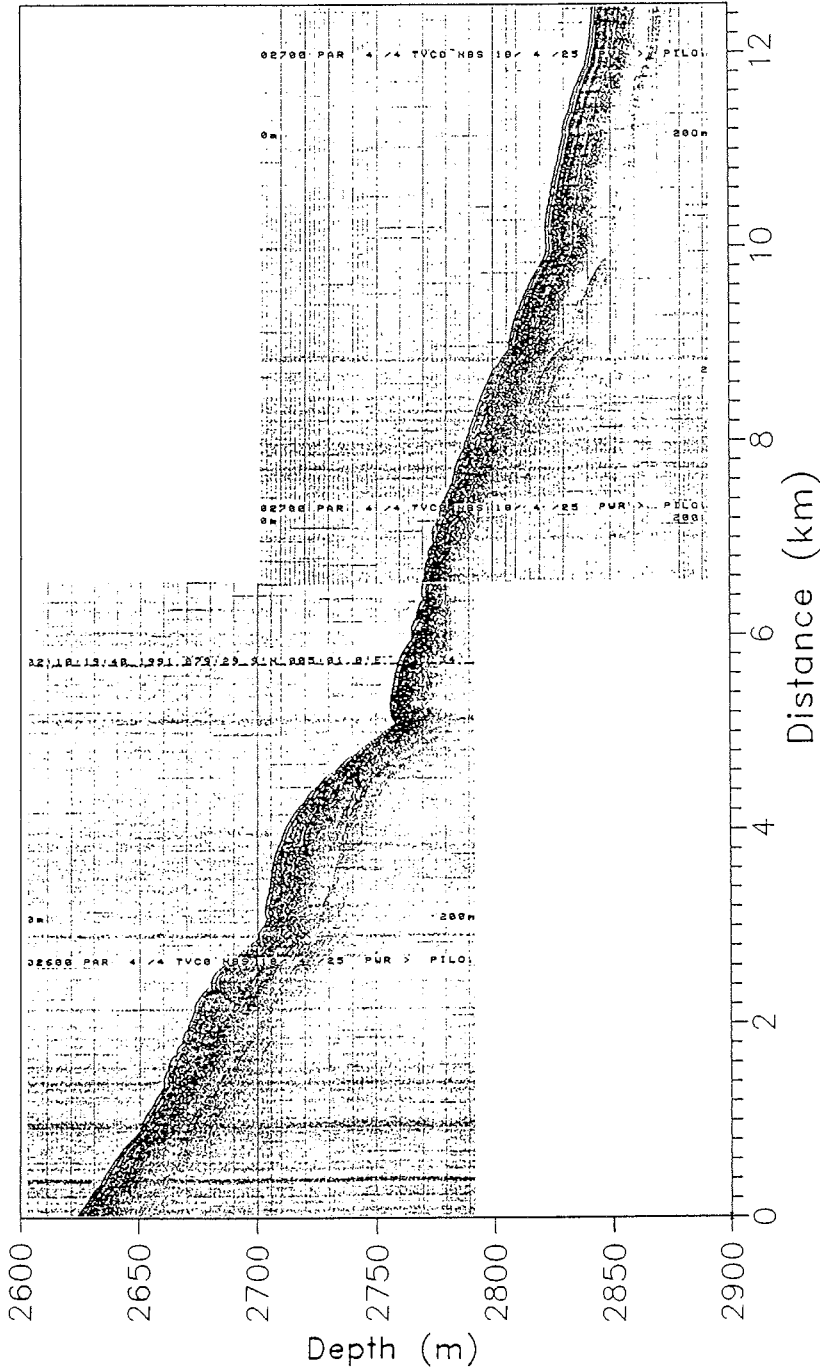


Fig. 6.2-5: Profile over the western flank of Yermak Plateau, recorded between 79° 30' N, 05° 18' W and 79° 30' N, 04° 41' W.

The record reflects acoustically well-stratified sediment features over the whole morphology of the ridge. The mean penetration of the acoustical signal shows only some variations and ranges between 20 and 30 m.

Figure 6.2-2 presents a profile on top of Morris Jesup Rise between 85° 16' N, 17° 05' W and 85° 08' N, 14° 38' W. Because of the steep slope in the first 1.5 km of the displayed section only a diffuse, diffracted signal could be recorded. The next 17.5 km exhibit a rough bathymetry with erosion channels. Below the rough seafloor down to a sub-bottom depth of about 40 m, a distinct stratification of sediments could be recorded by the PARASOUND system. These sediment features can be followed up to the end of this profile.

A profile of sediment coverage on top of Yermak Plateau between 80° 30' N, 10° 07' E and 80° 26' N, 08° 44' E is shown in Fig. 6.2-3. In contrast to Morris Jesup Rise, the topography on top of Yermak Plateau shows no erosional channels since the typical interruptions of sediment features were not observed. Whether the morphology follows the basement topography or not, has to be cleared by way of a link to reflection seismic data shot parallel to this profile.

Figure 6.2-4 shows a profile in NE-SW direction at the eastern flank of Yermak Plateau between 81° 13' N, 13° 04' W and 80° 58' N, 12° 16' W. In the first 6-9 km at a waterdepth of about 2,220 m a possible debris flow can be seen. It is characterized by a transparent section caused non-layering of mixed up sediments within the debris flow. The debris flow is partly underlain by well-stratified sediments, which can also be seen at the slope without any disturbances. In this part of the profile the mean penetration of the Parasound signal is about 40 m.

The last Figure, Fig.6.2-5, is a record of the western flank of Yermak Plateau between 79° 30' N, 05° 18' W and 79° 30' N, 04° 41' W at a waterdepth between 2,620m and 2,840 m. The left part of this profile shows an example for larger mass movements of sediment cover. With decreasing inclination of the seafloor the acoustical pattern reflects a more smooth depositional regime with well-stratified sediments at a waterdepth of about 2820 m.

6.3 Sediment Sampling

Geological sampling and coring was one of the major topics of *Polarstern* during ARK-VIII/3 of ARCTIC '91. There had been two major approaches (i) to recover undisturbed surface and near surface samples for biological, paleoecological, geochemical and physical property investigations and (ii) to recover as undisturbed and long sediment sequences as possible for the various stratigraphic (stable isotope stratigraphy, biostratigraphy, paleomagnetism, AMS ¹⁴C, etc.), paleoenvironmental and sedimentological investigations.

Geological coring and sampling stations were carried out along two transects crossing all major structures, the topographic highs as well as the large basins of the Eurasian Arctic Ocean (Figures 6.3-1 through 4). The more eastern transect comprises about 30 stations from the continental slope north of Svalbard crossing Nansen Basin, Gakkel Ridge, central Amundsen Basin, Lomonosov Ridge up to Makarov Basin. The western transect comprises 24 stations and stretches from

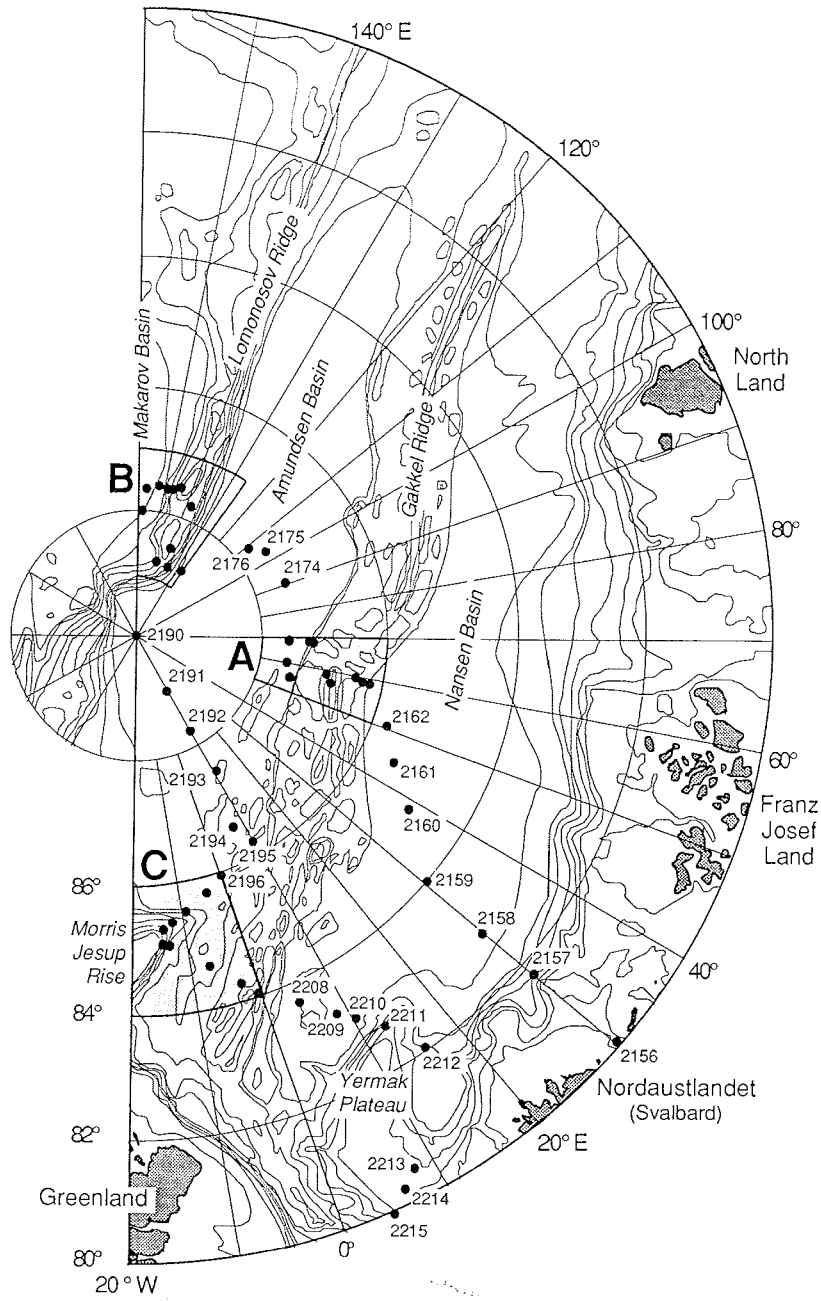


Fig. 6.3-1: Location map of geological sampling stations of ARK-VIII/3 - ARCTIC'91 (for details see Station List, Annex 9.1); blow up of area **A** see Fig. 6.3-2; blow up of area **B** see Fig. 6.3-3; blow up of area **C** see Fig. 6.3-4.

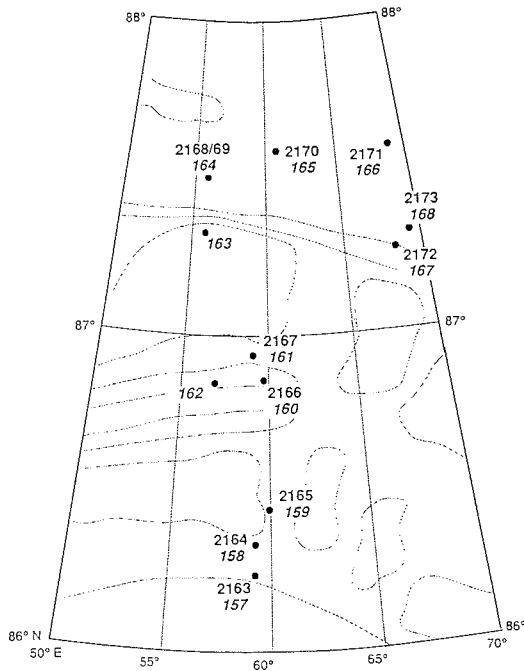


Fig. 6.3.-2: Location map of geological sampling stations on Gakkel Ridge (blow up of area A in Fig. 6.3-1; for further details see Station List, Annex 9.1).

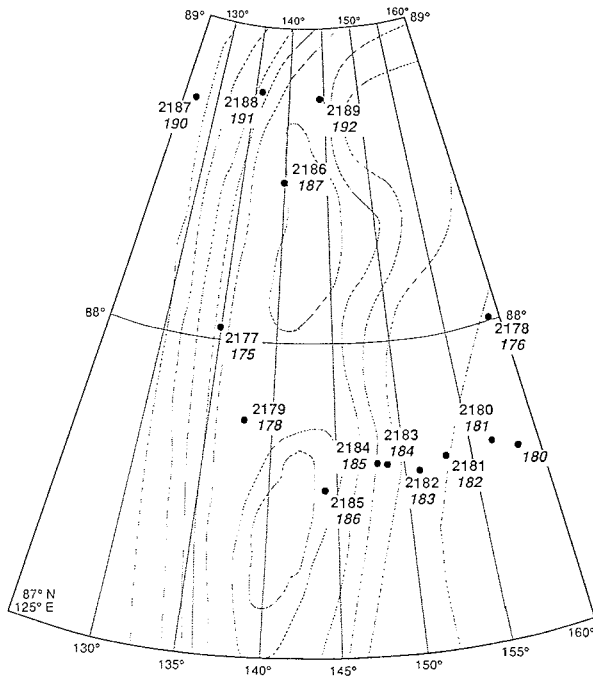


Fig. 6.3-3: Location map of geological sampling stations on Lomonosov Ridge and Makarov Basin (detail of area B in Fig. 6.3-1; see Station List, Annex 9.1).

North Pole, western Amundsen Basin, Morris Jesup Rise, Gakkel Ridge and western Nansen Basin as far as to the Yermak Plateau.

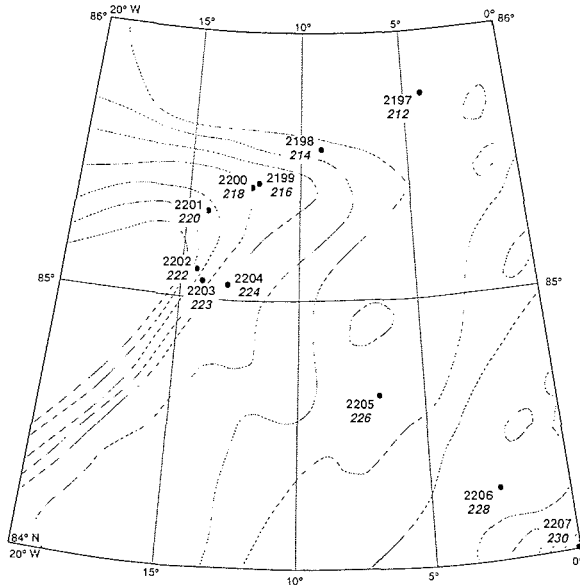


Fig. 6.3.-4: Detailed location map of geological sampling stations on Morris Jesup Rise and western Amundsen Basin (blow up of area C in Fig. 6.3-1; for further details see Annex 9.1).

6.3.1 Sampling of Near-surface Sediments (H. Bergsten, R. Spielhagen and R. Stein)

In order to get undisturbed near-surface sediment samples, the giant box corer (GKG) and the multicorer (MUC) were used. In addition to high quality sediment sampling the multicorer also samples the bottom water directly overlaying the sediment surface.

Giant Box Corer (GKG)

Sampling with the giant box corer (50 x 50 x 60 cm) was carried out routinely on all geological stations. It was carried out along the entire transect from the Barents Sea continental margin to the Makarov Basin and back to the Yermak Plateau to recover surface sediment from all visited morphological features. In total, 117 box cores were run, of which 82 recovered a sedimentary sequence with an average thickness of approximately 30 cm. 23 box cores were empty or contained only very little sediment and 12 box cores did not trigger due to technical problems. On 30 stations, separate box cores were taken for geological and biological studies to supply sufficient sediment volumes.

Multicorer (MUC)

Two types of multicorer (both manufactured by Fa. Wuttke, Henstedt-Ulzburg) were used, the standard 12-tubes-version with a tube diameter of 6 cm and the 8-tubes version with a diameter of 10 cm. The penetration weight was up to 250 kg. On 45 of the 60 geological stations multicorer were run, of which 42 recovered sedimentary sequences with an average thickness of about 32 cm; only three times the multicorer did not trigger.

6.3.2 Coring of Long Sediment Cores (H. Grobe, H. Kassens, K. Manchester and R. Stein)

One major aim of geological investigations was to obtain undisturbed sediment cores as long as possible. For this purpose the (i) giant piston corer (GPC), (ii) kastenlot (KAL), and (iii) gravity corer (SL) were used.

Giant Piston Corer (GPC)

The piston coring system used was the AGC LARGE CORING SYSTEM (Atlantic Geoscience Centre of the Geological Survey of Canada). This system has the capability of using a 30.5 m core barrel made up of up to ten 305 cm core barrels coupled together to a core head.

On the *Polarstern* it was feasible to easily handle this corer with up to a 21.55 m core barrel in the standard *Polarstern* core handling system. The core head can weight between 1,365 kg and 2,250 kg by adding of lead weights. On this cruise all but the first few cores were taken with the 2,250 kg core head. The core barrels use CAB plastic liner in them with an inner diameter of 9.92 cm and an outer diameter of 10.5 cm for easy removal and storage of the cores. The steel core barrels are all 305 cm long and available in three wall thicknesses, of 25.4, 19.1, and 9.53 mm with corresponding weights of 254.5, 182, and 84 kg each. The corer is tripped at 4.5 m above the bottom with a 225 kg trip weight. The weight in air of the coring system varied between 1,925 kg and 3,420 kg with most stations using the system with its weight equal or greater than 3,000 kg.

The "CHATS" (core head acceleration and tilt system) instrumentation package was used on all the piston cores. This system digitally records the pressure (depth), acceleration and two component of tilt of the coring system at a cycle rate of 100/sec. for up to a three minute period during the time of core triggering and sea floor penetration. This data will be compared to the core stratigraphy and physical properties data in the final analysis of the cores.

Kastenlot (KAL)

The kastenlot (KÖGLER 1963), a gravity corer without piston, has a rectangular cross section of 30 x 30 cm. It is a type 390 with a penetration weight of 3.5 t and a corebox segment sized 30 x 30 x 575 cm (manufactured by Hydrowerkstätten Kiel,

Germany). The length of the core boxes used were 5.75 m and 11.75 m plus 35 cm for the core catcher. The great advantage of this kastenlot is the wall-thickness of only 0.2 cm. Because of the great cross-sectional area (900 cm²) and the small thickness of the walls, the quality of the sediment cores was generally excellent. The minimum degree of disturbance was also verified by x-ray radiographs.

There have been 16 successful attempts of kastenlot with a total sediment recovery of 102 m. The average recovery to penetration ratio, an important factor in terms of core-disturbances, is 94 % which means that almost all penetrated sediments have been recovered. Only one kastenlot core (2173-1) has shown over-penetration because it touched the sea floor twice.

Gravity Corer (SL)

The gravity corer has a penetration weight of 1.5 t and a core barrel segment of 5.00 m (5.75 m) in length and 120 mm in diameter. The core barrels used during ARK-VIII/3 had a length of 10 m or 5.75 m.

6.4 Sediment Descriptions and Lithostratigraphy

6.4.1 Sediments in the Nansen Basin (T. Vorren, G. Gard, K. Moran and N. Nowaczyk)

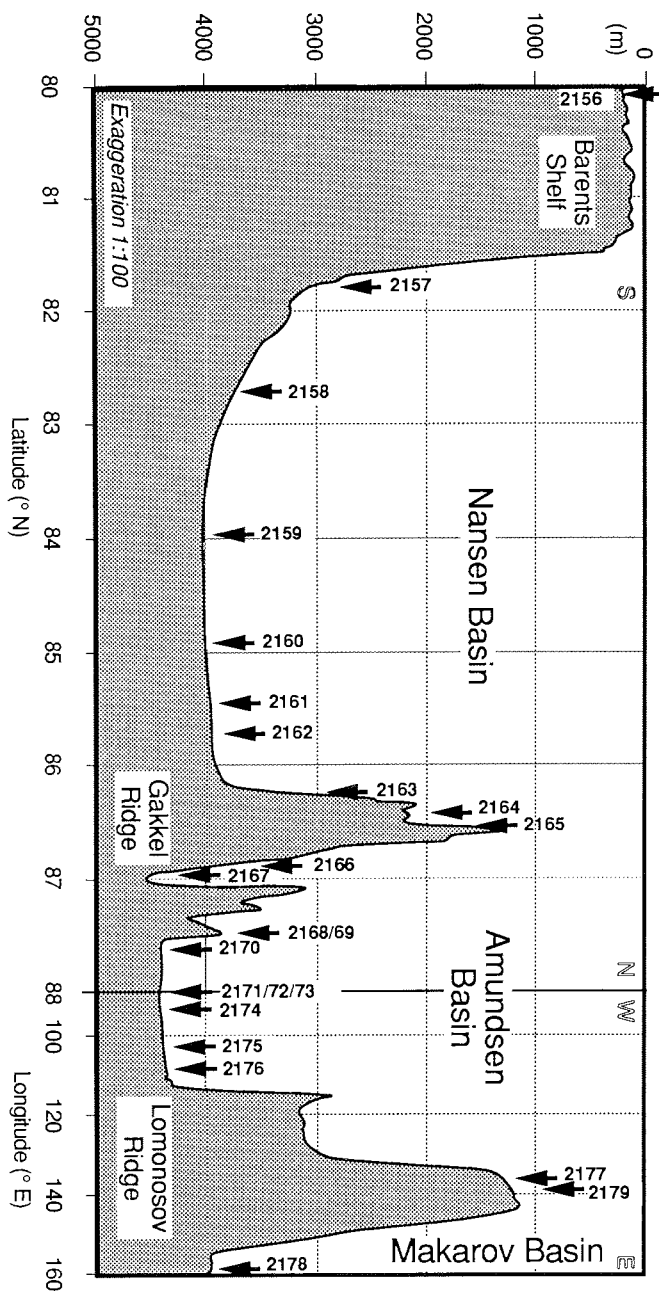
With the expedition of the *Fram* across the Arctic Ocean in 1893-96, Nansen demonstrated a scientific courage and ingenuity unparalleled in polar research. This expedition for the first time observed that the Arctic Ocean was a deep-sea rather than a shallow epicontinental sea. The *Fram* expedition drifted with the Transpolar Current along the Nansen Basin.

The deepest part (4,000-4,100 m) of the Nansen Basin is located in its western part. To the east, sediments of probably originating from the Kara and Laptev shelves, have filled the basin and partly buried the bordering Gakkel Ridge.

ARCTIC'91 recovered four piston cores, seven box-cores and four multicores from the Nansen Basin. The cores were sampled along two southwest-northeast transects; one in the east from 81° 45' N, 30° 00' E to 85° 27' N, 44° 30' E (Fig. 6.4.1-1); and the other in the west from 83° 40' N, 03° 00' E to 83° 00' N, 12° 00' E (Fig. 6.4.1-2).

The uppermost 20-50 cm of sediments in the Nansen Basin normally comprise soft dark brown, brown-grayish and brown clay. Except for the topmost clay, the four piston cores retrieved, contained quite different lithologies: a muddy diamicton with outsized clasts (PS2157-6), sandy-silt beds alternating with clay beds (PS2159-6), and silty clay beds of brownish and grayish colours (PS2161-3). Core PS2208-3 was retrieved from a plateau on a seamount. The plateau was semi-encircled by hills. The upper 250 cm of this core comprise brown and olive brown clays. Below these are several sandlayers and a 74 cm thick unit of a sandy mud with mud-clasts up to 20 cm in diameter.

Fig. 6.4-1-1: Sketch of a bathymetric section from south to north and west to east showing major topographic features: Barents shelf, Nansen Basin, Gakkel Ridge, Amundsen Basin, Lomonosov Ridge and Makarov Basin. Geological stations are indicated by arrows



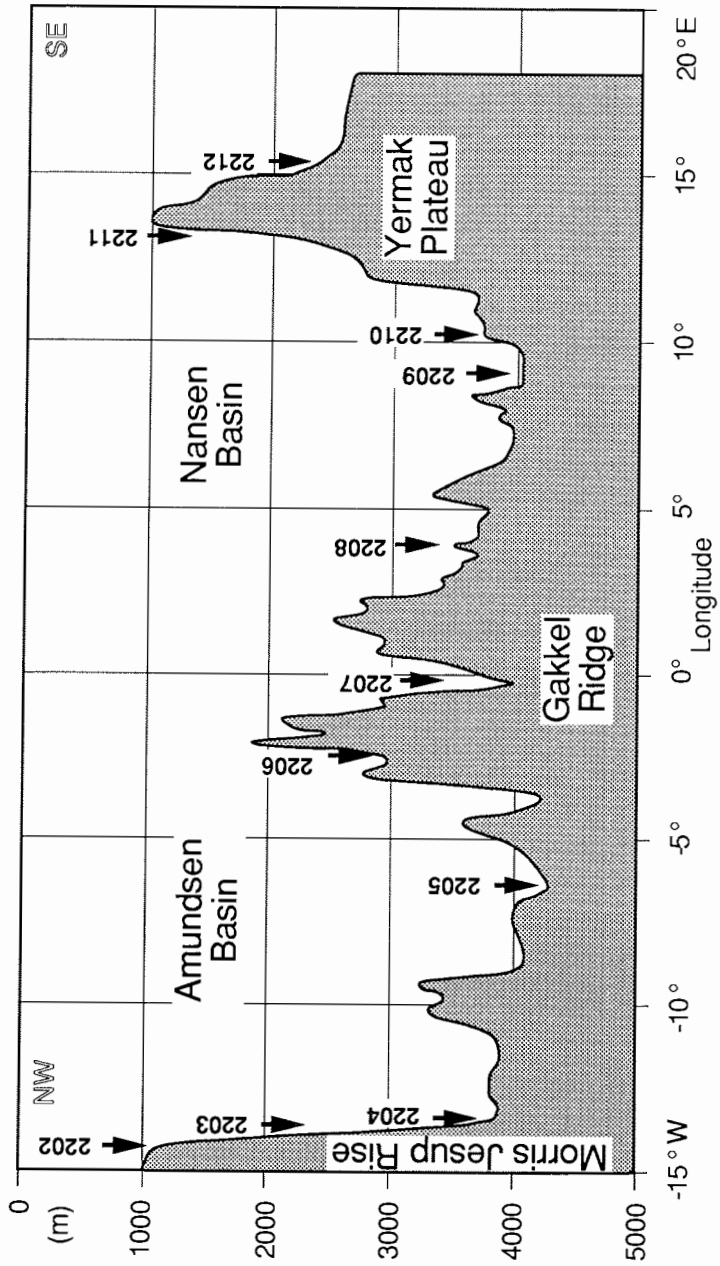


Fig. 6.4.1-2: Sketch of a bathymetric section from Morris Jesup Rise to Yermak Plateau crossing the western parts of Amundsen Basin, Gakkel Ridge and Nansen Basin. Geological stations are indicated by arrows.

Biostratigraphy

The Holocene is represented in the uppermost brownish clays at all investigated sites by rare to common nannofossils, mainly *Emilliana huxleyi* and *Coccolithus pelagicus*. Linear sedimentation rates are in the order of several cm per 1,000 years. Below the Holocene assemblages, the sediments are usually barren of nannofossils but rare specimens of *Gephyrocapsa* spp. are occasionally present.

Magnetic Properties

The level of magnetic susceptibility of sediments recovered in the Nansen Basin varies in the range of 250 to 500 x 10E⁻⁶ (SI). Some distinct peaks in the susceptibility logs in the range of 1,000 to 10,000 x 10 E⁻³ (SI) are caused either by large stones (PS2157-6) or by sand-layers (PS2159-6). Because of large differences in depositional environment of the three cores, it is not possible to achieve a correlation based on magnetic susceptibility (Fig. 6.4.1-3).

Physical Properties

The upper 80 cm of sediments of Core PS2157-6 represents a clay with low shear strength which increases with depth; high water content and porosity; low bulk density; and acoustic compressional wave velocities (p-wave) close to that of seawater. Below 80 cm, the sediment properties are radically different. The water content/porosity (low) and bulk density (high) profiles do not vary with depth indicating that the sediment was deposited as one mass flow deposit.

The physical properties of the two cores collected in the deeper part of the basin (PS2159-6 and PS2161-3) are characteristically similar to deep ocean basin sites. The longest core in the basin (PS2159-6, Fig. 6.4.1-4) suffered from coring disturbances. Limited physical property data show the upper 20 cm of sediments with low density and high water content/porosity. Shear strength could not be measured in the upper metre of core due to disturbance, but between 100-218 cm, the shear strength generally increases with depth, representative of a normally consolidating sediment sequence. Within this normally consolidated trend, shear strength peaks occur. These peaks represent thin layers of sandy sediments.

Sedimentary Environment.

The upper brownish soft clay, probably mostly of Holocene age according to the coccolith-stratigraphy, must be of pelagic/hemipelagic origin. The small amount of dropstones and coarser grain-sizes in general is noticeable. It indicates that the sea-ice is not a large contributor of coarser grain-sizes. The brownish colour indicates oxidizing condition within this unit.

The older sediments are partly hemipelagic but also, to a large degree, derived from various types of mass movements/gravity flows. The diamicton in Core PS2157-6 bears many resemblances to glacial diamictons on the Barents Sea shelf. Most likely it was transported from the shelfbreak down the continental slope

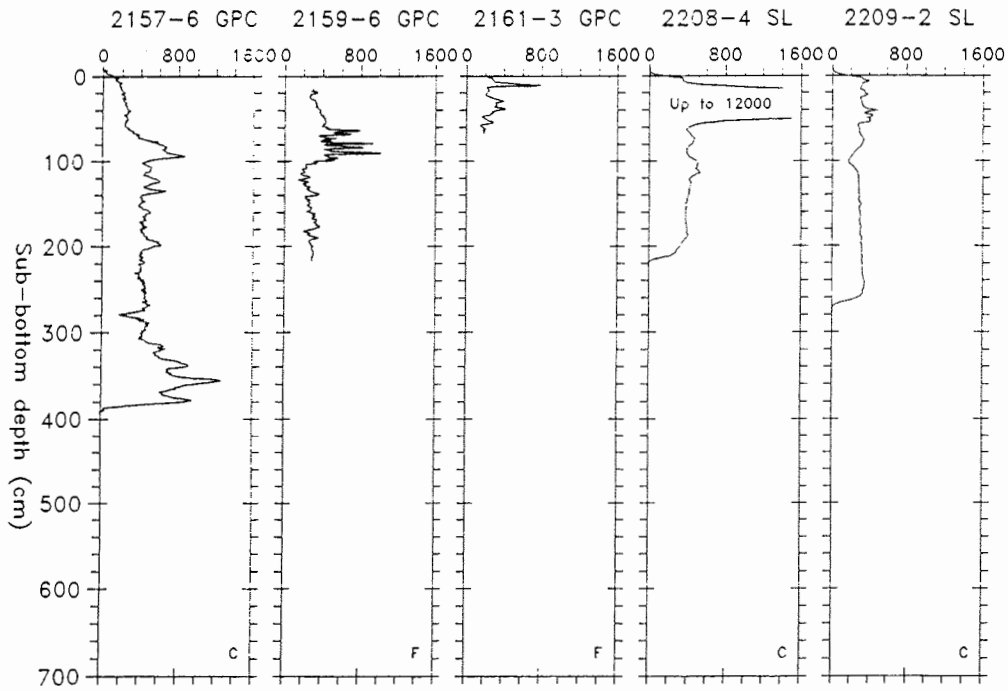


Fig. 6.4.1-3: Magnetic susceptibility ($10E^{-6}$ SI) profiles of various sediment cores from the Nansen Basin. There is no distinct pattern for inter-core correlation.

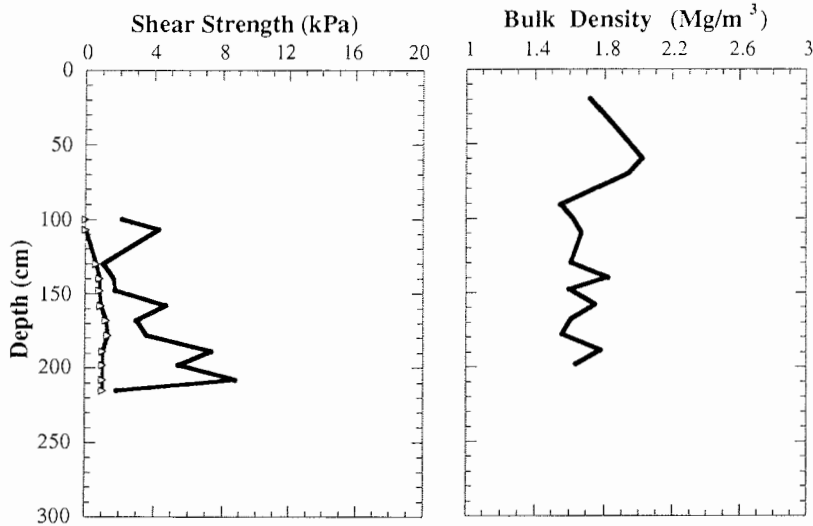


Fig. 6.4.1-4: Physical properties (shear strength and bulk density) of sediment from Core PS2159-6 in the Nansen Basin.

as a debris flow. Core PS2159-6 obviously contains several, mostly distal, turbidites derived from the continental margin. Core PS2208-2 contains several more proximal turbidites and also a 74 cm thick unit of probable slump deposits. These latter sediments are probably of intra-basinal origin.

The mostly olive gray/dark gray colours of the older sediments indicate less oxidizing conditions. These conditions may be due to more rapid sedimentation rates, to a decrease in the oxygen content of the bottom water or to variations in mineralogical composition and/or organic carbon content.

Important problems to be further studied are :

- What are the present and past sedimentary processes on the continental slope?
- What is the ratio of gravity flow sediments to pelagic/hemipelagic sediments in the Nansen Basin?
- Is there any criterion for distinguishing between sea ice rafted and iceberg rafted sediments?
- What are the reasons for the different colours of the hemipelagic sediments?

6.4.2 Sediments on the Gakkel Ridge (T. Vorren, G. Gard, K. Moran and N. Nowaczyk)

An extension of the mid-oceanic ridge system into the Arctic Ocean was suggested on the basis of earthquake epicenters and a few soundings by HEEZEN & EWING (1961) and GAKKEL (1962). The Gakkel Ridge has a width of approximately 300 km and rises more than 2 km above the ocean floor in the southwest. Towards the Laptev Sea in the east, it becomes a more subdued feature.

The ARK-VIII/3 expedition made two crossings of the Gakkel Ridge. The first and northernmost sailed approximately along 60° E between 86° and 87° 30' N (Fig. 6.4.1-1 and 6.3-2). The second from 84° 30' N, 05° 00' W to 83° 40' N, 03° 00' E (Fig. 6.4.1-2). On the northern crossing there were seven geological sampling-stations (PS2163-PS2169); and on the southern crossing two stations (PS2206 and PS2207). Altogether seven piston cores, two kastenlots, seven box cores and seven multicores were recovered along the northern transect. Along the southern transect one piston core, one kastenlot, two box-cores and two multicores were recovered.

Sediment Composition and Lithostratigraphy

The smear slide analysis show that the sediments on the Gakkel Ridge are dominated by quartz, clay minerals and mica. In the cores collected near the spreading axis, there is abundant volcanic glass in some horizons. Ferromanganese crusts and nodules also occur.

The uppermost 20-50 cm of sediments on the Gakkel Ridge comprise soft dark brown, brown, grayish brown clay. In most of the cores there are two horizons of brown clay separated by olive brown clay. The upper horizon is darker.

The older stratigraphy is rather varied. Core PS2165-1 contains several thin gray sand/silt layers, probably distal turbidites. The same is found in Core PS2167-1. This core also has a thick (approx. 2 m) coarse grained turbidite containing large mud clasts and basaltic rock fragments. The color of the turbiditic layers is dark gray.

There are several horizons of hemipelagic sandy/silty clays with quite a variety in colours; black, gray, olive, brown, yellowish brown and reddish. The colour variation may be due to hydrothermal activity or provenance or a shift in redox potential.

Cores PS2168-2 and PS2169-1 have typical sequences of very dark gray sandy mud with sharp lower boundaries grading upwards into olive brown clay. Below the lower boundary is often a thin (1-2 cm) gray clay layer.

Biostratigraphy

The Holocene is represented at most sites by 10-40 cm of the brownish sediments containing rare to abundant specimens of *Emiliana huxleyi* and *Coccolithus pelagicus*. At Station PS2163, oxygen isotope stage 5, or part thereof, is represented by abundant specimens of *Gephyrocapsa* spp. Older sediments are barren of nanofossils.

Magnetic Properties

Three cores retrieved from the southern slopes of the Gakkel Ridge (PS2163-3, PS2164-6 and PS2165-1; Fig. 6.4.2-1) yielded magnetic susceptibilities of roughly 150×10^{-6} (SI). Two cores (PS2166-3 and PS2167-1) recovered from the central graben and two cores from the northern part of the ridge show mean susceptibility of around 300×10^{-6} (SI) (Figs. 6.4.2-1 and 6.4.2-2). Sediments in the coarse grained turbidite in Core PS2167-1 are characterized in parts by susceptibilities of several thousand 10^{-6} (SI) (Fig. 6.4.2-2). Even higher susceptibilities (up to $16,000 \times 10^{-6}$) were found in sediments recovered from a transect along 20° E during the 1987 ARK-IV/3 expedition of *Polarstern*. Increasing amplitudes of some correlated peaks with decreasing distance to the central graben indicated a significant influence on the magnetic properties by volcanic and/or hydrothermal activity (NOWACZYK 1991). This was confirmed by *in situ* heat flow measurements (THIEDE et al. 1987) and geochemical investigations on the recovered sediments (BOHRMANN 1991). The relatively low magnetic susceptibility of the sediments along 60° E may indicate that the hydrothermal activity on this part of the Gakkel Ridge has been lower during the past several hundred thousand years than in the region farther west.

A few susceptibility peaks in cores PS2168-2 and PS2169-1(TWC) reach 900×10^{-6} (SI). These are related to dark (reddish) brown sediments and may be caused by hydrothermal activity (Fig. 6.4.2-2). Cores PS2168-2 and PS2169-1 show cyclic susceptibility patterns. In Core PS2168-1 the interval from 75-165 cm shows almost the same type of variation as the interval from 165-225 cm. The same repetition is found in Core PS2169-1 at 145-200 cm and 200-260 cm. At the base of the

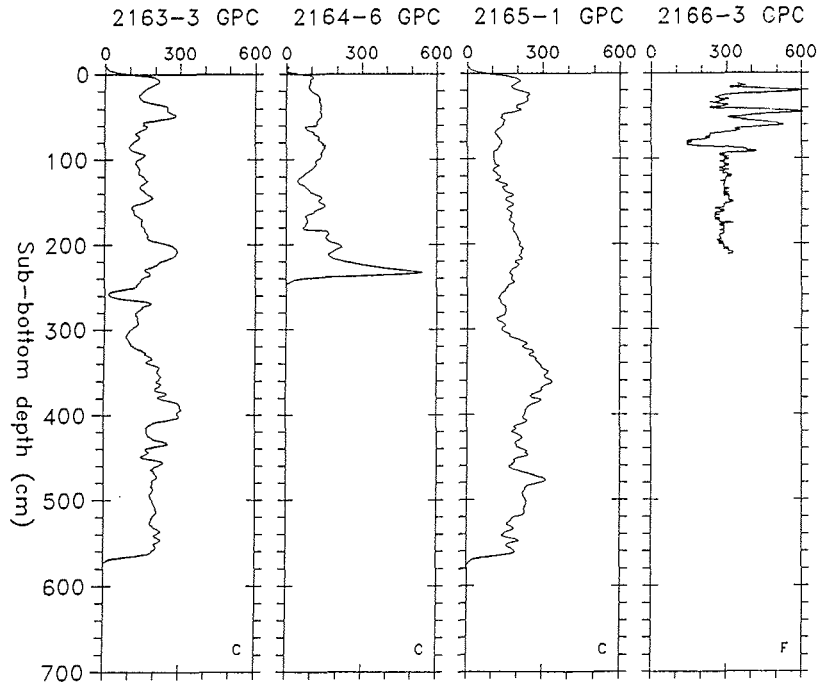


Fig. 6.4.2-1: Magnetic susceptibility ($10E^{-6}$ SI) of sediment cores retrieved from the Gakkel Ridge. Single letter in lower right corner indicates Barthington susceptibility sensor; **c** = whole core measurements; **F** = high-resolution measurements.

corresponding intervals in both cores there is always a dark grayish mud grading into an olive mud which has a sharp susceptibility peak.

Physical Properties

The cores collected on the Gakkel Ridge show physical property variations which are a reflection of the wide grain size and sediment source variations. In general, the shear strength, porosity, bulk density, and acoustic velocity profiles show no trends with depth below seafloor. This suggests that the grain size or sediment composition variations control the physical property changes, as would be expected on a steep spreading ridge where a combination of rapid sediment source changes and slope processes are present. When compared with other regions of the Arctic Ocean, the Gakkel Ridge cores, show high acoustic compressional wave velocity ($>1,500-1,700$ m/sec) and high bulk density (1.8 Mg/m³). Piston Core PS2163-3 (Fig. 6.4.2-3), located at mid-slope on the Nansen Basin side of the ridge shows physical properties which are typical of the region. The shear strength, although increasing with depth, does not have a clear trend. The bulk density is high throughout, the water content is low and the velocity is varying, but generally high. In this region, there is consistent peak to peak correlation between acoustic velocity and porosity,

suggesting that the reflectivity of the seafloor is controlled by the changes in sediment source with depth below seafloor on the ridge.

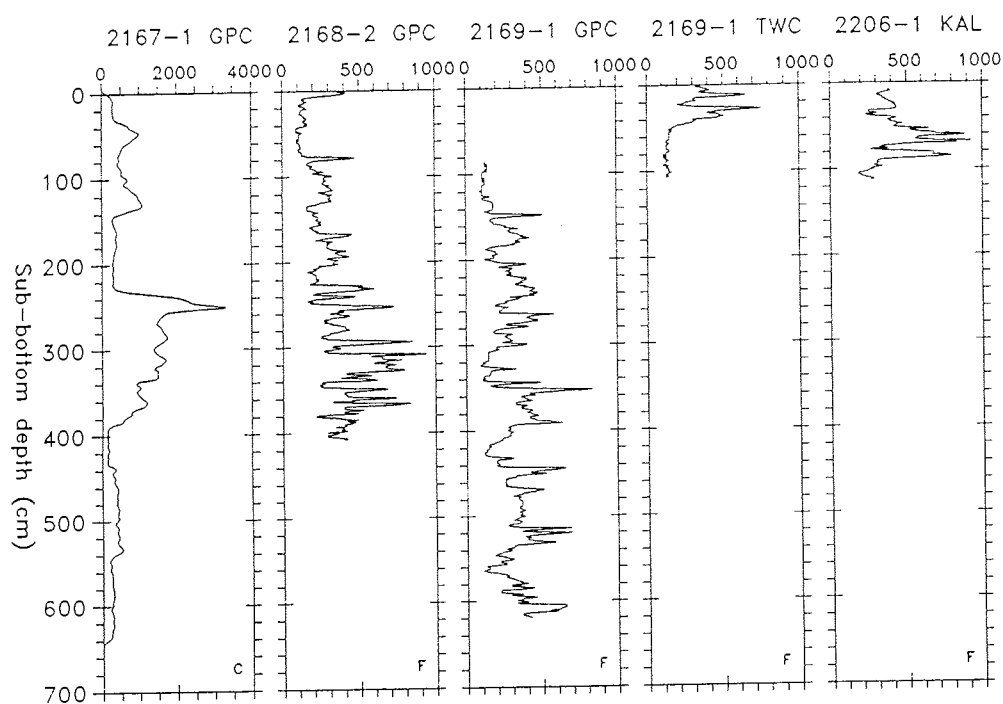


Fig. 6.4.2-2: Magnetic susceptibility of sediment cores retrieved from the Gakkel Ridge. Single letter in lower right corner indicates Barthington susceptibility sensor: **c** = whole core measurements; **F** = high-resolution measurements.

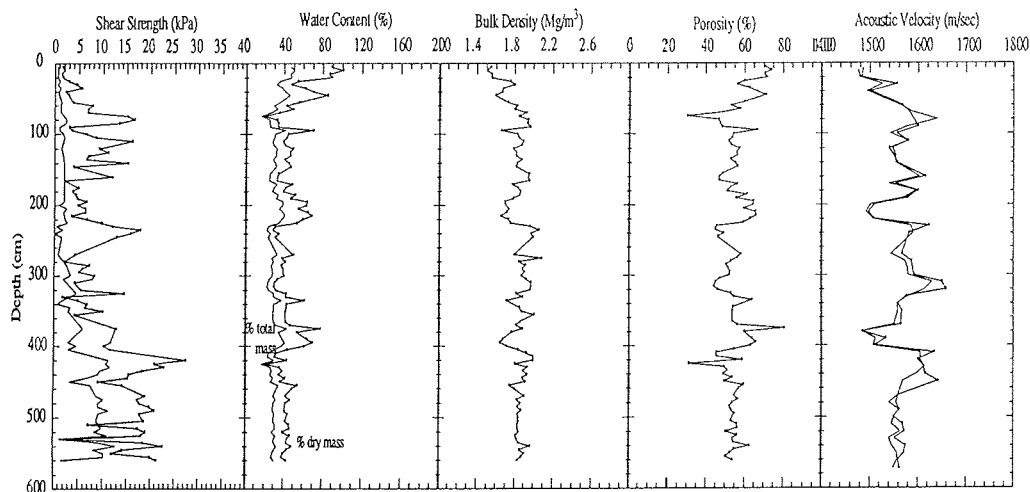


Fig. 6.4.2-3: Physical properties of sediment core 2163-3 from the Gakkel Ridge.

Sedimentary Environment

The sediments on the Gakkel Ridge originate from various sources. Outsized clasts, mud clasts and a high sand fraction in the hemipelagic sediments indicate an iceberg/sea ice transport. Fe- and Mn-rich horizons and crusts point to a hydrothermal source. Some calcareous material is of biogenic origin. Graded sand/silt beds and gravelly beds indicate redeposition by gravity flows. The gravity flows were released and deposited within the ridges and valleys of Gakkel Ridge. Most probably they were triggered by earthquakes in the mid-oceanic ridge.

As in the Nansen Basin, the color of the uppermost Holocene sediments is brownish indicating an oxidizing sedimentary environment. The typical turbiditic sequences are grayish, probably because of rapid deposition.

Cores PS2168-2 and PS2169-1 have some repetitive sediment sequences comprising a very dark gray sandy mud with sharp lower boundaries grading upwards into olive brown clay. Below the lower boundary is often a thin (1-2 cm) gray clay layer. The susceptibility pattern for these sequences is quite distinctive. These sequences may originate from a cyclic change in sedimentary environment between glacial, deglacial, and interglacial periods.

Further Studies

Some of the problems to be further studied are the same as in the Nansen Basin and some are more specific for the Gakkel Ridge:

- What is the ratio of gravity flow sediments to pelagic/hemipelagic sediments?
- Is there any criteria for distinguishing between sea ice rafted and iceberg rafted sediments?
- What is the provenance of the ice rafted debris?
- What are the reasons for the different colours of the hemipelagic sediments?
- Why is there a high susceptibility in clay layers directly underlying the dark gray sandy muds?
- Only stage 1 and part of stage 5 have been identified in the nannofossil stratigraphy. Is this simply due to non-representation of older sediments, or did stage 1 and 5 have specific environmental condition.
- Do the typical sediment sequences really reflect glacial-interglacial variations?

6.4.3 Sediments in the Amundsen Basin (J. Thiede, D.C. Mosher and N. Nowaczyk)

The Amundsen Basin of the Arctic Ocean (Fig. 6.3-1) is located between the northern crest of the Gakkel Ridge in the south and the margin of the Lomonosov Ridge towards the Eurasian Basin. It includes the Pole Abyssal Plain in its center and the Fram Basin where it abuts the continental margin of the Lincoln Sea and the Morris Jesup Rise. In its extension farthest to the east, the Amundsen Basin is bounded by the continental margin of the Laptev Sea adjacent to the New Siberian Islands. With the exception of the Morris Jesup Rise and the poorly defined transitions to the Laptev Sea and Lomonosov Ridge margins, it is completely

underlain by true oceanic crust which has been generated due to seafloor spreading along the Gakkel Ridge in a slow, but fairly regular fashion during the past 53 my (VOGT 1985, KRISTOFFERSEN 1990). As compared to other parts of the Arctic Ocean, the entire basin is seismically very quiet. Since it is exposed to only short segments of the continental margins from where major quantities of sediments can be supplied, the Amundsen Basin sediment fill does not exceed 1-3 km, whereas the Nansen Basin has received >4 km of sediments since its formation. Little is known about stratigraphy and age distributions of the deposits in both deep-sea basins of the Eurasian part of the Arctic Ocean.

It was one of the goals of the *Polarstern* Leg ARK-VIII/3 of ARCTIC'91 expedition to sample surface and subbottom sediments to describe the impact of the ice cover on sediment properties of the sea floor surface and to decipher the temporal and spatial variability of the depositional environment. The Amundsen Basin is located under the northern branch of the Transpolar Drift system.

The sea floor of the Amundsen Basin has been sampled during several segments of the ARCTIC'91 expedition, first in the east during the crossing from the Gakkel Ridge to the Lomonosov Ridge (between 60° and 160° E), then on the way from the North Pole to the Gakkel Ridge (between 0° and 20° E) and then on the way to and from Morris Jesup Rise (Figs. 6.3-1, 6.4.1-1 and -2, 6.4.6-1). More or less successful attempts to sample surface and subsurface sediments have been made on almost all stations, even though the Arctic abyssal plains are known to be covered by deposits which cannot be penetrated with ease (THIEDE et al. 1988). Most of the samples have been taken during the early part of the expedition.

Morphology and Sediment Distribution

A clear relationship can be observed between morphology and sediment distribution in the Amundsen Basin. Geophysical investigations have shown that with the exception of submarine highs, an increasingly thick layer of well stratified sediments covers the irregular surface of the oceanic basement with increasing distance from the Gakkel Ridge. The irregular topography of the abyssal hills north of the Gakkel Ridge (see Fig. 6.4.1-2) give space to the even abyssal plain whose rims are situated some 20-100 m higher than the central part of the basin. This peculiar morphology of the abyssal plain surface is probably caused by sediment properties and input processes. Semiquantitative considerations of the potential source regions indicate that neither Lomonosov Ridge nor Gakkel Ridge with their Cenozoic sediment cover of <500 m thickness can have supplied sufficient clastic sediments to generate a basinwide, several kilometer thick stratigraphic sequence during the same time span. Since low and high resolution reflection geophysics have shown that the dominant share of the basin fill consists of clastic turbidite sequences, the continental margins off the Greenland/Lincoln Sea and off the Laptev Sea have probably acted as source regions. Except for the surface layer, which has been sampled, little is known about the stratigraphic ages of the Amundsen Basin deposits.

Because of the combination with studies of other disciplines and of the difficulties to use *Polarstern* for pre-site surveys in the ice-covered waters, most sampling stations are located in the flat abyssal plain. Only on a few occasions, the position

of the ship and the slow ice drift allowed to sample submarine highs; they comprise stations PS2170, PS2195, PS2196 (see below for further details).

Composition and Properties of Surface Sediments

The giant box cores (GKG) provided in most cases excellently preserved sediment surfaces which consisted in the entire Amundsen Basin of dark brown to dark grayish brown silty clay with few dropstones and common calcareous microfossils (foraminifers and calcareous nannofossils). The brown and grayish brown color of the sediment surface is a result of the oxidizing conditions at the seafloor due to the rapid renewal of the bottom water masses. Planktic foraminifers and calcareous nannofossils are relatively frequent and well preserved despite the remote location of the basin and its water depths of >4000 m. Smear slide descriptions have shown that the surface sediments consist dominantly of clays to silty muds with clay minerals and quartz as the most important constituents. The coarse fractions contained besides planktic and benthic foraminifers and coarse clastic materials, rare bivalves, dropstones and mud clasts. The Station 2190 at the North Pole is a particular good example of the type of sediments deposited at the sea floor surface of the Amundsen Basin, with homogenous dark brown soft clay covering a sediment sequence of highly variable composition.

Numerous giant box cores also provide insight into the detailed lithostratigraphy of the uppermost sediment layers. Twelve box cores have been collected from the Amundsen Basin. Below the youngest unit of 5-20 cm thick silty clays deposits of variable stratigraphies have been found, mostly consisting of clays or silty clays. In a few instances turbidites have been observed. Benthic foraminifers have not been found in the surface sediments. Other fossils were extremely rare.

Bioturbation is weakly developed on all stations. Benthic animals seem to live only in and on the uppermost 2 cm of the uppermost sediment layer. They comprise amphipods (on all stations) and holothurians, bryozoans, polychaetes, and porifers at one station each.

Magnetic Properties

The magnetic susceptibilities of Amundsen Basin sediments range in general from 250 to 500 x 10 E⁻⁶ (SI) (Figs. 6.4.3-1 to 6.4.3-4). At three sites (PS2174, PS2175, PS2176), the mean level is increased to 800 x 10 E⁻⁶ (SI) in the sediment sequences below 6-8 m sub-bottom depth. Numerous sand layers within this section are supposed to be of turbiditic origin. They are related to the high-amplitude and high-frequency variations in the corresponding susceptibility logs. The onset of this pattern and other typical features in the variations of magnetic susceptibility allow a first correlation among these three cores.

At other sites in the Amundsen Basin (e.g. PS2190, PS2197; Figs. 6.4.3-3 and 6.4.3-4), sandlayers with increased susceptibility are abundant in the whole recovered sediment sequences. In addition to this observation, the concentration of the magnetic fraction at Site PS2197 (Fig. 6.4.3-4) is at least twice as high as in the sediments recovered at all other sites in the Amundsen Basin. In this case, the

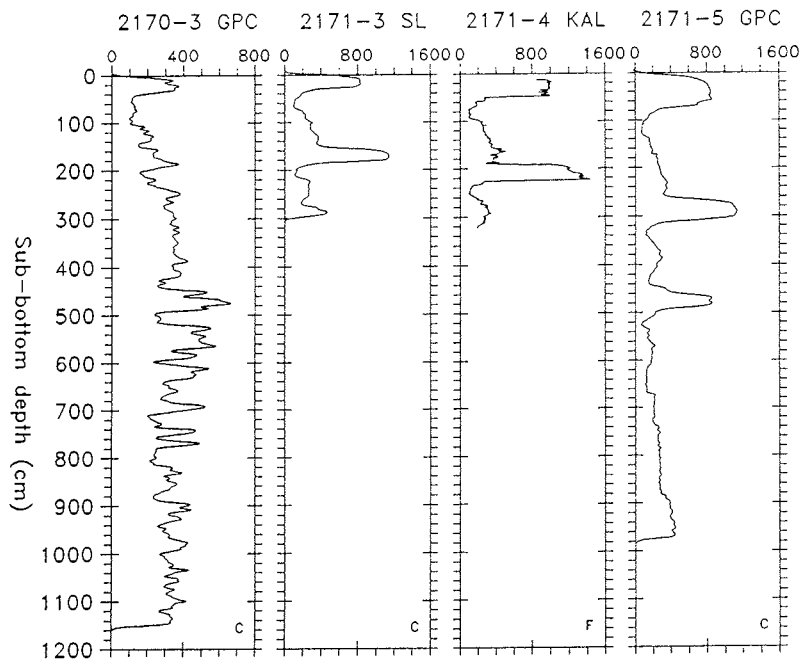


Fig. 6.4.3-1: Magnetic susceptibility of cores taken in the Amundsen Basin near Gakkel Ridge. For precise location see Fig. 6.3-2.

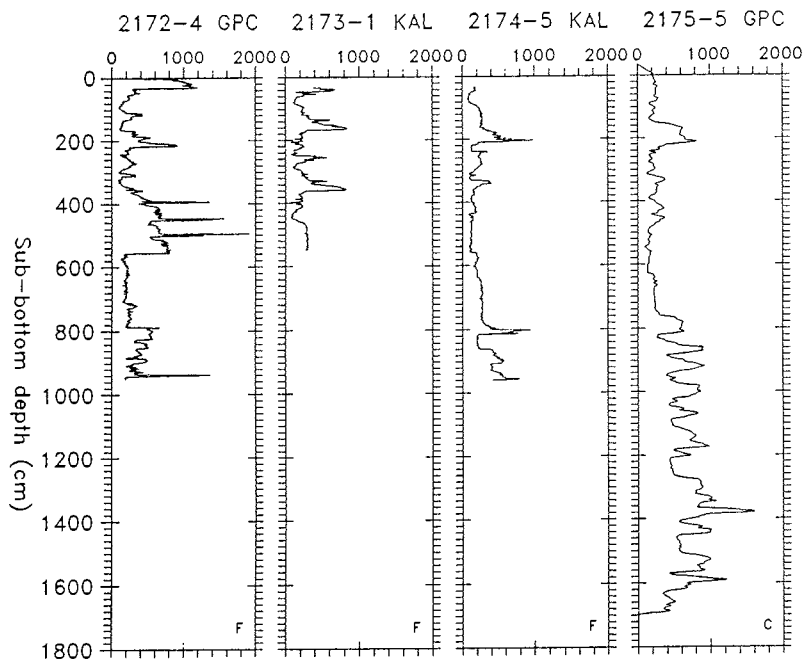


Fig. 6.4.3-2: Magnetic susceptibility of cores taken in the Amundsen Basin. For precise location see Figs. 6.3-1 and 6.3-2.

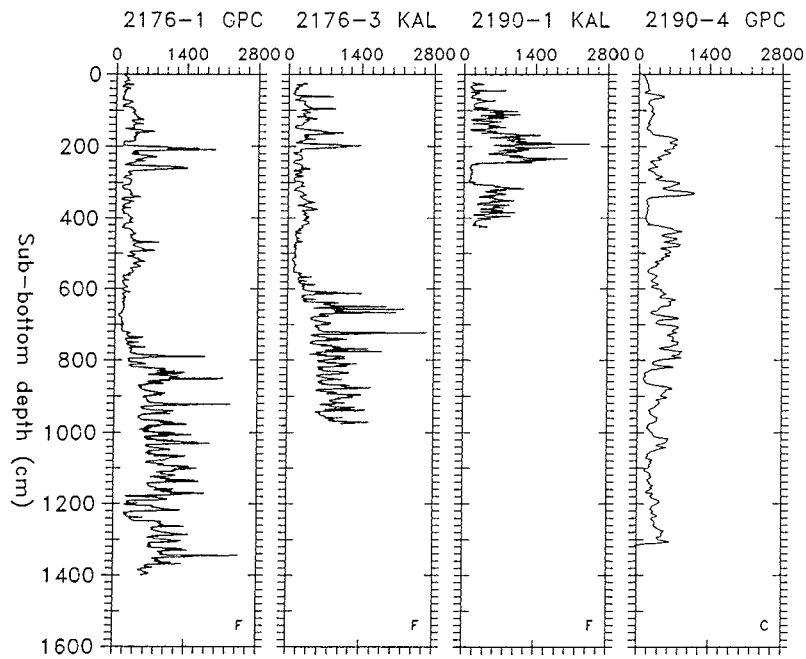


Fig. 6.4.3-3: Magnetic susceptibility of cores taken in the Amundsen Basin. For precise location see Fig. 6.3-1.

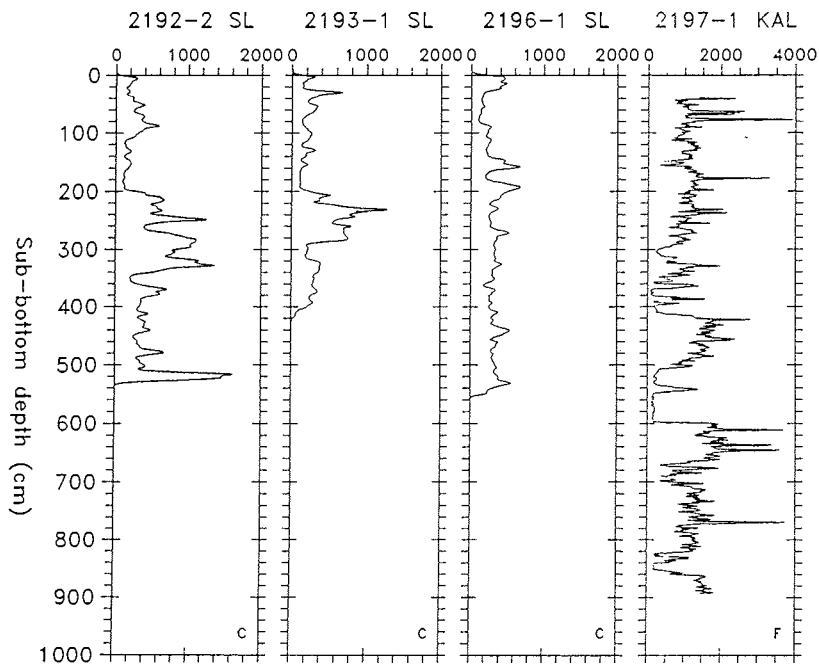


Fig. 6.4.3-4: Magnetic susceptibility of cores taken in the Amundsen Basin. For precise location see Figs. 6.3-1 and 6.3-4.

higher ground level of susceptibility is linked to very soft clays of reddish color. Such sediments are also found in two intervals of the cores at sites PS2171 and PS2172 (Figs. 6.4.3-1 and 6.4.3-2). Pronounced minima in the susceptibility log of Site PS2197 can be correlated to dark greyish coarse grained sediments. It is interesting to note that in Core PS2172-4 susceptibility peaks of up to $2,000 \times 10^{-6}$ (SI) are related to dark bluish clay (Fig. 6.4.3-2). A more smoothly varying whole core susceptibility log ($150-500 \times 10^{-6}$ SI) is typical for the long sediment sequence recovered by a piston core at Site PS2170 (Fig. 6.4.3-1). Almost the whole sediment column is composed of brownish sediments where in this case maximum values of susceptibility correlate with dark brownish layers. A more or less flat plateau of the whole-core log from 220-410 cm is probably due to sediments mixed up by a debris flow.

Physical Properties

Physical property measurements from cores of the Amundsen Basin typify turbidite sequences with relatively high sedimentation rates. The high frequency and high amplitude variations of the physical property curves represent alternating beds of sand and silt with beds of silty clay to clay. The beds with silt and sand (often sandy clay to, more rarely, sorted sand beds) have higher p-wave velocities, higher bulk densities, and lower water contents and porosities. The p-wave velocities in these turbidites show distinctly the sharp base of the bed, with a sudden increase in velocity, followed by a gradual decline in the velocity values up section, presumably representing the fining upwards of the turbidite bed.

The shear strengths depend less upon this grain size difference than the other parameters. With some variation, the shear strength curves show normally consolidated sequences, though the slope of the curves is shallow (less than 1 kPa/m), suggesting rapid sedimentation rates.

A number of the cores, such as PS2172-4, PS2174-3 and 5, PS2175-5, and PS2176-1 and 3, contain a distinctive thick (1-4 m) interval of clay, starting at about 2-4 m subbottom depth. This interval is characterized by very high water contents and porosities, with correspondingly low velocities and very low bulk densities. The shear strength curve over this interval shows either little significant change through the sequence, to slightly higher shear strengths in the middle of the zone. Figure 6.4.3-6 of Core PS2175-5 shows this interval distinctly. This physical property evidence suggests that the interval was deposited very rapidly. This core also shows the dependence of p-wave velocity on the porosity of the sediment in these cores, with a good peak to trough correlation between the two parameters.

Sedimentary Environment

Stratigraphic sequences were collected with all available tools and are documented (Appendix 9.2) to the degree that they have been opened and analysed onboard. During the expedition, sedimentologists have concentrated mostly on piston cores and kastenlots because they offered a combination of long stratigraphies and large volume undisturbed samples. In total, 16 stations have been sampled for stratigraphic sections in the Amundsen Basin.

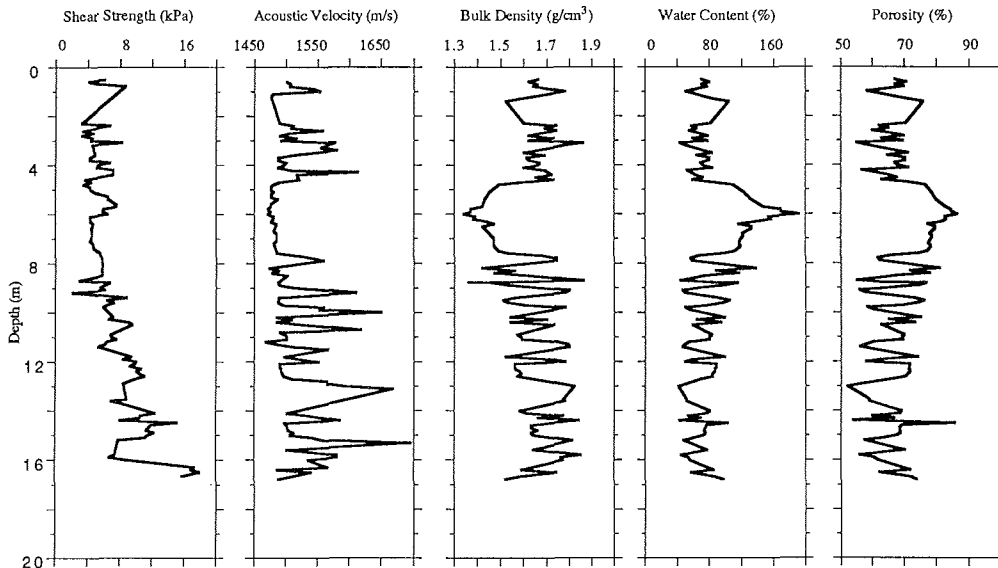


Fig. 6.4.3-6: Physical properties of Kastenlot Core 2175-5 taken in the Amundsen Basin.

The available cores can be subdivided into two groups, namely those representing true abyssal plain sediment records, and those coming from locations protected against turbidite sedimentation. The dominant share of the cores belongs to the first group. The core from the North Pole is a particular good example despite the location of its sampling site in a niche of the Lomonosov Ridge (Fig. 6.3-1) which we originally had hoped would be protected from turbidite sedimentation.

The abyssal plain sediment sequences consist commonly of brown to gray clays alternating sandy and silty muds at the base of the turbidites. The deeper parts of the cores consist entirely of terrigenous mostly relatively fine-grained materials, occasionally interrupted by rare coarse ice-rafted components and mud clasts, sometimes with traces of volcanic glass and few benthic fossils or signs of bioturbation. Fossils are mostly restricted to the upper sediment layers, but especially planktic remains such as foraminifers and calcareous nannofossils (*Emiliana huxleyi*, *Gephyrocapsa* spp., *Coccolithus pelagicus* and *Syracosphaera pulchra*, in decreasing order of abundance) were found. The abundance of the calcareous fossil material decreases towards the north, but they are present even at the North Pole at a great distance from the modern ice border.

The kastenlot Core PS2190-1 is a typical example of the abyssal plain sedimentation in the Amundsen Basin (Fig. 6.4.3-1), where turbidites are usually centimeters to meters thick with a base of fine-grained sand or silty mud. The dominant portion of the sediments, however, consists of clays in various shades of olive gray to black, with only the upper decimeters of the cores grading into brownish hues. Manganese crusts or enrichments, such as those found on the Lomonosov or Gakkel ridges, are the exception rather than the rule in the deep

Amundsen Basin although dark yellowish brown to brownish laminations have been observed in many of the cores.

Coarse, ice-rafted terrigenous components and horizons rich in mud-clasts which are also considered to be deposited from the ice, are surprisingly rare. Due to the lack of any age data, it is presently not clear if this a function of high accumulation rates of fine clastics or of the distance from potential source regions. Fossils seem to be extraordinary rare in the deeper portion of the Amundsen Basin sediment cores, but mottling has been observed repeatedly, suggesting the continued occurrence of benthic life in the deep Amundsen Basin.

The three stations located in positions above the floor of the abyssal plain provided sediments with generally less thick, fewer turbidites and more brownish hues than the deeper cores. Much hope is invested in these cores for good stratigraphic sequences, but it was virtually impossible to find regions with good PARASOUND records indicating the presence of undisturbed pelagic sediments.

The sample material collected from the Amundsen Basin will allow for the study of the following major scientific problems of the Arctic depositional environments:

- the sediment input from the northern branch of the Transpolar Drift system;
- the correlation between surface and bottom water and surface sediment properties (distribution of fossil assemblages, sediment constituents and light stable isotope ratios);
- the sediment structures and determination of major sediment transport processes as well as provenance provinces of turbidites;
- the paleoceanology of the Central Arctic Ocean during the Late Quaternary.

6.4.4 Sediments on the Lomonosov Ridge (G. Brass, G. Gard, K. Moran and N. Nowaczyk)

The Lomonosov Ridge runs across the Arctic Ocean (see Fig. 6.3-1) from the Eurasian continental margin north of the New Siberian Islands to the North American margin north of Nares Strait, between Greenland and Ellesmere Island. The ridge rises above the 2,000 meter depth contour throughout its length and forms the boundary between the Eurasian and Amerasian basins that is in the investigated area the boundary between Amundsen Basin and Makarov Basin of the Arctic Ocean (Fig. 6.4.4-1).

The Lomonosov Ridge has a crustal thickness of approx. 25 km and appears to represent a thin slice of the continental margin of Eurasia which was separated from the remainder of the continent by sea-floor spreading on the Gakkel Ridge beginning about 60 Ma ago. Because of its continental origin, rocks of virtually any age might be found on the Lomonosov Ridge. Seismic reflection studies carried out during ARK-VIII/3 of the ARCTIC'91 expedition show basement covered by an older sedimentary sequence which, in turn, has been tilted and eroded and then covered by a flat lying, younger sequence. All of the cores recovered from the Lomonosov Ridge during ARK-VIII/3 were from this younger sequence.

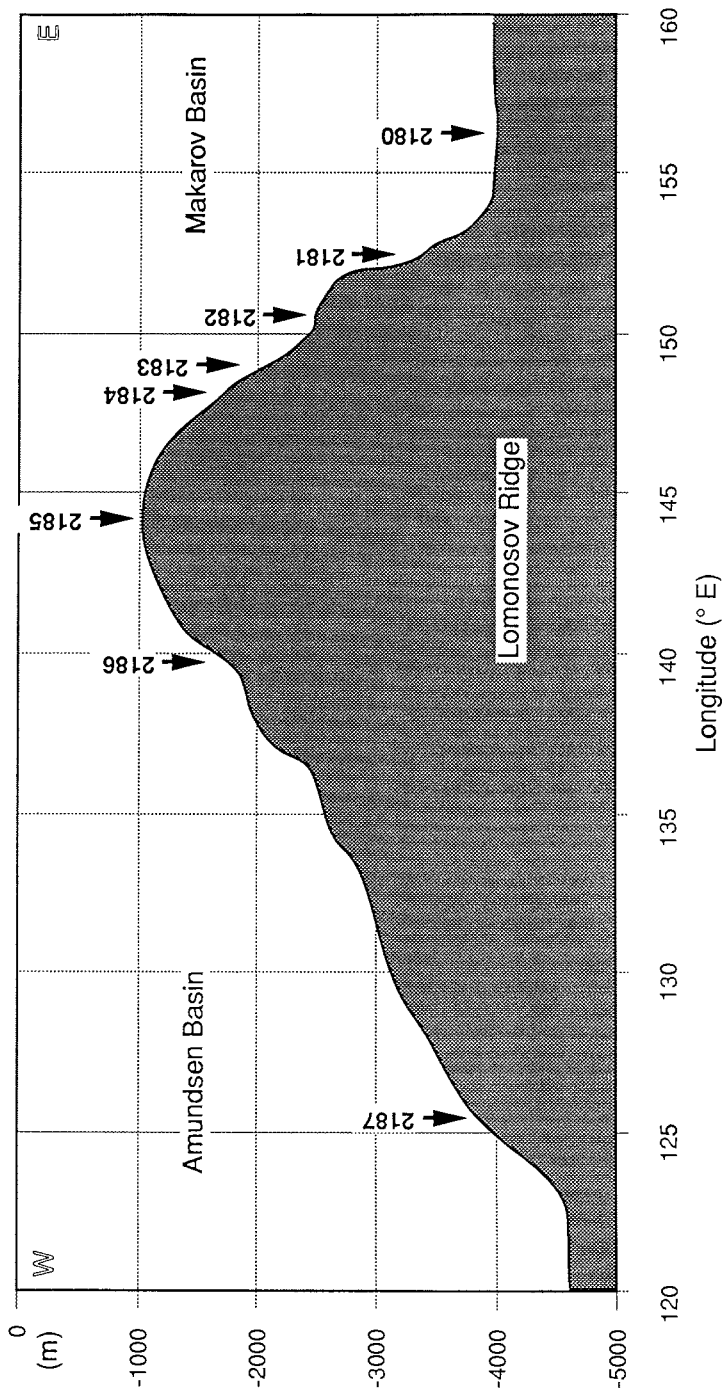


Fig. 6.4.4-1: Sketch of a bathymetric section from Amundsen Basin to Lomonosov Ridge and Makarov Basin. Sampling stations are indicated by arrows.

ARK-VIII/3 recovered five piston cores, three kastenlots, 22 box cores, ten multi-cores and six gravity cores. Coring operations were concentrated on two areas, one around 87° 30' N and 140° to 150° E (sites PS2177, PS2179, PS2181-PS2185) and the other about 100 km to the north at around 88° 30' N and 125° to 145° E (sites PS2186 through PS2189).

Sediment Composition and Lithostratigraphy

Sediments from the Lomonosov Ridge show a variety of colors and textures. Following smear slide analyses (Fig. 6.4.4-2) they are composed mostly of clay minerals and quartz with mica and feldspars, especially in the siltier and sandier parts. Volcanic glass, microcrystalline carbonate, opaque minerals and green amphibole are occasional accessories.

The sediments from the Lomonosov Ridge show a noticeable difference from sediments collected from the surrounding basins. Lomonosov Ridge sediments are richer in silt and sand than basin sediments. Occasional turbidites occur in ridge sediments but these must be of entirely local origin. The ridge sediments include frequent layers of "cottage cheese" texture made up of what appear to be small, angular mud clasts of a variety of colors.

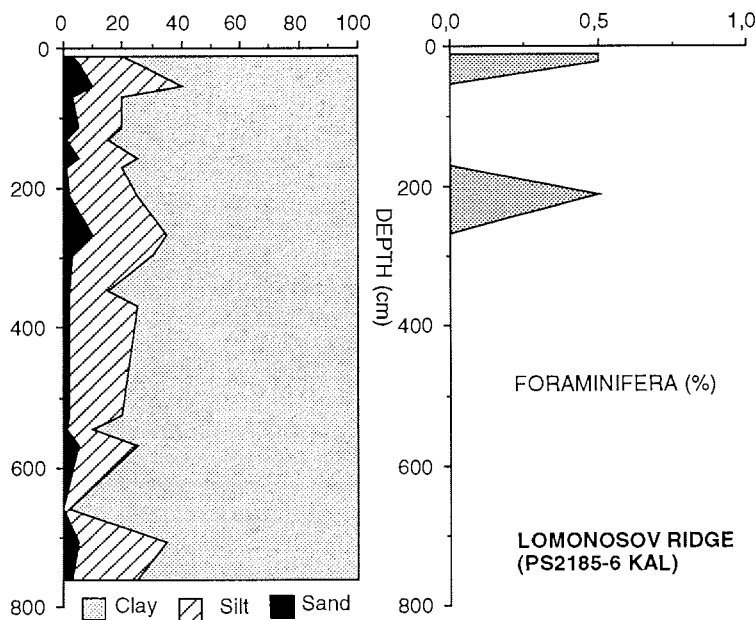


Fig. 6.4.4-2: Texture and composition of kastenlot Core PS2185-6 from top of Lomonosov Ridge from smear slide analyses.

Biostratigraphy

The top five to fifteen centimeters of sediment from the Lomonosov Ridge usually contained *Emiliana huxleyi*, *Coccolithus pelagicus* and *Gephyrocapsa* spp.. The sediment at Site PS2185 contained *Calcidiscus leptoporus* at the 1 cm level. Reworked Tertiary specimens were found at Sites PS2177 and PS2185 and reworked Cretaceous species were also found at Site PS2185. Below the highest level, cores are generally barren; only one core, PS2185-6 the kastenlot from Site PS2185, contained poorly preserved and reworked nanofossils at depth.

Magnetic Properties

Sediments recovered at the Lomonosov Ridge are typically characterized by mean magnetic susceptibilities of 200 to 300 x E⁻⁶ (SI) (Fig. 6.4.4-3). A quite good correlation is given between Kastenlot PS2177-4 and the gravity cores from sites PS2182, PS2183, PS2185 and PS2186. The sediment sequences recovered in kastenlot cores at Sites PS2177 and PS2185 are mainly of brownish color. Dark brown colors do not coincide with higher levels of magnetic susceptibility as was observed in cores from the Gakkel Ridge. The susceptibility patterns of the gravity cores from Sites PS2188 and PS2189 are noticeably different from the other cores from this region. Sediments from Kastenlot PS2187-4 appear to be disturbed by a large slump in the depth interval from roughly one to four meters. The susceptibility profile and sediment color were completely different from the cores discussed above.

Physical Properties

Lomonosov ridge sediment physical properties display a general trend of normally consolidated behaviour. In all cores, shear strength increases linearly with depth at a rate of 0.7 to 1.3 kPa/m (Fig. 6.4.4-4). This increase is typical for normally consolidated sediment. Zones of high shear strength which deviate from this linear trend occur to some extent in all cores, but particularly at Site PS2187 (Fig. 6.4.4-4). These high shear strength zones are approx. 25-30 cm thick and are associated with either mud clast or more sandy intervals. Because these zones of high strength do not effect the normally consolidating trend of the sediment section, it is not likely that these coarser intervals are associated with erosion on the ridges. Rather, these intervals are more likely associated with glaciomarine deposition with moderate sedimentation rates. The p-wave velocity and bulk density on the Lomonosov Ridge likely vary with sediment grain size due to the high sediment sand content. A good example of this dependance is seen at Site PS2189 where the sediment section is coarser in the upper 4 m and finer below (Fig. 6.4.4-4), resulting in higher p-wave velocities in the upper section.

Sedimentary Environment

The sedimentary materials on the Lomonosov Ridge are the product of weathering and erosion of the continents and, perhaps, the re-erosion and re-sedimentation of

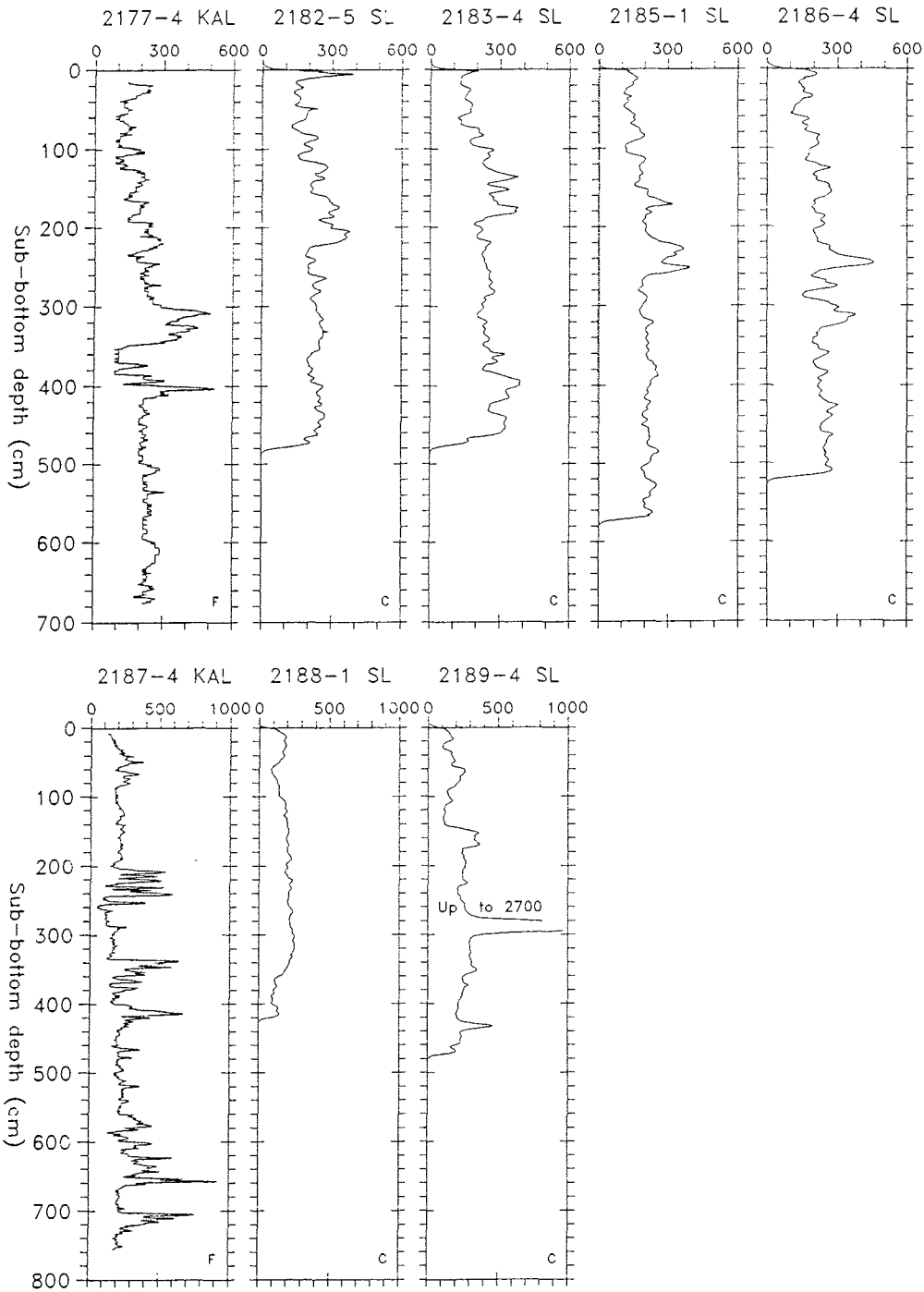
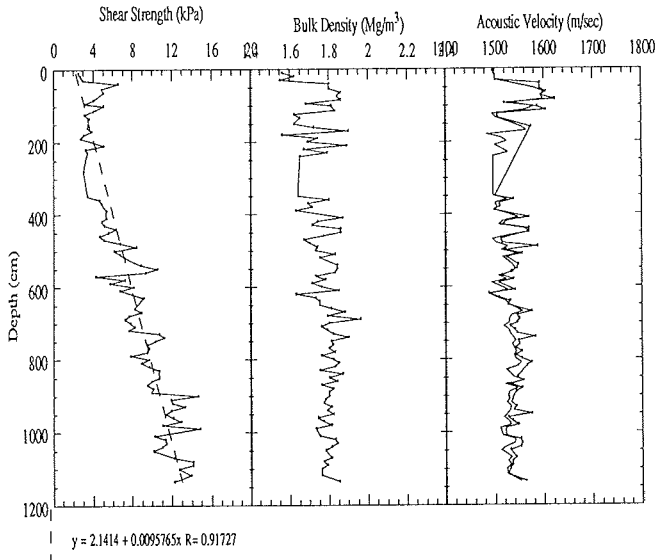
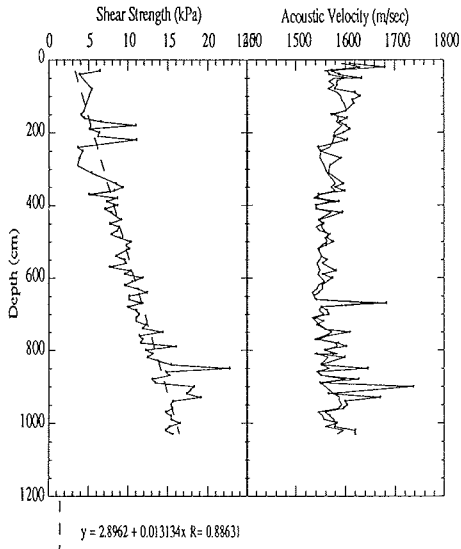


Fig. 6.4.4-3: Magnetic susceptibility in sediment cores from Lomonosov Ridge.

2177-6 Lomonosov Ridge



2189-5 Lomonosov Ridge



2187-3 Lomonosov Ridge

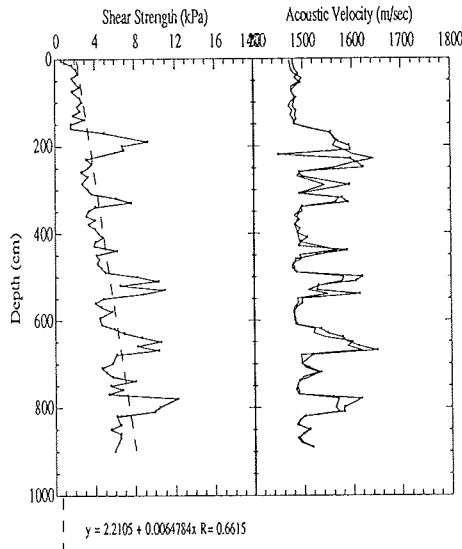


Fig. 6.4.4-4: Physical properties of selected cores taken on Lomonosov Ridge.

pre-existing sediments. Quartz, feldspar, mica and clay are the dominant components and come, no doubt, from a continental source.

The sediments of the Lomonosov Ridge are substantially richer in sand and silt than those from the surrounding basins. For example, in Core PS2189-5, a piston core from a depth of 1,000 m on the ridge, 45 % of the units described in the initial core description are classified as sand or sandy, 40 % as silt or silty and only 15 % as clay or clayey. By contrast, in Core PS2178-5, a piston core from 3,997 m in the Makarov Basin, 19 % are described as sand or sandy, 10 % as silt or silty and 71 % as clay or clayey. A more quantitative measure would show an even greater disparity as the clayey units are relatively thick and the sandy units thin in Core PS2178-5.

The origin of this difference is a puzzle. Turbidites, particularly coarse, sandy turbidites, should be scarce and entirely of local origin on this ridge which stands some 2,000 meters above the surrounding basins. The Lomonosov Ridge is a barrier to overflow of the deep water of the Amerasian Basin into the Eurasian Basin. Overflow currents might have winnowed the fine-grained, more easily suspended clay, but this process should be restricted to the low-lying saddles and should not cause a general coarsening.

It may be that these sediments represent the "true" glacio-marine sediment, transported to the Lomonosov Ridge frozen in icebergs and pack ice and undiluted by the rain of muddy to clayey turbidites which fill the basins. Further post-cruise work will be required to come to some settled conclusion as to the origin of these sediments.

6.4.5 Sediments in the Makarov Basin (R. Stein and K. Moran)

The wedge-shaped Makarov Basin lies between the Lomonosov Ridge and the Alpha-Mendeleev-Ridge (Fig. 6.3-1) and comprises two abyssal plains: (i) the Wrangel Abyssal Plain which is about 2,800 m deep and adjoins the East Siberian shelf, and (ii) the Siberian Abyssal Plain which is about 4,000 m deep and adjoins the Lomonosov Ridge. Both abyssal plains are connected via the Arlis Gap. The two geological stations (PS2178 and PS2180; Fig. 6.3-3) visited during ARK-VIII/3, were both in the Siberian Abyssal Plain in water depths of 4,005 m and 4,009 m, respectively. At these two stations, three box cores, one set of multicores, two piston cores, and one kastenlot core were recovered. These are the first sediment cores ever recovered from this area.

Sediment composition and lithostratigraphy

The surface-near sediments from the Makarov Basin are composed of an uppermost 15-20 cm thick sequence of dark yellowish brown silty clay, underlain by a more grayish brown to olive brown clay. In the uppermost sequence, the coarse fraction is characterized by the dominance of planktic foraminifers (*Neogloboquadrina pachyderma*), rare occurrence of benthic foraminifers, sponge spicules, and ostracodes, and rare to abundant occurrence of quartz and rare occurrence of mica

and opaque minerals. Increased amounts of dropstones (quartz grains, terrigenous carbonate, and siltstones >1mm) were observed in the middle part of this sequence. In the underlain clay, only very small amounts of planktonic foraminifers occur and the coarse fraction is clearly dominated by fine-grained quartz.

The sediments from the long cores are mainly composed of olive, olive brown to brown clay. Occasionally, more sandy intervals and fining-upwards sequences occur. Between about 1.8 and 5 m sub-bottom depth, sequences of sandy mud with frequent mud clasts of 2-10 mm in diameter ("cottage cheese texture") were recorded. In the kastenlot Core PS2178-5 (2.1-2.4 m sub-bottom depth) several large dropstones of up to 7 cm in diameter were found. Based on smear-slide estimates, clay minerals and quartz are the dominant mineral phases; heavy minerals, opaques, micro-nodules, and volcanic glass occur in minor amounts (Fig. 6.4.5-1). Biogenic particles were not observed.

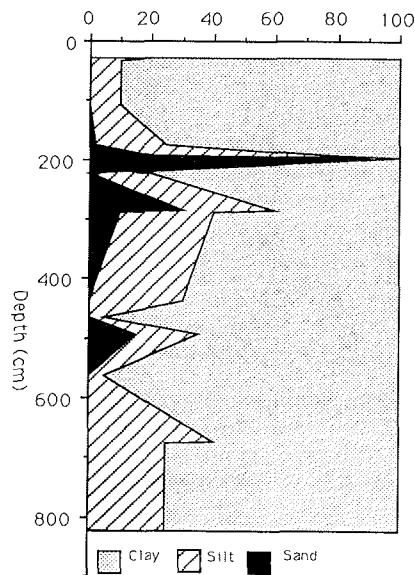


Fig. 6.4.5-1: Sediment texture of kastenlot Core PS2178-5 from smear slide analyses.

Biostratigraphy

In the uppermost 15-20 cm of the sediments from the Makarov Basin rare abundances of *Emiliana huxleyi*, *Gephyrocapsa* spp., and *Coccolithus pelagicus* were found. Below this depth, the sediment is barren of nannofossils and other microfossils.

Magnetic Susceptibility

In the Makarov Basin Cores 2178-5 and 2180-2, magnetic susceptibility ranges from $150\text{-}350 \times 10^{-6}$ SI (Fig. 6.4.5-2). Although the level is not very high the logs of both cores allow a reliable correlation which is confirmed by sediment colors. The large peak in the lowermost section of Core PS2180-2 is caused by the core cutter lamella which was torn off the core catcher during penetration.

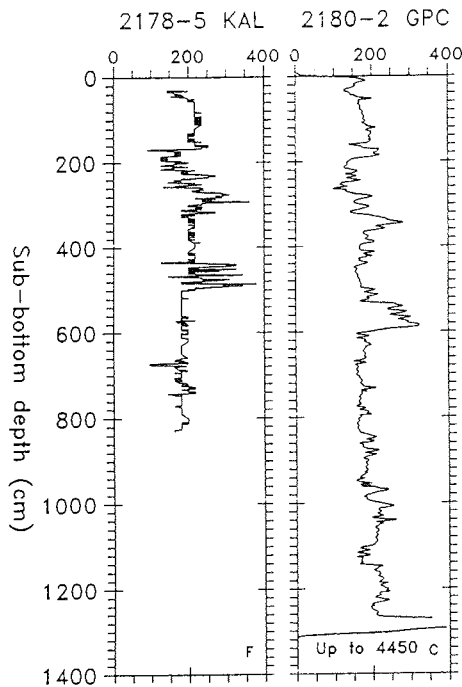


Fig. 6.4.5-2: Magnetic susceptibility of cores taken in the Makarov Basin.

Physical Properties

Physical properties of sediment from the Makarov Basin can be characterized in two types of depositional environments: (i) rapidly deposited sediment which show no increase in strength with depth and (ii) normally consolidated sediment with increasing strength with depth. In both of these sediment types, physical properties also vary with input of coarse-grained sediment and mud clasts. These variations show up in the physical property record as an 'overprint' on the general trend. For example, Core PS2180-2 shows the upper 4 m of sediment with no increase in shear strength with depth, indicating that the sediment is likely rapidly deposited (Fig. 6.4.5-3). Within this unit, peaks of shear strength occur and are associated with sand and mud clasts. From 4-11 m below seafloor (mbsf) in Core PS2180-2, the sediment is generally normally consolidating with increasing shear strength with depth. However, large peaks in shear strength occur within this general trend at intervals where sand, silty sand and mud clasts are also deposited. From 11 m to

the bottom of the core, shear strength decreases with depth. The acoustic velocity of Core PS2180-2 is predominantly low (1,490-1,520 m/sec) which is characteristic of clay dominated sediment. As with the shear strength profile, peaks in velocity are associated with grain size changes, specifically sand layers and intervals of mud clasts.

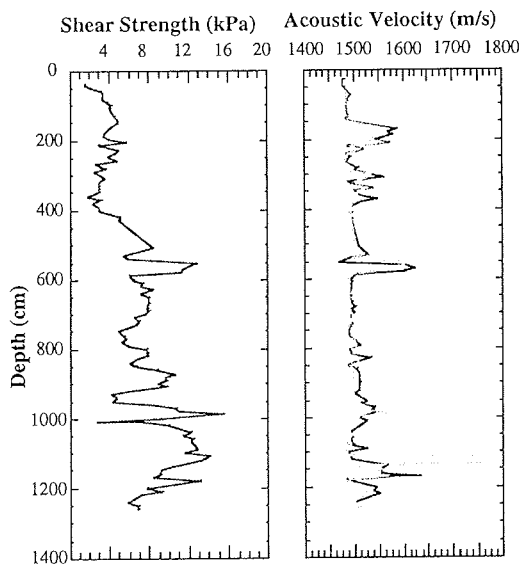


Fig. 6.4.5-3: Physical properties of sediment Core 2180-2 in the Makarov Basin.

Depositional Environment

The sediments in the Makarov Basin are clearly dominated by siliciclastic components such as quartz, clay minerals, and mica, indicating the continental origin of the sediment. Based on grain size distribution and sediment composition and texture, two major sediment types with different transport mechanisms can be distinguished:

- The occurrence of large dropstones as well as irregular-shaped mud clasts indicate an ice-rafted origin of these sediments. Several of the coarse-sand-sized quartz grains found in the coarse fraction of the surface-near sediments are well-rounded and highly-polished. This may suggest fluvial, current, or wave transport mechanisms in coastal and shallow shelf areas before the sediment was incorporated into grounded sea ice or icebergs and transported into the Central Arctic Ocean.
- The fining-upwards sequences with gradational changes from sandy mud to clay are interpreted as distal turbidites. The source area of the sediment might be the surrounding ridges or continental shelf areas.

The abundant occurrence of the planktonic foraminifer *N. pachyderma* in the coarse fraction of the uppermost sediments may indicate increased carbonate productivity

(possibly because of a reduced sea-ice cover during the Holocene) or decreased carbonate dissolution in the Makarov Basin.

More detailed sedimentological and geochemical investigations as well as a much better stratigraphic framework are absolutely necessary for a more detailed reconstruction of the origin of the different sediment types, their changes through time, and their paleoenvironmental significance.

6.4.6 Sediments on the Morris Jesup Rise (R. Stein)

The Morris Jesup Rise is a more than 200 km broad aseismic plateau that trends northeastward from the northern coast of Greenland into the Amundsen Basin (Fig. 6.3-1). It has probably been generated in connection with the Yermak Plateau as a single oceanic plateau in the period between magnetic anomalies 18 and 13 (40-34 Ma).

During the ARK-VIII/3 cruise, coring operations were concentrated on two transects, one transect at the northeastern slope (Figs. 6.3-1, 6.3-4 and 6.4.6-1, sites PS2198, PS2199, PS2200, and PS2201) and the other at the eastern slope of the Morris Jesup Rise (Figs. 6.3-1 and 6.3-4; sites PS2202, PS2203, and PS2204). A total of five box cores, four sets of multicores, two piston cores, one kastenlot core, and four gravity cores were recovered in water depths between 1,070 and 3,900 m (Appendix 8.1). The long piston and kastenlot cores are all taken at shallow water depth.

Sediment Composition and Lithostratigraphy

The near surface sediments from the Morris Jesup Rise (at 1,080 m water depth) are composed of an uppermost 10 cm thick unit of dark brown silty clay, underlain by a more grayish brown to olive brown silty clay. In the uppermost interval, the coarse fraction is dominated by planktonic foraminifers (*Neogloboquadrina pachyderma*). Benthic foraminifers, sponge spicules, bivalves, echinoderms, serpels, pteropodes, and ostracodes are rare to common. In one box corer (PS2201-1), the sediment surface was completely covered by siliceous sponge spicules and single sponges of up to 20 cm in diameter. The siliciclastic components in the coarse fraction of the uppermost unit, common to abundant in occurrence, are mainly quartz and very coarse-grained rock fragments (dropstones). The underlain silty clay is dominated by siliciclastic components, i.e. quartz, rock fragments, and opaque minerals. The rock fragments are very coarse-grained (dropstones) and composed of siltstones, terrigenous carbonates, and metamorphites. Biogenic components are restricted to rare to common occurrence of planktic foraminifers; benthic foraminifers are of very minor importance. Furthermore, coal fragments were observed in this unit.

The sediments recovered in the long cores mainly consist of (rhythmic?) alternations between light olive brown to brown sandy to silty mud and grayish brown to brown, often mottled, sometimes silty, clay. Mud clasts and large dropstones frequently occur in the sandy mud intervals. Based on smear-slide

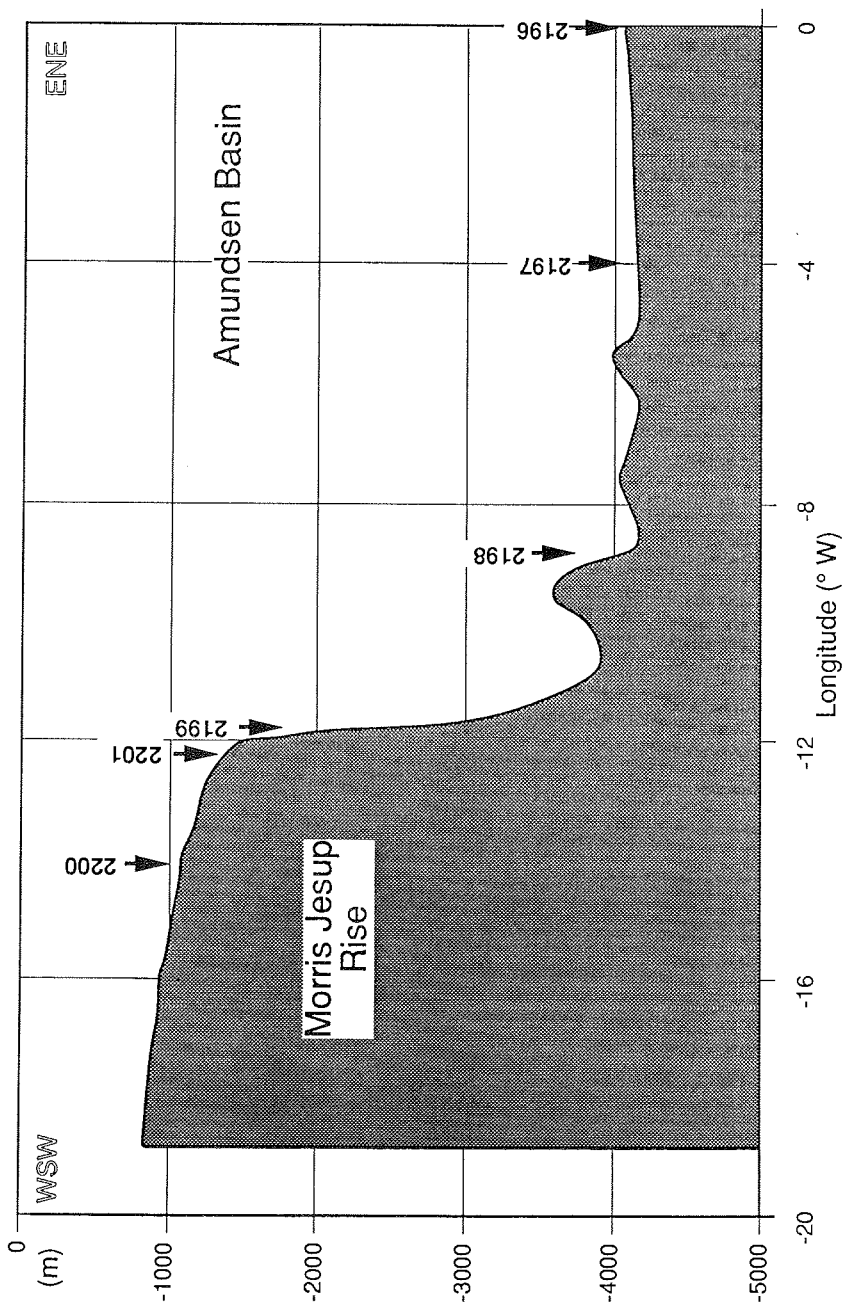


Fig. 6.4.6-1: Sketch of bathymetric section from Amundsen Basin to Morris Jesup Rise. Sample locations are indicated by arrows.

estimates, clay-sized particles (i.e. mainly clay minerals) are generally dominant reaching up to 80 % of the bulk sediment. Sand- and silt-sized material, however, may become a major proportion of the sediment in several intervals (Fig. 6.4.6-2). The silt and sand fractions are composed of quartz as the most important component, followed by terrigenous carbonates, feldspars, and opaques as less important components. Planktic foraminifers also occur - at least in minor amounts - in the deeper part of the sediment sequences of Morris Jesup Rise (Fig. 6.4.6-2).

Magnetic Susceptibility

A mean susceptibility of about 260×10^{-6} SI was detected for cores at the Morris Jesup Rise. Three cores taken on top of the rise (PS2200-1, PS2200-5, and PS2202-5) yielded almost identical patterns, but there is no obvious correlation to Core PS2198-2 from the lower slope of the rise (Fig. 6.4.6-3).

Sedimentary Environment

The sediments at the Morris Jesup Rise are composed dominantly by siliciclastic components, i.e., mainly clay minerals and quartz as well as rock fragments. The common occurrence of irregular-shaped mud clasts and coarse-sand-sized rock fragments suggests a glacio-marine origin of these sediments. The large dropstones occasionally found in the sequence may indicate transport by icebergs. The composition of the dropstones, mainly dark gray terrigenous carbonates, metamor-

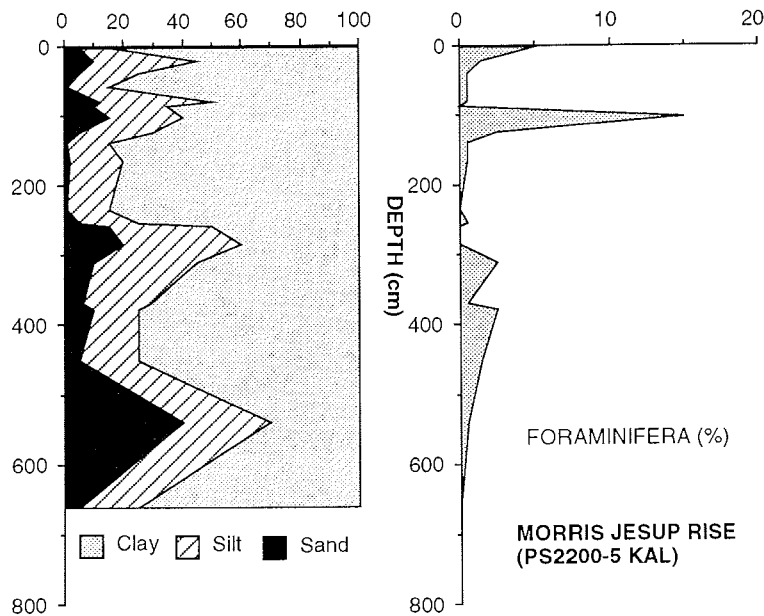


Fig. 6.4.6-2: Sand-silt-clay ratios and content of planktic foraminifers in Kastenlot Core PS2200-5, as based on smear-slide estimates.

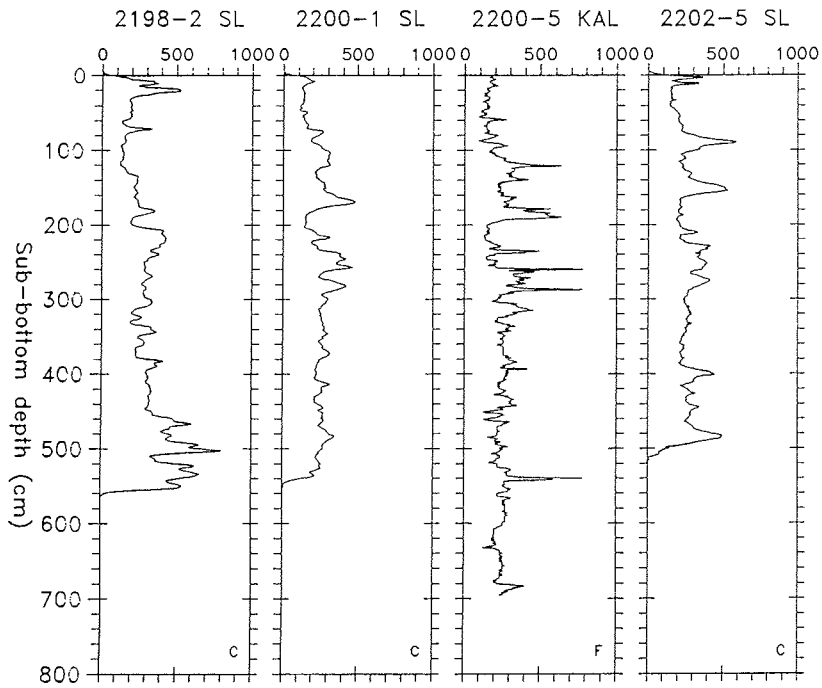


Fig. 6.4.6-3: Magnetic susceptibility of cores taken at the Morris Jesup Rise.

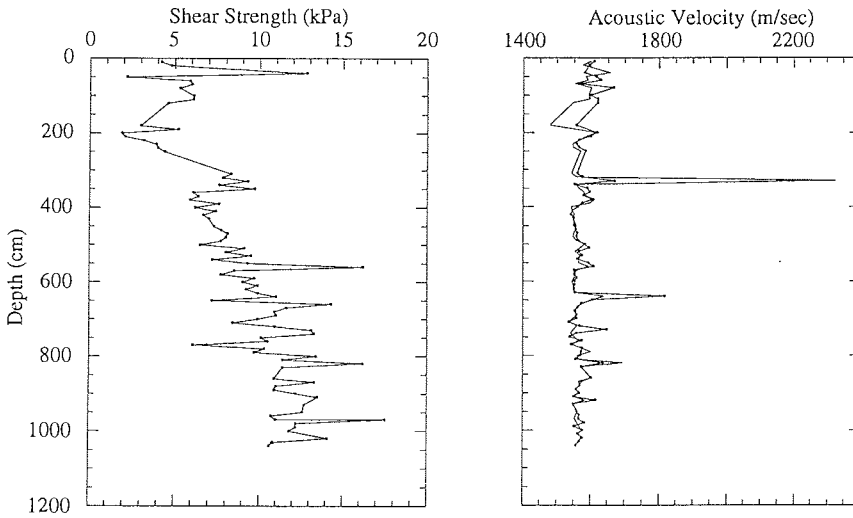


Fig. 6.4.6-4: Physical properties of sediment Core PS2202-7 on Morris Jesup Rise.

phites, and siltstones, suggest the palaeozoic rocks on Greenland to be the source area of the siliciclastic material deposited on Morris Jesup Rise. The rhythmic changes in sediment composition may have been triggered by changes in paleoclimate (i.e. glacial/interglacial cycles). These may result in variations of availability of weathered source rocks, sea-ice cover, iceberg abundance, or surface-water circulation which all are factors controlling terrigenous sediment supply. Further detailed shore-based studies are necessary before a more precise reconstruction of the depositional environment is possible.

Although the siliciclastic components are the dominant proportion of the sediments at the Morris Jesup Rise, biogenic carbonate particles (foraminifers, echinoderms, serpents) occur in significant to trace amounts throughout the entire sediment sequences. The occurrence of well-preserved planktic foraminifers and, especially, pteropods suggest a good carbonate preservation environment, i.e., a position well above the lysocline. The distinct changes in abundance of planktonic foraminifers in the uppermost interval may reflect changes in paleoceanographic conditions.

6.4.7 Sediments on the Yermak Plateau (Y. Kristoffersen, J. Thiede and R. Stein)

The Yermak Plateau was first charted by the Soviet icebreakers *Ob* and *Lena* in 1956-1957 in search for the "Nansen sill" and the northeastern part was not outlined until 1982 by helicopter landings on ice during the *FRAM-IV* expedition. The two distinct trends in its morphology appear to have different geophysical characteristics and suggest that the plateau may have a northern NE-trending (north of 81° 45' N) volcanic part and a southern part with predominantly continental crust (Fig. 6.3-1). High amplitude linear magnetic anomalies indicative of strongly magnetized material and relatively high seismic velocity characterize the crustal rocks in the northern part whereas the southern part is associated with a low amplitude magnetic field and the crustal seismic velocities are lower.

The conjugate position with respect to the Gakkel Ridge and similarity in morphology between northern part of Yermak Plateau and Morris Jesup Rise suggest they were formed by excessive volcanism during the sea-floor spreading process and they may have been above sea level at one point during their evolution.

Together with the Morris Jesup Rise it is believed to be the product of hotspot volcanism in Palaeogene times (if following the currently known magnetic anomaly ages of the adjacent oceanic crust somewhere between 53 and 34 Ma); both rises were later separated by sea-floor spreading. The boundary between continental and oceanic crust is not well known in the area of the eastern extension of Yermak Plateau which is separated from the Svalbard margin by a deep trough, as well as in its western section where a line of modern earthquakes, strange heat flow values and young volcanism as well as recent hydrothermal activity on NW Svalbard indicate a zone of neotectonics.

Despite its elevated position and its relatively young age, the outer Yermak Plateau volcanic basement is known to be covered by surprisingly thick sediments with

presently unknown stratigraphic relations. The sediment sampling stations (Fig. 6.3-1) on the Yermak Plateau had three purposes:

- The northern margin of the Yermak Plateau was assumed to comprise several canyons whose walls would offer suitable locations to sample outcropping sediments older than the Quaternary;
- The Quaternary sediment cover was to be sampled on the top and on the southern flank of the outer Yermak Plateau where widespread undisturbed pelagic sediment sequences were known from previous cruises (THIEDE et al. 1988).
- Several of the proposed ODP sites (RUDDIMAN et al. 1991) were to be crossed by seismic reflection profiles and the local sediment cover was to be sampled.

Suitable locations for all three aims were found and successfully sampled.

Morphology and Sediment Distribution

The first locality had been chosen in the northern flank of the outer Yermak Plateau where canyons provide for incisions with outcropping sediments older than Quaternary. A suitable location was found when searching the area immediately to the north of the plateau crest, on top of a region with steeply rising basement rocks. Sediment distribution in the area was very irregular, but according to previously available and new seismic reflection lines, the volcanic foundation of Yermak Plateau seems to be covered by a thick sequence of deposits of presently unknown stratigraphy.

The expedition then visited the trough between Svalbard continental margin and the outer Yermak Plateau to sample an area of widespread undisturbed pelagic sedimentation, which could also be followed further to the west where the locations of the proposed ODP sites are located. Proposed site locations are on the westernmost part of the Yermak Plateau and on its slope towards Fram Strait in areas of irregular sediment distributions.

Composition and Properties of Surface Sediments

The gravity corer at Site PS2211 recovered a short (0.2 m) core with pieces of gravel of a strange indurated yellowish brown sandy mud. Its surface was overgrown by sponges. The topmost two cm produced *Coccolithus pelagicus* and *Emiliana huxleyi* which belong to a Holocene assemblage (GARD 1988). Below, small placoliths are present, some of which are *Gephyrocapsa* spp., which occurs during the Pliocene to Recent. In addition, a significant amount of Eocene taxa were observed at 20 and at 26 cm depth.

The surface sediments at sites PS2211 and PS2212 consist of grayish to dark grayish brown silty clays. At Site PS2212 it also contained bivalve shells, small sponges and common benthic and planktonic foraminifers, PS2213 common brittle stars, echinoids and polychaete tubes. The last two sites of the expedition, which are located on the western Yermak Plateau (Sites PS2213 and PS2214), provided

surface sediments consisting of dark olive sandy to silty mud with abundant benthic life.

The surface sediments of the Yermak Plateau have been sampled in detail in four giant box cores. Below a surface consisting of sandy-silty clays without or with abundant dropstones variable stratigraphies silty and sandy clays have been found. The sediments contain rare to common planktonic and benthic foraminifers, usually also other benthic biota.

A rich and diverse benthic fauna has been found near the seafloor surface on the Yermak Plateau (the samples still await further analysis). Bioturbation reached down to 20-30 cm below the sediment surface, but polychaetes lived sometimes in deeper sediment layers.

Lithostratigraphy

The sediments of the KAL, GPC and SL from the Yermak Plateau consisted mainly of brownish and grayish clays and muds, with brown colors being dominant in the upper 4 m of the cores. Few sandy and silty layers are present. The smear slide analyses show the presence of heavy minerals, carbonate, planktonic and benthic foraminifers (Fig. 6.4.7-1). Sponge spicules, some diatoms and radiolarians were also observed. Some of the cored intervals are intensely mottled, particularly close to very dark sediment horizons. Dropstones and mudclasts were observed only rarely.

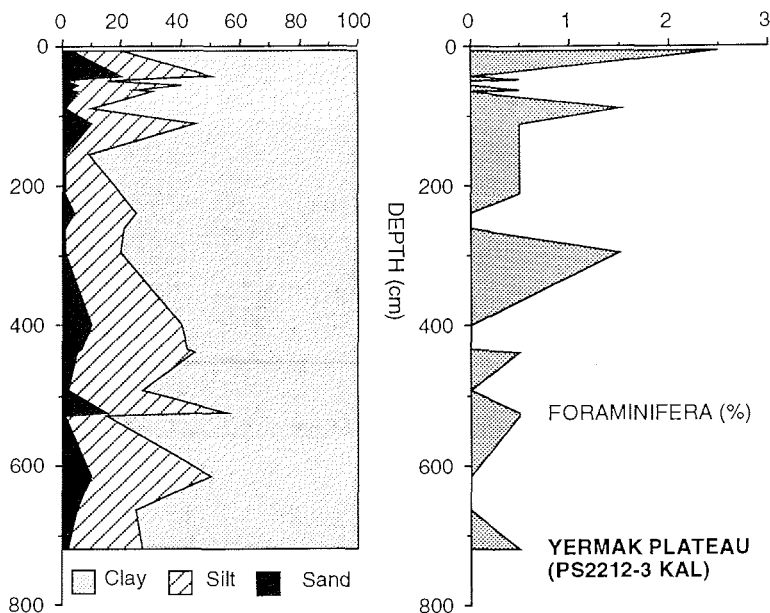
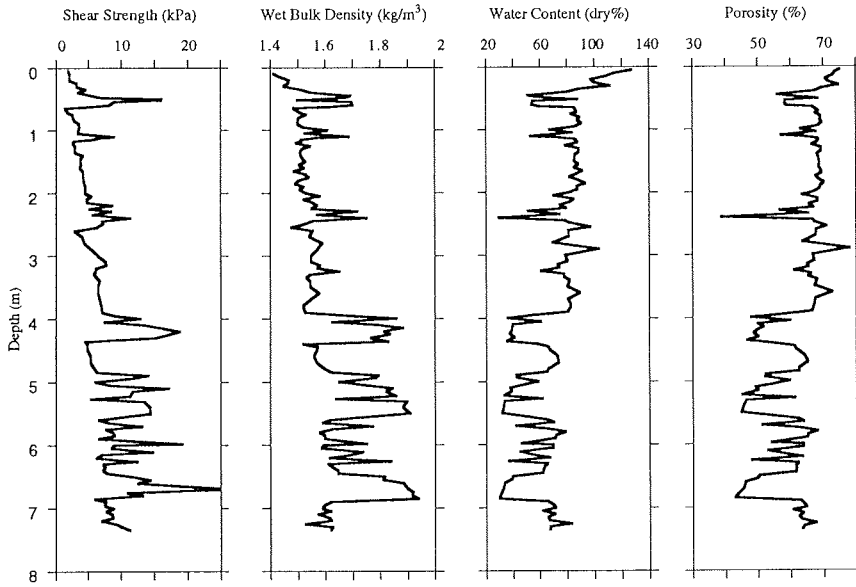


Fig. 6.4.7-1: Sediment texture and content of foraminifers of kastenlot Core PS2212-3 from Yermak Plateau as based on smear slide estimates.

2212-3 YERMAK PLATEAU



2213-6 YERMAK PLATEAU

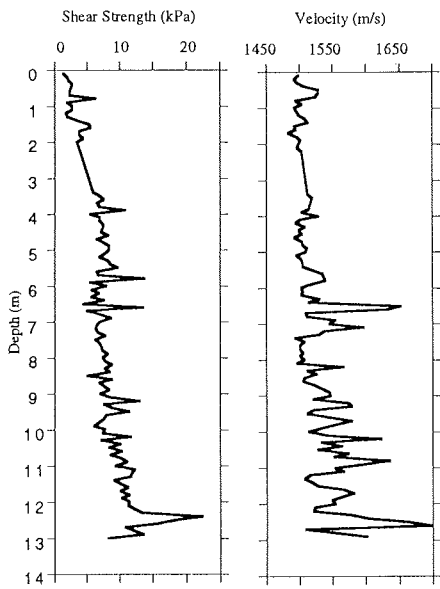


Fig. 6.4.7-2: Physical properties of sediment cores of Yermak Plateau.

Physical Properties

The sediments of the Yermak Plateau exemplify a normally consolidated sequence, represented by increasing shear strengths, bulk densities and velocities with depth, and decreasing porosities and water contents with depth (Fig. 6.4.7-2). Spikes in the curves can be correlated to coarser sediment beds, and to ice rafted debris layers (mud clasts and dropstone intervals). The property curves from the lower part of the sediment sequence in the cores (below 4 m in the Kastenlot PS2212-3 and below about 6 m in the Piston Core PS2213-6), show higher amplitude variations in the physical properties than above, reflecting the coarser sediment type of this interval. There appears to be good correlation between the cores from different sites, although all of the physical property data are not yet available.

Magnetic Susceptibility

The kastenlot Core PS2212-3 (water depth 2,550 m, Fig. 6.4.7-3) yielded almost the same susceptibility log as the gravity core of the nearby Site PS1533 (water depths 2,030 m) of ARK-IV/3 which is dated by different techniques (EISENHAUER unpubl., KÖHLER 1991, NOWACZYK 1991, NOWACZYK & BAUMANN in press). By correlation to this core it can be concluded that oxygen isotope stage 2 is located at

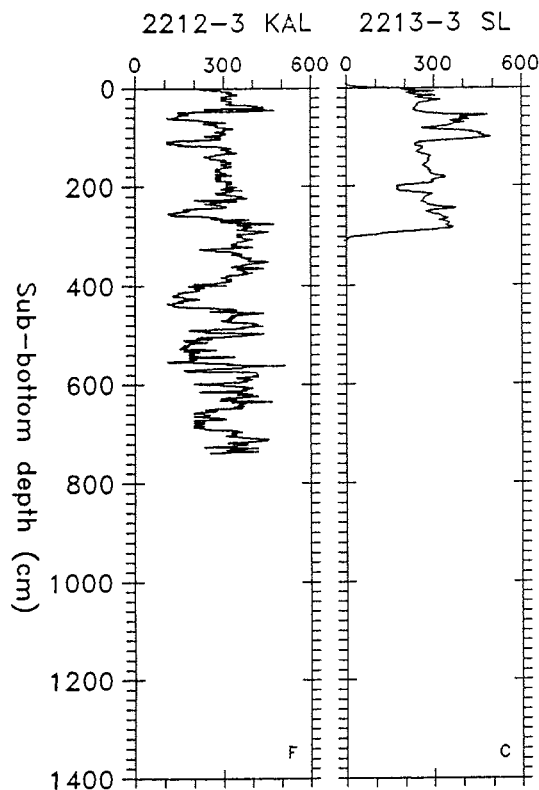


Fig. 6.4.7-3: Magnetic susceptibility of cores taken at the Yermak Plateau.

a depth of approximately 110 cm and stage 2/4 at a depth of around 390 cm. Therefore sedimentation rates based on this correlation are in the range of 3-5 cm/ky at Site PS2212. There is no clear correlation between this site and Site PS2213 to the southwest on top of the Yermak Plateau (water depth 848 m), although susceptibility oscillates within the same range ($100-500 \times 10^{-6}$, SI).

Further Studies

The samples collected from the Yermak Plateau during this expedition will allow to address a number of important scientific problems, namely:

- The pre-Quaternary deposits immediately above volcanic basement will aid in determining the minimum age of the build up of the volcanic foundation of the Yermak Plateau. Their age apparently is not easily reconciled with the presently assumed age of the outer part of Yermak Plateau. At the same time, this core means encouragement to sample systematically out-cropping pre-Quaternary sediments at suitable locations.
- The Quaternary deposits provide for excellent, detailed stratigraphies with relatively high fossil contents. The history of the Vestspitsbergen Current on its way under the Arctic pack-ice cover can be reconstructed in detail.
- Cores at the planned ODP positions provide a base for establishing a paleoceanographic record of the short-term variability of the eastern Arctic Basin, whose long-term variability will be studied by means of deep-sea drilling in 1993.

6.5 Physical Properties of Sediments

6.5.1 Physical Property Methods (H. Kassens, K. Moran and D. Mosher)

Physical properties measured on board included acoustic compressional wave velocity (p-wave), undrained shear strength, index properties (e.g. water content, porosity) and electrical resistivity.

P-wave velocity was measured using the Digital Sound Velocimeter (DSV). This velocimeter uses a standard travel time method for determination of sound velocity. In this method, four probes are pushed into the split section of the sediment core, two for measurement of velocity in the longitudinal direction (along the z-axis of the core) and two for measurement in the direction transverse to the axis of the core. The travel time from the transmitter to the receiver in each direction is measured. The transducer separation is measured by placing the transducer in distilled water of known velocity, whereby travel time is measured and separation can be calculated. The p-velocity is then determined by dividing the separation by the measured travel time. All p-wave velocity measurements reported here are uncorrected for *in situ* temperature and pressure.

Two different miniature vane shear instruments were used to measure undrained shear strength, the viscometer and the Wykeham-Farrance motorized vane shear device. The undrained shear strength of all box and kastenlot cores were determined using a Haake viscometer (Rotationsviskosimeter, RV3). A 20 mm x 8.8

mm vane was used with this instrument, inserted 1 cm deep into the sediment and rotated at a speed of 4 rotations per minute ($24^\circ/\text{sec}$). At each depth interval, two to three measurements were made in order to determine the scatter associated with sediment inhomogeneities, such as bioturbation. The measurement interval ranged from 2-10 cm. This instrument was kindly provided by F.C. Kögler, Univ. of Kiel for this cruise. The Wykeham-Farrance device was used to measure strength on the piston core and was run at $50^\circ/\text{min}$, using a standard 1:1 ratio vane. Measurements were made at intervals of 5 to 10 cm. Shear strength was measured at peak failure, and some tests were allowed to run to a constant post-peak value. All values are reported in kPa as "shear strength" and "residual strength", respectively.

Index properties of sediments include water content and bulk density. From these two basic properties, other sediment phase relationships can be derived (e.g. void ratio, porosity, dry density). The index properties can be determined from the direct measurement of the total mass of the sample (M_t), the dry mass of the sample (M_d), and the total volume of the saturated sample (V_t).

To compensate for ship's motion, mass is determined using a technique of differential counterbalancing on twin top loading electronic balances. The ship's motion is partially compensated by a reference balance (A), which has a matched load to the sample balance (B) with the sample of unknown mass (M_t). The balance are configured with an analog 0-5 volt output over a 50 g range. The voltage output of each balance is directed to a differential amplifier. The voltage difference is digitized and then processed on a microcomputer. This method of differential counterbalance is described by CHILDRESS & MICKEL (1980). The computerized precision electronic balance system (LUTZE et al. 1988) used during this cruise was kindly provided by M. Sarnthein, Univ. of Kiel.

A known mass (M_k), ideally within 1 g of unknown mass, is placed on a balance A. The unknown mass (M_t) is placed on balance B. The differential signal should then be the difference (in Volts) between M_k and M_t . This differential voltage is averaged over time (several cycles of ship's roll period). The differential mass (M_{diff}) is calculated by linear regression from the calibration curve. The unknown mass is then $M_t = M_{\text{diff}} - M_k$. The balance system was used in a non-counterbalance mode simply by using zero as the known mass.

Sample volume was determined using two different methods. One method was using a constant volume sampling tube of 10 cm^3 . The tube was carefully pushed into the sediment, then cut out, trimmed and weighed. The second method used a Helium gas pycnometer. The volume of a material can be determined using an ideal gas pycnometer. This method is based on Archimedes principle of fluid displacement for the determination of solid volume. The fluid used is an ideal gas (He) so that the finest pore spaces can be penetrated. The sample is placed in a chamber of known (calibrated) volume and pressurized, using He, to a known pressure. The pressurized sample is then ported (using a solenoid valve) to another chamber of known volume (which has been purged with He) and the subsequent pressure is measured. Using the ideal gas law, the sample volume can be calculated. The instrument used, was a commercial one manufactured by Quantachrome Corp., the Penta-Pycnometer.

After determination of the total (wet) mass and volume, samples were dried using the freeze drying method. In this method samples which are quickly frozen at temperatures less than -30°C to avoid formation of crystalline ice. Sublimation of the frozen water is then carried out in the freeze dryer at a temperature of -48°C . Samples were left in the freeze dryer for periods of 24-48 hours, depending on sample size and the total number of samples in the freeze dryer.

Water content is reported in two ways, either as a percent ratio of water to total mass (w_t) or as a percent ratio of water to dry mass (w_d). In addition, because any dissolved salts contained in the pore fluid will change phase during drying of the sample, a correction for pore fluid salinity (r) must be included in both calculations of water content (NOORANY 1984). If, for example, pore fluid salinity is 35 ‰, then $r = .035$. The formulation are as follows :

$$w_t = (M_t - M_d) (1 + r) / M_t$$

$$w_d = (M_t - M_d) / (M_d - r M_t)$$

Bulk density (M_w) is the density of the total sample, including pore fluid or:

$$M_w = M_t / V_t$$

No corrections are required for this calculations. Units are SI reported in Mg/m^3 which is numerically equivalent to g/cm^3 . In addition to being one of the most basic measurements for determining material properties, bulk density is also one of two variables required for the calculation of reflection coefficients used in synthetic seismograms for correlation to reflection seismic records.

The two different methods (constant volume and penta-pycnometer) for wet volume determination were compared. Both methods were used and checked by measuring the dry volume of the samples in the penta-pycnometer. Using the dry volume measurements and water content, bulk density was calculated, independent of wet volume showing a good correlation. The comparison result in a mean precision of $\pm 0.002 \text{ Mg}/\text{m}^3$ for both methods.

The electrical resistivity or conductivity was used on sediment cores to estimate porosity and wet bulk density. The parameter was measured using a miniaturized Wenner configuration. The method was tested and routinely applied during the cruise for the rapid and efficient logging of all sediment cores.

The Wenner probe consists of a narrow plastic strip (16 x 4 x 100 mm) in which four platinum wires ($\varnothing 0.6 \text{ mm}$) were embedded lengthwise, 4 mm apart. The end of the probe was sharpened to form a wedge to facilitate easy penetration into the sediment. The measurements were taken in steps of 5 cm by pushing the probe a few millimeters into the sediment. At each depth 2-6 readings were used on a line perpendicular to the core axis in order to get representative resistivity data. During the measurement a stabilized alternating square wave current (330 Hz, 0.4 mA) was applied to the outer pair of electrodes, while the voltage changes were measured across the inner pair of electrodes. After amplification, the square wave voltage output was converted to a direct voltage, which is proportional to the electrical resistivity of the material.

The formation factor F is given by the ratio of the electrical resistivity R_s of saturated sediment to the electrical resistivity R_w of the interstitial water at the same temperature and pressure.

$$F = k \times P^{-m} = R_s / R_w$$

The formation factor can be related to porosity P and salinity of sediments by ARCHIE (1942) and others. It is inversely proportional to the porosity with the cementation factor m as exponent. The parameter k depends on the water saturation of the sediment and is approximately 1. During the shipboard work the constants were chosen after BOYCE (1968): $k = 1.3$, $m = 1.45$. In addition, the electrical resistivity is controlled by the temperature and the concentration of dissolved electrolytes in the interstitial water. Assuming that the concentration of dissolved ions in the pore fluid is equivalent or close to that in sea water standard, a temperature calibration of the probe can be carried out using the sea water standard, so that the temperature dependence can be eliminated. Wet bulk density values can then be calculated from porosity values after BOYCE (1976):

$$M_w = (P \times M_f) + (1 - P)M_g$$

with a pore fluid density of $M_f = 1030 \text{ kg/m}^3$ and a grain density of $M_g = 2,670 \text{ kg/m}^3$.

Fig. 6.5.1-1 compares wet bulk density and porosity logs of square-barrel kastenlot Core PS2178-5 (Makarov Basin) derived from electrical resistivity measurements and from standard methods, as described above. Both methods reveal a similar downcore variation of the porosity values. Differences are observed in depth intervals from 150-330 cm and from 430-510 cm. They may be caused by different sample locations and spacing chosen for the two methods: The resistivity probe was inserted into the sediment at a regular 5 cm spacing but the sediment samples used for the standard method were taken in steps of 5 cm or 10 cm. Moreover the electrical resistivity measurements were carried out immediately after the cores were opened, the samples for the standard methods were taken some hours up to several days later. The comparison of the wet bulk density (WBD) curves derived from both methods (Fig. 6.5.1-1) also shows a good agreement for the complete core with only minor differences.

It should be pointed out that the porosity was determined assuming a constant parameter k , and a constant cementation factor m . To calculate wet bulk density, a constant grain density was used. Both, porosity and wet bulk density values derived from the electrical resistivity, show a very good agreement with the standard measured wet bulk density and porosity values. Within given implicit uncertainties, these measurements can be used well to estimate porosity and wet bulk density data of sediments.

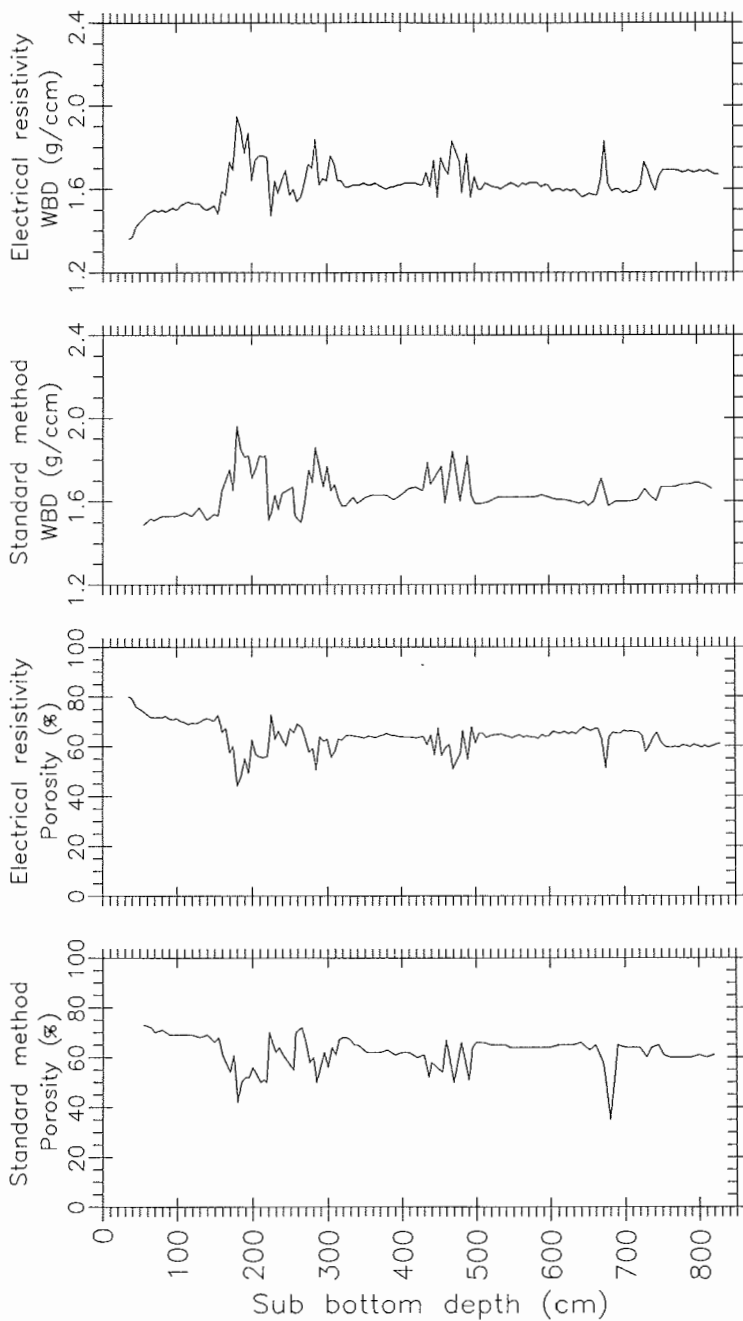


Figure 6.5.1-1: Comparison of porosity and wet bulk density (WBD) logs of square-barrel kastenlot Core PS2178-5 (Makarov Basin: 88° 01.5' N, 159° 42.2' E) derived from electrical resistivity measurements and from standard method.

6.5.2 Paleomagnetic and Mineral Magnetic Investigations (N. Nowaczyk and T. Frederichs)

Magnetostratigraphy

During the ARK-VIII/3 expedition an intense paleomagnetic sampling program was carried out on the sediment series recovered with the different coring tools. Vertically oriented paleomagnetic cubic samples of about 7 cm³ were generally taken at intervals of 5 cm or less from square barrel kastenlot (KAL) and giant piston cores (GPC). In addition, the kastenlot cores and the large box cores (GKG) were continuously sampled with U-shaped 28 x 28 mm plastic liners. The high sampling density is required to evaluate a high resolution Quaternary magnetostratigraphy based on short geomagnetic excursions and polarity events within the Brunhes normal polarity chron. Sediments from the Norwegian-Greenland Sea and the Arctic Ocean previously proved to contain almost ideal records of this type of geomagnetic variations (LØVLI 1989, BLEIL & GARD 1990, NOWACZYK 1991, NOWACZYK & BAUMANN in press).

A detailed shorebased paleomagnetic analysis will use the Bremen University laboratory facilities. The natural remanent magnetization (NRM) is measured with a cryogenic magnetometer (GM 400, Cryogenic Consultants). To remove unstable viscous overprints, the NRM of each sample will be treated by progressive alternating field (AF) demagnetization. Typically eight steps with maximum field amplitudes of up to 100 mT and, where necessary, additional steps up to 250 mT are applied using a 2G alternating field demagnetizer. A single step demagnetization based on the demagnetization characteristics of a few representative "pilot samples", as often reported in literature, must be regarded as insufficient for establishing high quality geomagnetic event stratigraphies (NOWACZYK 1991, NOWACZYK & BAUMANN in press).

Magnetic Susceptibility

Exposed to a magnetic field H , all material exhibits an induced magnetization M_i

$$M_i = k \times H$$

In general, the magnetic susceptibility k is an anisotropic parameter. The difference between maximum and minimum susceptibility may reach up to 15 % in natural rocks. For most purposes, however, an isotropic approximation is quite appropriate. Most rock-forming minerals are either paramagnetic or diamagnetic with susceptibilities of some -10^{-6} to $+10^{-6}$ SI. Only ferrimagnetic minerals, in particular (titano-) magnetites, have susceptibilities of up to $+10^{-2}$. The susceptibility of marine sediments thus mainly reflects their (titano-) magnetite concentration. Various sources can contribute to the flux of these magnetic minerals into marine sediments (THOMPSON & OLDFIELD 1986). For the study area, the influence of ice-rafted detritus is of special interest.

Measurements of magnetic volume (bulk) susceptibility were done with a BARTINGTON M.S.2. control unit applying two different sensors. The sensitivity of this device depends on the integration time used for the measurement. In the fast

but less precise mode, a reading can be taken in less than one second and the result is given in integer multiples of 10^{-5} . In the slower, high precision mode a measurement takes 10 sec, and the result is given in integer multiples of 10^{-6} .

The unsplit gravity and piston cores were logged with a loop sensor (BARTINGTON M.S.2.C) in intervals of 1 cm using the high precision mode only where necessary. This sensor is a single frequency device ($f = 565$ Hz) for cores with diameters of up to 130 mm. For comparing measurements taken on cores with different diameters, the results are converted to multiples of 10^{-6} using a correction curve supplied with the manual of the M.S.2.C sensor.

Measurements taken with the loop sensor are the result of a weighted integral along the core axis over a quite large volume. The response function of this sensor with respect to a thin test disk has the shape of a Gaussian curve with a half-width of 55 mm. By Fourier analysing the M.S.2.C sensor characteristic, it can be shown that wave-lengths shorter than about 3 cm are totally filtered out. Therefore, core logs obtained with the loop sensor contain only the low frequency component of the true distribution of the magnetic susceptibility (NOWACZYK 1991).

To define the actual zero level of the instrument, the profile has to be extended over both ends of each core section by at least 10 cm. These zero levels were used to calculate a linear instrument drift which was then subtracted from the data of the profile. The complete susceptibility log of a long sediment core is obtained by adding the overlap of adjacent segments.

The second sensor used for susceptibility logging is a cylinder-shaped single frequency ($f = 580$ Hz) BARTINGTON M.S.2.F probe with a diameter of about 15 mm and very narrow response function (half-width 12 mm). For the measurement, it is lowered directly onto the sediment surface. Even thin sediment layers of only a few mm with differing susceptibilities can be detected with this sensor. On the other hand, because of the small volume covered by one measurement, the sensitivity of this probe is lower than that of the M.S.2.C loop sensor.

Sub-cores with a size of 28 x 28 mm and a maximum length of 1,100 mm taken from the box cores (GKG) and the kastenlot cores (KAL) as well as the archive halves of the piston cores were scanned with the M.S.2.F probe. The logging was done in steps of 5 mm with zero readings every 50-100 mm for monitoring of the sensor stability. Any drift was then interpolated linearly between these readings and subtracted from the susceptibility log. Because of the large number of data points (200/m) measurements with the M.S.2.F probe could only be run in the fast (lower precision) mode.

Shorebased analyses of the paleomagnetic samples taken from the recovered sediments will be done with a BARTINGTON M.S.2.B dual frequency susceptibility sensor ($f_1 = 460$ Hz, $f_2 = 4,600$ Hz) in the high precision mode (integer multiples of 10^{-6}) to determine the grain size distribution of the ferrimagnetic mineral phases.

In addition, the complete anisotropy tensor of the magnetic susceptibility will be measured with a GEOFYZIKA BRNO Kappabridge KLY-2 (maximum sensitivity: integer multiples of 5×10^{-8}) for selected paleomagnetic samples. The results should give some detailed informations about the sedimentational environment.

Furthermore, the anisotropy of magnetic susceptibility provides a test for the reliability of paleomagnetic directions as this parameter allows to discriminate effects introduced by deformation of the sediment texture.

Comparison of Coring Tools

At Site PS2176 in the Amundsen Basin (see Fig. 6.3-2) three different coring tools were employed, a 12 cm diameter gravity corer (SL), a 30 x 30 cm kastenlot corer (KAL) and a 10 cm diameter giant piston corer (GPC). An unequivocal correlation of the three cores is given by a series of characteristic features in the susceptibility logs (Fig. 6.4.3-3). In particular, an interval of increased susceptibilities can be precisely traced in all three cores. In the gravity core, it is found between 150-187 cm sub-bottom depth of, at 190-227 cm in the kastenlot, and at 260-315 cm in the piston core.

More detailed high-resolution susceptibility logs were run with the M.S.2.F sensor

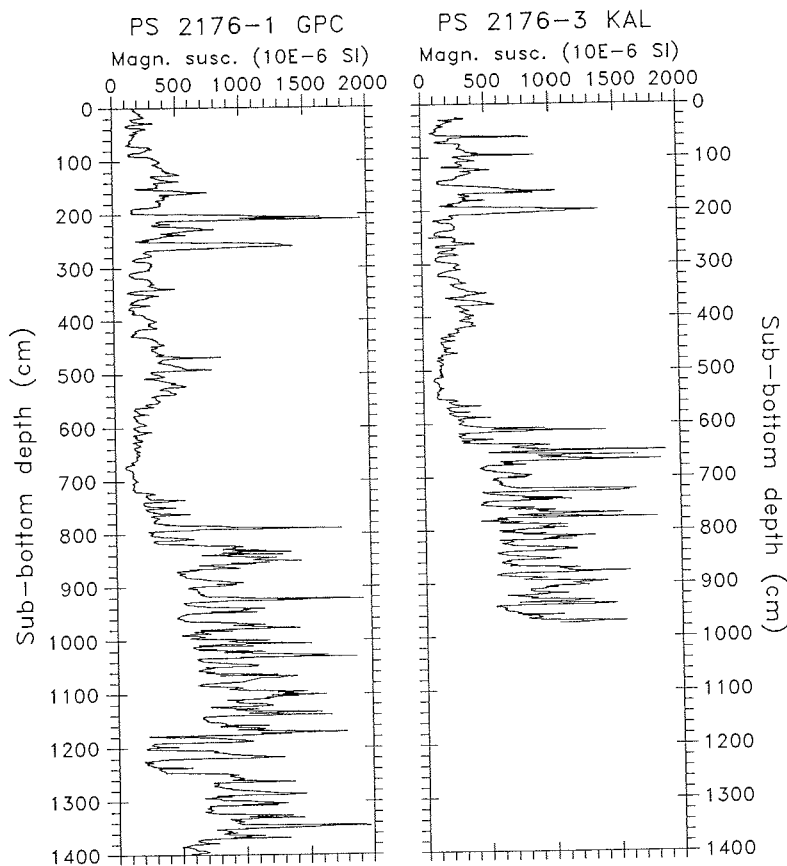


Fig. 6.5.2-1: High-resolution magnetic susceptibility logs for Piston Core 2176-1 (left) and Kastenlot 2176-3 (right), taken at the same site in the Amundsen Basin.

for the neighboring Piston Core PS2176-1 and Kastenlot Core PS2176-3 (Amundsen Basin, Fig. 6.5.2-1). On the basis of this data set (200 data points per meter) both cores can be correlated on a very fine scale. From about 60 peaks and troughs identified in the susceptibility profiles of both cores it was possible to define a "sub-bottom depth conversion graph" (Fig. 6.5.2-2). If both cores would have recovered identical sediment sequences without any disturbances, a linear function with slope 1 and intercept 0 should result. Instead, the Piston Core PS2176-1 (penetration 1850 cm; recovery 1421 cm) is apparently stretched relative to the Kastenlot PS2176-3 (penetration 1080 cm; recovery 976 cm). Moreover, there is an offset of about 20 cm at a sub-bottom depth of Core PS2176-3, indicating that this amount of material is missing in the piston core PS2176-1 (this, however, might be due to a bag sample that was not taken into account when the depth scale was defined for piston core PS2176-1).

In the present case stretching of Piston Core PS2176-1 can be corrected in detail by using the graph of Figure 6.5.2-2 as shown in the susceptibility logs of Figure 6.5.2-3. From this it can be concluded that the piston core 2176-1, although it contains a 400 cm longer recovery than the kastenlot PS2176-3, from the stratigraphic point of view is only 210 cm longer. Such systematic discrepancies of sediment sequences recovered by different coring tools have to be taken into account when calculating and comparing sedimentation rates.

Other examples illustrating differences between sediment sequences recovered by different gears at the same site (gravity corer and piston corer of different diameter and kastenlot) have been discussed by GARD (1987), NOWACZYK (1991), and in THIEDE & HEMPEL (1991).

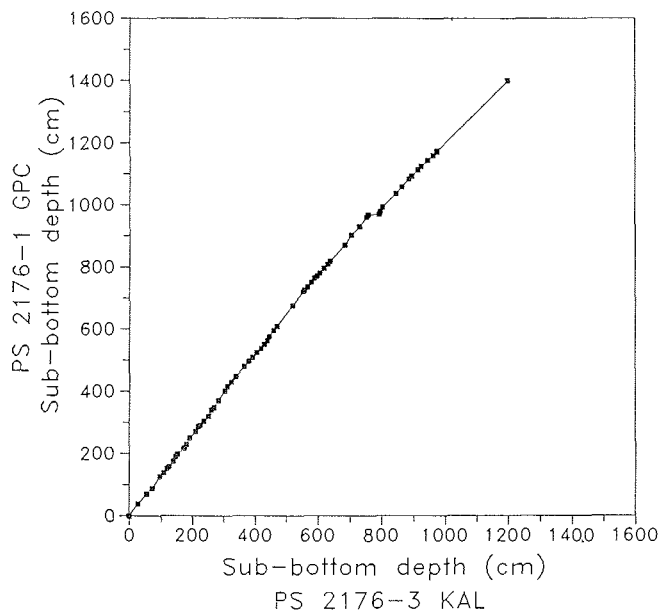


Fig. 6.5.2-2: "Sub-bottom depth conversion graph" for Piston Core 2176-1 and Kastenlot 2176-3 (Amundsen Basin) derived from Figure 6.5.2-1.

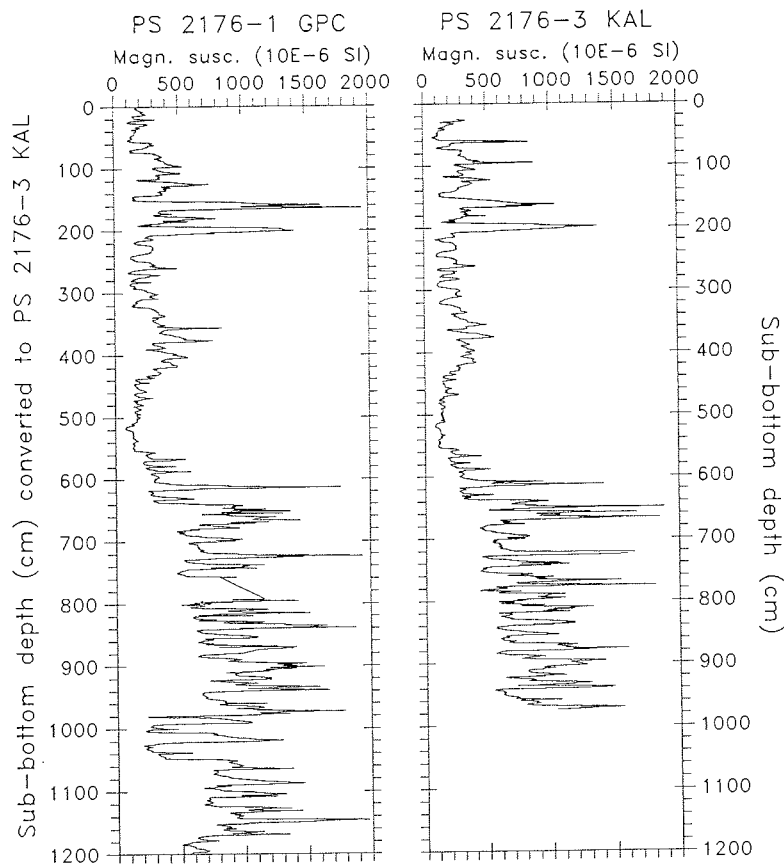


Fig. 6.5.2-3: High-resolution magnetic susceptibility log of Piston Core 2176-1 converted to the sub-bottom depth of Kastenlot 2176-3 using the conversion function of Figure 6.5.2-2.

6.5.3 Electrical Resistivity in Sediment Cores (U. Bergmann, T. Frederichs and N. Nowaczyk)

Electrical resistivity logs were run on all sediment cores recovered during the cruise with the aim to test this parameter as a measure for porosity and wet bulk density.

A miniaturized Wenner configuration has been used for the measurements consisting of a narrow plastic strip (16 x 4 x 100 mm) in which four platinum wires (\varnothing 0.6 mm) were embedded lengthwise, 4 mm apart. The lower end of the probe was sharpened to form a wedge to facilitate an easy penetration of a few mm into the sediment. At depth intervals of typically 5 cm, two to six readings were taken on a transect perpendicular to the core axis in order to get representative resistivity data at each horizon. For the measurement a stabilized alternating square wave current

(330 Hz, 0.4 mA) is applied to the outer pair of electrodes and the electric field gradient determined across the inner pair of electrodes. After amplification, their square wave voltage output is converted to a direct voltage which is proportional to the electrical resistivity of the sediment.

The porosity P of sediments is related to the so-called formation factor F , defined as the ratio of the electrical resistivity R_s of the sediment to the electrical resistivity R_w of the interstitial water at the same temperature and pressure:

$$F = k \times P^{-m} = R_s / R_w \quad (\text{ARCHIE 1942})$$

The formation factor is inversely proportional to the porosity with the cementation factor m as exponent. The parameter k is controlled by the water saturation of the sediment and amounts to approximately 1. For the shipboard data evaluation the constants were chosen according to BOYCE (1968): $k = 1.3$, $m = 1.45$.

The electrical resistivity readings critically depend on the temperature and the concentration of dissolved electrolytes in the interstitial water. On the assumption that the concentration of dissolved ions in the pore fluids were equivalent or close to that in sea water, a calibration of the probe was carried out using a seawater standard to eliminate the temperature dependence.

After BOYCE (1976) wet bulk densities D_w can be calculated from porosity data:

$$D_w = (P \times D_f) + (1 - P) D_g$$

with a pore fluid density of $D_f = 1.03 \text{ Mg/m}^3$ and a grain density of $D_g = 2.67 \text{ Mg/m}^3$.

Figure 6.5.1-1 compares porosity and wet bulk density logs of Kastenlot PS2178-5 (Makarov Basin) derived from electrical resistivity measurements with those determined by the traditional methods described before. Both data sets show an almost identical downcore variation in porosity. Minor differences are observed only in depth intervals from 150-330 cm and from 430-510 cm sub-bottom. This may be caused by slightly different sample locations of the two methods, and perhaps also by the fact that the electrical resistivity measurements were carried out immediately after the cores had been opened while the samples for the standard methods were taken hours to several days later. The wet bulk density (WBD) curves derived from both methods reveal a similar good agreement for the entire core with only some small discrepancies.

In summary, within given implicit uncertainties, both porosity and wet bulk density data derived from electrical resistivity measurements on Arctic Ocean sediments show convincing consistency with conventional weighting method results. Electrical resistivity measurements should be well suited therefore as a rapid and efficient onboard logging technique to determine sediment porosity and wet bulk density. Further shorebased analyses will have to validate in some detail the present simple assumptions of a constant parameter k , a constant cementation factor m , and a constant grain density D_g .

6.6 Biostratigraphy: Calcareous Nannofossils (G. Gard)

Shipboard analyses of calcareous nannofossils were made for biostratigraphic purposes. In addition, samples were taken for onshore studies of planktic and benthic foraminifers, diatoms, ostracods and palynology. Some of these studies will yield biostratigraphic information, as will further onshore studies of calcareous nannofossils.

In the Nansen Basin, the late Holocene is indicated by the presence of *Coccolithus pelagicus* (GARD 1988) in the uppermost few to over 30 cm at all investigated sites. This suggests that linear sedimentation rates for the late Holocene are in the order of cm per 1000 years in the Nansen Basin. Other taxa present are *Emiliana huxleyi*, *Calcidiscus leptoporus*, *Gephyrocapsa* sp. and the occasional *Helicosphaera carteri* and *Syracosphaera pulchra*. Below the Holocene interval, the sediments are usually barren of nannofossils but rare specimens of *Gephyrocapsa* spp. are occasionally present. These represent the late Quaternary.

On the Gakkel Ridge the late Holocene is represented by a few cm of rare to common nannofossils, mainly *E. huxleyi* and *C. pelagicus*. At Site PS2163, oxygen isotope stage 5, or a part thereof, is represented by abundant specimens of *Gephyrocapsa* spp. in conjunction with few *C. pelagicus* (GARD 1988). Deeper sediments are barren of calcareous nannofossils.

Only traces of calcareous nannofossils are found at most investigated sites in the Amundsen Basin, on the Lomonosov Ridge, in the Makarov Basin, and on the Morris Jesup Rise. These are Quaternary, however, no other age assignments have so far been done as the Arctic nannofossil biostratigraphy, to a large extent, rely on abundance variations (GARD 1988, GARD & BACKMAN 1990) which require that a statistically significant number of specimens is observed.

From the Yermak Plateau, only a short gravity core (26 cm) was analysed for calcareous nannoplankton shipboard. This core contained abundant *C. pelagicus* and *E. huxleyi* in the top two cm, which is indicative of the Holocene. Below the assemblage is mixed, with Quaternary *Gephyrocapsa* spp. and a significant amount of reworked late Eocene taxa.

Methods

Smear slides were prepared from toothpick samples and studied in a light microscope at x1500 magnification in normal light and with crossed nicols.

Taxonomic List

Helicosphaera carteri (Wallich 1877) Kamptner 1954
Emiliana huxleyi (Lohmann 1902) Hay & Mohler in HAY et al. 1967
Calcidiscus leptoporus (Murray & Blackman 1898) Loeblich & Tappan 1978
Coccolithus pelagicus (Wallich 1877) Schiller 1930
Syracosphaera pulchra Lohmann 1902
Gephyrocapsa sp. Kamptner 1943

2157 -4, GKG	2174 -3, GKG
-6, GPC + TWC	-5, KAL
2158 -1, GKG	2175 -3, GKG
2159 -4, GKG	-5, GPC + TWC
-6, GPC	2176 -3, KAL
2161 -3, GPC + TWC	-4, GKG
-4, GKG	2177 -1, GKG
2162 -1, GKG	-5, KAL
2163 -2, GKG	2178 -2, GKG
-3, GPC + TWC	-5, KAL
2164 -4, GKG	2179 -1, GKG
-6, GPC	2180 -1, GKG
2165 -1, GPC	2181 -3, GKG
-3, GKG	2182 -1, GKG
-4, KAL	2183 -1, GKG
2166 -2, GKG	2184 -1, GKG
2167 -1, GPC	2185 -6, KAL
-2, GKG	2187 -1, GKG
2168 -1, GKG	-4, KAL
2170 -1, GKG	2189 -5, GPC + TWC
-3, GPC	2197 -1, KAL
2171 -1, GKG	2200 -5, KAL
-3, KAL	2211 -1, SL
2172 -1, GKG	
2173 -1, KAL	

Tab. 6.6-1: List of cores analysed for calcareous nannofossils.

7. GEOPHYSICAL INVESTIGATIONS

From a geophysical point of view the Arctic Ocean is still the least known region of the world's oceans. More or less systematic mapping activities began after the second world war but due to the permanent ice cover geological and geophysical knowledge increased only slowly.

The Arctic Ocean is divided into the Eurasia Basin and the Amerasia Basin by the submarine transpolar Lomonosov Ridge which has an elevation of more than 3,000 m above the adjacent abyssal plains. The ridge was discovered in 1948 by Soviet oceanographers although the existence of a barrier had already been postulated in 1904 and 1936 on theoretical grounds from tidal analysis. In 1961 it was first postulated that the Mid-Atlantic rift system extend into the Eurasia Basin. The seismicity and bathymetric profiles collected by submarines supported the presence of a plate boundary accommodating the present motion between the Eurasian and North American continents. Aeromagnetic surveys carried out by Soviet and United States institutions during the late 1960's and early 1970's mapped a pattern of lineated magnetic anomalies that are symmetric with respect to the Gakkel Ridge. By correlation of this magnetic pattern to the geomagnetic polarity time scale, it was inferred that the Eurasia Basin formed by Cenozoic crustal accretion at the Gakkel spreading center concurrently with the opening of the Norwegian-Greenland Sea to the south. The Gakkel Ridge represents an end-member of the global oceanic rift system as the rate of total opening are among the lowest observed anywhere due to the relative proximity of the pole of rotation which describe the motion between Eurasia and North America. The present rate is 1.6 cm/yr. and was as low as 1.2 cm/yr during the late Oligocene.

Geophysical Data Base

Besides the aeromagnetic data set the present geophysical data base from the Eurasia Basin contains more than 1,700 km of seismic reflection, depth and gravity measurements collected from drifting ice stations. 1,500 km of the seismic data are single-channel data of which 350 km have been collected with a small airgun (0.15-0.7 l) and the remainder with a 5-9 kJ sparker. Most of the sparker data are of poor quality. In 1982, 200 km of multi-channel seismic data were obtained with a 20 channel sonobuoy array and a 2 litre air gun north of Yermak Plateau. 22 seismic refraction experiments have been carried out and over 30 heat flow measurements have been made. Traverses by nuclear submarines since 1958 have contributed towards mapping of the main bathymetric features.

Scientific Objectives

The main scientific objectives of the marine geophysical program were to:

- obtain a seismic reflection profile across the Eurasia Basin for first order mapping of the sediment distribution and its seismic stratigraphy above oceanic crust of known age;
- investigate the sedimentary cover and the crustal structure of the Lomonosov Ridge to elucidate its origin and subsidence history;

- determine the extent of a sedimentary cover and the nature of the basement of the marginal plateaus Morris Jesup and Yermak;
- obtain further data on the thickness of the oceanic crust to evaluate any dependence of crustal thickness with very slow spreading rate.

Geophysical data acquisition in ice-covered waters is foremost a challenge in engineering which has received little attention among explorationists. The marine geophysical program on *Polarstern* was designed with a multifaceted approach to the practical problems of moving through or on the ice with instruments under tow, including the unique opportunity of having two icebreakers moving in tandem. In combination with favourable ice conditions we were able to collect approximately 1,500 km of multi-channel seismic data. The seismic lines are displayed in Figure 7-1. The main components of the program are listed in Table 7-1.

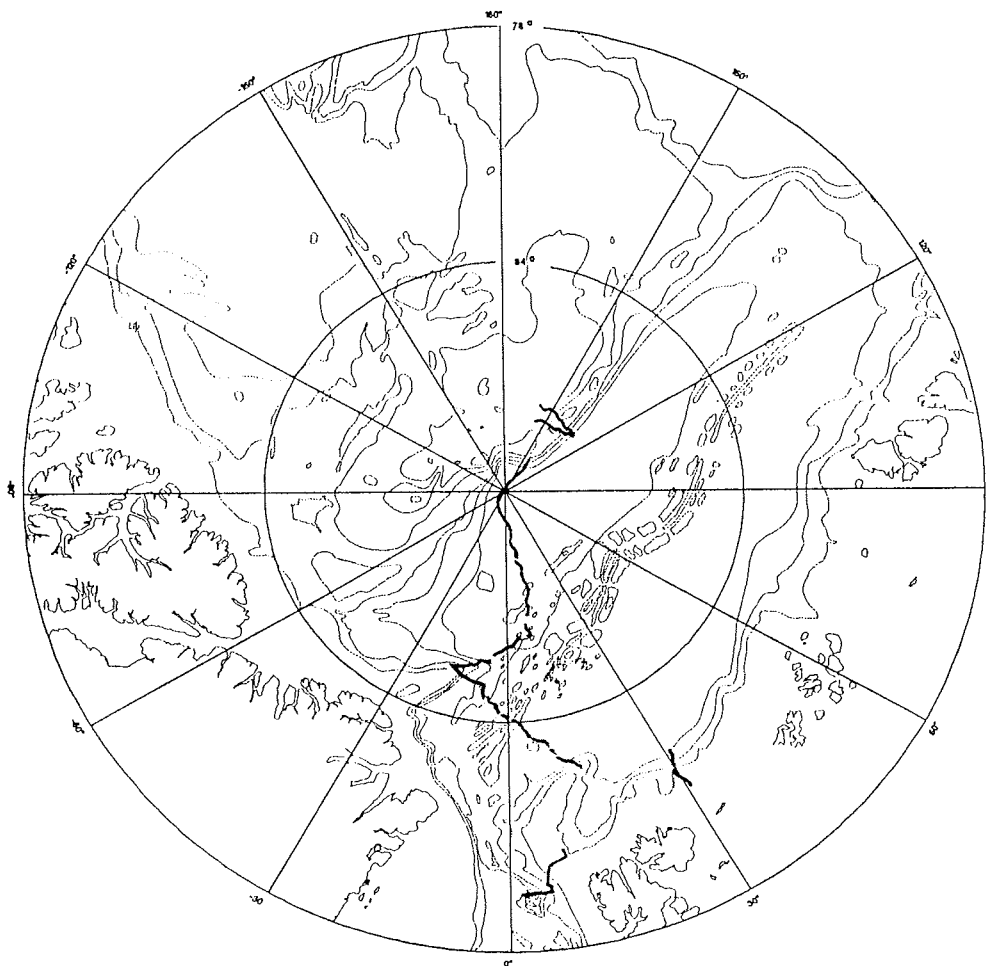


Fig. 7-1: Positions of seismic reflection lines and sonobuoy locations measured during *Polarstern* ARK-V/III/3 cruise / ARCTIC'91.

Program	Sources	Receivers
Marine seismic reflection	8x3 litre tuned array mounted under frame	12 channel , 500 m long streamer 24 channel , 800 m long streamer
	2x3 litre air guns	12 channel, 500 m long streamer
	2x3 litre air guns below 1.5 ton weight	50 channel, 100 m long streamer
Over-ice seismic reflection	dynamite 0.55-11 kg	10-12 channel, 250-600 m snow streamer group int. 25-50 m.
Seismic refraction and wide angle reflection	8x3 litre tuned array mounted under frame; 2x3 litre air guns below 1.5 ton weight	12 channel Reftek 3-comp. seismometer, geophone arrays and two hydrophones sonobuoys (Fairfield), 12 channel, 375 m long snowstreamer
Gravity		KSS 31/25 sea gravimeter
Magnetotelluric measurement	natural electromagnetic fields	

Table 7-1: Summary of the geophysical program components and equipment.

7.1 Marine Geophysics (W. Jokat, M. Alvers, V. Bouravtsev, B. Heesemann, Y. Kristoffersen and G. Uenzelmann-Neben)

For the marine part of the experiment it was essential to have an icebreaking vessel moving ahead of the ship towing the geophysical equipment to break a more or less ice free channel so that the towing ship could avoid any long stops. For several operational and scientific reasons, *Oden* and *Polarstern* did not rendezvous until their departure from the Lomonosov Ridge. Nevertheless, it was possible to collect some 400 km of MCS data in single ship operation in 7/10 to 9/10 of ice cover. Data of excellent quality were collected when *Oden* broke a channel ahead of *Polarstern* (profile 91097 and onwards). Table 7.1-1 summarizes the collected seismic lines.

Seismic Equipment and Towing Techniques

Continuous movement of the ship and secure towing of the equipment especially under heavy ice conditions, are essential for marine seismic measurements in the arctic basin. We therefore describe briefly some modifications and problems:

S o u r c e

Two different seismic source configurations were used. The big array (Fig. 7.1-1) consisted of eight PRAKLA SEISMOS airguns (3 l each) with a total volume of 24 l. The guns were tuned to produce a signal spectrum up to 120 Hz. In most cases sufficient guns were operating and no significant bubble pulse was visible. The total weight of the system is approximately 1 ton.

Table 7.1-1: Summary of all seismic profiles shot during the cruise ARK-VIII/3.

Profile	Time Range	Leadin	Streamer (m)	Chan	dx Chan	Airgun	Shots	x [km]	Start Lat	Start Lon	End Lat	End Lon
91010	05.08.91 10:26:59 - 06.08.91 03:19:37	42	50	6	8	8x3	4457	81	81,0366	30,2560	81,7522	29,8534
91020	06.08.91 16:34:02 - 06.08.91 23:22:00	42	50	6	8	8x3	1930	35	81,8040	30,2542	82,1161	30,6183
91030	10.08.91 19:10:00 - 10.08.91 20:07:00	none	Sonobuoy	1	none	8x3	none	none				
91041	13.08.91 10:50:00 - 13.08.91 15:09:00	none	Overice/REFTEK	3	none	8x3	475	1	86,2425	59,2272	86,2406	59,3390
91042	16.08.91 01:10:13 - 16.08.91 09:03:00	none	Overice/REFTEK	6	none	8x3	372	2	86,8538	56,7375	86,8425	56,9081
91043	23.08.91 16:47:00 - 23.08.91 23:05:00	none	Overice/REFTEK	6	none	8x3	179	4	87,5767	103,6447	87,6101	103,8639
91060	21.08.91 09:28:00 - 21.08.91 10:08:00	none	only Sonobuoy	1	none	8x3	1217	6	87,7647	108,7852	87,7982	107,7931
91070	25.08.91 11:23:00 - 26.08.91 09:04:00	none	Overice/REFTEK	6	none	8x3	544	14	88,0574	140,4788	88,0369	144,0262
91080	27.08.91 20:38:00 - 27.08.91 22:27:24	42	50	6	8	1x3	4009	144	88,0170	156,9241	87,7611	130,1684
91090	29.08.91 15:53:24 - 30.08.91 09:00:00	195	300	12	25	2x3	4622	126	87,7391	130,0788	87,5982	157,8986
91091	30.08.91 10:14:00 - 31.08.91 05:54:44	195	300	12	25	2x3	817	9	87,5307	144,2736	87,5301	146,1029
91092	02.09.91 07:07:00 - 02.09.91 20:42:00	none	Overice/REFTEK		none	8x3	626	12	87,5511	147,2977	87,6383	145,8996
91093	03.09.91 01:52:12 - 03.09.91 04:46:24	195	300	12	25	2x3	79	0	88,0160	145,3065	88,0197	145,2663
91094	03.09.91 12:36:48 - 03.09.91 12:52:00	195	300	12	25	2x3	359	4	88,5173	140,5216	88,5389	141,4486
91095	04.09.91 11:13:00 - 04.09.91 17:09:00	none	Overice/REFTEK		none	8x3	843	6	88,7311	129,4985	88,7617	127,6793
91096	05.09.91 04:45:00 - 05.09.91 18:20:00	none	Overice/REFTEK		none	8x3	5395	90	88,8926	143,8108	89,9913	-128,2500
91097	06.09.91 15:47:00 - 07.09.91 09:47:47	200/183	300	12	25	2x3	3283	104	89,8687	-49,0501	89,0068	9,4353
91098	08.09.91 10:58:35 - 09.09.91 02:21:00	183	300	12	25	8x3	2040	76	88,9515	7,8683	88,2761	9,8422
91100	09.09.91 11:15:56 - 09.09.91 20:20:03	183	300	12	25	8x3	2079	80	88,2116	7,2762	87,5066	11,7204
91101	10.09.91 10:41:20 - 10.09.91 19:52:48	183	300	12	25	8x3	2613	80	87,4870	11,5485	86,7773	9,7371
91102	11.09.91 04:38:00 - 11.09.91 16:13:54	183	300	12	25	2x3		24	86,7443	9,7329	86,5984	7,1230
91103	11.09.91 21:16:00 - 12.09.91 02:44:00	none	REFTEK			8x3	877	38	86,5608	7,3471	86,2500	9,4215
91104	12.09.91 10:26:19 - 12.09.91 14:19:59	183	300	12	25	8x3	551	24	86,2012	8,4484	86,1324	5,4091
91105	13.09.91 00:42:07 - 13.09.91 03:08:21	183	300	12	25	8x3	1013	40	86,1673	4,7862	85,9822	0,3128
91106	13.09.91 13:57:00 - 13.09.91 18:24:31	183	300	12	25	8x3	905	41	85,9521	-0,4150	85,7776	-4,8523
91107	14.09.91 02:37:11 - 14.09.91 06:38:15	183	300	12	25	8x3	552	21	85,6337	-5,4674	85,5780	-7,7901
91108	15.09.91 06:52:31 - 15.09.91 09:19:11	183	300	12	25	8x3	598	26	85,5561	-9,2700	85,4460	-11,8326
91109	15.09.91 18:26:15 - 15.09.91 21:05:10	183	300	12	25	8x3	450	18	85,4074	-12,0054	85,3409	-13,7798
91110	16.09.91 07:01:08 - 16.09.91 08:45:40	183	300	12	25	8x3	605	21	85,3013	-13,9642	85,4119	-12,0778
91111	17.09.91 03:03:00 - 17.09.91 18:13:00	183	300	12	25	8x3	1700	50	85,4149	-12,5285	85,3356	-18,0310
91112	17.09.91 12:35:31 - 17.09.91 22:31:00	183	300	12	25	8x3	1094	23	85,3356	-18,0310	85,2160	-15,9851
91113	17.09.91 18:13:00 - 17.09.91 22:31:00	183	300	12	25	8x3	973	23	85,2160	-15,9851	85,0965	-13,9958
91114	17.09.91 22:31:00 - 18.09.91 02:00:00	183	300	12	25	8x3	622	12	85,0965	-13,9958	85,0494	-12,8193
91115	18.09.91 02:00:00 - 18.09.91 04:25:27	183	300	12	25	8x3	3639	66	85,0651	-12,5824	84,7582	-6,6212
91116	20.09.91 08:33:18 - 20.09.91 22:42:51	183	300	12	25	8x3	316	10	84,7131	-6,8413	84,6299	-6,6212
91117	21.09.91 01:18:37 - 21.09.91 02:59:25	183	300	12	25	8x3	1684	54	84,6396	-5,5771	84,2373	-2,7404
91118	22.09.91 06:44:05 - 22.09.91 13:16:46	183	300	12	25	8x3	564	20	84,1971	-1,9277	84,0929	-0,4551
91119	22.09.91 22:34:41 - 23.09.91 00:46:03	183	300	12	25	2x3	1197					
91120	23.09.91 11:09:00 - 23.09.91 18:39:59	none	REFTEK		none	8x3	2144	65	84,0658	0,8832	83,6282	4,4970
91121	23.09.91 20:39:44 - 24.09.91 05:00:14	183	300	12	25	8x3	1820	55	83,5462	5,1860	83,2637	8,6668
91122	24.09.91 23:10:41 - 25.09.91 06:15:21	183	300	12	25	2x3	1105					
91123	25.09.91 10:52:59 - 25.09.91 18:47:18	none	REFTEK		none	8x3	811	21	83,1776	8,7528	83,0641	9,9972
91124	26.09.91 21:08:15 - 27.09.91 00:46:02	183	300	12	25	8x3	1479	60	82,9669	9,8228	82,6603	13,3704
91125	28.09.91 05:01:19 - 28.09.91 12:59:47	183	300	12	25	8x3	425	15	82,6519	13,2919	82,5758	14,1735
91126	28.09.91 16:52:39 - 28.09.91 18:31:21	183	300	12	25	8x3	334	12	80,5660	7,8849	80,4725	8,2352
91127	01.10.91 06:47:21 - 01.10.91 08:04:49	183	300	12	25	8x3	321	12	80,4721	8,2364	80,3623	8,3227
91128	01.10.91 08:05:17 - 01.10.91 09:19:57	183	300	12	25	8x3	824	32	80,3615	8,3237	80,2716	6,7248
91129	01.10.91 09:20:25 - 01.10.91 12:32:27	183	300	12	25	8x3	610	22	80,2756	6,7504	80,2016	5,6936
91130	01.10.91 15:40:42 - 01.10.91 18:02:48	183	600	24	25	8x3	1457	53	80,2014	5,6919	79,7343	5,2463
91131	01.10.91 18:03:02 - 01.10.91 23:42:46	183	600	24	25	8x3	213	8	79,7340	5,2466	79,6754	5,4387
91132	02.10.91 00:32:28 - 02.10.91 00:32:28	183	600	24	25	8x3	700	25	79,6989	5,3279	79,5053	5,9919
91133	02.10.91 14:45:53 - 02.10.91 17:28:58	183	600	24	25	8x3	2449	91	79,5050	5,9923	79,4999	1,5156
91134	02.10.91 17:29:12 - 03.10.91 03:01:20	183	600	24	25	Test	268					
91135	03.10.91 03:08:42 - 03.10.91 04:56:01	183	600	24	25							

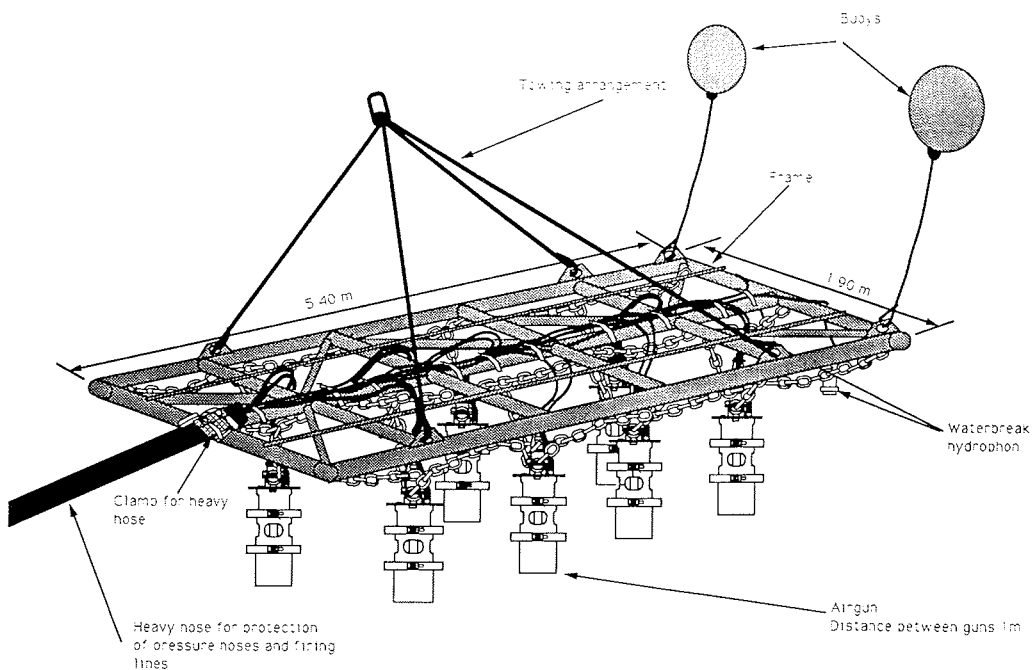


Fig. 7.1-1: Arrangement details of the 24 litre airgun cluster.

The second set-up (Fig. 7.1-2) consisted of a 1.5 t weight with two airguns (3 l each). This configuration was used during the single ship operation on the Lomonosov Ridge. As this was not a tuned array a significant bubble pulse is present in the data.

Problems

The 24 l airgun setup was especially designed for seismic experiments under ice conditions and successfully tested in 1990 off East Greenland. For ship speeds below six knots this setup worked satisfactorily. Problems arose when the ship had to increase the speed up to eight knots in order to obtain sufficient momentum to penetrate ice flows without coming to a stop and consequently having to retrieve the seismic equipment before backing up and pushing ahead again. As long as the ship steamed in a straight line the high speed produced only minor problems. However, when the ship made sharp forced turns while passing ice flows and ridges, the frame made contact with larger pieces of ice as it moved only 1 m below the water surface due to the high towing speed. The frame was forced out of the water and towed over such flows several times but luckily without major damages. Consequently we further restricted use of the frame during single ship operation.

Inspired by the success of *Polar Star* in acquiring seismic data in heavy ice on the Northwind Ridge in 1988 (A. Grantz pers. comm.) we built a second towing system on *Polarstern*. It consisted of a heavy weight with two airguns (Fig. 7.1-2) towed at approximately 6-10 m depth. This configuration worked very well even at high speeds and sharp curving of the ship. Negative aspects were the breaks in the

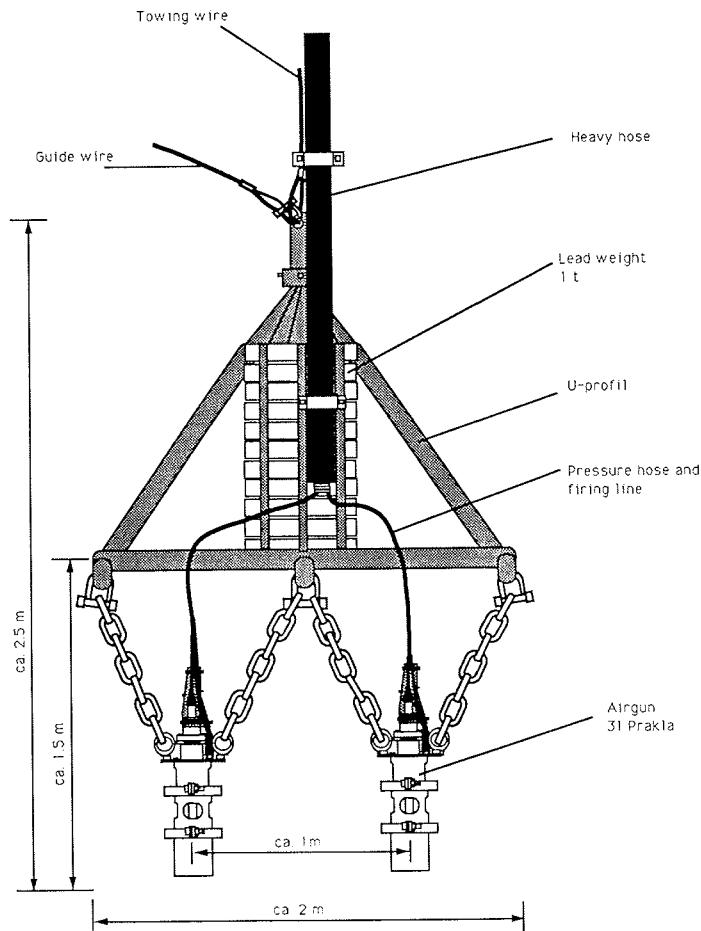


Fig. 7.1-2: Design of heavy weight airgun array (2 airguns) as used during single ship operation.

profile due to gun maintenance and lower seismic energy compared to the larger array.

Receiver

The streamers were, like the airguns, towed midships. At the very beginning of the cruise we deployed a 50 m streamer with a 50 m lead-in cable to record the signals. Despite the 24 litre airgun array, the ambient noise level of the ship due to ice breaking and forced manoeuvring was so high, that the signal to noise ratio was degraded close to a value of 1 even for the water bottom reflection. The essential increase in data quality occurred when we changed to a 300 m long streamer (12 channels, group spacing 25 m) towed 200 m behind the vessel with a heavy lead-in cable. The noise decreased to an acceptable level even when the ship made large course changes. The towing depth of the streamer was highly dependent on the ship's speed. The depth ranged between 5-15 m and occasionally it went as deep

as 60 m. This created a receiver ghost with very variable delays. All seismic lines from line 91075 onwards were observed with the 300 m long streamer and the 24 litre air gun array.

D a m a g e s

Most damages due to ice action were sustained by the high pressure lines along the frame of the airgun array. The high pressure lines as well as the firing lines between the ship and the frame were enclosed in a thick walled tube of 10 cm diameter and were not damaged at all. Generally however damages could be kept to a reasonable limit because the frame was towed very close to the stern and midships.

The streamer showed only minor damages even after it had been towed over ice floes numerous times. Since we did not use any depth leveling birds or tail buoy, the likelihood of losing the streamer was considerably lowered. The critical depth rating of the hydrophones (50 m) was unfortunately exceeded several times when the ship was to stop for longer periods (10-30 minutes).

Brief Summary of the Reflection Seismic Results

L o m o n o s o v R i d g e

The Lomonosov Ridge is about 1,500 km long and 50-70 km wide. The seismic data from the Canadian LOREX-expedition show the ridge near the North Pole to consist of a series of tilted fault blocks (SWEENEY et al. 1982). Sea-floor sediments recovered from the top of the ridge are mostly gravelly lag deposits which also contain reworked mid-Cretaceous palynomorphs and poorly preserved Devonian spore fragments. The geological and geophysical data all indicate that the Lomonosov Ridge is formed by continental type crustal rocks rather than denser, predominantly volcanic material. A reconstruction of the Eurasia Basin for the early Tertiary (Chron 24 B) places the 1,500 km long and 50-70 km wide Lomonosov Ridge close to the margin between Svalbard and Severnaya Zemlya. The ridge probably originated as a crustal sliver severed off the margin concurrent with rifting between Norway and Greenland. The subsidence history of the Lomonosov Ridge is unknown. A shallow sea-way extended from the Arctic Ocean into western Siberia during the early Tertiary, but the Eurasia Basin had no deep oceanic gateway until opening of the Fram Strait in the early Miocene.

Excellent ice conditions in this region allowed us to shoot two multichannel reflection seismic profiles (91090, 91091) across the Lomonosov Ridge with between 3 and 12 fold CDP coverage depending on the ship's speed (Fig. 7.1-3). Both profiles show a characteristic flat-topped ridge with a 600 ms TWT (two-way travel time) thick acoustically stratified and undisturbed seismic sequence above a distinct angular unconformity. The sequence becomes attenuated at the ridge perimeter towards the Nansen Basin on one profile and shows erosion in its upper part at the Makarov Basin side in both profiles.

Below the unconformity, a sequence of horizontal apparently undisturbed strata in the central part of the ridge is flanked by a series of fault bounded half-grabens on the Nansen Basin side and a prograding sequence above shallow basement structures on the Makarov Basin part. There are also distinct differences in the

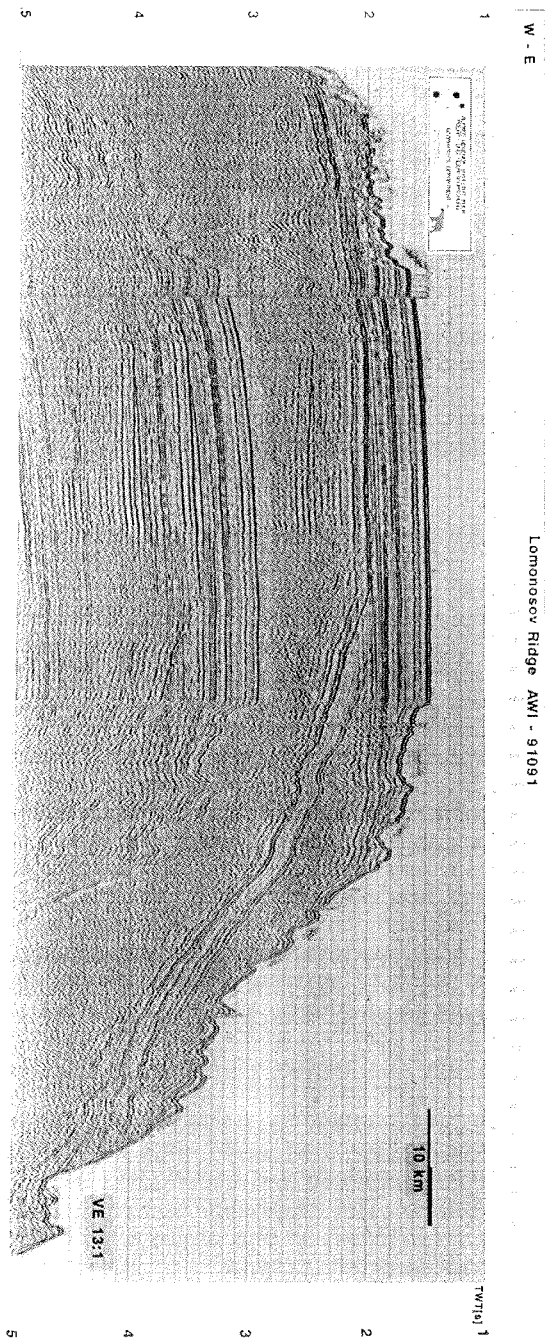


Fig. 7.1-3: Seismic line (AWI 91091) across the Lomonosov Ridge.

deeper strata at the foot of the ridge. Throughout the whole section in the Nansen Basin the turbidites show a regular onlap relationship as basement shallows towards the ridge. On the Makarov Basin side, the onlap is not clear and there is a distinct unconformity at 300-1100 ms which separates the typical basin turbidites from the deeper strata. A provoking thought may be that the Lomonosov Ridge contains the remnants of a former prograding continental shelf towards the Makarov Basin and that any oceanic crust in the basin may be beyond the edges of these profiles.

Five sonobuoys were launched on the Lomonosov Ridge in order to resolve the velocity structure more accurately. Four of them showed good signals.

Amundsen Basin

The Amundsen Basin is about 500 m deeper than the Nansen Basin although they both evolved by symmetric generation of oceanic crust at the Gakkel spreading center during the Cenozoic. This is considered to be a result of differences in sediment thickness as the Amundsen Basin has, throughout its evolution, mainly received its terrigenous input from its Siberian- and North Greenland ends with limited contribution from the Lomonosov Ridge.

We acquired multichannel seismic data during the whole transit starting at the Lomonosov Ridge through the Amundsen Basin. The top of the oceanic basement could be mapped on all profiles and the total sediment thickness is up to 2 s TWT. The strata are ponded in topographic lows typical of predominantly turbidite deposition. The characteristic features of the acoustic stratigraphy are a uniformly stratified lower half of the section and an upper half with more than four strong regional reflectors. The lower uniform unit appears to pinch out towards Gakkel Ridge on crust associated with Chron 2. There is also a rough spatial relation between this isochron and the far edges of Morris Jesup and Yermak plateaus which mark the initiation of a volcanic constructional episode that ended before Chron 13 during which the plateaus were formed. Thus turbidite deposition during the first 10-15 Ma. of basin evolution yielded an acoustically monotonous sequence, but later the depositional environment changed repeatedly to generate regional acoustic impedance contrasts.

Basement topography appears to increase in roughness towards the Gakkel Ridge. Sediments are present in pockets or basins between seamounts and ridges. The acoustic image of the sediments is an upper 150 ms transparent unit above a uniformly stratified unit which may reach 800 ms in pockets.

Morris Jesup Rise

The plateau named after the adjacent Kap Morris Jesup extends out from the northern tip of Greenland with water depths shallower than 500 m. It was first traversed by Soviet ice drift stations NP-3 in 1955 and NP-7 in 1959. It was first shown on the 1954 Soviet bathymetric map of the Arctic Ocean but misplaced 200 km towards the southeast and in the 1959 edition it was mapped as a broad shelf. The geologic structure of the plateau is best documented by the U.S. ice drift station Arlis II seismic profile from 1964 (OSTENSO & WOLD 1977) and later aeromagnetic data. The plateau has a flat-topped nose bounded to the east by a steep scarp and to the west by a series of progressively deeper sediment covered fault blocks. The

geophysical characteristics and the conjugate position of the plateau with respect to the northern part of the Yermak Plateau argue for it being a volcanic constructional feature.

The acquired seismic data show, that the plateau has a relatively smooth top and is covered with about 200 ms of flatlying strata overlying assumed volcanic basement. There is a hint of sub-basement reflections. In the deeper parts to the west, sediment thickness increases to 500 ms and reaches 900 ms in downfaulted halfgrabens. Here, the sediments show clear evidence of current controlled deposition and erosion. Due to ice conditions and the time schedule we were not able to obtain better coverage in the western and southern part of the plateau.

G a k k e l R i d g e

The sea-floor topography becomes rougher towards the Gakkel spreading center. The search for an easy passage between large floes generated a sinuous ship's track which together with a short streamer were not optimal for imaging rough oceanic crust. Bathymetric swath mapping at the spreading center suggests a fairly two-dimensional sea-floor morphology and a rift which is slightly asymmetric south of 84° 02' N where the axial valley is offset about 5 km towards southeast.

N a n s e n B a s i n

Sediment thickness in the Nansen Basin is less than 1 s TWT along the profile. The acoustic stratigraphy shows similarities to that of the Amundsen Basin in that the lower part of the section appears acoustically uniform whereas the upper part contains several distinct reflectors. We also note that bathymetric highs and seamounts tend to have a thicker sediment cover in this basin compared to the opposite flank of the Gakkel Ridge which may be indicative of a higher contribution from pelagic deposition and/or more sluggish bottom currents.

Y e r m a k P l a t e a u

The Yermak Plateau can be divided into a northern part (north of 82° N) and a southern part based on its morphology and regional differences in the magnetic properties of the crust. The northern part is associated with high amplitude (>1,000 nT) magnetic anomalies and a single refraction line shows relatively high velocities in a 18 km thick crustal section. These characteristics have been interpreted as evidence of oceanic crust. The magnetic field is very smooth over the southern part, lower crustal velocities and - less certain - dredged gneiss boulders of unknown provenance argue for crustal material of continental affinity (JACKSON et al. 1982).

The northern part of Yermak Plateau and Morris Jesup Rise probably formed by excessive volcanic extrusions at a spreading center which initially was above sea level. This condition would in many ways be similar to the extrusion of the Upper Series basalt on the Vøring Plateau. On the top of these marginal plateaus we therefore expect to find a series of sub-basement reflectors dipping towards the Gakkel Ridge.

The northern slope of Yermak Plateau has a sediment section that is up to 800 ms thick in 2,500 m water depth. The lowermost part of the slope is dissected by a

number of deep canyons which cut through the stratigraphy. The sedimentary cover on the shallowest part along the profile (water depth 1,000 m) shows chaotic layering and is up to 300 ms thick. There is only weak evidence of discontinuous sub-basement reflections. We note that a 30 cm sediment core recovered from a steep slope in 1,300 m water depth indicates a Middle to Late Eocene marine environment and a submerged ridge at this location during which it was formed.

The cruise tracks of *Oden* and *Polarstern* diverged on top of Yermak Plateau. Seismic profiling during single vessel operation was suspended until the ice edge was reached due to heavy ice.

Seismic Reflection Survey in Support of ODP Drill Sites North of Svalbard

Five sites on the southern part of Yermak Plateau, northwest of Spitsbergen, have been proposed to the Ocean Drilling Program for sampling in order to investigate the Cenozoic paleoceanographic history of the Arctic Ocean and evolution of the Fram Strait gateway. In response to a request from the ODP Site Survey Panel for improved data quality, it was decided to shoot a seismic line through the sites and carry out a sediment coring program as well. The northernmost site YERM 1 had to be excluded due to ice conditions, but sites YERM 2, 3 and 4 were tied with a seismic line using the 24 litre airgun array and a 24 channel streamer (800 m long).

Reflection Measurements in a Passive Drift Mode

Ice conditions prevented marine seismic data acquisition during the first part of the cruise. We therefore collected reflection data at each geological station while the vessel was drifting passively with the ice. The 24 litre airgun array was used as a source and two REFTEK recording systems with hydrophones and geophones as receivers. The time base for firing the airguns was GPS time and the portable REFTEK recording systems received the OMEGA time signal with only minor problems. Previewing of the data has confirmed good signal quality.

Marine Wide Angle Reflection and Refraction

We deployed a total of 25 sonobuoys (Fairfield, USA) for wide angle reflection and refraction measurements parallel to seismic profiling. Targets of specific interest included the velocity structure of the upper crust on the Lomonosov Ridge and the Morris Jesup Rise, the thickness of oceanic crust in the Amundsen and the Nansen Basins as well as in the axial region of the Gakkel Ridge. The results of sonobuoy information are summarized in Table 7.1-2. The frequent changes in ship's speed and course gave a complicated data set which could not be analyzed with available software on board. This will be done in Bremerhaven after the cruise.

It was also planned to fly out REFTEK recording systems ahead of the ship in order to record the signals of the reflection seismics. Due to the rapid changes in the weather conditions, this approach had to be abandoned as the likelihood of losing the instruments with the data were too high.

Sonobuoy #	Type	Profile	Time Range (Carrier)	Shot Range	Quality	Latitude	Longitude
9101	30L	91030	06.08.91 19:07:40 - 06.08.91 20:07:00	no profile	6	81.8783	30.4799
9102	30L	91060	10.08.91 09:11:00 - 10.08.91 10:08:00	no signal	6	84.7260	36.9475
9103	10L	91060	10.08.91 09:55:00 - 10.08.91 10:08:00	no profile	6	84.7452	37.2958
9104	30L	91090	30.08.91 01:32:00 - 30.08.91 05:50:00	2000 - 2850	1	87.9532	142.6719
9105	10L	91090	30.08.91 02:48:00 - 30.08.91 10:14:00	2494 - 3800	1	87.9397	139.6751
9106	30L	91090	30.08.91 06:14:00 - 30.08.91 06:30:00	no signal	6	87.8370	135.1049
9107	10L	91091	30.08.91 10:38:00 - 30.08.91 14:24:00	0121 - 1100	1	87.7275	130.8674
9108	10L	91091	30.08.91 18:25:00 - 30.08.91 23:44:00	1480 - 3000	1	87.7220	139.8429
9109	10L	91098	08.09.91 11:25:00 - 08.09.91 17:12:00	0115 - 0600	3	89.8394	-48.1446
9110	30L	91098	08.09.91 20:20:00 - 08.09.91 23:52:00	1928 - 2734	1	89.3580	-5.1549
9111	10L	91100	09.09.91 13:28:00 - 09.09.91 13:50:00	no signal	6	88.7534	5.2596
9112	30L	91100	09.09.91 13:56:00 - 09.09.91 14:20:00	no signal	6	88.7140	5.2254
9113	10L	91101	10.09.91 12:04:00 - 10.09.91 15:08:00	0320 - 1230	2	88.0999	9.3610
9114	30L	91101	10.09.91 16:55:00 - 10.09.91 19:52:00	1420 - 1900	1	87.7039	10.8003
9115	30L	91102	11.09.91 05:42:00 - 11.09.91 06:00:00	no signal	6	87.4473	13.0665
9116	10L	91102	11.09.91 11:55:00 - 11.09.91 14:00:00	1634 - 2111	1	87.0688	9.9296
9117	10L	91104	12.09.91 10:50:00 - 12.09.91 14:19:59	0001 - 0877	1	86.5330	7.6175
9118	10L	91106	13.09.91 14:07:00 - 13.09.91 16:40:00	0048 - 0623	1	86.1743	4.5590
9119	10L	91112	17.09.91 12:40:00 - 17.09.91 15:01:00	30 - 634	3	85.4096	-12.6020
9120	10L	91116	20.09.91 13:25:00 - 20.09.91 15:38:00	1252 - 1821	3	85.0170	-9.8309
9121	10L	91122	25.09.91 03:16:00 - 25.09.91 06:15:21	1053 - 1820	1	83.4449	7.3626
9122	30L	91124	26.09.91 21:30:00 - 27.09.91 00:46:02	76 - 811	1	83.1655	9.0563
9123	30L	91125	28.09.91 05:37:00 - 28.09.91 08:25:00	136 - 766	4	82.9527	10.3161
9124	30L	91128	01.10.91 09:32:00 - 01.10.91 09:40:00	no signal	6	-	-
9125	30L	91130	01.10.91 16:03:00 - 01.10.91 18:10:00	98 - 611	2	80.2632	6.5806

Table 7.1-2: Information on all sonobuoys deployed during ARK-VIII/3.

With the assistance of *Oden* on station near the REFTEK instruments, we carried out three wide angle reflection and refraction measurements to an offset of 27 km; two measurements in Amundsen and Nansen basins and one measurement within the rift valley of the Gakkel Ridge. The basin profiles were carried out over oceanic crust within the age range of 20-36 Ma at which period spreading rates were at a minimum during the Cenozoic. Previous refraction measurements from this area suggest that the oceanic crust is only 2-3 km thick and that there is a possible relation between thin crust and slow spreading rate (JACKSON et al. 1982).

Seismic Data Processing on Board Polarstern

A CONVEX C120 vector computer is available for seismic processing on board *Polarstern*. The computer is networked with a VAX cluster and a SUN SPARC 1+ workstation via DECNET and ETHERNET (Fig. 7.1-4). For seismic processing we used the DISCO Basic software package.

The status of the processing after finishing the cruise in Bremerhaven is shown in Table 7.1-3. All profiles were processed up to a brute stack (demultiplexing, geometry, sorting and stack). The data were sorted into a CDP grid of 25 m bins which resulted in a 6-15 fold mean coverage. Noise and signal distortion due to large course changes and lack of streamer depth control at very low speeds, can clearly be identified. They will be removed at a later stage by wavelet processing techniques and trace editing.

Table 7.1-3: Overview on the seismic processing on board Polarstern during cruise ARK-VIII/3 of ARCTIC'91.

Profile	Exp. Type	Field Tape #	Demultiplex	Geometry	Sorting	Velocity Ana.	Brute Stack	Mute	Plot	Sonobuoys	RFR-SHOTL	RFR-DEMUX
91010	Marine	002 - 009	5.9.91	9.9.91	9.9.91	11.9.91	11.9.91	x	x		none	none
91020	Marine	010 - 012	5.9.91	12.9.91	12.9.91	13.9.91	13.9.91	x	x		none	none
91030	Marine	13	5.9.91	SB only	none	none	none	-	-	9101	none	none
91040	Overice/REFTEK			SHOTL	none	none	none	-	-			
91041	Overice/REFTEK			SHOTL	none	none	none	-	-			
91042	Overice/REFTEK	14	5.9.91	SHOTL	none	none	none	-	-			
91043	Overice/REFTEK	16	6.9.91	SHOTL	none	none	none	-	-			
91050								-	-			
91060	Marine	15	6.9.91	SB only	none	none	none	-	-	9102/9103	none	none
91070	Overice/REFTEK	017 - 018	6.9.91	SHOTL	none	none	none	-	-			
91080	Marine	19	6.9.91	12.9.91	12.9.91	13.9.91	13.9.91	x	x			
91090	Marine	020 - 028	7.9.91	10.9.91	10.9.91	12.9.91	12.9.91	x	x	9104/9105/9106	none	none
91091	Marine	029 - 037	7.9.91	10.9.91	10.9.91	13.9.91	13.9.91	x	x	9107/9108	none	none
91092	Overice/REFTEK	38	7.9.91	SHOTL	none	none	none	-	-			
91093	Marine	039 - 040	7.9.91	12.9.91	12.9.91	18.9.91	20.9.91	x	x		none	none
91094	Marine	41	8.9.91	12.9.91	12.9.91	18.9.91	20.9.91	x	x		none	none
91095	Overice/REFTEK	42	8.9.91	SHOTL	none	none	none	-	-			
91096	Overice/REFTEK	043 - 044	8.9.91	3.10.91	3.10.91	3.10.91	3.10.91	x	x			
91097	Marine	045 - 056	8.9.91	15.9.91	15.9.91	16.9.91	16.9.91	x	x		none	none
91098	Marine	057 - 064	9.9.91	20.9.91	20.9.91	20.9.91	20.9.91	x	x	9109/9110	none	none
91100	Marine	065 - 069	10.9.91	20.9.91	20.9.91	20.9.91	20.9.91	x	x	9111/9112	none	none
91101	Marine	070 - 074	10.9.91	19.9.91	19.9.91	20.9.91	22.9.91	x	x	9113/9114	none	none
91102	Marine	075 - 081	12.9.91	20.9.91	20.9.91	22.9.91	23.9.91	x	x	9115/9116	none	none
91103	REFTEK	82		SHOTL	none	none	none	-	-			
91104	Marine	083 - 085	12.9.91	26.9.91	26.9.91	26.9.91	28.9.91	x	x	9117	none	none
91105	Marine	086 - 087	13.9.91	26.9.91	26.9.91	26.9.91	28.9.91	x	x		none	none
91106	Marine	088 - 090	13.9.91	26.9.91	26.9.91	26.9.91	28.9.91	x	x	9118	none	none
91107	Marine	091 - 093	14.9.91	21.9.91	21.9.91	22.9.91	22.9.91	x	x		none	none
91108	Marine	094 - 095	14.9.91	21.9.91	21.9.91	22.9.91	23.9.91	x	x		none	none
91109	Marine	096 - 097	15.9.91	21.9.91	21.9.91	22.9.91	23.9.91	x	x		none	none
91110	Marine	098 - 099	16.9.91	26.9.91	26.9.91	28.9.91	29.9.91	x	x		none	none
91111	Marine	100 - 101	17.9.91	21.9.91	21.9.91	22.9.91	24.9.91	x	x		none	none
91112	Marine	102 - 105	19.9.91	21.9.91	22.9.91	22.9.91	24.9.91	x	x	9119	none	none
91113	Marine	105 - 107	20.9.91	21.9.91	22.9.91	23.9.91	24.9.91	x	x		none	none
91114	Marine	107 - 109	20.9.91	24.9.91	24.9.91	26.9.91	26.9.91	x	x		none	none
91115	Marine	109 - 111	20.9.91	24.9.91	24.9.91	26.9.91	26.9.91	x	x		none	none
91116	Marine	112 - 120	21.9.91	21.9.91	25.9.91	26.9.91	26.9.91	x	x	9120	none	none
91117	Marine	121	23.9.91	26.9.91	26.9.91	27.9.91	28.9.91	x	x		none	none
91118	Marine	122 - 125	23.9.91	26.9.91	26.9.91	28.9.91	29.9.91	x	x		none	none
91119	Marine	126 - 127	24.9.91	27.9.91	27.9.91	28.9.91	30.9.91	x	x		none	none
91120	REFTEK	128	24.9.91	SHOTL	none	none	none	-	-			
91121	Marine	129 - 134	24.9.91	27.9.91	27.9.91	28.9.91	30.9.91	x	x		none	none
91122	Marine	135 - 139	25.9.91	27.9.91	27.9.91	29.9.91	30.9.91	x	x	9121	none	none
91123	REFTEK	140	27.9.91	SHOTL	none	none	none	-	-			
91124	Marine	141 - 142	27.9.91	30.9.91	30.9.91	1.10.91	1.10.91	x	x	9122	none	none
91125	Marine	143 - 146	29.9.91	4.10.91	4.10.91	6.10.91	6.10.91	x	x	9123	none	none
91126	Marine	147	29.9.91	4.10.91	4.10.91	6.10.91	6.10.91	x	x		none	none
91127	Marine	148	1.10.91	5.10.91	5.10.91	6.10.91	6.10.91	x	x		none	none
91128	Marine	148 - 149	1.10.91	5.10.91	5.10.91	6.10.91	6.10.91	x	x	9124	none	none
91129	Marine	149 - 151	1.10.91	5.10.91	5.10.91	6.10.91	7.10.91	x	x		none	none
91130	Marine	152 - 153	2.10.91	5.10.91	6.10.91	7.10.91	8.10.91	x	x	9125	none	none
91131	Marine	154 - 158	2.10.91	5.10.91	5.10.91	6.10.91	7.10.91	x	x		none	none
91132	Marine	158 - 159	2.10.91	5.10.91	5.10.91	6.10.91	7.10.91	x	x		none	none
91133	Marine	160 - 162	3.10.91	5.10.91	6.10.91	7.10.91	8.10.91	x	x		none	none
91134	Marine	162 - 171	3.10.91	6.10.91	7.10.91	7.10.91	8.10.91	x	x		none	none
91135	Marine	172	3.10.91	-	-	-	-	-	-			

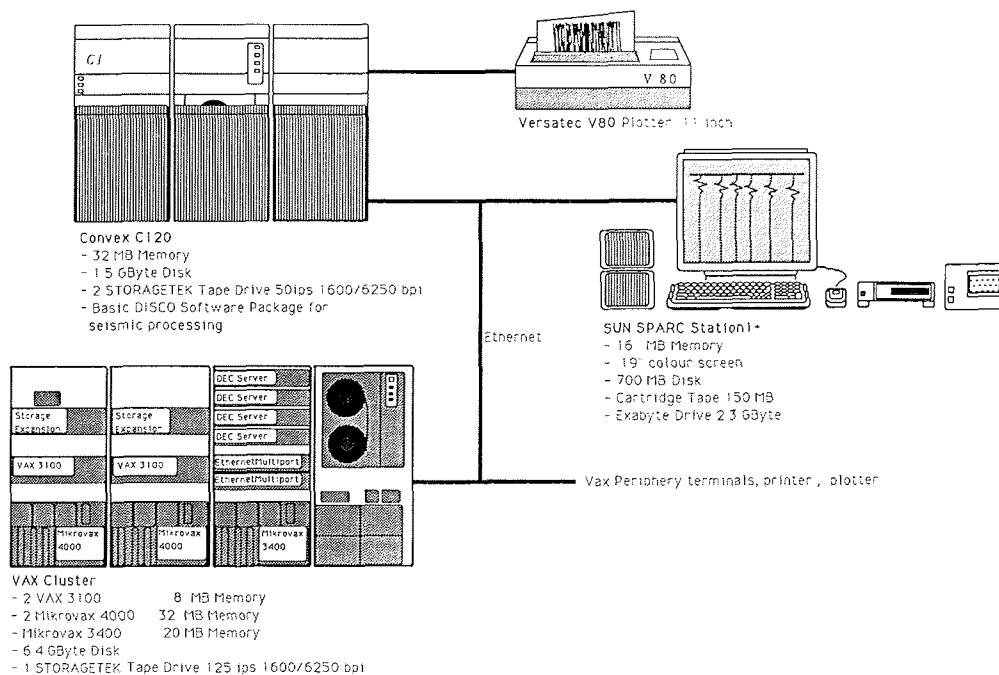


Fig. 7.1-4: Sketch of available computer configuration on *Polarstern* for geophysical processing.

7.2 Over-ice Seismic Surveys (Y. Kristoffersen, J.P. Fjellanger, A. Lif, P.J. Lindgren and T. Rasmussen)

Mobile seismic surveys on sea ice in the deep Arctic Ocean have not been performed to any extent up until now, mainly due to lack of technology efficient enough to make it worthwhile. With the proven performance of the snowstreamer this becomes an interesting approach. The objective of the seismic program on the sea ice was to test the feasibility of seismic reflection and refraction data acquisition on sea ice during the summer season using the snow streamer. Three types of experiments were carried out; the location of which are given in Table 7.2-1:

- mobile seismic reflection measurements;
- deep reflection measurements in passive drift mode;
- seismic wide-angle reflection and refraction.

In the deep ocean environment, good quality single channel seismic reflection data are often adequate for reconnaissance surveys. We may therefore use the multichannel array to obtain single fold coverage by firing one shot at intervals of half the streamer length. The seismic reflection survey team consisted of four persons, each driving a skidoo towing a sled. One person was assigned for drilling shot holes through the ice with a power auger, the second for shooting and the third managed the recording unit and the snowstreamer under tow. The fourth person

Date	Experiment	Shots	Charge [g]	Streamer length [m]	Channels	Length [km]	Latitude	Longitude
6.8.91	refl. test	4	270-550	250	5			
7.8.91	refl. test	3	270	250	5			
11.8.91	refl. test	10	550	375	8	1,7	85° 44'N	44° 41'E
16.8.91	refl.	14	550	375	8	2,8	86° 50'N	57° 00'E
25.8.91	rfl. ice drift	80	550-1100	250	5	4,8	87° 46'N	108° 32'E
27.8.91	rfl. ice drift	34	550	250	5	1,5	88° 02'N	134° 38'E
28.8.91	rfl. ice drift	75	550-1100	250	10	2,7	87° 59'N	158° 44'E
2.9.91	rfl. ice drift	67	1100	250	10	7,2	87° 32'N	144° 50'E
5.9.91	rfl. ice drift	700	airgun	250	10	3,2	88° 45'N	127° 00'E
9.9.91	rfl. ice drift	35	550-2200	250	10	3,2	88° 16'N	100° 22'E
11.9.91	rfl. ice drift	12	5500	250	10	0,4	86° 45'N	10° 01'E
12.9.91	rfl. ice drift	11	5500	250	10	1,1	86° 36'N	07° 16'E
13.9.91	rfl. ice drift	10	5500	250	10	0,6	86° 09'N	05° 07'E
13.9.91	rfl. ice drift	7	2750-5500	250	10	0,9	85° 57'N	00° 08'E
14.9.91	rfl. ice drift	5	5500	250	10	0,4	85° 45'N	04° 14'W
16.9.91	pulse test	36	138-1100	250	12		85° 19'N	13° 53'W
21.9.91	rfl. ice drift	8	5500	250	10	0,3	84° 39'N	06° 53'W
23.9.91	rfl. ice drift	7	5500	250	10	0,5	83° 59'N	00° 21'W
24.9.91	rfl. ice drift	7	5500	250	10	0,4	83° 38'N	04° 34'W
26.9.91	rfl. ice drift	7	5500	250	10	0,4	83° 12'N	08° 26'E
27.9.91	rfl. ice drift	9	5500-11000	250	10	0,8	83° 01'N	10° 07'E

Table 7.2-1: Summary of all seismic over-ice profiles during ARK-VIII/3.

carried out line reconnaissance and assisted where needed. A skidoo pulled a 600 m long, 12 channel snowstreamer with relative ease. Each group contained four gimbaled geophones and group spacing was 50 m. A Geometrics ES-2401 digital recording unit was used for collecting the data. It had capabilities for monitoring of noise on all channels in real time as well as print-out of shot files for data quality control. The seismic source was 550 grams of dynamite suspended at 7.5 m depth below the ice. For navigation we used a portable GPS receiver.

Seismic tests in August were strongly impeded by the abundance of meltponds and only 1.5-2 km/hour was achieved with one shot point every 175 m. A more severe constraint was the limited sizes of individual flows. Flow sizes observed during the traverse from Svalbard to the Makarov Basin and return via the North Pole, were generally less than 1 km across with 10-20 % open water in between in August and September. Only in a few instances were floes as large as 5 km across encountered.

Deep seismic reflection measurements in a passive drift mode were made when the vessel was on station next to an ice floe. 5.5-11 kg dynamite charges at 15 m depth were used as source and the source signature was monitored by a hydrophone at 100 m depth. The signals were received by a 10 channel 250 m long snowstreamer on the ice. A typical record is shown in Fig. 7.2-1. Due to format conversion problems, it was not possible to process these data onboard. On one station, the snowstreamer was hooked up to the onboard seismic acquisition system and the 8 x 3 l airgun array was used as a source.

Wide-angle reflection and refraction measurements were carried out with the snowstreamer on the ice while the ship was on station firing the airgun array on a one minute schedule. The streamer was moved up one length at a time and a sequence of shots recorded. It was only possible to reach a maximum offset of 8 km due to the limited flow sizes.

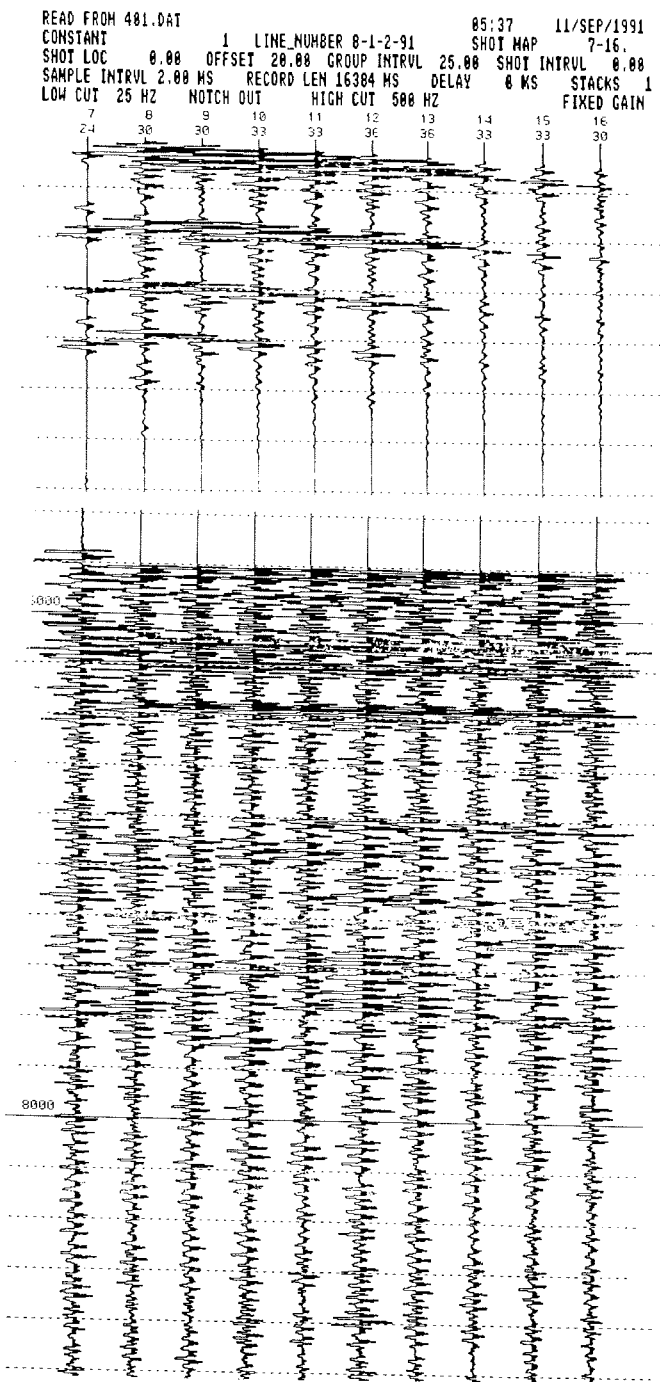


Fig. 7.2-1: Signals from 5.5 kg dynamite at 15 m depth recorded by snowstreamer on the ice. Upper panel shows the direct waves recorded for the first 1.4 s with the source signature on the left trace. Lower panel shows reflections in the time interval of 6-9 s TWT.

The efficiency of over-ice seismic reflection surveys is strongly dependent on the capability to move across an ice surface interrupted by leads. For transportation across the mosaic of small ice floes pitted by meltwater ponds and separated by small leads, we tested a small hovercraft (vehicle weight 250 kg) capable of carrying a payload of 350 kg. The craft was able to tow a 250 m long snowstreamer with relative ease and an electrically driven drum mounted on the hovercraft proved efficient for deployment and recovery of the streamer. However, the load became excessive for efficient operation with the added weight of an additional observer and the recording equipment (100+50 kg).

The experience gained from this test strongly suggests that operation of a team of 2-3 modified light hovercrafts may be a viable approach to increase the efficiency of seismic data acquisition by single icebreaker expeditions during summer time.

7.3 Magnetotelluric Measurements (T. Rasmussen)

A magnetotelluric experiment was carried out on the Lomonosov Ridge. The instrumentation was deployed on a large ice floe and the electrodes placed a few meters below the ice. The electromagnetic field in the period range of 2-3,600 s was recorded for about 17 hours.

A number of difficulties are encountered in performing magnetotelluric measurements in the Arctic. Firstly, the proximity of the sources might invalidate the requirement for a uniform source field. Secondly, the attenuation of the electromagnetic field in sea water limits the resolution at depth. A third complication, related to the drift of the ice, is the movement of the magnetometers in the static magnetic field which could induce noise in the data.

The magnetotelluric transfer function obtained from the experiment, has a clear two dimensional signature which can be explained by the bathymetry. The presence of a conductive layer below the uppermost resistive layer is indicated, but careful analysis is needed in order to exclude any influences from a non-uniform source field.

7.4 Gravity Measurements (W. Jokat)

For continuous gravity measurements we operated a sea gravity meter KSS 31/25 (Bodenseewerke, Überlingen). The gravity values were recorded digitally via a serial interface on the VAX onboard computer. The logging interval was 20 s which at a speed of 5 knots represents a spatial sampling distance of 50 m. The VAX computer also sends navigation information to the meter every second to support stabilizing the sensor platform.

A failure occurred for unknown reasons at the very beginning of the cruise just after leaving Tromsø. After this incident, the meter worked well even under severe ice conditions. During the single ship operation, the data are highly disturbed due to large and sudden changes in ship's heading from collisions with ice flows. The data quality improved when the vessel was able to proceed in the channel behind

Oden. Gravity ties were made in Tromsø with the international network of absolute gravity values. In total we collected nearly 5,000 nautical miles of gravity data.

7.5 Measurements of Streamer Noise (V. Bouravtsev, W. Jokat)

For seismic acquisition the noise at the receiver is as important as the energy which is transmitted by the source. To investigate this problem under heavy ice conditions we recorded at the beginning of each seismic profile 10 files only with noise.

For the data processing and analysis of these noise recordings we used a constant gain value for all traces, for RMS noise level calculation, the calculation of the spectral density, the autocorrelation function and the calculation of the signal to noise ratio in open waters and under ice conditions.

The RMS level of the streamer noise and the corresponding parameters during the recording are summarized in Tab. 7.5-1. The dependence of the streamer noise level on the distance from the ship is presented in Fig 7.5-1. The highest RMS noise level was present, when *Polarstern* operated as a single ship during seismic profiling (profiles 91090/91091). A strong decrease of the RMS noise can be observed when *Polarstern* followed *Oden* (profiles 91116/91126). But also in this case the RMS noise level can be higher than 10 μbar (first channels, profile 91116) the limit of the noise for industrial seismic exploration. On the open sea the RMS noise level of the PRAKLA streamer equals $\approx 2.5\text{-}3.0 \mu\text{bar}$ for all channels, which are farther away than 400 m from the ship's stern. This is a normal value for this type of streamer.

Figure 7.5-2 shows examples of the noise recordings. The set N1 represents the normal streamer noise during operation in open waters ($\approx 2.5\text{-}3.0 \mu\text{bar}$). The records N2 and N3 are dominated by reflection waves, which are generated from the ship. This reflection signals have different apparent velocities for different profiles ($\approx 3,000 \text{ m/s}$ for line 91112; $\approx 6,000 \text{ m/s}$ for line 91130).

The sets N4 and N5 represent the lower and upper limits of the streamer noise during the joined operation with *Oden*. The last record shows the noise character, when *Polarstern* carried out seismic profiling as a single ship. It is obvious from the analysis, that the propeller is dominating the records of the sets N5 and N6. This is due to the operation of all engines and the increased hydrodynamic forces on the propellers during operation in heavy ice. The autocorrelation functions show that the propeller noise is a coherent acoustic wave with an amplitude modulation. The main frequency is $f_1 = 11.3 \text{ Hz}$.

On Figure 7.5-3 the spectral density of the streamer noise for the two different types is displayed. The shaded spectrum shows the normal shape of the streamer noise during heavy ice conditions. The second one is generated when reflection noise from the sea floor (N2, N3) is present. It overlaps with the frequency band of seismic signals. The peaks are corresponding to the harmonics of the propeller noise ($f_2 = 22.6 \text{ Hz}$; $f_3 = 33.9 \text{ Hz}$; $f_4 = 44.2 \text{ Hz}$).

Table 7.5-1: Summary of the most important parameters of the streamer noise analysis.

Number of the Profile	RMS noise level [μ bar]						Velocity [ktn]	Waterdepth [m]	Depth of streamer [m]					Active Length of streamer [m]	Ice Conditions	Machine [rpm]
	Number of streamer channel								h1	h2	h3	h4	h5			
	1	5	11	16	20	24										
91020	2957	2217											80			
91090	30,2	16,6	12,4				3900						300	H(ice)=2-2.5 m; D=100%		
91091	27,3	14,0	10,0				4300	8	18				300	H(ice)=2-2.5 m; D=100%		
91097	13,2	11,2	11,0				1200	21	14				300	H(ice)=2-2.5 m; D=100%		
91098	35,1	20,9	14,8				4220	6	9				300	H(ice)=2-2.5 m; D=100%		
91100	9,7	6,9	5,3				4350						300	H(ice)=2-2.5 m; D=100%		
91101	9,7	6,3	4,4				4370	10	10				300	open channel after the ship	n1=171;n2=172	
91102	12,5	8,3	5,2				4360	6	6				300	H(ice)= 2-2.5 m, x=200 m; D=100%	n1=171;n2=172	
91104	8,3	9,2	5,4				4380	8	10				300	H(ice)= 2-2.5 m; D=100%		
91106	14,8	8,5	5,9				4240	6	6				300	H(ice)= 10-15 cm; Nilas		
91107	10,0	5,8	3,7				4250	8	14				300	big lead during deploying	n1=n2=171	
91108	7,1	4,9	3,4				3400	7	14				300	H(ice)= 2-2.5 m; D=100%		
91110	11,1	9,4	8,8				1370	5	5				300	H(ice)= 2-2.5 m; D=100%		
91112	12,9	9,7	9,7				1300	5	2				300	H(ice)= 2.0 m; floating ice in channel		
91116	10,1	5,6	3,4				3885	8	6				300	H(ice)= 2.0m		
91126	21,4	9,1	5,6				990	3	4				300	H(ice) < 2 m; x=100 m; D= 100%	n1=n2=173	
91127	26,0	10,9	5,0				835	2	7				300	heavy ice		
91129	15,5	13,2	10,5				555	15	8				300	open sea		
91130	17,2	16,2	14,0	12,5	10,0	12,5	560	8	8	5	15	15	600	open sea; BN 2		
91133	10,4	4,9	3,1	2,9	4,7	4,5	2040	4	10	5	11	8	600	open sea; BN 4		

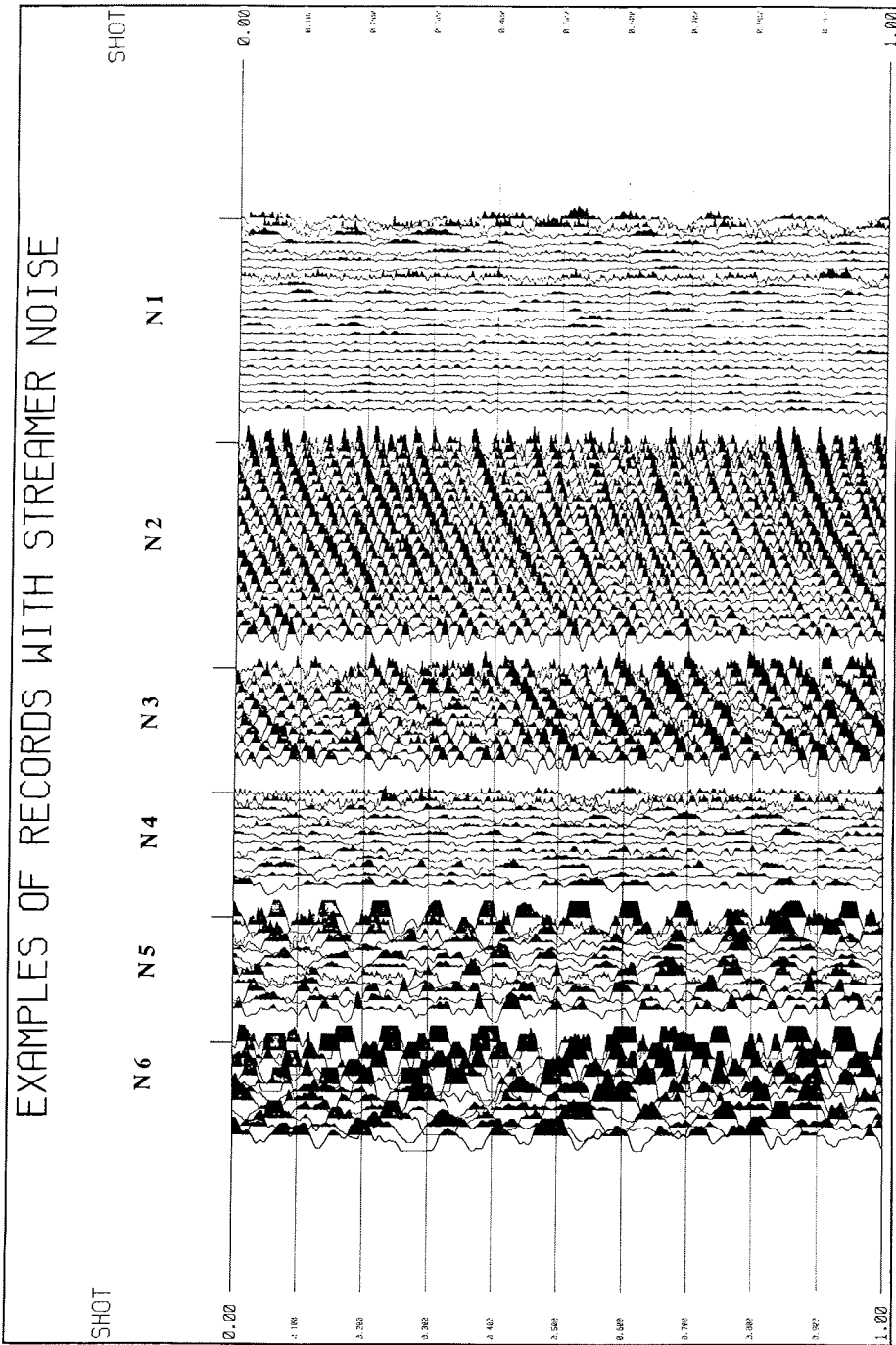


Fig. 7.5-1: Typical record of streamer noise for different environments.

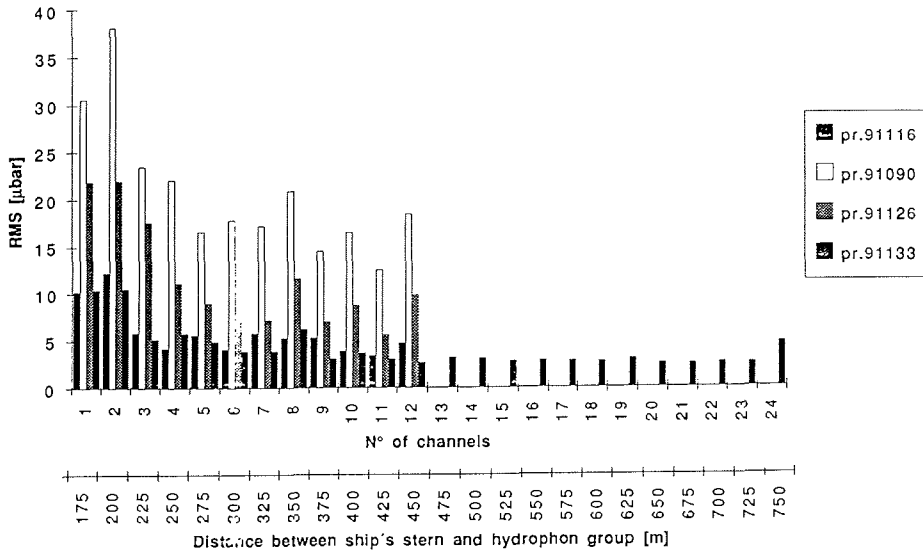


Fig. 7.5-2: RMS streamer noise level depending on hydrophon distance from the ship.

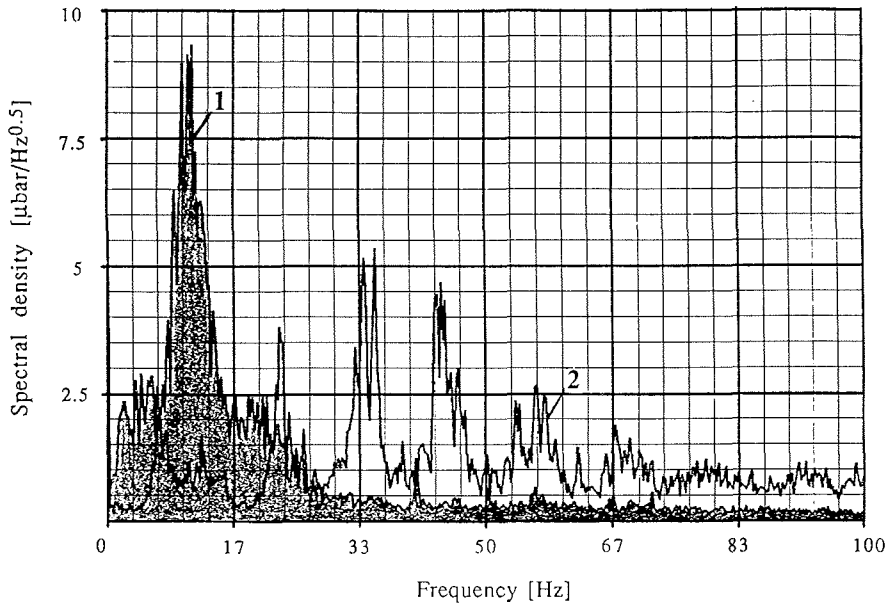


Fig. 7.5-3: Spectral density function of two typical streamer noise records.

The values of the signal to noise ratio for the 300 m and the 50 m streamer are displayed in Figure 7.5-4. The ratio has been calculated within the time gates 0-50 ms, 0-100 ms, 100-200 ms *et cetera*. Zero is corresponding to the arrival of the first seismic signal (sea-floor reflection). It is obvious, that the use of the 300 m streamer has increased the S/N value by up to 20 db (factor 10) for the first channel close to the ship and by up to 40 db (factor 100) for the last channel of the streamer. In both cases we used the 24 l airgun array as a source. The use of the long streamer provided a S/N ratio greater than 1 until 800 ms for the first channel and until 1,800 ms for the last channel. Note the very low S/N ratio of the 50 m streamer!

The analysis of the streamer noise data show very clearly that the usage of the 24 litre airgun array and the long streamer were essential for the good seismic data quality. All results are confirmed by the data quality of the seismic sections. This detailed analysis of the streamer noise is the first one under such heavy ice conditions. It shows that up to a certain level it is possible to collect high quality data in the Arctic basins.

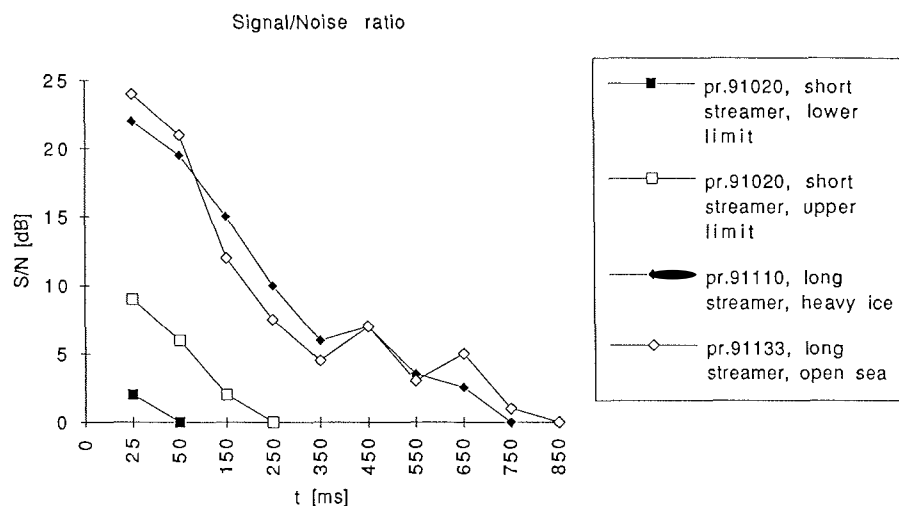


Fig. 7.5-4: Comparison of the signal to noise ratio for the short (50 m) and the long (300 m) streamer. Note that the S/N ratio for the long streamer is a factor 100 better than for the short streamer.

8. REFERENCES

- Archie G. E. (1942): Electrical resistivity log as an aid in determining some reservoir characteristics.- *Trans. A.I.M.E.* 146: 54-62.
- A S T M (1990): Annual Book of ASTM Standards, Section 4, Construction, volume 04.08, Sediment and Rock; dimension stone; geosynthetics.- American Society for Testing and Materials, Philadelphia, 1092 pp.
- Bleil, U. & Gard, G. (1989): Chronology and correlation of Quaternary magnetostratigraphy and nannofossil biostratigraphy in Norwegian-Greenland Sea sediments.- *Geol. Rundschau* 78: 1173-1187.
- Bohrmann, H.W. (1991): Radioisotopenstratigraphie, Sedimentologie und Geochemie jungquartärer Sedimente des östlichen Arktischen Ozeans.- Unpubl. Ph.D. Thesis, University of Kiel, 114 pp.
- Boyce, R.E. (1968): Electrical resistivity of modern marine sediments from Bering Sea.- *J. Geophys. Res.* 73: 4759-4766.
- Boyce, R.E. (1976): Sound velocity-density parameters of sediment and rock from DSDP drill sites 315-318 on the Line Island Chain, Manihiki Plateau, and Tuamotu Ridge in the Pacific Ocean.- *Initial Reports DSDP* 33: 695-728.
- Champion, D. E., Lanphere, M. A. & Kuntz, M. A. (1988): Evidence for a new geomagnetic reversal from lava flows in Idaho: discussion of short polarity reversals in the Brunhes and late Matuyama Polarity Chrons.- *J. Geophys. Res.* 93B: 11667-11680.
- Chang, S.-B. R. & Kirschvink, J. L. (1989): Magnetofossils, the magnetization of sediments, and the evolution of magnetite biomineralization.- *Ann. Rev. Earth Planet. Sci.* 17: 169-195.
- Childress, J.J. & Mickel, T.J. (1980): A motion compensated shipboard precision balance system.- *Deep Sea Res.* 27: 965-970.
- Drewry, D. (1986): *Glacial geologic processes*.- Edward Arnold, 276 pp.
- Gard, G. (1987): Late Quaternary calcareous nannofossil biostratigraphy and sedimentation patterns: Fram Strait, Arctica.- *Paleoceanography* 2: 519-529.
- Gard, G. (1988): Late Quaternary calcareous nannofossil biochronology and paleo-oceanography of Arctic and Subarctic Seas.- *Medd. Stockholm Univ. Geol. Inst.* 275.
- Gard, G. (1988): Late Quaternary nannofossil biozonation, chronology and paleo-oceanography in areas north of the Faeroe-Iceland-Ridge.- *Quat. Sci. Rev.* 7: 65-78.
- Gard, G. & Backman, J. (1990): Synthesis of Arctic and Sub-Arctic coccolith biochronology and history of North Atlantic drift water influx during the last

500,000 years.- In: U. Bleil and J. Thiede (eds.), Geological History of the Polar Oceans: Arctic versus Antarctic, NATO ASI Ser. C 308, Kluwer Acad. Publ., Dordrecht, 417-436.

Heezen, B.C. & Ewing, M. (1961): The Mid-Oceanic Ridge and its extension through the Arctic Basin.- In: Rasch, G. O. (ed.) Geology of the Arctic, V.1, University of Toronto Press, Toronto, 622-642.

Horner, R. A. (1985): Sea Ice Biota.- CRC Press, Boca Raton.

Horner, R. A. (1989): Arctic Sea-Ice Biota.- In: Herman, Y. (ed.), The Arctic Seas, van Nostrand Reinhold, New York, 123-146.

Jackson, H.R., Reid, I. & Falconer, R.K.H. (1982): Crustal structure near the Arctic mid-ocean ridge.- J. Geophys. Res. 79: 3347-3352.

Kögler, F. C. (1963): Das Kastenlot.- Meyniana 13: 1-7.

Köhler, S. (1991): Spätquartäre paläo-ozeanographische Entwicklung des Nordpolarmeeres und Europäischen Nordmeeres anhand von Sauerstoff- und Kohlenstoffisotopenverhältnissen der planktischen Foraminifere *Neogloboquadrina pachyderma* (sin.).- Unpubl. Ph.D. Thesis, Kiel University, 103 pp.

Kristoffersen, Y. (1990): Eurasia Basin.- In: The Geology of North America. Vol. L. The Arctic Ocean region, Geol. Soc. Amer., Boulder, 365-378.

Løvlie, R. (1989): Paleomagnetic stratigraphy: a correlation method.- Quaternary Int. 1: 129-149.

Nansen, F. (1902-1906): The Norwegian North Polar Expedition 1893-1896.- Scientific results Vol. I-VI, Oslo.

Noorany, I. (1984.): Phase Relations in Marine Soils.- ASCE Journal Geotech. Eng., 1984: 539 - 543.

Nowaczyk, N. R. (1991): Hochauflösende Magnetostratigraphie spätquartärer Sedimente arktischer Meeresgebiete (High-resolution magnetostratigraphy of Arctic Ocean marine sediments).- Ber. Polarforsch 78: 187 pp.

Nowaczyk, N. R. & Baumann, M. (in press): Combined high-resolution magnetostratigraphy and nannofossil biostratigraphy for late Quaternary Arctic Ocean sediments.- Deep-Sea Res.

Oestlund, H.G., Possnert, G. & Swift, J.H. (1987): Ventilation rate of the deep Arctic Ocean from carbon-14 data- J. Geophys. Res. 92: 3769-3777.

Ostenso, N. & Wold R.J. (1977): A seismic and gravity profile across the Arctic Ocean Basin.- Tectonophysics 37:1-24.

Ruddiman, W. & NAAG-DPG (1991): North Atlantic-Arctic gateways.- JOIDES Journ. 17(2): 38-50.

Schlosser, P., Boenisch, G., Kromer, B., Muennich, K.O. & Koltermann, K.P. (1990): Ventilation Rates of the Waters in the Nansen Basin of the Arctic Ocean Derived from a Multitracer Approach.- J. Geophys. Res. 95: 3265-3272.

Spieß, V., Villinger, H., Pototzki, F. & Zöllner, T. (1990): The Expeditions ANTARKTIS VIII/3 and VIII/4 of RV "Polarstern" in 1989.- In: Gersonde, R. & Hempel, G. (ed.), The Expeditions ANTARKTIS VIII/3 and VIII/4 of RV "Polarstern" in 1989.- Ber. Polarforsch. 74: 58-71.

Sweeney, J.F., Weber, J.R. & Blasco, S.M. (1982): Continental ridges in the Arctic Ocean: LOREX constraints.- Tectonophysics 89: 217-232.

Thiede, J. (ed.) (1988): Scientific cruise report of Arctic Expedition ARK IV/3.- Ber. Polarforsch. 43: 237 pp.

Thiede, J. & Hempel, G. (1991): The Expedition ARKTIS-VII/1 of RV "POLARSTERN" in 1990.- Ber. Polarforsch. 80: 137 pp.

Thompson, R. & Oldfield, F. (1986): Environmental Magnetism.- Allen and Unwin, London.

Vogt, P. (1985): Sea floor topography, sediments, and paleoenvironments.- In: Hurdle, B. G. (ed.), The Nordic Seas, Springer Verlag, New York, 237-410.

Wollenburg, I. (1991): Sedimenttransport durch das arktische Meereis.- Unpubl. Ph.D. Thesis, Kiel University, 132 pp.

9. ANNEX

9.1 Station List

Station	AWI-No.	Date	Time	Latitude	Longitude	Depth	Activity
19/148 Test- station	PS 2156-1	4.8.91	10:05	80° 05.3' N	30° 18.4' E	253	GWS
			10:45	80° 05.3' N	30° 16.3' E	243	ISP+CTD
			12:12	80° 05.2' N	30° 13.8' E	258	GKG (33)
			12:20-14:46				Seismic
19/149		5.8.91	06:08-09:40	81° 00.2' N	30° 49.9' E	124	Sea-ice sampling
		6.8.91	10:02-03:30				Seismic
19/150	PS 2157-1		4:45	81° 45.3' N	29° 54.9' E	2874	GKG (0)
			05:39	81° 45.3' N	29° 54.9' E	2874	GKG (0)
	06:56-10:50		81° 45.4' N	29° 56.3' E	2946	Sea-ice sampling	
	7:29		81° 45.3' N	29° 54.9' E	2875	MUC (35) +CTD	
	9:36		81° 45.4' N	29° 57.9' E	2960	ISP (test)	
	9:50-14:44		81° 45.3' N	29° 59.5' E		Sea-ice sampling	
	10:30		81° 45.3' N	29° 59.9' E	2900	GKG (37)	
	11:40		81° 45.3' N	30° 00.7' E	2965	TWC (165/77)	
	13:57		81° 45.5' N	30° 02.3' E	2978	GPC (625/377/TWC78)	
	15:05		81° 45.6' N	30° 03.6' E	3000	PS-frequency test	
		16:14-23:20				Seismic	
19/151	PS 2158-1	7.8.91	12:14-19:00	82° 46.5' N	29° 53.4' E	3799	Sea-ice sampling/Meteo-Boje
			13:38	82° 46.5' N	29° 55.5' E	3800	GKG (34)
			6:55-7:12				Seismic
19/152			19:50	83° 59.3' N	30° 28.6' E	4018	GWS
			18:30-21:20	83° 59.3' N	30° 28.6' E	4018	Sea-ice sampling
			13:38-22:50	83° 59.3' N	30° 28.5' E	4019	Ice-seismic
			0:45	83° 58.5' N	30° 24.8' E	4055	GWS+ISP
			6:07	83° 57.9' N	30° 23.6' E	4055	GWS
			8:00	83° 57.6' N	30° 22.1' E	4055	GKG (0)
			9:40	83° 57.3' N	30° 20.7' E	4054	GKG (30) bio
			9:42-12:00	83° 57.4' N	30° 20.7' E	4044	Sea-ice sampling
			11:41	83° 57.1' N	30° 18.6' E	4044	MUC (34)
			11:06-15:18				Seismic
			13:32	83° 56.9' N	30° 17.1' E	4010	GKG (27)
			13:20-16:25	83° 56.9' N	30° 17.1' E	4044	Sea-ice sampling
			15:15	83° 56.7' N	30° 16.9' E	4010	SL (40/20)
			18:14	83° 56.4' N	30° 16.4' E	4055	GPC (345/218/TWC0)
19:38	83° 56.2' N	30° 15.4' E	3950	PS-frequency test			
19/153		10.8.91	13:10-18:39	84° 53.0' N	37° 57.2' E	3757	Sea-ice sampling
			14:07	84° 52.9' N	37° 57.1' E	4029	GKG (0)
			15:53	84° 52.7' N	37° 55.6' E	4029	GKG (0)
			18:39	84° 52.8' N	37° 56.2' E	3989	Sonarboje
			17:46	84° 52.6' N	37° 53.5' E	4029	MUC (40) +CTD
		19:08-20:20				Seismic	
19/154	PS 2161-1	11.8.91	10:55	85° 27.2' N	44° 29.5' E	3966	GWS
			10:10-11:55	85° 27.2' N	44° 29.4' E		Sea-ice sampling
			13:36	85° 27.0' N	44° 25.2' E	4005	MUC (40) +CTD
			12:30	85° 27.1' N	44° 26.0' E		Ice-seismik

Station	AWI-No.	Date	Time	Latitude	Longitude	Depth	Activity
	PS 2161-2		15:15	85° 26.7' N	44° 23.6' E	4005	GKG (55) bio
			16:45	85° 26.7' N	44° 23.6' E	3967	GWS
	PS 2161-3		19:33	85° 26.4' N	44° 20.3' E	4005	GPC (1000/70/TWC92)
	PS 2161-4		21:42	85° 26.3' N	44° 18.2' E	4005	GKG (36)
19/155	PS 2162-1	12.8.91	13:13	85° 47.7' N	50° 49.6' E	3981	GKG (44)
			12:35-14:15	85° 47.7' N	50° 49.3' E	3941	Sea-ice sampling
			14:51-15:34				Video/Linescan flight
19/156			19:23	85° 56.0' N	52° 20.4' E	3938	GWS
19/157	PS 2163-1	13.8.91	9:58	86° 14.5' N	59° 12.9' E	3040	MUC (30) +CTD
			9:30-15:40	86° 14.5' N	59° 12.7' E	3025	Sea-ice sampling
			10:40-15:05				Seismic
	PS 2163-2		11:21	86° 14.5' N	59° 14.0' E	3047	GKG (23)
			11:00-17:10	86° 14.5' N	59° 13.8' E	3025	Sea-ice activity
	PS 2163-3		13:34	86° 14.5' N	59° 14.5' E	3075	GPC (1000/582/TWC72)
	PS 2163-4		16:27	86° 14.4' N	59° 21.6' E	3173	KAL (40/30)
			18:35	86° 14.3' N	59° 22.7' E	3174	GWS
			19:50	86° 14.2' N	59° 24.1' E	3205	PS-frequency test
19/158	PS 2164-1	14.8.91	0:28	86° 20.3' N	59° 10.5' E	2004	MUC (18) +CTD
	PS 2164-2		1:33	86° 20.2' N	59° 12.6' E	2004	MUC (18)
	PS 2164-3		2:32	86° 20.1' N	59° 14.6' E	1974	GKG (0)
	PS 2164-4		3:20	86° 20.1' N	59° 16.0' E	2030	GKG (33)
	PS 2164-5		4:28	86° 20.0' N	59° 17.8' E	2035	GKG (30) bio
	PS 2164-6		8:38	86° 15.9' N	59° 21.4' E	2111	GPC (740/238/TWC57)
			8:45-10:14	86° 19.9' N	59° 21.6' E	2114	Sea-ice sampling
			10:15	86° 19.9' N	59° 24.1' E	2140	PS-frequency test
19/159	PS 2165-1		14:06	86° 26.8' N	59° 57.6' E	2011	GPC (1115/567/TWC88)
	PS 2165-2		15:30	86° 26.5' N	60° 03.8' E	1798	GKG (0)
			14:25-17:08	86° 26.6' N	60° 02.0' E	1816	Sea-ice sampling
	PS 2165-3		16:27	86° 26.4' N	60° 04.3' E	1794	GKG (36)
	PS 2165-4		17:22	86° 26.3' N	60° 06.1' E	1835	KAL (300/227)
	PS 2165-5		18:40	86° 26.1' N	60° 08.4' E	1911	MUC (30)
			19:11	86° 26.1' N	60° 08.9' E	1939	PS-frequency test
19/160	PS 2166-1	15.8.91	5:42	86° 51.6' N	59° 41.9' E	3618	MUC (30) +CTD
	PS 2166-2		7:28	86° 51.6' N	59° 45.9' E	3636	GKG (37)
			6:53-9:38	86° 51.6' N	59° 44.7' E	3555	Sea-ice sampling
	PS 2166-3		9:40	86° 51.4' N	59° 48.2' E	3555	GPC (250/215/TWC54)
19/161	PS 2167-1	15.8.91	15:36	86° 56.7' N	59° 00.9' E	4434	GPC (750/640/TWC169)
			14:20-17:01	86° 56.7' N	59° 00.9' E	4499	Sea-ice sampling
	PS 2167-2		17:55	86° 56.1' N	59° 04.5' E	4425	GKG (41)
	PS 2167-3		20:12	86° 56.0' N	59° 08.3' E	4427	MUC (32)
			21:05	86° 55.8' N	59° 10.4' E	4400	PS-frequency test
19/162		16.8.91	0:23-10:40	86° 51.3' N	56° 43.6' E	3772	Sea-ice sampling
			1:06-9:16				Seismic
			1:20	86° 51.2' N	56° 44.4' E	3779	GWS (test)
			6:41	86° 50.7' N	56° 48.7' E	3779	GWS (300 m) +CTD
			9:20-11:32	86° 50.6' N	56° 55.0' E	3371	Sea-ice sampling
			11:08-16:06	86° 50.3' N	57° 06.7' E	3467	Ice-seismic
	228H		13:20-14:47				Sea-ice sampling flight
			11:37	86° 50.4' N	56° 59.4' E	3449	GWS
19/163		17.8.91	1:45	87° 20.0' N	55° 56.9' E	4104	GWS
19/164	PS 2168-1		6:22	87° 30.6' N	55° 56.0' E	3846	GKG (39)

Station	AWI-No.	Date	Time	Latitude	Longitude	Depth	Activity
	PS 2168-2		9:31	87° 30.9' N	56° 05.8' E	3790	GPC (1200/409/TWC34)
			9:42-12:04	87° 31.1' N	56° 16.1' E	3681	Sea-ice sampling
	PS 2168-3		11:51	87° 31.1' N	56° 15.0' E	3685	MUC (30) +CTD
			13:12-14:40	87° 31.1' N	56° 26.7' E	3655	Sea-ice sampling
	PS 2169-1!		16:52	87° 30.2' N	55° 58.3' E	3846	GPC (1050/622/TWC109)
			17:46	87° 30.2' N	56° 00.6' E	3825	PS-frequency test
19/165			23:55	87° 34.4' N	60° 13.9' E	4448	GWS
		18.8.91	2:45	87° 34.4' N	60° 23.1' E	4459	GWS+ISP
			8:38	87° 35.0' N	60° 39.0' E	4375	GWS
	PS 2170-1		10:47	87° 35.4' N	60° 46.0' E	4226	GKG (38)
			10:15-11:47	87° 35.3' N	60° 44.1' E	4279	Sea-ice sampling
	PS 2170-2		12:24	87° 35.7' N	60° 51.5' E	4186	MUC (0)
	230H		14:20-15:35				Sea-ice sampling flight
	PS 2170-3		15:34	87° 35.7' N	60° 52.2' E	4112	GPC (1220/1151/TWC76)
	PS 2170-4		17:20	87° 35.8' N	60° 53.7' E	4083	MUC (45)
			18:00	87° 36.5' N	61° 09.8' E	4033	PS-frequency test
19/166	PS 2171-1	19.8.91	1:53	87° 35.1' N	68° 58.7' E	4384	GKG (50)
	PS 2171-2		3:23	87° 35.6' N	69° 12.0' E	4384	MUC (43)
	PS 2171-3		6:45	87° 35.6' N	69° 11.2' E	4395	SL (400/300)
			6:20-8:50	87° 35.7' N	69° 10.1' E	4395	Sea-ice sampling
	PS 2171-4		9:15	87° 36.1' N	69° 22.8' E	4395	KAL (400/325)
	231		12:43-13:28	87° 36.6' N	69° 45.4' E		Laser-altimetry flight
	PS 2171-5		13:06	87° 36.6' N	69° 48.2' E	4397	GPC (1487/986/TWC182)
			14:44	87° 36.8' N	69° 56.9' E	4429	PS-frequency test
19/167		20.8.91	8:25-11:00	87° 15.3' N	68° 17.7' E	4344	Sea-ice sampling
	PS 2172-1		9:22	87° 15.4' N	68° 22.7' E	4391	GKG (49)
	PS 2172-2		11:14	87° 15.7' N	68° 32.2' E	4479	GKG bio
	PS 2172-3		13:04	87° 15.9' N	68° 41.6' E	4480	MUC (35)
	PS 2172-4		15:45	87° 16.1' N	68° 53.9' E	4481	GPC (1265/951/TWC170)
			17:12	87° 16.2' N	68° 59.8' E	4468	PS-frequency test
	232		18:13-18:53	87° 16.4' N	69° 01.6' E		Laser-altimetry flight
	232H		19:15-20:50				Sea-ice sampling flight
19/168	PS 2173-1	21.8.91	7:19	87° 18.4' N	69° 19.3' E	4558	KAL (700/550)
			6:11-7:46	87° 18.3' N	69° 13.6' E	4558	Sea-ice sampling
19/169			9:30-10:20				Seismic
19/170			17:15	87° 29.7' N	79° 53.6' E	4431	GWS surface
19/171		22.8.91	1:10	87° 30.1' N	89° 58.7' E	4396	GWS surface
			2:39	87° 30.0' N	90° 10.5' E	4427	GWS
	PS 2174-1		5:05	87° 29.8' N	90° 24.2' E	4427	GKG (0)
	PS 2174-2		6:40	87° 29.5' N	90° 43.2' E	4427	MUC (34)
			8:47-12:20	87° 29.3' N	90° 56.9' E	4395	Sea-ice sampling
	234		10:00-10:38	87° 29.2' N	91° 02.1' E		Laser-altimetry flight
	PS 2174-3		10:08	87° 29.2' N	91° 06.5' E	4394	GPC (1930/1300/TWC110)
	PS 2174-4		12:48	87° 29.1' N	91° 20.3' E	4426	GKG (43)
	PS 2174-5		14:37	87° 29.1' N	91° 32.6' E	4427	KAL (1130/960)
	234H		16:10-17:31				Sea-ice sampling flight
	PS 2174-6		16:22	87° 29.1' N	91° 41.5' E	4427	GKG (40) bio
			18:21	87° 29.1' N	91° 46.2' E	4394	GWS
			19:14	87° 29.1' N	91° 52.1' E	4399	PS-frequency test
19/172	235	23.8.91	10:22-11:05	87° 33.0' N	103° 23.4' E		Laser-altimetry flight
			11:00-24:00	87° 33.3' N	103° 26.0' E	4381	Ice-seismic

Station	AWI-No.	Date	Time	Latitude	Longitude	Depth	Activity
			11:46	87° 33.4' N	103° 26.8' E	4381	GWS surface
			13:00-16:00	87° 33.7' N	103° 29.9' E	4379	Sea-ice sampling
	PS 2175-1		14:36	87° 34.1' N	103° 34.0' E	4379	GPC (1750/1124/TWC61)
			16:38-23:10				Seismic
	PS 2175-2		17:51	87° 34.9' N	103° 40.9' E	4412	GKG (40) bio
	PS 2175-3		19:39	87° 35.4' N	103° 43.6' E	4411	GKG (36)
	PS 2175-4		21:14	87° 36.0' N	103° 47.6' E	4411	MUC (24)
	PS 2175-5	24.8.91	8:52	87° 39.8' N	104° 04.9' E	4313	GPC (1950/1692/TWC102)
			9:45	87° 40.0' N	104° 04.1' E	4410	PS-frequency test
19/173		25.8.91	1:10	87° 43.5' N	109° 20.8' E	4363	GWS
			4:12	87° 45.2' N	108° 59.1' E	4395	GWS + ISP
			9:35-9:00 (26.)	87° 45.6' N	108° 54.9' E	4395	Ice-seismic
			10:35-11:25				Sea-ice sampling flight
	PS 2176-1		11:54	87° 46.0' N	108° 44.8' E	4395	GPC (1850/1421/TWC72)
			13:10-17:00	87° 46.1' N	108° 38.9' E	4395	Sea-ice sampling
	PS 2176-2		14:37	87° 46.2' N	108° 32.5' E	4396	MUC (30)
	PS 2176-3		16:26	87° 46.3' N	108° 23.6' E	4363	KAL (1080/976)
			18:17	87° 46.4' N	108° 18.8' E	4359	GWS
	PS 2176-4		20:11	87° 46.6' N	108° 10.0' E	4364	GKG (37)
	PS 2176-5		21:56	87° 46.8' N	108° 08.9' E	4364	GKG (40) bio
		26.8.91	0:20	87° 47.0' N	108° 08.5' E	4362	GWS
	PS 2176-6		9:04	87° 47.8' N	107° 52.2' E	4364	GPC (1800/863/TWC86)
	238		9:13-10:00	87° 47.9' N	107° 47.3' E		Laser-altimetry flight
			10:12	87° 47.9' N	107° 43.8' E	4363	PS-frequency test
			10:45-12:15				Sea-ice sampling flight
19/174			19:41	88° 01.7' N	119° 51.4' E	3166	GWS surface
19/175		27.8.91	6:06	88° 02.2' N	134° 55.7' E	1357	GWS
	PS 2177-1		6:36	88° 02.2' N	134° 55.1' E	1388	GKG (40)
			7:16-11:00	88° 02.2' N	134° 54.3' E	1357	Ice-seismic
	PS 2177-2		7:22	88° 02.2' N	134° 53.7' E	1388	GKG (40) bio
	PS 2177-3		8:12	88° 02.2' N	134° 50.7' E	1390	MUC (35) +CTD
	PS 2177-4		9:12	88° 02.1' N	134° 48.6' E	1391	KAL (575/575, top lost)
			9:42-12:00	88° 02.1' N	134° 46.0' E	1391	Sea-ice sampling
	PS 2177-5		11:27	88° 02.1' N	134° 36.7' E	1400	KAL (900/780)
	PS 2177-6		15:48	88° 02.3' N	134° 19.6' E	1419	GPC (1612/1157/TWC161)
			16:25	88° 22.3' N	134° 18.9' E	1431	PS-frequency test
			18:50-23:30				Seismic
19/176		28.8.91	8:55	88° 01.2' N	158° 30.3' E	3971	GWS surface
			9:10	88° 00.2' N	158° 31.6' E	3970	GWS
			13:20	88° 00.0' N	158° 51.8' E	4010	GWS + ISP
			10:00-11:45 (29)	88° 00.6' N	158° 41.0' E	3970	Ice-seismic
	240H		11:10-12:28				Sea-ice sampling flight
			13:15-17:59	88° 00.0' N	158° 51.8' E	4010	Sea-ice sampling
	240		13:20-13:35	88° 00.0' N	158° 59.5' E		Laser-altimetry flight
			18:44	88° 02.0' N	159° 01.7' E	4009	GWS
			19:42-20:03	88° 00.3' N	159° 06.9' E	4009	Sea-ice sampling
	PS 2178-1		20:39	88° 00.3' N	159° 07.8' E	4009	GKG bio
	PS 2178-2		22:14	88° 00.2' N	159° 14.0' E	4009	GKG (43)
	PS 2178-3	29.8.91	8:06	88° 00.3' N	159° 10.1' E	4009	GPC (1930/1372/TWC124)
	PS 2178-4		10:40	88° 01.3' N	159° 35.1' E	4008	MUC (35)
			9:55-11:00	88° 01.2' N	159° 31.3' E	4008	Sea-ice sampling

Station	AWI-No.	Date	Time	Latitude	Longitude	Depth	Activity
	PS 2178-5		12:33	88° 01.5' N	159° 42.2' E	4008	KAL (880/831)
			13:21	88° 01.6' N	159° 44.4' E	4008	PS-frequency test
19/177		30.8.91	15:18-15:07				Seismic
19/178	242		15:20-16:09	87° 45.0' N	138° 09.0' E		Laser-altimetry flight
			15:32-16:58	87° 44.7' N	138° 00.4' E	1231	Sea-ice sampling
	PS 2179-1		15:46	87° 44.8' N	138° 01.7' E	1230	GKG (37)
	PS 2179-2		16:31	87° 44.9' N	138° 06.0' E	1229	GKG bio
	PS 2179-3		17:13	87° 45.0' N	138° 09.4' E	1228	MUC (28)
19/179		31.8.91	18:06-06:00				Seismic
19/180			7:15	87° 35.6' N	158° 22.2' E	3969	GWS
19/181	PS 2180-1		11:14	87° 37.6' N	156° 40.5' E	4005	GKG (48)
			10:40-13:25	87° 37.4' N	156° 37.4' E	3968	Sea-ice sampling
	PS 2180-2		13:47	87° 38.6' N	156° 58.0' E	3991	GPC (1760/1296/TWC87)
			14:38	87° 39.0' N	157° 06.1' E	3967	PS-frequency test
19/182	PS 2181-1		20:29	87° 35.8' N	153° 03.6' E	3112	GKG bio
	PS 2181-2		21:58	87° 35.7' N	153° 15.4' E	3226	GKG (10)
	PS 2181-3		23:16	87° 35.8' N	153° 22.5' E	3331	GKG (16)
	PS 2181-4	1.9.91	0:36	87° 35.9' N	153° 29.0' E	3418	MUC (19)
19/183	PS 2182-1		3:24	87° 34.3' N	151° 07.2' E	2489	GKG (10)
	PS 2182-2		4:29	87° 34.5' N	151° 14.4' E	2547	GKG (0)
	PS 2182-3		5:26	87° 34.6' N	151° 21.2' E	2609	GKG bio
	PS 2183-4		6:31	87° 34.7' N	151° 29.9' E	2619	MUC (35)
	PS 2182-5		7:58	87° 34.7' N	151° 42.6' E	2628	SL (600/480)
19/184	244		9:59-10:23	87° 35.3' N	150° 16.8' E		Laser-altimetry flight
	PS 2183-1		11:32	87° 36.1' N	148° 49.8' E	2016	GKG (15)
	PS 2183-2		12:28	87° 36.2' N	148° 55.3' E	2031	GKG bio
	PS 2183-3		13:24	87° 36.3' N	149° 00.4' E	2022	MUC (15)
			12:15-14:35	87° 36.2' N	148° 54.0' E	2032	Sea-ice sampling
	PS 2183-4		14:30	87° 36.4' N	149° 06.5' E	2032	SL (700/481)
19/185	PS 2184-1		16:20	87° 36.7' N	148° 08.4' E	1640	GKG (31)
	PS 2184-2		17:11	87° 36.7' N	148° 12.1' E	1654	GKG bio
	PS 2184-3		17:56	87° 36.7' N	148° 15.2' E	1674	MUC (30)
19/186			23:50-23:00 (02	87° 30.8' N	143° 31.6' E	1051	Ice-seismic
	PS 2185-1	2.9.91	6:18	87° 31.8' N	144° 10.0' E	1051	SL (1000/580)
	PS 2185-2		7:10	87° 31.9' N	144° 16.2' E	1051	GKG bio
			7:01-11:45	87° 31.8' N	144° 15.8' E	1051	Sea-ice sampling
	PS 2185-3		7:53	87° 32.0' N	144° 22.9' E	1051	GKG (33)
	PS 2185-4		8:34	87° 32.0' N	144° 28.9' E	1051	MUC (30)
	PS 2185-5		10:02	87° 32.1' N	144° 40.2' E	1051	GPC (1750/800/TWC114)
	245		10:32-11:15	87° 32.1' N	144° 43.3' E		Laser-altimetry flight
	PS 2185-6		12:00	87° 32.2' N	144° 55.6' E	1052	KAL (840/835)
			13:22-22:10	87° 32.3' N	145° 07.0' E	1078	Sea-ice sampling
	PS 2185-7		15:44	87° 32.3' N	145° 25.1' E	1069	GPC (1725/738/TWC121)
			16:43	87° 32.3' N	145° 34.1' E	1082	PS-frequency test
19/187		3.9.91	1:28-4:46				Seismic
	246		9:42-10:08	87° 53.7' N	146° 22.9' E		Laser-altimetry flight
19/188			12:35-14:05				Seismic
19/189	PS 2186-1	4.9.91	6:29	88° 30.7' N	139° 54.4' E	1867	GKG (38)
	PS 2186-2		7:36	88° 30.8' N	140° 11.0' E	1898	GKG bio
	PS 2186-3		8:30	88° 30.8' N	140° 21.8' E	2004	MUC (30)
			8:46-10:50	88° 30.8' N	140° 23.2' E	1976	Sea-ice sampling

Station	AWI-No.	Date	Time	Latitude	Longitude	Depth	Activity
	PS 2186-4		9:30	88° 30.8' N	140° 27.0' E	2034	SL (700/525)
	PS 2186-5		10:33	88° 30.9' N	140° 29.4' E	2036	GKG (37)
			10:34-17:24	88° 30.9' N	140° 29.4' E	1996	Ice-seismic
			11:00-16:19	88° 31.0' N	140° 31.0' E	1996	Sea-ice sampling
19/190		5.9.91	3:24-19:30	88° 31.4' N	126° 16.3' E	3842	Ice-seismic
			5:28	88° 43.8' N	126° 24.9' E	3841	GWS
	PS 2187-1		7:35	88° 44.1' N	126° 51.5' E	3813	GKG (41)
	PS 2187-2		9:03	88° 44.1' N	126° 59.6' E	3807	GKG bio
			8:58-12:00	88° 44.1' N	126° 59.7' E	3804	Sea-ice sampling
	PS 2187-3		11:41	88° 44.5' N	126° 52.0' E	3819	GPC (1890/907/TWC158)
			12:50	88° 44.7' N	126° 51.6' E	3853	PS-frequency test
	248		13:06-14:20	88° 44.8' N	126° 51.2' E		Laser-altimetry flight
	PS 2187-4		14:55	88° 45.3' N	127° 02.4' E	3908	KAL (840/827)
			14:58-16:13				Video/Linescan flight
	248H		16:35-18:20				Sea-ice sampling flight
	PS 2187-5		16:38	88° 45.5' N	127° 12.6' E	3898	MUC (35)
			18:15	88° 45.7' N	127° 34.9' E	3868	GWS
19/191	PS 2188-1	6.9.91	2:08	88° 47.5' N	135° 57.1' E	2479	SL (700/420)
19/192	PS 2189-1		6:16	88° 46.9' N	144° 33.0' E	1018	GKG (20)
	PS 2189-2		6:52	88° 46.8' N	144° 40.7' E	1036	GKG bio
	PS 2189-3		7:31	88° 46.8' N	144° 47.9' E	1064	MUC (10)
	PS 2189-4		8:16	88° 46.8' N	144° 55.0' E	1080	SL (700/473)
			9:00-10:50	88° 46.8' N	145° 00.1' E	1095	Sea-ice sampling
	PS 2189-5		12:30	88° 47.8' N	144° 00.9' E	1001	GPC (1445/1035/TWC93)
			12:55	88° 47.9' N	144° 05.5' E	1001	PS-frequency test
19/193			15:31-10:00 (07.)				Seismic
19/194	PS 2190-1	7.9.91	11:46	90° N		4240	KAL (550/467)
	PS 2190-2		13:26	89° 59.4' N	86° 45.0' W	4236	GKG bio
			11:20-15:30	89° 59.8' N	115° 0.0' W	4240	Sea-ice sampling
	PS 2190-3		14:57	89° 59.0' N	84° 44.7' W	4240	GKG (35)
	PS 2190-4		17:22	89° 58.2' N	96° 29.5' E	4237	GPC (1365/1293/TWC58)
	PS 2190-5		20:07	89° 57.8' N	110° 49.1' E	4267	MUC (30) +CTD
19/195		8.9.91	11:00-2:38 (09.)				Seismic
	251		16:19-16:42	89° 33.8' N	24° 4.2' W		Laser-altimetry flight
19/196	PS 2191-1	9.9.91	3:50	88° 59.6' N	09° 00.7' E	4346	MUC (30) +CTD
			3:00-5:55	88° 59.9' N	09° 24.9' E	4348	Sea-ice sampling
	PS 2191-2		5:37	88° 59.5' N	08° 12.6' E	4347	GKG (0)
	PS 2191-3		7:03	88° 59.7' N	07° 46.6' E	4348	SL (100/60)
	PS 2191-4		8:42	88° 59.7' N	07° 33.4' E	4346	GKG bio
19/197			11:20-20:30				Seismic
19/198			21:25-23:15	88° 16.2' N	10° 09.7' E	4375	Sea-ice sampling
			22:15-7:50 (10.)	88° 16.4' N	10° 08.1' E	4375	Ice-seismic
		10.9.91	1:03	88° 16.3' N	10° 11.6' E	4374	GWS
	PS 2192-1		3:08	88° 15.7' N	09° 52.7' E	4375	GKG (44)
	PS 2192-2		4:46	88° 15.3' N	09° 21.8' E	4411	MUC (30)
			6:31	88° 15.1' N	08° 58.9' E	4374	GWS
	PS 2192-3		8:26	88° 15.3' N	07° 56.0' E	4409	SL (900/528)
19/199			10:26-20:05				Seismic
19/200	PS 2193-1		21:05	87° 30.7' N	11° 28.5' E	4399	SL (600/418)
			20:38-23:00	87° 30.6' N	11° 34.2' E	4365	Sea-ice sampling
			21:50	87° 30.9' N	11° 22.4' E	4366	PS-frequency test

Station	AWI-No.	Date	Time	Latitude	Longitude	Depth	Activity
	PS 2193-2		22:39	87° 31.1' N	11° 15.5' E	4337	GKG (40)
	PS 2193-3	11.9.91	0:16	87° 31.6' N	11° 05.1' E	4158	MUC (35) +CTD
19/201			4:33-16:15				Seismic
19/202			16:45-20:50	86° 45.4' N	09° 55.7' E	4357	Ice-seismic
			18:03	86° 45.4' N	09° 55.9' E	4358	GWS
			17:08-20:30	86° 45.4' N	09° 56.9' E	4358	Sea-ice sampling
19/203			21:15-2:48 (12.)				Seismic
19/204		12.9.91	3:20-6:40	86° 35.8' N	07° 07.9' E	4324	Ice-seismic
			4:58	86° 35.8' N	07° 12.9' E	4326	GWS
			3:54-5:55	86° 35.9' N	07° 11.8' E	4324	Sea-ice sampling
	PS 2194-1		7:39	86° 35.6' N	07° 29.3' E	4326	GKG (20)
19/205			10:25-14:29				Seismic
19/206	PS 2195-1		15:27	86° 15.2' N	09° 37.0' E	3793	GKG (0)
			15:30-17:55	86° 15.2' N	09° 37.2' E	3778	Sea-ice sampling
	PS 2195-2		16:45	86° 15.0' N	09° 39.7' E	3743	GKG bio
	PS 2195-3		18:54	86° 14.2' N	09° 41.0' E	3966	GPC (1240/959/TWC45)
	PS 2195-4		20:53	86° 13.7' N	09° 35.6' E	3873	GKG (39)
19/207		13.9.91	0:40-3:20				Seismic
19/208			4:10-7:55	86° 09.0' N	05° 05.3' E	4421	Ice-seismic
			6:28	86° 09.0' N	05° 05.6' E	4423	GWS
			9:15-11:40	86° 07.8' N	05° 02.9' E	4423	Sea-ice sampling
19/209			13:46-18:30				Seismic
19/210	PS 2196-1		19:35	85° 57.7' N	00° 09.9' E	3958	SL (800/552)
			19:35-22:48	85° 56.4' N	00° 00.0' E	3894	Ice-seismic
			19:15-23:10	85° 57.9' N	00° 09.9' E	4141	Sea-ice sampling
	PS 2196-2		21:05	85° 57.1' N	00° 06.9' E	3958	GKG (28)
	PS 2196-3		22:35	85° 56.4' N	00° 00.6' E	3888	MUC (0) +CTD
			23:50	85° 56.1' N	00° 04.0' W	4032	PS-frequency test
19/211		14.9.91	2:36-6:48				Seismic
19/212	PS 2197-1		8:45	85° 46.0' N	04° 08.5' W	4154	KAL (960/937)
			9:30-11:40	85° 45.7' N	04° 10.0' W	4117	Sea-ice sampling
	PS 2197-2		10:42	85° 45.4' N	04° 13.7' W	4156	GKG (0)
			9:55-14:10	85° 45.6' N	04° 11.3' W	4117	Ice-seismic
	PS 2197-3		12:09	85° 45.1' N	04° 18.1' W	4156	GKG (0)
	PS 2197-4		14:27	85° 44.8' N	04° 22.7' W	4115	GPC (1800/1011/TWC0)
			15:33	85° 44.8' N	04° 23.5' W	4116	PS-frequency test
19/213		15.9.91	6:52-9:35				Seismic
19/214	PS 2198-1		12:01	85° 33.9' N	09° 03.5' W	3767	GKG (28)
	PS 2198-2		13:20	85° 33.8' N	09° 02.8' W	3820	SL (900/555)
			12:40-15:33	85° 33.8' N	09° 03.3' W	3794	Sea-ice sampling
	PS 2198-3		14:46	85° 33.8' N	09° 00.5' W	3838	GKG bio
	PS 2198-4		16:10	85° 33.6' N	08° 56.8' W	3818	MUC (30) +CTD
19/215			18:20-21:15				Seismic
19/216	PS 2199-1		22:01	85° 26.1' N	11° 54.8' W	1789	SL (0)
	PS 2199-2		22:53	85° 26.0' N	11° 55.5' W	1670	GKG (0)
	PS 2199-3		23:30	85° 25.9' N	11° 55.8' W	1633	GKG (15)
	PS 2199-4	16.9.91	0:20	85° 25.9' N	11° 56.3' W	1614	GKG (30)
	PS 2199-5		1:05	85° 25.8' N	11° 56.6' W	1591	GKG (0)
			1:28	85° 25.8' N	11° 56.4' W	1590	PS-frequency test
19/217			6:52-8:55				Seismic
19/218	PS 2200-1		9:53	85° 19.7' N	14° 01.0' W	1073	SL (900/546)

Station	AWI-No.	Date	Time	Latitude	Longitude	Depth	Activity
			9:50-11:58	85° 19.7' N	14° 01.2' W	1073	Sea-ice sampling
			10:15-22:00	85° 19.6' N	14° 00.0' W	1073	Ice-seismic
PS 2200-2			10:35	85° 19.6' N	14° 00.0' W	1074	GKG (30)
259			10:44-10:54	85° 19.6' N	14° 00.0' W		Laser-altimetry flight
PS 2200-3			11:16	85° 19.5' N	14° 00.3' W	1072	GKG bio
PS 2200-4			11:58	85° 19.4' N	14° 00.3' W	1072	MUC (30) +CTD
PS 2200-5			12:45	85° 19.4' N	14° 00.0' W	1073	KAL (770/768)
259H			13:08-14:31				Sea-ice sampling flight
PS 2200-6			16:15	85° 19.2' N	13° 52.3' W	1087	GPC (1700/585/TWC93)
			20:58	85° 17.8' N	13° 44.0' W	1099	PS-frequency test
19/219		17.9.91	3:01-5:40				Seismic
19/220	PS 2201-1		6:48	85° 25.3' N	12° 08.6' W	1353	GKG (32)
	PS 2201-2		7:29	85° 25.1' N	12° 07.1' W	1350	GKG bio
	PS 2201-3		8:50	85° 25.2' N	12° 02.1' W	1388	GPC (0/0/TWC0)
	PS 2201-4		10:32	85° 25.0' N	12° 00.8' W	1380	SL (30/29)
19/221			12:30-4:30 (18.)				Seismic
19/222	PS 2202-1	18.9.91	8:10	85° 06.5' N	14° 22.2' W	1081	GKG (0)
	PS 2202-2		8:36	85° 06.4' N	14° 22.7' W	1083	GKG (30)
	PS 2202-3		9:16	85° 06.4' N	14° 22.9' W	1083	GKG bio
			9:18-11:40	85° 06.4' N	14° 22.9' W	1084	Sea-ice sampling
			9:42-11:20	85° 06.3' N	14° 23.2' W	1083	Ice-seismic
	PS 2202-4		9:58	85° 06.3' N	14° 23.4' W	1083	MUC (30) +CTD
	PS 2202-5		10:45	85° 06.2' N	14° 24.0' W	1082	SL (900/510)
	PS 2202-6		11:24	85° 06.1' N	14° 24.6' W	1081	GKG bio
			12:30-18:00	85° 06.1' N	14° 25.1' W	1081	Ice-seismic
	PS 2202-7		13:31	85° 06.0' N	14° 25.2' W	1081	GPC (1475/1043/TWC110)
			13:21-14:03	85° 06.0' N	14° 25.2' W	1081	Sea-ice sampling
	PS 2202-8		14:29	85° 05.9' N	14° 24.9' W	1085	GKG bio
	PS 2202-9		15:04	85° 05.8' N	14° 24.5' W	1088	GKG bio
	PS 2202-10		15:41	85° 05.8' N	14° 24.5' W	1088	GKG bio
	PS 2202-11		16:12	85° 05.7' N	14° 24.0' W	1091	GKG bio
			16:27-18:03				Sea-ice sampling flight
	261		16:45-17:05	85° 05.6' N	14° 23.6' W		Laser-altimetry flight
19/223	262	19.9.91	14:09-14:56	85° 03.9' N	14° 05.9' W		Laser-altimetry flight
	PS 2203-1		14:16	85° 03.9' N	14° 05.7' W	2584	GKG (0)
	PS 2203-2		15:19	85° 04.0' N	14° 04.6' W	2584	GKG (0)
	PS 2203-3		16:14	85° 04.0' N	14° 03.5' W	2614	GKG (0)
	PS 2203-4		17:25	85° 04.1' N	14° 02.2' W	2541	MUC (0) +CTD
19/224	PS 2204-1		23:28	85° 03.3' N	13° 01.2' W	3899	GKG (0)
	PS 2204-2	20.9.91	0:44	85° 03.5' N	12° 59.9' W	3899	GKG (0)
	PS 2204-3		3:12	85° 03.5' N	13° 02.1' W	3899	MUC (35) +CTD
19/225			8:14-3:09 (21.)				Seismic
	263		10:12-10:42	85° 02.8' N	11° 52.4' W		Laser-altimetry flight
	263H		11:17-12:11				Sea-ice sampling flight
19/226		21.9.91	4:55	84° 38.2' N	06° 44.7' W	4260	GWS
	PS 2205-1		7:17	84° 38.6' N	06° 46.0' W	4283	MUC (44) +CTD
			6:50-21:10	84° 38.5' N	06° 45.6' W	4285	Ice-seismic
	PS 2205-2		9:38	84° 38.8' N	06° 47.3' W	4298	GKG (0)
			9:28-11:50	84° 38.8' N	06° 47.1' W	4288	Sea-ice sampling
	PS 2205-3		11:20	84° 38.9' N	06° 49.1' W	4318	GKG bio
	PS 2205-4		12:53	84° 39.2' N	06° 50.0' W	4327	GKG (0)


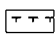
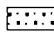
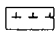

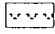

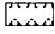
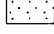
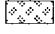
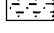




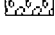
Station	AWI-No.	Date	Time	Latitude	Longitude	Depth	Activity
			13:11-16:55	84° 39.3' N	06° 50.0' W	4324	Sea-ice sampling
	PS 2205-5		14:28	84° 39.2' N	06° 50.0' W	4327	SL (?/63)
	PS 2205-6		15:59	84° 39.9' N	06° 46.8' W	4329	SL (?/49)
	PS 2205-7		17:32	84° 40.1' N	06° 43.1' W	4330	GKG (0)
19/227		22.9.91	6:40-13:27				Seismic
19/228	PS 2206-1		14:29	84° 15.8' N	02° 33.4' W	3020	KAL (250/187)
	PS 2206-2		16:07	84° 16.1' N	02° 36.6' W	3025	GKG (0)
	PS 2206-3		18:01	84° 16.3' N	02° 32.9' W	3025	GPC (600/105/TWC105)
			18:09	84° 16.4' N	02° 32.6' W	3027	PS-frequency test
	PS 2206-4		19:58	84° 16.7' N	02° 30.3' W	2993	MUC (30) +CTD
19/229			21:45-01:01 (23.)				Seismic
19/230		23.9.91	6:00-10:45	83° 59.6' N	00° 07.3' W	3687	Ice-seismic
	PS 2207-1		7:49	84° 00.0' N	00° 05.1' W	3687	GKG (0)
			7:20-20:03	83° 59.9' N	00° 05.7' W	3671	Sea-ice sampling
	PS 2207-2		9:17	84° 00.5' N	00° 01.4' W	3639	MUC
19/231			11:08-15:36				Seismic
19/232			15:58-18:50				Seismic
19/233			20:28-05:15 (24)				Seismic
19/234	PS 2208-1	24.9.91	6:48	83° 38.4' N	04° 36.2' E	3681	MUC (30)
	PS 2208-2		9:20	83° 38.6' N	04° 39.5' E	3682	GPC (900/685/TWC132)
			8:50-11:35	83° 38.5' N	04° 38.6' E	3682	Ice-seismic
			9:12-10:40	83° 38.5' N	04° 39.3' E	3682	Sea-ice sampling
	267		10:46-11:10	83° 38.6' N	04° 41.9' E		Laser-altimetry flight
	267H		11:10-12:58				Sea-ice sampling flight
	PS 2208-3		11:15	83° 38.7' N	04° 43.4' E	3721	GKG (0)
	PS 2208-4		13:07	83° 38.7' N	04° 47.8' E	3623	SL (300/214)
			13:50-15:08				Video/Linescan flight
	PS 2208-5		14:32	83° 38.6' N	04° 50.7' E	3503	MUC (30) +CTD
			13:54	83° 38.7' N	04° 49.6' E	3527	Ice-seismic
	PS 2208-6		15:52	83° 38.5' N	04° 52.3' E	3444	GKG (0)
19/235			23:08-06:17 (25.)				Seismic
19/236		25.9.91	07:15-08:32	83° 15.9' N	08° 35.2' E	4047	Ice-seismic
19/237			09:10-14:02				Seismic
	268H		12:50-14:25				Sea-ice sampling
	268		14:55-15:27	83° 02.1' N	07° 37.3' E		Laser-altimetry flight
19/238			15:42-18:53				Seismic
19/239			20:30	83° 14.8' N	08° 36.6' E	4039	GWS
		26.9.91	3:16	83° 13.9' N	08° 36.4' E	4046	GWS+ISP
	PS 2209-1		5:37	83° 13.5' N	08° 34.4' E	4046	GKG (47)
	PS 2209-2		7:20	83° 13.3' N	08° 32.8' E	4046	SL (750/276)
			8:55	83° 13.1' N	08° 31.7' E	4045	PS-frequency test
	269a		10:02-10:31	83° 12.9' N	08° 31.5' E		Laser-altimetry flight
	PS 2209-3		10:08	83° 12.9' N	08° 31.9' E	4048	GKG bio +CTD
			9:48-11:08	83° 13.0' N	08° 31.5' E	4046	Sea-ice sampling
			9:48-11:30	83° 13.0' N	08° 31.5' E	4046	Ice-seismic
	PS 2209-4		12:24	83° 12.4' N	08° 31.9' E	4048	GPC (600/122/TWC0)
			12:40-16:53	83° 12.3' N	08° 32.0' E	4044	Ice-seismic
			13:00-16:26	83° 12.2' N	08° 32.0' E	4046	Sea-ice sampling
	269b		16:10-17:00	83° 12.9' N	08° 31.5' E		Laser-altimetry flight
19/240			21:09-00:56 (27.)				Seismic
19/241	PS 2210-1	27.9.91	2:15	83° 02.7' N	10° 07.5' E	3949	GKG (34)

Station	AWI-No.	Date	Time	Latitude	Longitude	Depth	Activity
	PS 2210-2		3:39	83° 02.5' N	10° 06.8' E	3897	GKG bio
	PS 2210-3		5:10	83° 02.3' N	10° 05.4' E	3806	MUC (35) +CTD
	PS 2210-4		7:05	83° 02.1' N	10° 04.0' E	3702	SL (50/0)
			9:32-11:30	83° 01.7' N	10° 01.7' E	3485	Sea-ice sampling
			10:00-11:30	83° 01.7' N	10° 01.0' E	3466	Ice-seismic
19/242		28.9.91	05:00-13:09				Seismic
19/243	271		13:02-13:33	82° 39.6' N	13° 21.8' E		Laser-altimetry flight
	PS 2211-1		13:58	82° 40.9' N	13° 11.7' E	1297	SL (30/20)
	PS 2211-2		15:12	82° 39.3' N	13° 06.5' E	961	GKG (gravel) +CTD
			15:09-15:26	82° 39.3' N	13° 06.5' E	962	Sea-ice sampling
	PS 2211-3		15:44	82° 39.2' N	13° 05.5' E	961	GKG (0) +CTD
	PS 2211-4		16:09	82° 39.2' N	13° 04.7' E	959	GKG (0)
19/244			16:50-18:32				Seismic
19/245	PS 2212-1	29.9.91	7:21	82° 01.4' N	15° 40.3' E	2531	GKG bio
	PS 2212-2		8:32	82° 01.3' N	15° 37.1' E	2484	GKG (0)
			10:45-12:58	82° 04.2' N	15° 52.5' E	2563	Sea-ice sampling
			11:15-12:40				Video/Linescan flights
	PS 2212-3		11:17	82° 04.2' N	15° 51.2' E	2550	KAL (815/802)
	PS 2212-4		12:23	82° 04.0' N	15° 47.9' E	2480	GKG (0)
			12:26	82° 04.0' N	15° 47.8' E	2471	PS-frequency test
	PS 2212-5		13:17	82° 04.0' N	15° 46.0' E	2485	GKG (39)
	PS 2212-6		14:50	82° 03.8' N	15° 43.0' E	2439	MUC (40) +CTD
	272		15:15-15:36	82° 03.8' N	15° 42.4' E		Laser-altimetry flight
19/246	PS 2213-1	30.9.91	11:49	80° 28.4' N	08° 12.3' E	897	GKG (36)
	PS 2213-2		12:22	80° 28.3' N	08° 10.9' E	888	GKG bio
	PS 2213-3		13:02	80° 28.2' N	08° 09.4' E	884	SL (1000/300)
			13:42	80° 28.0' N	08° 08.2' E	879	PS-frequency test
	PS 2213-4		14:05	80° 28.0' N	08° 07.7' E	874	MUC (35) +CTD
	PS 2213-5		15:42	80° 27.8' N	08° 05.3' E	866	GPC (900/41/TWC169)
	PS 2213-6		17:41	80° 27.6' N	08° 02.6' E	853	GPC (1670/1317/TWC161)
19/247			19:40-05:39 (1.10.)				HydroSweep-survey
19/248		1.10.91	06:47-12:42				Seismic
19/249	PS 2214-1		13:06	80° 16.1' N	06° 37.6' E	552	GKG (34)
	PS 2214-2		13:36	80° 16.5' N	06° 36.6' E	560	GKG bio
	PS 2214-3		13:58	80° 16.7' N	06° 36.2' E	563	SL (250/57)
	PS 2214-4		14:41	80° 17.2' N	06° 34.7' E	562	MUC (40) +CTD
19/250			15:39-00:51 (2.)				Seismic
19/251		2.10.91	1:02-6:15				HydroSweep-survey
19/252	PS 2215-1		7:04	79° 41.7' N	05° 20.4' E	2045	MUC (42) +CTD
	PS 2215-2		8:18	79° 42.4' N	05° 15.6' E	2019	GKG (35)
	PS 2215-3		10:36	79° 41.7' N	05° 18.9' E	2073	GPC (1100/985/TWC155)
	PS 2215-4		13:20	79° 41.9' N	05° 18.1' E	2075	SL (800/437)
			13:44	79° 42.1' N	05° 16.9' E	2055	PS-frequency test
19/253			14:45-05:00 (3.)				Seismic
19/254		3.10.91	6:15	79° 41.4' N	01° 29.3' E	2367	CTD for HydroSweep
19/255		3.10.91	7:00- 6.10.91 11:26				HydroSweep-survey
19/256		7.10.91	6:20-17:00	75° 00.6' N	04° 08.5' W	3596	Search for mooring

9.2 Graphical Core Descriptions

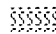





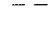

Legend:

Lithology

	sand		foraminiferal ooze
	sandy silt		nannofossil ooze
	sandy clay		diatomaceous ooze
	sandy mud		radiolarian ooze
	silt		volcanic ash
	mud		chert / porcellanite
	clay		pebbles, drop stones
	diamicton		sediment clasts

* = smear slides

Structure

	bioturbation
	stratification
	lamination
	coarsening upward sequence
	fining upward sequence
	sharp boundary
	gradational boundary
	transition zone

PS2157-4 (GKG)

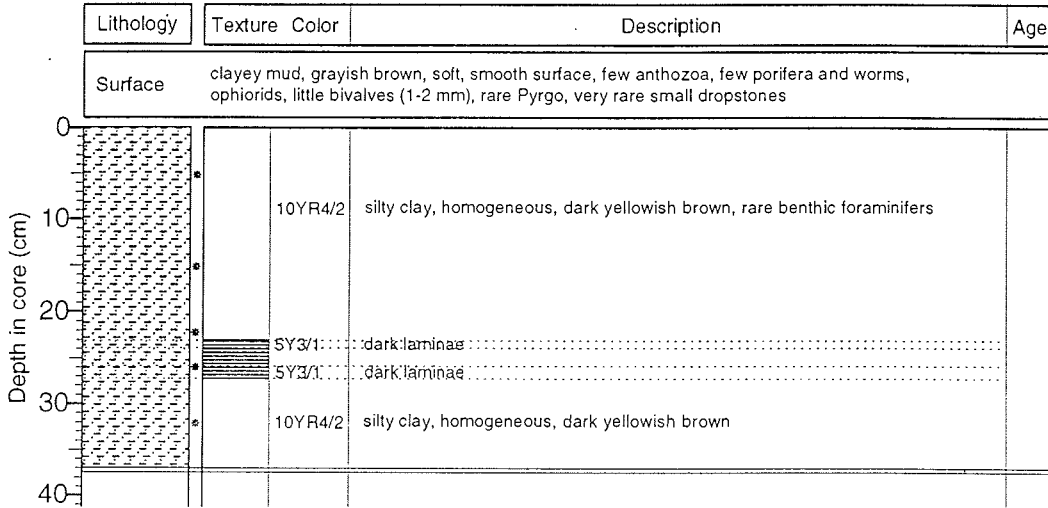
N Svalbard

ARK VIII/3 (ARCTIC 91)

Recovery: 0.37 m

81° 45.3' N, 30° E

Water depth: 2900 m



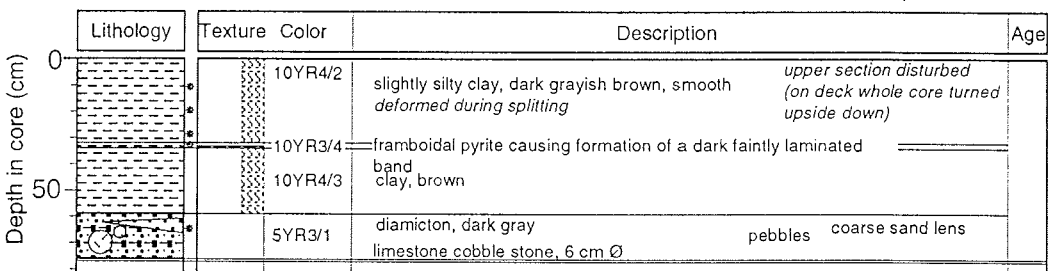
PS2157-5 (TWC as gravity corer) Slope N Svalbard

ARK VIII/3 (ARCTIC 91)

Recovery: 0.77 m

81° 45.3' N, 30° 0.7' E

Water depth: 2965 m



PS2157-6 (TWC)

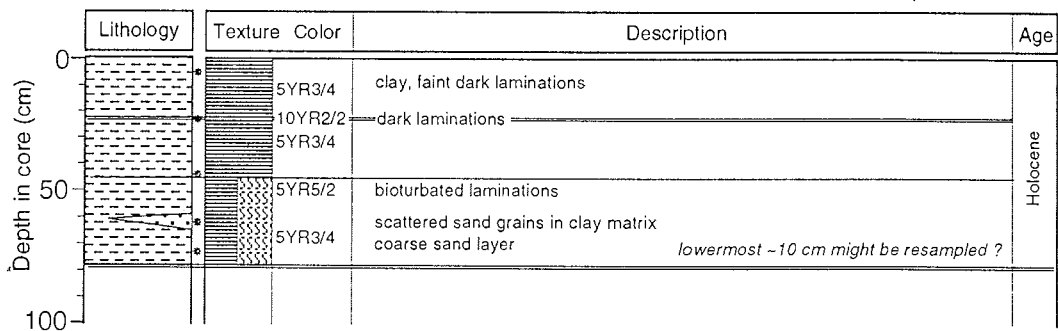
N Svalbard

ARK VIII/3 (ARCTIC 91)

Recovery: 0.78 m

81° 45.5' N, 30° 2.3' E

Water depth: 2978 m



PS2157-6 (GPC)

Slope N' Svalbard

ARK VIII/3 (ARCTIC 91)

Recovery: 3.77 m

81° 45.5' N, 30° 2.3' E

Water depth: 2978 m

Depth in core (m)	Lithology	Texture	Color	Description	Age
0			2.5Y3/2	clay, very dark grayish brown	Holocene
			10YR3/3	clay, dark brown, dark bands	
			2.5Y5/4	clay, light olive brown sand layer at 39-40 cm	
			10YR3/3	clay, dark brown brown layer, bioturbated at 55-57 cm	
			5Y4/1	diamicton, pebbles up to 3-4 cm Ø diamicton, poorly consolidated, dark gray	?
1				92-93 diamicton, poorly consolidated, dark gray	Pleistocene
			5Y3/1	diamicton (pebbly sandy mud) consolidated, homogeneous, very dark gray (similar to Barents Sea shelf diamictons)	
2				chert	
				chert	
				striated pebble (amphibolite?)	
3				sharp boundary carbonate rocks	?
				clasts more rounded clayey diamicton (pebbly sandy mud) poorly consolidated, homogeneous, very dark gray higher content of coarse sand and gravel than in unit above (similar to Barents Sea shelf diamictons)	Stage 5 ?
4					
5					

PS2158-1 (GKG)

Nansen Basin

ARK VIII/3 (ARCTIC 91)

Recovery: 0.34 m

82° 46.6' N, 29° 55.5' E

Water depth: 3800 m

Lithology	Texture	Color	Description	Age
Surface silty clay, dark grayish brown, smooth, common worm tubes, ophiurids, rare small dropstones and mud clasts				
<p>Depth in core (cm)</p>				
	10YR4/2		silty clay, homogeneous, dark grayish brown, at 4-7 cm dark gray burrows (2-3 mm Ø)	
	10YR4/2		silty clay, homogeneous, dark yellowish brown, horizontal brownish and grayish streaks and common brownish mottles	
	10YR4/2		clayey silt, slightly olive with brownish mottles and rare dropstones (2-5 mm Ø)	
	10YR5/2 10YR4/2		silty clay, dark yellowish brown, intercalations of stiff and soft layers	

PS2159-4 (GKG)

Nansen Basin

ARK VIII/3 (ARCTIC 91)

Recovery: 0.27 m

83° 56.9' N, 30° 17.1' E

Water depth: 4010 m

Lithology	Texture Color	Description	Age
Surface		silty clay, dark yellowish brown, soft, slightly sandy, smooth, common planktonic foraminifers	
0-10 cm	2.5Y4/2	clay, dark grayish brown, homogeneous, common planktonic foraminifers at very top	
10-13 cm	2.5Y4/2	silty clay, dark grayish brown, homogeneous, stiff	
13-16 cm	10YR3/3	clay, dark brown, homogeneous, brownish and grayish horizontal streaks at 13-16 cm	
16-30 cm	10YR3/3	silty clay, dark brown, homogeneous, stiff	

PS2159-6 (GPC)

Nansen Basin

ARK VIII/3 (ARCTIC 91)

Recovery: 2.18 m

83° 56.4' N, 30° 16.4' E

Water depth: 4055 m

Lithology	Texture Color	Description	Age
0-15 cm	10YR3/3	clayey mud, dark brown, more silty at the base no visible structures	0-15 cm bag sample
15-20 cm	10YR4/3	clay, brown to dark grayish brown, sticky, poorly consolidated disturbed during coring, possibly originally faintly laminated	sharp boundary
20-25 cm	10YR4/2	clayey sand, dark yellowish brown, laminated	core catcher was found in this part and did cause considerable disturbance transitional boundary
25-30 cm	10YR4/4	upper part of turbidite	transitional boundary
30-35 cm	10YR4/1	sand, dark gray, dark yellowish brown in upper part, fining upwards lower part of turbidite	sharp boundary
35-40 cm	10YR4/2 10YR5/2 10YR4/3	clay, dark greyish brown, in parts faintly laminated	layer of gray mud clasts
40-45 cm	10YR3/3	clay, dark brown	0.5-2 mm Ø sand lense due to coring disturbance
45-200 cm	10YR4/2 to 5Y4/2	clay, silty sand layers (2-7 mm), color varies between olive gray and dark grayish brown, poorly consolidated, in some parts heavily disturbed	late Pleistocene

PS2161-3 (TWC)

Nansen Basin

ARK VIII/3 (ARCTIC 91)

Recovery: 0.92 m

85° 26.4' N, 44° 20.3' E

Water depth: 4005 m

Lithology	Texture Color	Description	Age	
	10YR5/2-1	clay, grayish brown, homogeneous to laminated		
	10YR3/4	silty clay, dark yellowish brown, homogeneous		sharp boundary
	10YR4/3	silty clay, grayish brown to dark gray, homogeneous to laminated, slightly bioturbated in the lower part		
	10YR4/1			
	10YR5/2			sharp boundary
	10YR3/4 10YR4/2 to 10YR4/3	silty clay, dark yellowish brown to grayish brown, homogeneous to laminated		
	silty clay, grayish brown, dark gray spots ("cloudy"), 75-89 slightly bioturbated, 89-92 homogeneous to laminated			
		silty layers, dark gray at: 10, 35, 45, 47 cm black clast (weathered pyrite?) at 64 cm	<i>presumably double penetration</i>	

PS2161-3 (GPC)

Nansen Basin

ARK VIII/3 (ARCTIC 91)

Recovery: 0.70 m

85° 26.4' N, 44° 20.3' E

Water depth: 4005 m

Lithology	Texture Color	Description	Age	
	10YR5/2-1	clay, grayish brown, homogeneous to laminated		
	10YR3/4	silty clay, dark yellowish brown, homogeneous		sharp boundary
	10YR4/2	silty clay, grayish brown to dark gray, homogeneous to laminated, slightly bioturbated in the lower part		
	10Y3/2			
	2.5Y5/2			sharp boundary
	10YR3/4 2.5Y4/2 and N4	silty clay, dark yellowish brown, homogeneous		
	silt, dark grayish brown and dark gray, coring disturbance			
		silty layers, dark gray at 11, 37 cm dark layers at 46, 48 cm <i>Interval 0-57 cm fits well with the 0-57 cm interval of the TWC; 57-70 of the PC has been succed in from deeper parts</i>		

PS2161-4 (GKG)

Nansen Basin

ARK VIII/3 (ARCTIC 91)

Recovery: 0.36 m

85° 26.3' N, 44° 18.2' E

Water depth: 4005 m

Lithology	Texture Color	Description	Age
Surface		clay, olive gray, smooth, even surface, rare worm feeding traces, (pseudofaeces) rare benthic foraminifers	
	5Y4/2	clay, soft, olive gray with slight brownish horizontal streaks and mottles	
	5Y4/2	silty clay, olive gray, stiff	
	5Y4/2	clay, soft, olive gray	
	10YR3/2	silty clay, very dark grayish brown	
	10YR4/2	clay, soft, dark grayish brown with common light olive grayish mottles	
	10YR4/2	clay, stiff, dark grayish brown	
10YR3/3	silty clay, dark brown, with slight olive mottles, dark olive borrows at 28-30 cm		
2.5Y4/2	clay, dark grayish brown, with slight brownish horizontal streaks		

PS2162-1 (GKG)

Nansen Basin

ARK VIII/3 (ARCTIC 91)

Recovery: 0.44 m

85° 47.7' N, 50° 49.6' E

Water depth: 3981 m

Lithology	Texture	Color	Description	Age
Surface	clay, olive gray, smooth, even surface, one Actinea, small spots (0.1 mm Ø) of grayish black color			
	2.5Y4/2		clay, dark grayish brown, soft	
	10YR3/2		silty clay, very dark grayish brown, 16-17 cm with common planktonic foraminifers	
	10YR5/2		clay, grayish brown, soft, with slight grayish horizontal streaks	
	2.5Y4/2		clay, dark grayish brown, soft, with slight grayish horizontal streaks	
50				

PS2163-3 (GPC)

Gakkel Ridge

ARK VIII/3 (ARCTIC 91)

Recovery: 5.82 m

86° 14.5' N, 59° 14.5' E

Water depth: 3075 m

Lithology	Texture Color	Description	Age
0	10YR4/4	clay, dark yellowish brown, soft, getting darker towards the top	
	10YR4/3	clay, dark brown, lighter diffuse horizon between 18-20 cm	
0	2.5Y4/2	sandy clay, dark grayish, more grayish towards the base	
	10YR5/4	clay, yellowish brown	
0	10YR4/4	clay, dark yellowish brown, soft (similar to top unit)	
	2.5Y4/2	silty, sandy clay, dark grayish brown,	
0	2.5Y5/4	clay, light olive brown	
	2.5Y4/2	sandy mud, dark grayish brown, sand layers	
0	10YR5/4		sharp boundary
	2.5Y5/4	clay, light olive brown	
1	2.5Y5/4	sandy mud, light olive brown, frequently scattered lighter mud-clasts	
	10YR4/4	sandy silt, dark yellowish brown, scattered mud-clasts	
1			sand layer at 149-150 sand lens, pebble at 152-155 cm
	10YR3/1	sandy mud, very dark gray, dropstone 5 cm Ø	
2	5Y4/2	clayey mud, olive gray, mud clasts, lighter color at top	
	5Y4/3	silty clay, olive, sandy at base	
2	2.5Y4/2	clay, dark grayish brown	
	2.5Y4/2	sandy mud (diamicton?), common dropstones and dark spots	
2	missing		
	2.5Y4/4	sandy clay, olive brown	
3	10YR4/3 to 2.5Y4/2	sandy mud, dark grayish brown grading upwards to dark yellowish brown, few sand laminae, lighter spots (bioturbation ?)	transitional boundary
	5Y3/1	sandy mud, very dark gray	
3	5YR4/6	sandy clay, yellowish red, few dark dropstones	
	2.5Y4/2	clay sandy clay, yellowish red, few dark dropstones	
3	2.5Y4/4-5YR4/4	sandy mud, reddish brown clay, dark grayish brown (2.5Y4/2), sand laminae	
	2.5Y4/4	sandy clay, olive brown	
3	2.5Y4/2	clay, dark grayish brown	uneven boundary
	10YR5/4	clay, yellowish brown, few sand	
4	2.5Y4/4	sandy clay, olive brown	
	10YR5/4	sandy clay, color grading from dark grayish brown to yellowish brown, more sand at the base	
4	2.5Y4/4	sandy clay, olive brown, black laminae/streaks between 410-416 cm, scattered black spots, two clay layers at base	
	10YR5/6	clay, few sand, yellowish brown, dark spots	
4	10YR5/4	sandy clay, brownish yellow, scattered dark spots, irregular dark layers/streaks,	
5.82			566-582 is CC

PS2164-4 (GKG)

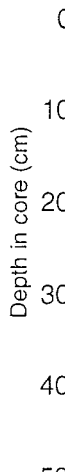
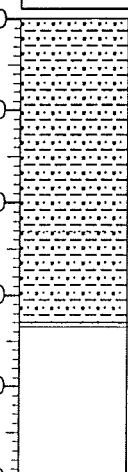
Gakkel Ridge

ARK VIII/3 (ARCTIC 91)

Recovery: 0.33 m

86° 20.1' N, 59° 16.0' E

Water depth: 2030 m

Lithology	Texture	Color	Description	Age
Surface			sandy silty clay, dark grayish brown, smooth surface, common planktonic and benthic foraminifers common dropstones (1-10 mm Ø), 1 big dropstone (4 cm Ø), abundant sponge spicules	
		2.5Y4/2	sandy silty clay, dark grayish brown, common planktonic and benthic foraminifers, common dropstones (1-5 mm Ø), abundant grayish and brownish mottles	
		2.5Y4/4	sandy silty clay, olive brown, common planktonic and benthic foraminifers, common dropstones (1-5 mm Ø), common grayish and brownish horizontal streaks and mottles	
		uneven boundary ..	

PS2164-6 (TWC)

Gakkel Ridge

ARK VIII/3 (ARCTIC 91)

Recovery: 0.57 m

86° 15.9' N, 59° 21.4' E

Water depth: 2111 m

Depth in core (m)	Lithology	Texture	Color	Description	Age
0				10YR3/3 sandy mud, dark brown	
				2.5Y4/2 clayey mud, dark grayish brown	
				10YR4/4	
				10YR3/2 sandy silty mud, dark grayish brown, darker bands at 26, 29 cm, slight color changes, mottled, slightly layered	
				2.5Y4/2	
				2.5Y4/4 clay to clayey mud, olive brown, slightly darker layer at 54 cm	
				<i>presumably double penetration</i>	
1					

PS2164-6 (GPC)

Gakkel Ridge

ARK VIII/3 (ARCTIC 91)

Recovery: 2.38 m

86° 15.9' N, 59° 21.4' E

Water depth: 2111 m

Depth in core (m)	Lithology	Texture	Color	Description	Age
0				5Y4/2 silty mud, olive gray, thin slightly darker mottled layer on top, mottles filled with darker material from above	
				5Y4/3 fine silty mud	
				5Y4/4 silty mud, olive, slightly brownish, homogeneous, mud layer at 35-36 cm	
				5Y4/2 clayey mud to clay, olive gray, slightly banded, no clear boundaries	
				5Y4/3 sandy silt, olive, homogeneous, slightly mottled, brownish sandstone at 52 cm	
				5Y4/2 silty mud, olive gray, homogeneous, slightly mottled, dark spot at 67 cm	
				10YR5/6 silty, sandy mud, yellowish brown, abundant mud clasts (yellowish, gray, black), unsorted, big clast at 96 cm, homogeneous	
1				10YR5/6 to 10YR4/3 sandy silt, yellowish brown (at 110-120 cm grading brown to dark brown), slightly deformed sand layer at 130 cm, four mudclasts, sand layers, black spot at 110 cm	
				10YR3/1 silty sand/sandy silt, very dark gray, inclusions and clasts, very homogeneous, 130-132 cm grading into gray	
				10YR3/2 silty sand/sandy silt, very dark grayish brown, homogeneous, slight layering indicated by minor changes of lines of gray to brown, shell fragment at 152 cm	
				10YR3/1 silty sand, very dark gray, homogeneous	
				2.5Y5/2 silty mud, dark grayish brown, homogeneous	
				2.5Y3/2 mud clasts in silty mud matrix, very dark grayish brown	
				2.5Y3/2 silty mud, few mud clasts, very dark grayish brown, slightly mottled	
2				2.5Y4/2 3 fine sand layers in silty matrix, dark grayish brown	
				2.5Y4/2-3/1 silty mud, grading to very dark gray, slightly layered, thin sand layer at 207 cm	
				2.5Y3/1 sandy silt to silty mud, very dark gray, homogeneous, big sand lens at 205 cm	
				2.5Y5/4 sandy silt, light olive brown, very homogeneous, upper boundary color grading over 1 cm, 231-238, block, crust, yellow, manganese nodule or part of crust layer	

PS2165-1 (GPC)

Gakkel Ridge

ARK VIII/3 (ARCTIC 91)

Recovery: 5.67 m

86° 26.8' N, 59° 57.6' E

Water depth: 2011 m

Lithology	Texture Color	Description	Age
	10YR3/3	clay, dark brown	
	2.5Y4/4	sandy clay, olive brown, bioturbated with infill of sediments of the overlying unit	
	10YR5/4		
	10YR4/3	clay, brown, with few sand, bioturbated, 19-21 cm yellowish brown	
	2.5Y4/4	sand, olive brown, with lenses of clay from the unit above	
	2.5Y4/4	sandy clay, olive brown	
	2.5Y4/4	sandy mud, olive brown, darker towards top, clay/mud clasts, faint laminations, mottled sand lense at 115-120 cm, sand laminae at 88, 103 cm	
	5Y3/1	sandy mud, very dark gray, thin laminae between 177 and 230 cm, few black mud clasts, particularly in the upper part	
	5Y4/2	sandy clay, olive gray, lighter at top	
	5Y4/3	sandy mud, olive (top) to dark olive (base), abundant sand laminae, few coal clasts	
	5Y3/2	clay, very dark brown, light layer on top	
	10YR2/2		
	5Y3/2 to 5Y4/2	sandy mud, olive to dark olive, darker at 290-300 cm	dropstone, 1 cm Ø at 277 cm
	5Y4/2	sandy mud, olive gray,	
5Y3/1	sandy mud, very dark gray, abundant sand layers at the lower part (distal turbidites ?), spacing of sand laminae is about 1 cm		
5Y4/3	sandy clay, olive, mottled, sand laminae at base, color changes on top		
5Y3/1	sandy clay, very dark gray, sand laminae at top (488-472 cm)		

PS2165-1 (GPC)

Gakkel Ridge

ARK VIII/3 (ARCTIC 91)

Recovery: 5.67 m

86° 26.8' N, 59° 57.6' E

Water depth: 2011 m

Depth in core (m)	Lithology	Texture Color	Description	Age
5		5Y3/1	sandy clay, very dark gray, sand lense at 502-504 cm	
		5Y4/3 to 2.5Y4/4	sandy clay, olive to olive brown, sand lenses at 533-539 cm	
		2.5Y4/4	sandy mud, olive brown, sand laminae on top	
		5Y4/3-3/1	clay, olive brown to very dark gray, sand layers at 549, 555 cm	

PS2165-1 (TWC)

Gakkel Ridge

ARK VIII/3 (ARCTIC 91)

Recovery: 0.88 m

86° 26.8' N, 59° 57.6' E

Water depth: 2011 m

Depth in core (m)	Lithology	Texture Color	Description	Age
0		10YR3/3	clay, dark brown, mottled	
		2.5Y4/4	silty clay, olive brown, few mud clasts in lower part, brown mottles	
		10YR5/4	clay, very dark grayish brown	
		10YR4/3	clay, brown mottled, yellowish brown mottles in upper part	
		2.5Y4/4	medium/coarse sand, olive brown	
		2.5Y5/4	sandy mud, light olive brown	
		mix	clay, varying brownish colors	
		2.5Y4/4	medium/coarse sand, olive brown	disturbed at 50-60 cm
		2.5Y5/4	sandy mud, light olive brown, sand layer at 71.5 cm, mud clasts at 77-79 cm	double penetration
1		10YR4/3	sandy mud, brown, several mud clasts, dark brown at top	

PS2165-3 (GKG)

Gakkel Ridge

ARK VIII/3 (ARCTIC 91)

Recovery: 0.36 m

86° 26.4' N, 60° 04.3' E

Water depth: 1794 m

Depth in core (cm)	Lithology	Texture Color	Description	Age
Surface			sandy, silty clay, dark grayish brown, smooth surface, common benthic and planktonic foraminifers, common dropstones (1-10 mm Ø), one dropstone 40 mm Ø, abundant sponge spicules, bivalves (1 cm Ø)	
0		2.5Y4/2	like surface	
		10YR5/3	sandy, brown, silty clay with grayish horizontal streaks and mottles	
10		10YR4/2	sandy, silty clay, dark grayish brown, with brownish and grayish horizontal streaks and mottles	
20		10YR5/3	sandy, silty clay, brown, with slight grayish horizontal streaks	
		10YR4/3	sandy, silty clay, dark brown	
		10YR5/4	sandy, silty clay, yellowish brown, slight grayish horizontal streaks	
		10YR4/4	sandy, silty clay, dark yellowish brown	
30		10YR4/3	sandy, silty clay, dark brown, grayish mottles	
40				

PS2165-4 (KAL)

Gakkel Ridge

ARK VIII/3 (ARCTIC 91)

Recovery: 2.27 m

86° 26.3' N, 60° 6.1' E

Water depth: 1835 m

Lithology	Texture	Color	Description	Age
	10YR3/3		sandy clay, dark brown	
	10YR5/3		clay, brown	
	10YR3/3		clayey mud, dark brown	
	10YR3/4		sandy clay, dark yellowish brown, worm tubes	
	10YR4/3		medium to coarse sand, dark brown bedding visible	Pecten sp., 1.5 cm Ø Clast of sandy silt
	10YR5/4		sandy mud, yellowish brown	
	10YR5/4		sand, yellowish brown	uneven surface
	2.5Y5/4 to 10YR5/4		silty mud, folded and contorted layers, color varying between yellowish brown and light olive brown	
	5Y5/3		clay, olive, disturbed	
	2.5Y5/4 to 10YR5/4		silty mud, folded and contorted layers, color varying between yellowish brown and light olive brown	sand lense
	10YR4/3		sand, yellowish brown, sorted	
	10YR3/4		pebbly sand, yellowish brown	
	10YR4/4		sandy mud with lighter and darker parts, contorted ?	
<p><i>The upper 120 cm of the core has slid upwards causing faulting and disturbance of the layers</i></p>				

Depth in core (m)

3

4

5

PS2166-2 (GKG)

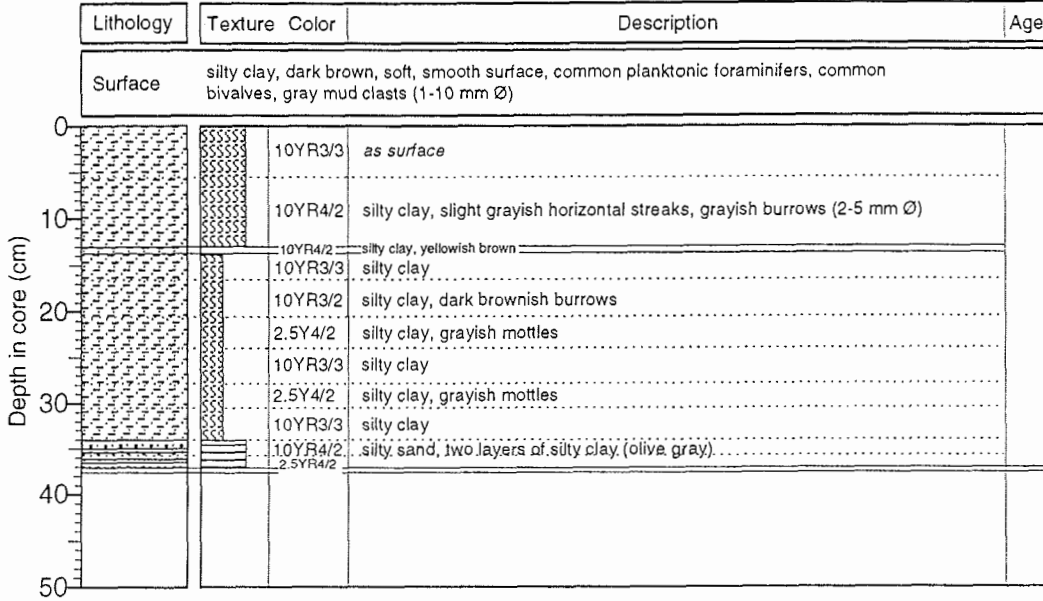
Gakkel Ridge

ARK VIII/3 (ARCTIC 91)

Recovery: 0.37 m

86° 51.6' N, 59° 45.9' E

Water depth: 3636 m



PS2166-3 (TWC)

Gakkel Ridge

ARK VIII/3 (ARCTIC 91)

Recovery: 0.54 m

86° 51.4' N, 59° 48.2' E

Water depth: 3555 m

Depth in core (m)	Lithology	Texture	Color	Description	Age
	0			10YR3/3	clay, dark brown, soft, mottled, 2 laminae of calcareous material
			2.5Y4/4	clay, olive brown, mottled	
			2.5Y4/2	sandy mud, dark grayish brown, black lamina at lower sharp boundary	
0.5			10YR4/3	clay, dark brown, mottled, two sand laminae in the upper part,	
			10YR3/4	olive brown at 45-47 cm, thin bands of sandy and silty mud,	
			10YR4/3	dark yellowish brown at 50 cm	

PS2166-3 (GPC)

Gakkel Ridge

ARK VIII/3 (ARCTIC 91)

Recovery: 2.14 m

86° 51.4' N, 59° 48.2' E

Water depth: 3555 m

Depth in core (m)	Lithology	Texture	Color	Description	Age
	0			10YR3/3	clay, dark brown, soft, mottled, small lenses of sand at 17 cm
			2.5Y4/4	clay, olive brown, mottled	
			2.5Y4/2	sandy mud, dark grayish brown, black lamina at lower sharp boundary	
			10YR4/3	clay, brown, mottled, sand laminae at base	
			2.5Y5/4	clay, light olive brown, mottled, sand lamina at 79 cm and at base	
1			10YR4/6	clay, dark yellowish brown, common very dark brown (10YR2.5/2) spots, mud clasts? at 160-214 cm, dropstone at 159 cm	
2					

↑
coring
disturbance
↓

PS2167-1 (GPC)

Gakkel Ridge

ARK VIII/3 (ARCTIC 91)

Recovery: 6.40 m

86° 56.7' N, 59° 0.9' E

Water depth: 4434 m

	Lithology	Texture	Color	Description	Age
0			10YR3/2	clayey mud, very dark grayish brown, soft, very homogeneous	
			10YR4/2	clay, dark grayish brown, homogeneous, slightly mottled, thin bands of silt	
			10YR4/1	sand, dark gray	
			10YR4/6	silty clay, dark yellowish brown, color grading	
			10YR4/3	silty clay, brown, homogeneous	
			10YR4/2	sand, dark yellowish brown	
			10YR4/4	clayey mud, dark yellowish brown, homogeneous, thin sand layer at 88 cm	
			5Y3/2	clayey mud, dark olive gray	
			2.5Y4/2	clayey mud, dark grayish brown, dark bands on top and bottom	
			10YR4/4	clay, dark yellowish brown, homogeneous	
			10YR3/6	manganese layer, dark yellowish brown	
1			10YR4/4	silty mud, dark yellowish brown, numerous mud clasts dropstone at 134-136 cm	
			2.5Y4/2	clayey mud, dark grayish brown, homogeneous	
			10YR4/3	clayey mud, dark brown, homogeneous	
			10YR4/1	sand, dark gray, heavy minerals?	
			10YR4/3	clayey mud, dark brown, homogeneous	
			10YR3/4	silt, dark yellowish brown	
			10YR4/3	silty mud, dark brown	
2		▲	2.5Y4/2	sand, dark grayish brown, homogeneous, fining upwards	
		▲	5Y3/1	coarse to medium sand, very dark gray, fining upwards	
3		▲	5Y4/3	coarse to medium sand, olive to olive gray, fining upwards	
		▲		rounded dropstone (3 cm Ø) at 315 cm	
			5Y4/2	mixture of sandy, in parts silty matrix with coarse rounded to unrounded pebbles, olive gray, mud clasts (dark gray, 3 cm Ø), sedimentary rock, numerous volcanic ash/glass conglomerate, unsorted (debris flow, proximal turbidite ?)	
		▲	5Y4/2	silty sand to sandy silt, olive gray, layered, slightly graded within layers	
		▲	5Y5/3	fine sand to silty clay, olive, fining upwards	
4		▲	5Y3/1	numerous changes of clay and sandy to sandy silt layers, layers fining upwards	
			2.5Y3/1	clayey mud, very dark gray, homogeneous	
			2.5Y3/2	sand, fine to medium graded, very dark grayish brown	
		▲	2.5Y4/3	sandy mud, homogeneous, very dark gray sand layers, fining upwards from medium sand to silty mud	
5					

PS2167-2 (GKG)

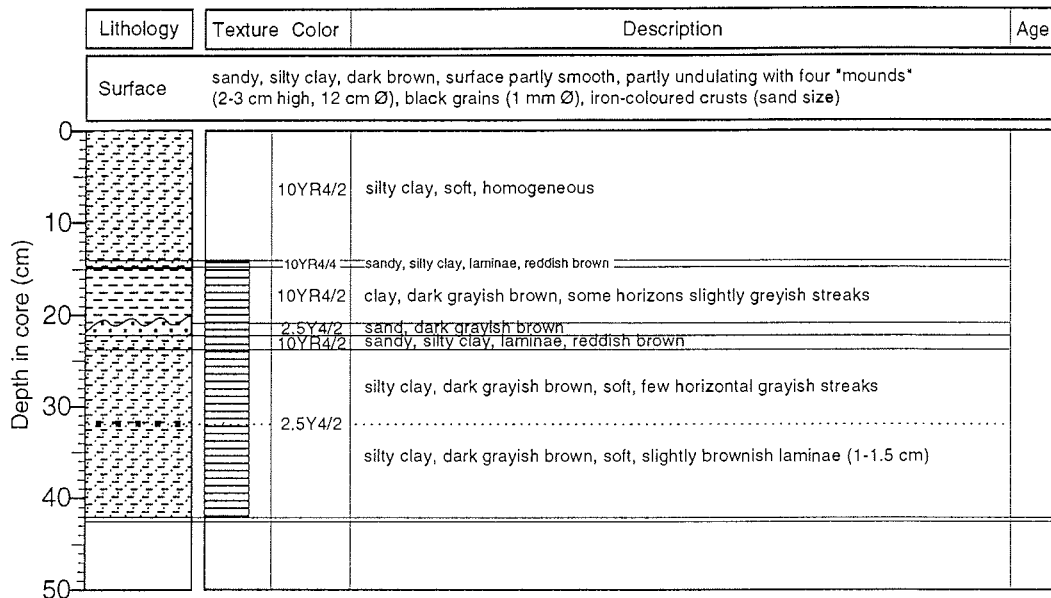
Gakkel Ridge

ARK VIII/3 (ARCTIC 91)

Recovery: 0.42 m

86° 56.1' N, 59° 04.5' E

Water depth: 4425 m



PS2167-1 (TWC)

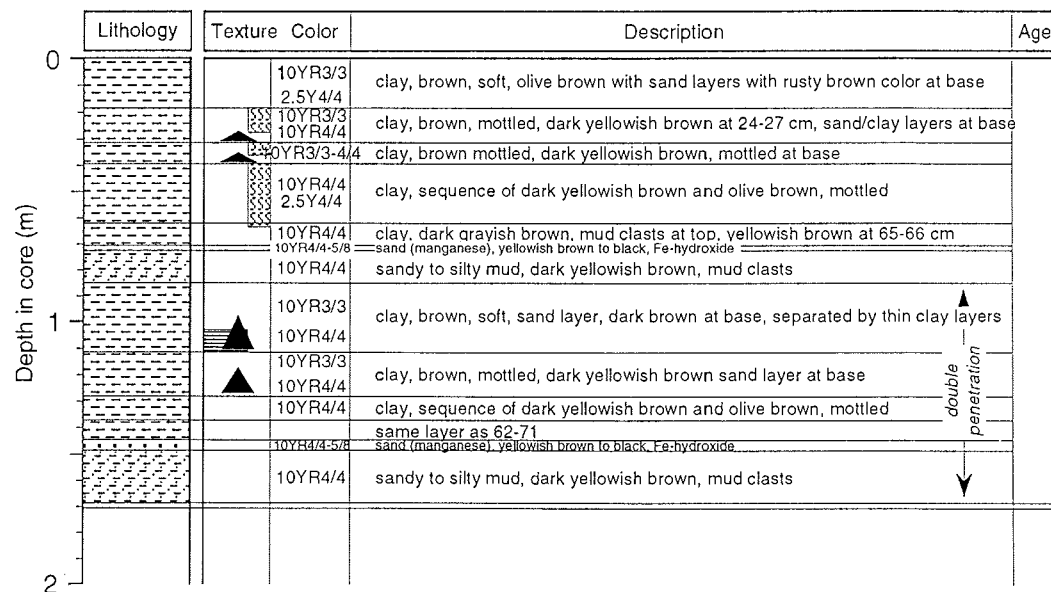
Gakkel Ridge

ARK VIII/3 (ARCTIC 91)

Recovery: 1.69 m

86° 56.7' N, 59° 0.9' E

Water depth: 4434 m



PS2168-1 (GKG)

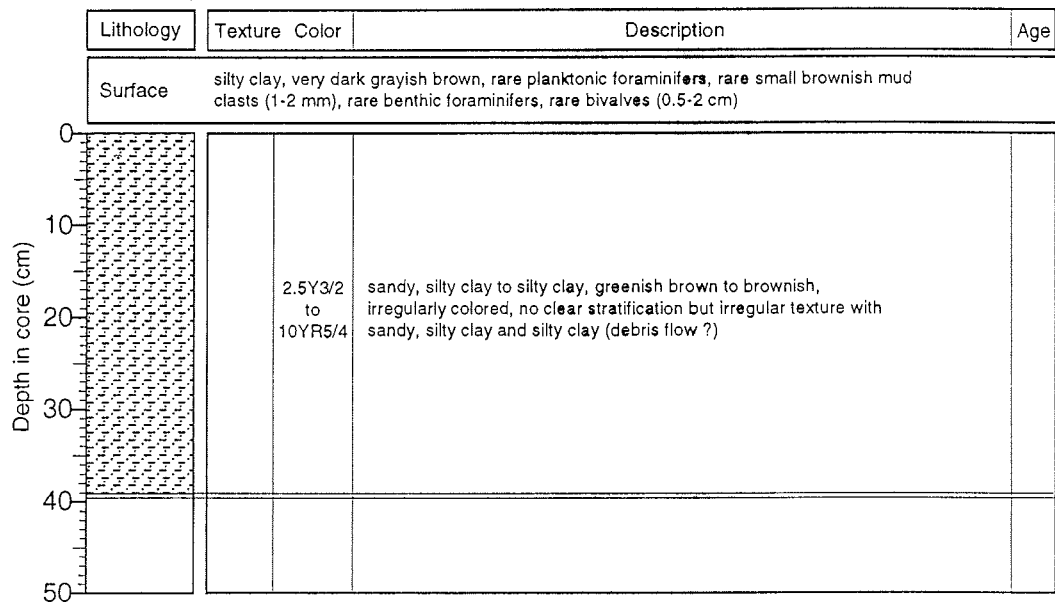
Gakkel Ridge

ARK VIII/3 (ARCTIC 91)

Recovery: 0.39 m

87° 30.6' N, 55° 56.0' E

Water depth: 3846 m



PS2168-2 (TWC)

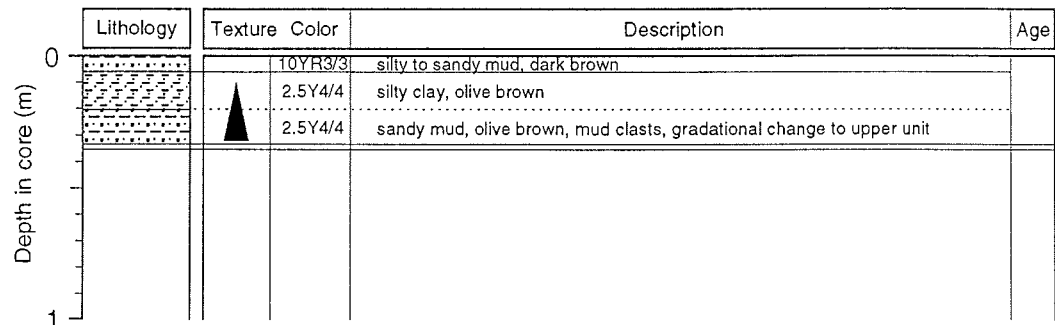
Gakkel Ridge

ARK VIII/3 (ARCTIC 91)

Recovery: 0.34 m

87° 30.9' N, 56° 5.8' E

Water depth: 3790 m



PS2168-2 (GPC)

Gakkel Ridge

ARK VIII/3 (ARCTIC 91)

Recovery: 4.09 m

87° 30.9' N, 56° 5.8' E

Water depth: 3790 m

	Lithology	Texture Color	Description	Age
0		2.5Y4/4 2.5Y4/4	silty mud, dark brown	
		10YR4/4	clayey mud, very dark grayish brown grading into dark yellowish brown grading into olive brown, upper part mottled with mud clasts (0.5-1 cm Ø), sandy layers (0.5-1 cm thick) at 60-210 cm	
		2.5Y3/2		
1		2.5Y4/4	clay, olive brown, mottled, weakly layered grading into	
		2.5Y3/2	silty-sandy mud, very dark grayish brown, sandy mud layer at 120, 112 cm	
		5Y2.5/1	sandy mud, black, homogeneous	
		5Y4/4		
		5Y4/3	sandy to silty mud, olive, sandy mud layers, mottled weakly at 175 cm	
2		5Y3/2	silty mud, dark olive gray, mud clasts grading into	
		2.5Y4/3	sandy to silty mud, very dark gray, homogeneous, sharp lower boundary	
		10YR3/4	silty mud, dark yellowish brown, sand layers, dark grayish brown with mud clasts	
		10YR3/6	clayey mud, dark yellowish brown	
		2.5Y4/4	silty mud, olive brown, mud clasts, weakly layered	
		10YR3/4	clay, dark yellowish brown, dark specks grading into	
		2.5Y4/4	clay to clayey mud, olive brown	
3		10YR3/3	clay, olive brown grading into dark brown, mottled	
		2.5Y4/4	clayey mud, dark yellowish brown grading into dark brown mud	
		10YR3/4	silty mud, dark grayish brown to dark yellowish brown, mud clasts	
		10YR3/4-6	silty mud, dark yellowish brown, grading into clayey mud, weakly mottled	
		2.5Y4/2	silty mud, dark grayish brown, grading into different colors, mud clasts	
		2.5Y4/2	silty mud, dark grayish brown, grading into different colors, mud clasts	
		10YR3/3	sandy to silty mud, dark grayish brown grading into dark brown clay	
		2.5Y4/2		
4		10YR3/4	clay, dark yellowish brown, layered and laminated, black specks at 398-409 cm, main color alternating with dark grayish brown (24 layers, 1-2 cm thick), sandy layer at 399 cm	
			<i>section 313-409 is possibly upside down !</i>	
5				

PS2169-1 (GPC)

Gakkel Ridge

ARK VIII/3 (ARCTIC 91)

Recovery: 6.22 m

87° 30.2' N, 55° 58.3' E

Water depth: 3846 m

Lithology	Texture	Color	Description	Age
0-1.06 m			0-84 bag sample	
1.06-1.13 m		10YR4/4	sandy mud, dark yellowish brown, 2 sandy laminae at 106, 113 cm, layers/laminae of dark color at 116-125 cm	
1.13-1.58 m		5Y4/1	sandy mud, dark gray	
1.58-1.59 m	▲	2.5Y4/4 2.5Y4/2	sandy mud, olive brown to dark grayish brown, mud clasts, clayey layer at 158-159 cm, fining upwards in the upper 10 cm	
1.59-2.00 m		5Y2.5/1	sandy mud, black, grading upwards into very dark grayish brown	
2.00-2.25 m	▲	2.5Y4/4 2.5Y4/2	sandy mud, dark grayish brown, grading upwards into olive brown clay, mottled in the upper part	
2.25-2.40 m		N3	sandy mud, very dark gray	
2.40-2.44 m		5Y4/3	clay, olive, mottled, mud clasts at lower part	
2.44-2.48 m		2.5Y4/4	clay, olive brown	
2.48-2.52 m		2.5Y4/2	sandy mud, dark grayish brown, few dark spots	
2.52-2.56 m		2.5Y4/2	sandy mud, dark grayish brown	
2.56-2.60 m		5Y4/4	clay, olive	
2.60-2.64 m		2.5Y4/2	sandy mud, dark grayish brown	
2.64-2.68 m		2.5Y4/4	clay, olive brown	
2.68-2.72 m		2.5Y4/2	sandy mud, dark grayish brown	
2.72-2.76 m	▲	2.5Y4/2	sandy mud, dark grayish brown	
2.76-2.80 m		10YR4/4	clay, dark yellowish brown, mud clasts	
2.80-2.84 m		2.5Y4/4	sandy mud, olive brown	
2.84-2.88 m		10YR4/4	clay, dark yellowish brown, mud clasts	
2.88-2.92 m		10YR4/6	clay, brown, grading upwards into dark yellowish brown	
2.92-3.00 m		10YR5/4	disturbed silty clay, yellowish brown, mud clasts, 2 clasts of olive brown sandy mud	
3.00-3.04 m		2.5Y3/2	disturbed silty mud, very dark grayish brown	
3.04-3.08 m		10YR5/4	disturbed silty mud, yellowish brown, common mud clasts in upper and lower part	
3.08-3.12 m		2.5Y4/2	disturbed sandy mud, dark grayish brown	
3.12-3.16 m		2.5Y4/2	disturbed sandy mud, dark grayish brown	
3.16-3.20 m		2.5Y4/4	disturbed silty clay, very dark grayish brown, grading upwards into olive brown sandy mud, dark streaks and specks at 414, 420-428 cm	
3.20-3.24 m		2.5Y3/2	disturbed sandy mud, very dark grayish brown, clayey and mottled in the upper part	
3.24-3.28 m		2.5Y3/2	disturbed sandy mud, very dark grayish brown, clayey and mottled in the upper part	
3.28-3.32 m		2.5Y4/2	disturbed silty mud, dark grayish brown (more grayish at base), laminated at base, mottled	
3.32-3.40 m		5Y4/2	disturbed clay, olive gray, mottled	
3.40-3.50 m		2.5Y4/2	disturbed sandy mud, dark grayish brown, several mud clasts in the upper 3 cm	

disturbed/deformed

PS2169-1 (GPC)

Gakkel Ridge

ARK VIII/3 (ARCTIC 91)

Recovery: 6.22 m

87° 30.2' N, 55° 58.3' E

Water depth: 3846 m

Depth in core (m)	Lithology	Texture	Color	Description	Age
5			2.5Y4/2 2.5Y3/2	clay, very dark grayish brown, grading upwards into dark grayish brown sandy mud	
			2.5Y4/4	clay, olive brown, sandy mud at 517 cm	
			2.5Y4/2 2.5Y4/4	sandy mud, dark grayish brown and olive brown, many small (< 3 mm) mud clasts at 524-533 cm, sand laminae at 548, 558 cm, 2 clay layers at 531, 532 cm	
			N3 5Y3/1	sandy mud, very dark gray, homogeneous clay, very dark gray	
			2.5Y4/2 5Y3/2	sandy mud, dark grayish brown and dark olive gray, mottled	
6			N3 5Y3/1	sandy mud, very dark gray, homogeneous clay, very dark gray	
			5Y3/2	sandy mud, dark olive gray, several dark mud clasts (3 mm Ø), clayey layer at 611.5-612.5 cm	

PS2169-1 (TWC)

Gakkel Ridge

ARK VIII/3 (ARCTIC 91)

Recovery: 1.09 m

87° 30.2' N, 55° 58.3' E

Water depth: 3846 m

Depth in core (m)	Lithology	Texture	Color	Description	Age
0			10YR3/3 2.5Y4/4	clay, dark brown silty clay, olive brown, mottled	
			10YR3/3 2.5Y4/4	clay, dark brown, mottled clay, olive brown, mottled, mud clasts below 20 cm, mud clasts layer at 23-24 cm	
			10YR4/3	clay, brown, mottled	
			10YR5/4 2.5Y4/4	sandy mud, yellowish brown, contorted layer or big mud clasts at 63-74 cm of olive brown sandy mud	
			10YR5/4 2.5Y4/2	sandy mud, dark grayish brown,	
1			10YR4/6 2.5Y4/2	lense of dark yellowish brown sandy mud at 98-105 cm	

PS2170-1 (GKG)

Amundsen Basin

ARK VIII/3 (ARCTIC 91)

Recovery: 0.38 m

87° 35.4' N, 60° 46.0' E

Water depth: 4226 m

Lithology	Texture	Color	Description	Age
Surface				
silty clay, dark brown, smooth, common planktonic foraminifers, few dropstones (0.1-1 cm), few bivalves, small mudclasts				
		10YR3/3	silty clay, dark brown, homogeneous, few planktonic foraminifers	
		10YR4/3	silty clay, brown, mottled by grayish streaks, small coal? particles	
		-2.5Y3/2	sand, reddish brown, laminae	
		5YR3/4	silty clay, brownish gray to gray	
		10YR4/3 -2.5Y3/2	silty clay, brown to gray, color gradually changing, some lamination	
		2.5Y4/4- 2.5Y4/2		

PS2170-3 (TWC)

Amundsen Basin

ARK VIII/3 (ARCTIC 91)

Recovery: 0.76 m

87° 35.7' N, 60° 52.2' E

Water depth: 4112 m

Lithology	Texture	Color	Description	Age
		10YR3/2	clay, very dark grayish brown	
		2.5Y4/4	clay, olive brown, mud clasts at 22-20 cm	
		10YR3/6	silty clay, dark yellowish brown, layering due to faint color changes	
		2.5Y4/4	silty sand, olive brown	
		2.5Y4/4	silty mud, olive brown, mud clasts	
		2.5Y4/4	sandy mud, olive brown, slight layering due to faint color changes	

PS2170-3 (GPC)

Amundsen Basin

ARK VIII/3 (ARCTIC 91)

Recovery: 11.51 m

87° 35.7' N, 60° 52.2' E

Water depth: 4112 m

Lithology	Texture Color	Description	Age
0	10YR3/3	clay, dark brown, soft, sand layer at 6 cm, lower boundary mottled/bioturbated	
	10YR4/8	clay, dark yellowish brown, at base layer with mud clasts (1-2 mm)	
	10YR4/3	clay, brown to dark brown at base, soft, lighter from 26-28 cm, mottled throughout, sand layer/lense at base	
	10YR3/3		
	10YR5/3	sandy clay, brown to dark grayish brown, yellowish brown at base, mottled throughout, traces of laminae preserved, black clasts at 55, 59, 75 cm	
	2.5Y4/2		
	10YR5/6	sandy clay, olive gray to dark gray, mottled throughout, lighter from 91-94 cm, black spots at base (90-102 cm)	
	5Y4/2		
1	5Y4/1	clay, olive	
	5Y4/4		
	5Y4/3	sandy clay, olive, mottled	
	2.5Y4/2	clay, sandy clay at base, dark grayish brown	
	5Y4/3	sandy mud, dark gray to olive, mottled throughout, particularly down to 133 cm, at 149 cm gradational boundary towards darker color	
	5Y4/3	clay, olive, darker layer between 162-163 cm, sand laminae at 160 + at base	
2	5Y4/2	sandy clay/mud, olive gray, mottled throughout, black clast at 192 cm	
	5Y3/1	sandy clay/mud, dark gray	
3	5Y5/2	clayey mud, olive gray, layered piece of clay, olive (5Y4/3)	
	10YR4/2	dark grayish brown, dark specks, mottled	
	10YR5/4	yellowish brown, on top grayer, mottled and slightly layered throughout, grain size very homogeneous	
	2.5Y4/4	sandy clay, olive brown, generally homogeneous, lenses of dark brown mud at 378-390 cm, black lenses/spots at 357-363 cm, dropstones at 348, 323 cm, sharp lower boundary <i>section may be disturbed</i>	
4	10YR3/3	clay, dark brown, black disturbed laminae	
	2.5Y4/4	sandy mud, olive brown, sharp lower boundary	
	10YR4/3	clay, dark brown, mottled	
	2.5Y4/4	sandy mud, olive brown	
	10YR3/3	clay, dark brown, mottled	
	2.5Y4/4	sandy mud, olive brown, mud clasts, sharp lower boundary	
5	10YR3/3	clay, dark brown, mottled	
	2.5Y4/2	sandy mud, dark grayish brown, mottled	

PS2170-3 (GPC)

Amundsen Basin

ARK VIII/3 (ARCTIC 91)

Recovery: 11.51 m

87° 35.7' N, 60° 52.2' E

Water depth: 4112 m

	Lithology	Texture	Color	Description	Age
5			2.5Y4/2	sandy mud, dark grayish brown, mottled	
			10YR3/3	clay, dark brown, mottled	
6			2.5Y4/4	sandy mud, olive brown, mud clasts	
			10YR4/3	clay, brown, mottled, dark specks	
			2.5Y4/4	sandy mud, olive brown, brownish layer at 563-570 cm, layered sandy mud at 596-580 cm, higher sand content, black lenses/laminae at 592-596 cm	
			5YR3/4	sandy mud, dark reddish brown	
7			2.5Y5/4	clay, light olive brown, mottled	
			10YR4/3	clay, brown, black specks, mottled	
			2.5Y4/4	sandy mud, olive brown, mottled, sharp lower boundary	
			10YR5/4	clay, yellowish brown, sandy lenses, mottled, sharp lower boundary	
			10YR4/3	clay, brown, mottled, dark specks	
			2.5Y4/4	sandy mud, olive brown, mottled, black lamina at 718 cm	
8			10YR4/4	sandy mud, dark yellowish, black specks	
			2.5Y4/4	sandy mud, olive brown	
			2.5Y5/2	clay, grayish brown	
			10YR5/4	clay, yellowish brown	
			2.5Y4/4	sandy mud, olive brown	
			5YR4/3	sandy mud, reddish brown	
			10YR5/4	clay, yellowish brown	
			10YR4/3	clay, brown, dark specks, mottled	
			2.5Y4/4	sandy mud, olive brown, dark specks at 775-785 cm	
			10YR4/4	sandy mud, dark yellowish brown, black specks	
9			2.5Y4/4	sandy mud, olive brown, dark yellowish brown layer at 810-811 cm	
			10YR4/4	sandy mud, dark yellowish brown, black specks	
			2.5Y4/4	sandy mud, olive brown	
			5YR4/4	sandy mud, reddish brown	
			10YR3/3	clay, dark brown, mottled, black specks, dropstone at 848 cm	
			2.5Y4/4	sandy mud, olive brown, mottled, sharp mottled lower boundary	
			10YR4/2	clay, brown, mottled, few black specks	
			2.5Y4/4	sandy mud, olive brown, mottled	
			10YR3/3	clay, dark brown, mottled, black specks	
			2.5Y4/4	sandy mud, olive brown, mottled	
10			10YR3/3	clay, dark brown, mottled, black specks	
			10YR3/3	sandy mud, olive brown, dark specks and mottled throughout, 2 horizons of sandy mud, dark yellowish brown at 975-980, 988-996 cm, gradational boundaries to the olive brown sandy muds above and below	
			10YR4/4		

PS2170-3 (GPC)

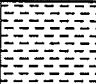

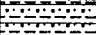
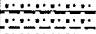
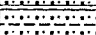
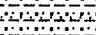
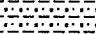
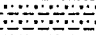
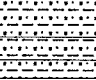
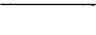

Amundsen Basin

ARK VIII/3 (ARCTIC 91)

Recovery: 11.51 m

87° 35.7' N, 60° 52.2' E

Water depth: 4112 m

Depth in core (m)	Lithology	Texture	Color	Description	Age
	10			10YR3/3	clay, dark brown, mottled, black specks
			2.5Y4/4	sandy mud, olive brown, dark specks	
			10YR4/4	sandy mud, reddish brown	
			2.5Y4/4	sandy mud, olive brown	
			10YR4/4-3/3	sandy mud, dark yellowish brown and dark brown, darker specks	
			2.5Y4/4	sandy mud, olive brown	
			10YR5/4-3/2	clay, yellowish brown-brown clay	
			2.5Y4/4	sandy clay, olive brown	
11				sandy mud, brown and olive brown <i>folding and deformation, disturbed during coring</i>	
			10YR3/3	sandy mud, brown/dark brown, laminated in the lower 3 cm	
			2.5Y4/4	sandy mud, olive brown	CC
12					
13					
14					
15					

PS2171-1 (GKG)

Amundsen Basin

ARK VIII/3 (ARCTIC 91)

Recovery: 0.50 m

87° 35.1' N, 68° 58.7' E

Water depth: 4384 m

Lithology	Texture Color	Description	Age
Surface	silty clay, dark brown, smooth, common light brownish mud clasts (same color as unit 2!), common planktonic foraminifers, 1 bivalve shell		
	10YR3/3	silty clay, homogeneous, dark brown, common planktonic foraminifers	
	10YR4/2	clay, homogeneous, dark grayish brown, rare benthic foraminifers	
		irregluar broken slightly grayish, horizontal streaks (30-45 cm)	
	5Y4/1	silty clay, homogeneous, dark gray	

PS2171-4 (KAL)

Amundsen Basin

ARK VIII/3 (ARCTIC 91)

Recovery: 3.25 m

87° 36.1' N, 69° 22.8' E

Water depth: 4395 m

Lithology	Texture Color	Description	Age
	10YR5/3	clay, brown, soft, disturbed dark specks between 25 and 40 cm 32-49 cm finely laminated, 1-2 mm thick laminae	
	2.5Y4/2	clay, dark grayish brown, grading to olive brown, mottled in the lower part clay, olive brown, homogeneous, mottled in the upper part	Dark layer
	2.5Y4/4	silty clay, olive brown, 77-80 cm clay, very dark grayish brown	
	2.5Y3/2	clay, very dark grayish brown, faint silt/sand laminae at the base	
	5Y3/1	clay, very dark gray, homogeneous, dark layer (2 cm thick) at top	
	7.5Y5/2	clay, brown, homogeneous, dark layer at base, few dark specks	
	10YR4/3	clay, brown/dark brown, homogeneous	
	2.5Y4/4	clay, olive brown, laminated, more grayish in the lower part, brownish laminae at 232, 236, 238, 245 cm	
	5Y3/1	clay, very dark gray, dark laminae at 238, 252 cm	
	5Y4/2-1	clay, olive gray, dark specks, gradational color boundary, dark gray at base	
5Y4/3 to 2.5Y4/4	clay, gradational color change from olive brown to olive, mottled throughout, dark specks and laminae at 305-310 cm		
2.5Y4/2	clay, dark grayish brown, laminae slightly darker		

PS2172-1 (GKG)

Amundsen Basin

ARK VIII/3 (ARCTIC 91)

Recovery: 0.49 m

87° 15.7' N, 68° 32.2' E

Water depth: 4479 m

Lithology	Texture Color	Description	Age
Surface	silty clay, dark brown, soft, common planktonic foraminifers, common mud clasts (0.2-1 cm Ø)		
	10YR3/3	silty clay, dark brown, homogeneous, common planktonic foraminifers	
	10YR4/3	clay, brown, homogeneous	
	10YR3/3	clay, dark brown, light brownish burrows in lower part	
	2.5Y4/2	clay, dark grayish brown, light brownish burrows	
	10YR3/3 to 2.5Y4/2	clay, dark brown, light brownish burrows	
	10YR4/6	clay, dark yellowish brown, homogeneous	
	10YR4/2 to 2.5Y4/2	clay, dark grayish brown, slightly silty, with fine brownish and grayish laminae, coal clast (0.5 cm Ø) at 44 cm	
	10YR4/3	clay, brown, slightly silty	

PS2172-4 (TWC)

Amundsen Basin

ARK VIII/3 (ARCTIC 91)

Recovery: 1.70 m

87° 16.1' N, 68° 53.9' E

Water depth: 4481 m

Lithology	Texture Color	Description	Age
	10YR3/4	clay, dark yellowish brown, grading into	
	5YR4/2	clay, dark reddish gray, very homogeneous	
	2.5Y4/2	clay, dark yellowish brown, sand layers at 37-39, 36 cm, grading into dark grayish brown	
	2.5Y4/4	clay, dark yellowish brown, grading into olive brown	
	2.5Y3/2	clay, olive gray, layering due to weak color changes, grading to very dark gray	
	5Y4/2		
	5Y3/2	clay, dark olive gray	
			<i>same sequence as above due to double penetration</i>
	5Y4/3	clay, olive, sand layer at 146-148 cm	

PS2172-4 (GPC)

Amundsen Basin

ARK VIII/3 (ARCTIC 91)

Recovery: 9.51 m

87° 16.1' N, 68° 53.9' E

Water depth: 4481 m

Lithology	Texture	Color	Description	Age
0		10YR3/4	clay, dark yellowish brown, grading into	
		5YR4/2	clay, dark reddish gray, homogeneous	
		2.5Y4/2	clay, dark grayish brown, grading into dark yellowish brown,	
		10YR3/4	sandy mud at 46-40 cm	
		2.5Y4/4	clay, olive brown, grading into dark yellowish brown	
		10YR3/6		
1		2.5Y3/2	clay, brown to very dark grayish brown to olive gray,	
		5Y4/2	layering due to color changes	
		5Y3/2	clayey mud, very dark grayish brown grading into dark olive gray,	
		2.5Y4/2	homogeneous	
		5Y4/3	clay, olive, sandy mud layer at 114-117 cm	
		5Y4/2	clay, olive gray, mottled	
		5Y4/1	clay, dark gray, mottled in the upper 2 cm	
		5Y5/1	clay, gray, mottled	
		5Y4/4	clay, olive, mottled	
2		2.5Y4/4	clay, olive brown, mottled in the upper 2 cm	
		10YR4/4	clay, dark yellowish brown, mottled	
		10YR5/4	clay, yellowish brown, mottled	
		10YR4/4	clay, dark yellowish brown, mottled	
		10YR5/4	sand and clay, yellowish brown, thick sand layers are graded	
		2.5Y4/4	clay, olive brown, mottled	
3		2.5Y4/4	clay, olive brown/yellowish brown, laminated, few dark specks, mottled at	
		10YR5/4	277-287 cm, layer of mud clasts, brown, at 296-301 cm	
		5Y4/3	clay, olive, mottled at 301-310 cm	
4			sandy/silty mud layer at 350-352 cm	
		5Y3/2	clay, dark olive gray, silt layers, very homogeneous	
			sandy/silty mud layer at 389 cm	
5		5Y3/2	clay, dark olive gray, silt layers, very homogeneous	
			silty/clayey mud layer (10 mm thick) at 447-448 cm	
			sandy/silty mud layer (13 mm thick) at 495 cm, slightly darker color below	

PS2172-4 (GPC)

Amundsen Basin

ARK VIII/3 (ARCTIC 91)

Recovery: 9.51 m

87° 16.1' N, 68° 53.9' E

Water depth: 4481 m

Depth in core (m)	Lithology	Texture	Color	Description	Age
	5			5Y4/1	clay, dark gray, homogeneous, thin sand layer at base
6			5Y4/2	sand, silt and clay laminae and layers, olive gray to dark gray to very dark gray, sand layers at 561-563, 566-579, 582-583, 598-599, 601-602, 603-605, 619-620, 621-622, 631-644 cm	
			5Y4/1		
			5Y3/1		
7			5Y3/1	sandy mud, very dark gray, homogeneous, scattered dropstones	
8			5Y3/2	clay, dark olive gray, weakly mottled below 790 cm	
			5Y4/1	clay, dark gray, homogeneous, black laminae at base	
			5Y3/2	clay, dark olive gray, mottled	
			5Y3/1	clay, dark gray, at base 0.5 cm lighter gray layer, grading into upper unit	
			5Y4/2	clay, olive gray, mottled, mud clasts, very dark gray at 873.5 cm, sandy mud at base 878-875 cm	
9			5Y4/3	clay, dark gray, grading into olive clay, mottled, sand at 881-883 cm,	
			5Y4/1	0.5 cm lighter gray clay at base	
			5Y4/2	silt, sand and clay layers, very dark gray (917-904 cm),	
			5Y3/1	grading into olive gray clay and sand	
			5Y4/4	clay and sand, olive	
			5Y3/2	sand and clay, dark olive gray	
			5Y3/1	sandy mud, very dark gray, sand layer	
10			5Y3/2	silty clay, dark olive gray, laminated	
			5Y4/2	silt/clay, olive gray, laminae	
			5Y3/1	silt/clay, very dark gray, laminae	

PS2173-1 (KAL)

Amundsen Basin

ARK VIII/3 (ARCTIC 91)

Recovery: 5.50 m

87° 18.4' N, 69° 19.3' E

Water depth: 4558 m

Lithology	Texture	Color	Description	Age
<i>uppermost 2 m lost in weight</i>				
		5Y3/2	clay, dark olive gray, collapsed core top	
		10YR3/3	sand, reddish brown	
		2.5Y4/2	sand, olive (see 263-264 t)	
		2.5Y3/2	slightly sandy mud, faintly laminated	
		5Y3/1	clay, dark gray, massive	
		5Y3/2	clay, gray, layered, dark (Mn?) stain	
		5Y4/3	clay, variegated olive, mottled	
		5Y3/2	transition zone with burrows	
		5Y4/3	clay, olive, massive	
		10YR5/3		
		10YR4/3	clay, brown, burrowed	
		10YR5/3	clay, brown	
		10YR3/2	clay, very dark grayish brown, (Mn?)-staining, Pyrite ?	
		10YR4/2	clay, dark grayish brown	
		10YR4/4	silt, dark yellowish brown	
		2.5Y4/4	clay, olive, homogeneous, slightly mottled at base	
<i>coring disturbance at 237-255 cm</i>				
		5Y5/3	clay, abundant color changes, partly laminated,	
		5Y4/2	sand/silt layers at 213-214, 228-229, 241-242, 262-263, 283 cm	
		2.5Y4/0	clay, abundant color changes, partly laminated,	
		5Y5/3	sand/silt layers at 385-388, 395-398, 403-404, 405, 407, 411-412, 428, 438 cm	
		2.5Y4/0	clay, dark gray, massive, structureless	

PS2174-3 (GPC)

Amundsen Basin

ARK VIII/3 (ARCTIC 91)

Recovery: 13.0 m

87° 29.2' N, 91° 6.5' E

Water depth: 4394 m

Depth in core (m)	Lithology	Texture Color	Description	Age
0		10YR3/3	clay, dark brown, homogeneous, mottling at 7-9 cm	
		5Y3/2	clay, dark olive gray, slightly mottled	
		2.5Y4/4	clay, olive brown, mottled at 18-21 cm	
		10YR4/3 10YR4/1 2.5Y4/2	silty clay, very dark grayish brown, dark gray, brown, alternating with dark brown sandy layers, laminated	
1		5Y4/1	clay, dark gray, soft, homogeneous	
2		5Y4/1	silty sand to sandy mud, dark gray, laminated, fining upwards, (turbidite)	
		5Y4/1	clay, dark gray, mottled	
		5Y4/2	clay, olive gray, mottled	
3		5Y4/1	clayey mud, dark gray, faintly laminated, gradational color change to upper unit	
		5Y4/4	clay, olive, mottled, gradational color change at 308 cm to gray, uppermost sharp boundary is marked by 1 mm black lamina	
		5Y4/2	clay, olive gray, very finely laminated, laminae are marked by brownish colors	
		5Y4/2	clay, olive gray, mottled	
4		5Y4/1	clay, dark gray, homogeneous	
		5Y3/1	clay, dark gray, homogeneous	
		5Y5/4	clay, gray, mottled in the lower part, laminated in the upper 0.5 cm	
		5Y4/4	sandy mud and clay, olive, coarsening upwards, mottled throughout, intensely mottled below 451 cm	
		2.5Y4/4	clay, olive brown, mottled	
		5Y4/2	clay, olive gray, mottled, mottles have lighter color	
		5Y4/3	clay, olive, mottled, mottles have lighter color	
5		5Y4/3	clay, olive, laminated, few mottles	

PS2174-4 (GKG)

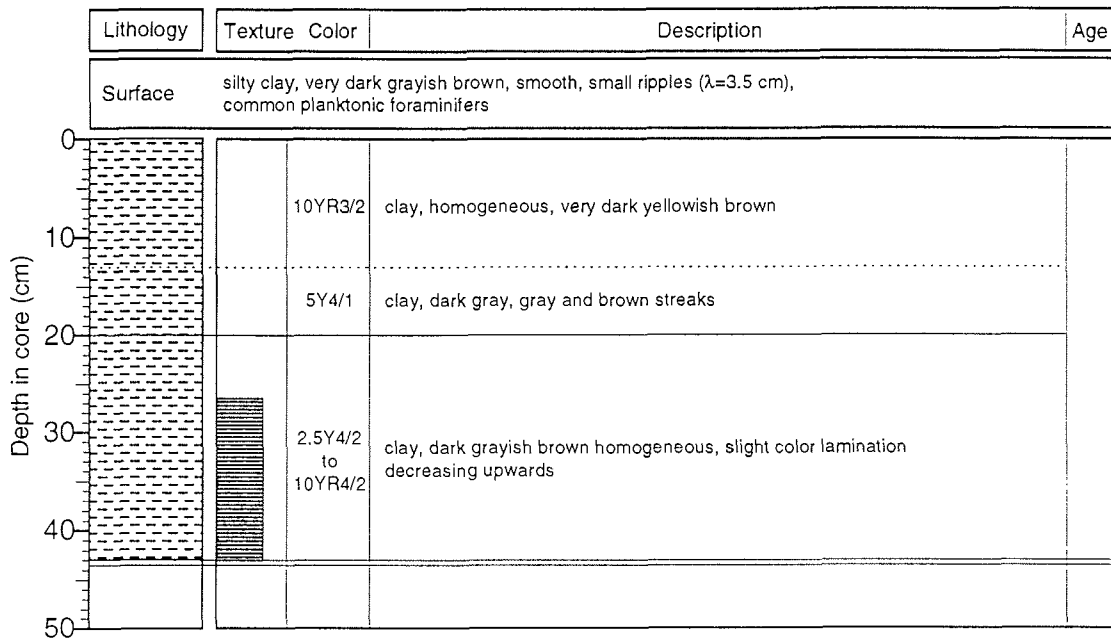
Amundsen Basin

ARK VIII/3 (ARCTIC 91)

Recovery: 0.43 m

87° 29.1' N, 91° 20.3' E

Water depth: 4426 m



PS2174-3 (TWC)

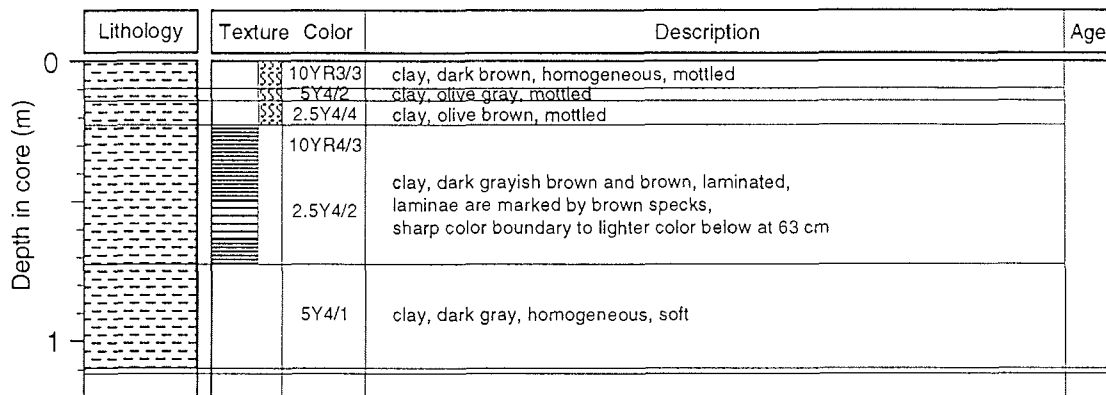
Amundsen Basin

ARK VIII/3 (ARCTIC 91)

Recovery: 1.10 m

87° 29.2' N, 91° 6.5' E

Water depth: 4394 m



PS2174-3 (GPC)

Amundsen Basin

ARK VIII/3 (ARCTIC 91)

Recovery: 13.0 m

87° 29.2' N, 91° 6.5' E

Water depth: 4394 m

	Lithology	Texture	Color	Description	Age
5			5Y4/3	clay, olive, laminated, few mottles	
			5Y4/2 and 5Y4/1	clay, olive gray/dark gray, laminated, some mottles in the interval 526-545 cm	
			5Y4/1	clay, dark gray, homogeneous, mottled in the upper 5 cm, sharp boundaries	
			5Y4/1	clay, dark gray, homogeneous, mottled in the upper 5 cm, sharp boundaries	
6			5Y4/1	clay, dark gray, homogeneous, mottled in the upper 5 cm, sharp boundaries	
			5Y4/1	clay, dark gray, homogeneous, mottled in the upper 5 cm, sharp boundaries	
			5Y4/1	clay, dark gray, homogeneous, mottled in the upper 5 cm, sharp boundaries	
			5Y4/1	clay, dark gray, homogeneous, mottled in the upper 5 cm, sharp boundaries	
7			5Y4/1	clay, dark gray, homogeneous, mottled in the upper 5 cm, sharp boundaries	
			5Y4/1	clay, dark gray, homogeneous	
8		5Y3/2			
		5Y4/1	clay, dark (olive) gray, homogeneous, faint mottles in the upper 5 cm, black clouds/spots between 962 and 966 cm		
		5Y4/1	clay, dark gray, homogeneous		
9		5Y3/1	clay, dark gray to very dark gray, mostly homogeneous		
10					

PS2174-3 (GPC)

Amundsen Basin

ARK VIII/3 (ARCTIC 91)

Recovery: 13.0 m

87° 29.2' N, 91° 6.5' E

Water depth: 4394 m

Lithology	Texture Color	Description	Age
	<p>5Y4/1</p> <p>5Y4/1</p> <p>5Y4/1</p>	<p>intervals of alternating clay and sand layers at 985-993, 1057-1069 cm, black layers (pyrite) at 998, 1001, 1029, 1069, 1071 cm, vertical sand lense at 1041-1049 cm as part of turbidite at 991-996 cm ? <i>coring disturbance</i></p> <p>clay, dark gray, mostly, homogeneous, finely laminated (clay/silt alternations) at 1092-1096, 1132-1143, 1160-1170 cm, dark gray sand layers at 1097-1098, 1099, 1105, 1144; dark grayish brown sand layer at 1151-1152 cm (sharp boundary at top), black (pyritic ?) layers at 1101, 1107, 1146, 1153, 1154 and 1170 cm</p> <p>laminations at 1256-1271, 1203-1204 cm, sand interval at 1272-1282 cm, fining upwards, black layers/lenses at 1206, 1215 cm</p> <p>foam 1282-1285 cm, sand, dark gray, black spots at 1285-1287 cm, clay, dark gray, homogeneous at 1287-1300 cm, black (pyritic?) lense/layer at 1290 cm</p>	

PS2174-5 (KAL)

Amundsen Basin

ARK VIII/3 (ARCTIC 91)

Recovery: 9.60 m

87° 29.1' N, 91° 32.6' E

Water depth: 4427 m

Lithology	Texture	Color	Description	Age
0		10YR3/4 10YR3/3 10YR3/2	clay, dark yellowish brown, soft, grading to dark brown at 27 cm and to very dark grayish brown at 33 cm	
			sharp boundary	
		2.5Y4/4 2.5Y3/2	clay, color changes from olive brown to grayish brown, mottled layer at 65-68 cm, grayish layer at 54-56 cm	
			sharp boundary	
1		N3	clay, very dark gray, homogeneous	
2			numerous 1-5 mm thick silt layers and laminae, slightly graded, sharp boundaries at base	
		2.5Y4/2 2.5Y4/4 5Y4/2-3/2	clay, grading color changes, white specks at 214-217 cm, mottled	
3			sharp boundary	
		2.5Y4/2 5Y4/4	clay, dark grayish brown (240-241 cm) grading to olive, mottled down to 268 cm	
		5Y3/2	faint lamination at 268-280, 302-312 cm mottled horizon at 250-294, 296-302 cm dark olive gray at base	
4			sharp boundary	
		N4	clay, dark gray, homogeneous, grading to lighter color at top	
		5Y4/2	clay, dark grayish brown, grading into olive gray, partly laminated, mottled at 370-405, 410-428 cm	
5			sharp boundary	
		2.5Y4/2	lamination often brownish with sharp lower boundaries, grading into grayish hues upwards	
		N3	clay, very dark gray, homogeneous	

PS2174-5 (KAL)

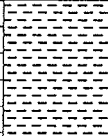
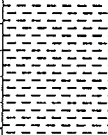
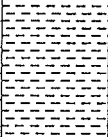
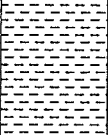
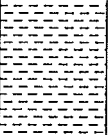
Amundsen Basin

ARK VIII/3 (ARCTIC 91)

Recovery: 9.60 m

87° 29.1' N, 91° 32.6' E

Water depth: 4427 m

Depth in core (m)	Lithology	Texture	Color	Description	Age
5			N3	clay, very dark gray, homogeneous	
				faint color-change from darker to lighter	
6			N4	clay, very dark gray, homogeneous	
				faint color-change from darker to lighter	
				sharp boundary	
7			N4	clay, very dark gray, homogeneous	
8				silt/fine sand laminae	
9			5Y3/1	clay, very dark gray, homogeneous, black laminae	
10					

PS2175-3 (GKG)

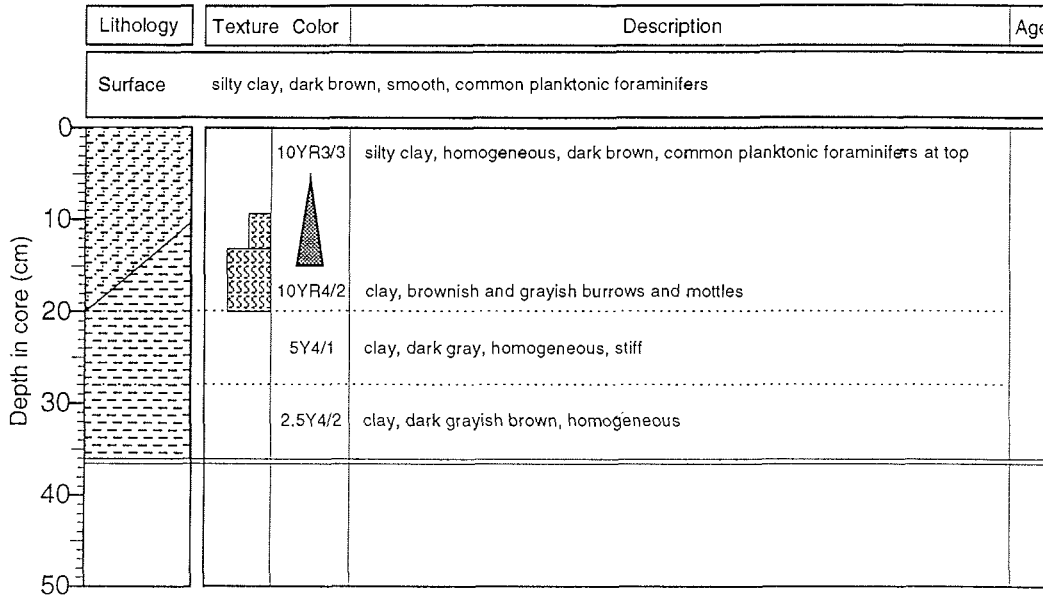
Amundsen Basin

ARK VIII/3 (ARCTIC 91)

Recovery: 0.36 m

87° 35.4' N, 103° 43.6' E

Water depth: 4411 m



PS2175-5 (TWC)

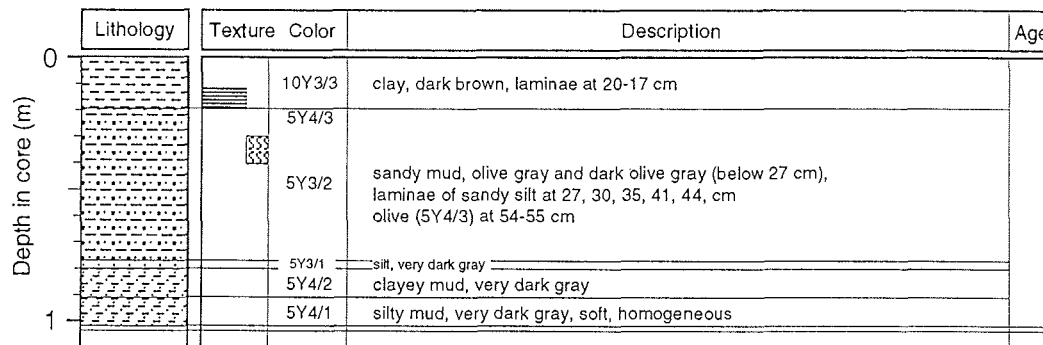
Amundsen Basin

ARK VIII/3 (ARCTIC 91)

Recovery: 1.02 m

87° 39.8' N, 104° 04.9' E

Water depth: 4313 m



PS2175-5 (GPC)

Amundsen Basin

ARK VIII/3 (ARCTIC 91)

Recovery: 16.92 m

87° 39.8' N, 104° 04.9' E

Water depth: 4313 m

	Lithology	Texture Color	Description	Age
0		10YR3/3	clay, dark brown, mottled down to 23 cm, laminated at 23-28 cm, dark gray with brown specks at base	
		5Y4/3 5Y4/2	clay, olive to olive gray, slightly mottled, brownish at base	
		5Y4/2	clayey mud, olive gray, partly laminated at 53-67, 83-88 cm, partly mottled	
1		5Y3/1	silty mud, very dark gray, soft and soupy	
		5Y4/1	clay, dark gray	
		5Y4/2	clay, olive gray	
		5Y4/1	clay, dark gray, black laminae at 194 cm	
2		5Y3/1	sand, layer-grading to silty sand, very dark gray	
		5Y3/2	clay, dark olive gray, homogeneous	
		5Y4/2	clay, olive gray, homogeneous, mottled ?	
		5Y4/1	sandy silt, laminated clay, dark gray, laminated in the lower part	
		5Y4/2	clay, olive gray, homogeneous	
3		5Y4/3	clay, olive gray, stratified	
		5Y3/1	silt to clay, graded and stratified, laminated at top	
		5Y4/1	clay, dark gray, homogeneous	
		5Y4/3-2	clay, olive gray to olive	
		5Y4/4 5Y4/3	clay, olive to olive gray, gray lamina at base, mottled throughout	
4		5Y4/3	clay, olive to olive gray to dark gray, mottled	
		5Y4/1	sandy silt, graded, laminated at top	
		5Y4/1	clay, dark gray, laminated at base	
		5Y4/2	clay, olive gray, homogeneous	
5		10YR5/4 10YR4/4 10YR5/3 10YR4/3	clay, brown-yellowish brown- dark yellowish brown, mottled throughout 492-499 black spots	

PS2175-5 (GPC)

Amundsen Basin

ARK VIII/3 (ARCTIC 91)

Recovery: 16.92 m

87° 39.8' N, 104° 04.9' E

Water depth: 4313 m

	Lithology	Texture	Color	Description	Age
5			2.5Y4/2	clay, dark yellowish brown to olive brown, mottled, brown laminae at 517 and 519 cm	
			2.5Y4/4		
6			5Y4/3	clay, olive, mottled, olive gray laminated bed at 592-599 cm, brown laminae at 581, 556 cm	
			5Y4/2 5Y4/3		
7			5Y4/1	clay, dark gray, homogeneous, slight color change from lighter to darker at 628 cm	
			5Y3/1		
			5Y4/1		
8			5Y3/1	fining upwards sequence, graded sand-laminated silty sand-laminated silty mud-clay, very dark gray, homogeneous, sharp lower boundary	
			5Y4/1		
9			5Y4/1	clay, dark gray, homogenous laminated silty mud at 805-818, 830-835, 854-857 cm	
			5Y4/1		
			5Y4/1		
10			5Y4/1	fining upwards sequence, sand to clay, laminated at 915-895 cm, black horizons at 878-886 and 882 cm, sharp lower boundary	
			5Y4/1		
			5Y3/1	clay, very dark gray, 3 mm thick sandy clay at top	
			5Y4/1	fining upwards sequence, sand to clay, laminated at 970-1000 cm, sharp lower boundary	

PS2175-5 (GPC)

Amundsen Basin

ARK VIII/3 (ARCTIC 91)

Recovery: 16.92 m

87° 39.8' N, 104° 04.9' E

Water depth: 4313 m

Depth in core (m)	Lithology	Texture	Color	Description	Age
10			5Y4/1	silty sand, dark gray, fining upwards	
			5Y4/1	clay, dark gray, black horizon at 1018-1020, 1034-1035, 1040, 1046-1047 cm 2 mm thick olive gray, sandy clay laminae with small mud clasts at 1034 cm	
			5Y3/2	clayey mud, dark gray, very finely laminated	
			5Y3/2	sandy silt, dark olive gray, fining upwards	
11			5Y3/2	clay, dark olive gray, laminated?, black layers at 1082, 1110 cm	
			5Y3/2	clayey silt, dark olive gray, laminated, folded in the upper part	
			5Y3/2	silty sand, dark olive gray, graded, fining upwards sequence	
			5Y3/2	clay, dark olive, black laminae at 1179, 1182, 1186 cm	
12			5Y3/2	silt, laminated, dark olive	
			5Y3/1	clay, very dark gray, homogeneous, black horizon and mottled at top	
	<i>disturbed</i> 		5Y3/1	silty sand, very dark gray, laminated, disturbed on top	
13			5Y3/2	sand, dark olive gray, fining upwards	
			5Y3/1	clay, very dark gray, folded and faulted laminae	
			5Y3/1	sand to sandy silt, very dark gray, folded and faulted laminae	
14			5Y3/1	clay, very dark gray, black horizon at 1408 cm, faintly laminated at 1415 cm	<i>after opening the core, there were "gas pits" between 1400 and 1450 cm</i>
			5Y3/1	sandy silt, very dark gray, faintly laminated, fining upwards	
			5Y3/1	clay, very dark gray, dark layers at 1427, 1428 cm	
			5Y3/1	sandy silt, very dark gray, folded and faulted laminae	
15			5Y3/1	clay, very dark gray, homogeneous, stiff, dark layer at top (1447-1449 cm)	

PS2176-4 (GKG)

Amundsen Basin

ARK VIII/3 (ARCTIC 91)

Recovery: 0.37 m

87° 46.6' N, 108° 10.0' E

Water depth: 4364 m

Lithology	Texture	Color	Description	Age
Surface				
			clay, brown, smooth, common planktonic foraminifers	
0				
		7.5YR5/2	clay, brown, homogeneous, common planktonic foraminifers	
10		10YR4/2	clay, dark grayish brown, abundant brownish and grayish mottles, common yellowish nodules	
20		10YR4/2	clay, dark grayish brown, common brownish and grayish mottles	
30		5Y4/1	clay, dark gray, homogeneous	
		5Y4/2	clay, olive gray, homogeneous	
		2.5Y4/2	clay, dark grayish brown, common horizontal brownish and grayish streaks	
40				
50				

PS2176-1 (TWC)

Amundsen Basin

ARK VIII/3 (ARCTIC 91)

Recovery: 0.72 m

87° 46' N, 108° 44.8' E

Water depth: 4395 m

Lithology	Texture	Color	Description	Age
0		10YR3/6	clay, dark yellowish brown	
		2.5Y3/2	clay, very dark grayish brown, grading into upper unit	
		10YR3/4	clay, dark yellowish brown, laminated	
		2.5Y4/2	clay, dark grayish brown, slightly brownish bands at 47-48 cm	
		2.5Y3/2	clay, very dark grayish brown, layering indicated by slight color changes, grading boundaries	
		2.5Y3/1	sand, very dark gray	
		10YR3/1	clay, very dark gray, grading into very dark grayish brown	
		10YR3/2	clay, very dark grayish brown	
			<i>presumably double penetration</i>	
1				

PS2176-1 (GPC)

Amundsen Basin

ARK VIII/3 (ARCTIC 91)

Recovery: 14.00 m

87° 46' N, 108° 44.8' E

Water depth: 4395 m

	Lithology	Texture Color	Description	Age
0		10YR3/6	clay, dark yellowish brown	
		2.5Y3/2	clay, very dark grayish brown, grading into upper unit	
1		10YR3/4	clay, dark yellowish brown, laminated, brown specks	
		2.5Y4/2	clay, dark grayish brown, brownish bands	
		2.5Y3/2	clay, very dark grayish brown, layering indicated by slight color changes, slight brownish band at 48-50 cm, grading into upper unit	
		5Y3/1	silty mud to clay, very dark gray	
		2.5Y4/2	clay, very dark gray	
		5Y3/2	clay, dark olive gray, grading into upper unit	
		5Y4/2	clay, olive gray	
		5Y3/1	clay, very dark gray, silty mud at base, grading into upper unit	
		5Y3/2	clay, dark olive gray	
		2		2.5Y3/2
2.5Y3/2	clay, very dark grayish brown			
5Y3/1	clay, very dark gray, homogeneous			
5Y4/2	clay, olive gray, mottled in the upper part			
5Y3/1	silt, very dark gray, fining upwards			
5Y4/1	silty clay, dark gray, fining upwards to dark gray clay, black spots in the upper 8 cm			
5Y4/2	clay, dark gray and olive gray, mottled in the upper part, black laminae at 251 cm, black spots at 249 cm			
5Y4/1	clay, dark gray and olive gray, mottled			
5Y3/1	sandy silt, very dark gray, fining upwards			
5Y4/1	silt, very dark gray, fining upwards into olive gray and dark gray clay, mottled at top			
3		5Y4/2	fine silt, very dark gray, fining upwards to olive gray clay, weakly mottled at 288-305 cm	
		5Y3/1		
		5Y4/1		
		5Y4/2	silt, very dark gray, fining upwards to olive gray and dark gray clay, mottled at 317-340 cm	
		5Y3/1		
		5Y4/1	clay, dark gray and olive gray, mottled	
		2.5Y4/2	clay, dark grayish brown, weakly mottled	
		5Y3/1	silt, very dark gray, laminated, fining upwards	
		5Y4/1	clay, dark gray, mottled in the uppermost part	
		5Y4/3	clay, olive, mottled at 393-424 cm, silty clay at 429-426 cm, fining upwards	
4		5Y4/2	clay, olive gray, mottled, dark gray at top 1 cm, dark grayish brown silty clay, fining upwards at lowermost 3 cm	
		5Y4/2	clay, olive gray, mottled	
		5Y3/1	silt, very dark gray, fining upwards at base	
		5Y3/1	silty, very dark gray, grading upwards into clay, mottled in the upper part	
5		5Y3/1	silty, very dark gray, grading upwards into clay, mottled in the upper part	

PS2176-1 (GPC)

Amundsen Basin

ARK VIII/3 (ARCTIC 91)

Recovery: 14.00 m

87° 46' N, 108° 44.8' E

Water depth: 4395 m

	Lithology	Texture	Color	Description	Age
5			5Y4/1	silty clay, very dark gray, laminated, fining upwards into dark gray clay, black laminae at 496 cm	
			5Y3/1		
6			5Y4/1	clay, dark gray, black spots, mottled	
			2.5Y4/4		
			2.5Y4/2		
7			2.5Y4/2	clay, dark grayish brown, lighter mottles throughout, silt laminae at 596-603, 611-616 cm, brown postdepositional laminae, particular at 596, 622, 628, 647 cm	
			2.5Y3/2		
8			5Y3/1	clay, very dark gray, layering marked by slight color changes, silt layers at 736-739, 749-751, 762-765 cm	
			5Y4/1		
			5Y3/3		
			5Y2.5/2		
			5Y3/3		
			5Y3/3		
			5Y3/3		
			5Y3/3		
			5Y3/3		
			5Y2.5/2		
9			5Y2.5/2	silt, black, grading into clay, lowermost part laminated	
			5Y3/2		
			5Y3/2		
			5Y3/2		
			5Y3/2		
10			5Y3/1	silt, very dark gray, fining upwards, laminated	
			5Y3/1		

PS2176-1 (GPC)

Amundsen Basin

ARK VIII/3 (ARCTIC 91)

Recovery: 14.00 m

87° 46' N, 108° 44.8' E

Water depth: 4395 m

	Lithology	Texture	Color	Description	Age
10			5Y4/1	silt, dark gray, fining upwards into upper unit	
			5Y3/1	silt, dark gray, laminated, fining upwards into clay, mud clasts at 815 cm	
			5Y3/1	s.a.a.	
			5Y3/1	s.a.a.	
			5Y3/1	s.a.a.	
11			5Y3/1	s.a.a., black horizon at 1103-1105 cm	
			5Y3/1	s.a.a.	
			5Y3/1	s.a.a., black horizon at 1123-1127 cm	
			5Y3/1	s.a.a.	
			5Y3/1	silty sand, dark gray, grading into clay, laminated from 1163-1177, 1152-1160 cm	
			5Y4/1	sandy mud, dark gray, homogeneous	
			5Y3/2	sandy mud, dark gray, homogeneous	
12			5Y4/1	sandy mud, dark gray, mud clasts, clay at 1198-1199 cm	
			5Y3/2	silt, dark olive gray, laminated, grading upwards into clay	
			5Y4/1	sandy mud, dark gray, mud clasts, homogeneous	
			5Y3/2	clayey mud, dark olive gray, laminated, grading upwards into clay, black at top	
			5Y3/2	silt, dark olive gray, laminated, fining upwards into clay	
13			5Y3/2	s.a.a., black horizon at 1290-1296 cm	
			5Y3/2	s.a.a., black horizon at 1309-1314 cm	
			5Y3/2	s.a.a., black horizon at 1332-1337 cm	
			5Y3/2	s.a.a.	
			5Y3/2	clay, dark olive gray, homogeneous	
14			5Y2.5/1 5Y3/1	clay, very dark gray, grading into black clay	
				<p><i>sections exchanged (core barrel upside down):</i> 478-582 <> 683-784, 784-887 <> 989-1090 bag samples: 1090-1095, 1299-1303 sections with no indication of true depth: 1095-1196, 1196-1299</p>	
15					

PS2176-3 (KAL)

Amundsen Basin

ARK VIII/3 (ARCTIC 91)

Recovery: 9.76 m

87° 46.3' N, 108° 23.6' E

Water depth: 4363 m

Lithology	Texture Color	Description	Age
0	10YR4/4	0-16 clay, dark yellowish brown, soupy	
	16-30 clay, dark yellowish brown, brown-orange lenses, laminated 18-23 cm, hole (burrow ?) at 20-21 cm		
0	2.5YR5/0 to 2.5YR4/2	25-30 cm thin sandy laminae	
	2.5Y4/4	clay, dark grayish brown, partly laminated, "cloudes/lenses", larger mud lenses at 40-42 cm,	
1	5Y4/3	clay, olive to gray, mottling 79-80 cm, silty/sandy layer 97-98 cm	
	5Y5/1		
1	N4	clay, gray and silty/sandy clay, dark gray, alternating, laminations	
	N4	clay, dark gray, massive, black layers at 131 and 133 cm	
1	5Y5/1	clay, olive, homogeneous	
	N4	sand, dark gray, fining upwards	
2	10YR4/1	clay, olive gray to gray, partly laminated, black bands/spots at 169-173, 179-181, 188-190 cm	
	5Y4/2		
2	10YR3/2	clay, dark brownish gray and silty/sandy clay alternations	
	2.5Y5/2	clay, grayish brown, mottling (bioturbation) in the lower part	
2	5Y5/3	clay, olive to olive brown, in the lower part lamination and mottling/bioturbation, grayish sandy layer at 222 cm	
	2.5Y4/4	clay, dark gray, laminated, sandy layer at 245 cm	
2	N4	clay, olive to dark grayish olive, partly laminated, upper part light gray with black spots (pyrite?)	
	5Y5/3	sandy clay, dark gray	
2	N4	clay, olive to brownish olive, mottled/bioturbated in the upper part	
	5Y5/3		
3	N4	clay, dark gray, slightly mottled	
	N3	clay, very dark gray, laminated	
3	N5	clay, gray, mottled (black spots, pyrite ?), black layer at 298 cm	
	5Y5/3	clay, variegated olive to grayish brown, partly laminated and mottled/bioturbated, clay, light gray at 121-122 cm	
3	10YR4/2		
	N3	sandy clay, very dark gray, gradation	
4	N5	clay, light gray to very dark gray (N5), partly laminated	
	5Y4/1	clay and sandy silt alternating, very dark gray	
4	N5	clay, light gray to very dark gray (N5), bioturbated	
	5Y4/1	clay, olive	
4	5Y5/3	clay, dark gray, in the lower part laminated	
	5Y4/1	clay, light gray, black spots	
5	5Y5/3	clay, olive to very dark grayish olive, strongly mottled/bioturbated, dark brown laminae at 444, 454, 465, 486, 490 cm, sandy layers at 472-473 and 486 cm	
	5Y3/2		

PS2176-3 (KAL)

Amundsen Basin

ARK VIII/3 (ARCTIC 91)

Recovery: 9.76 m

87° 46.3' N, 108° 23.6' E

Water depth: 4363 m

	Lithology	Texture	Color	Description	Age
5		N4 5Y4/1-5/2		clay, dark gray to olive, partly laminated, thin dark brown laminae at 508.5, 509.5, 516, 517 cm	
				clay, dark gray to very dark gray, alternating sandy/silty and clayey layers at 566-568, 577-578, 587-599, 627-630, 658-660 cm	
6				more sandy intervals with cross bedding at 608-615, 646-650 cm	
				N2 clay, very dark gray to black (pyrite?)	
7		N4 to N3			
		N2			
		N4 to N3		clay, dark gray to very dark gray, alternating with sandy layers at 661-669, 695-699, 721-724, 738-743, 756-769 cm;	
		N2		cross bedding at 665, 738-740, 761-764 cm;	
		N4 to N3		directly underneath the sandy/clay alternations black intervals (N2), mottled	
		N4 to N3			
		N4 to N3			
		N4 to N3			
8		N4 to N3			
		N2			
		N4 to N3			
		N4 to N3		alternating clay sections and clayey/sandy laminated sections, cross bedding at 895-898, 932-936 cm	
		N2		directly underneath the sandy intervals black (pyritic?), mottled intervals	
		N4 to N3			
		N2			
9		N4 to N3			
		N2			
		N4 to N3			
		N4 to N3			
		N2			
		N4 to N3			
10		N2			
		N4 to N3			

PS2177-5 (KAL)

Lomonosov Ridge

ARK VIII/3 (ARCTIC 91)

Recovery: 6.94 m

88° 2.1' N, 134° 36.7' E

Water depth: 1400 m

	Lithology	Texture	Color	Description	Age
0			10YR3/4	clay, dark yellowish brown, soft	transitional boundary
			10YR4/3 10YR3/6	clay, dark yellowish brown to brown, soft, mottled	
1			10YR5/4	sandy mud, dark grayish brown to yellowish brown, more grayish towards base, coarsening upwards, faint layering/lamination	sharp boundary
			10YR4/2		
			5Y3/1	sandy mud, very dark gray, coarsening upwards	sharp boundary
2			5Y4/3	sandy clay, olive, thin sand layer at 111 cm	gradational boundary
			5Y4/3	sandy mud, olive to olive brown, coarsening upwards	bioturbated boundary
			10YR4/4 to 2.5Y4/4	clay, olive brown to dark yellowish brown, individual mud clasts, intensely mottled throughout, sand layer at 159-161 cm	
			10YR3/3-4/4 to 5Y5/3	sandy mud, olive grading to clay, dark yellowish brown, dark specks, dark layer at 183 cm, sandy layer at 186, 189, 192 cm, layered below 180 cm, dropstones and mud clasts	
3			10YR4/2 to 2.5Y4/4	clay, olive brown to dark grayish brown, yellowish brown at 222-224 cm, intensely mottled, light and dark, color boundary at 214/215, mud clasts, slightly more sandy at base	
			10YR3/2 2.5Y4/4	sandy mud, olive brown to very dark yellowish brown, intensely mottled, thin dark sandy layer at 235 cm, sand layer with mud clasts at 241-243 cm	
			10YR3/2 10YR4/4 2.5Y5/2	sandy mud, dark yellowish brown, intensely mottled throughout, grading at 265 cm to grayish brown	transitional boundary
4			10YR4/3	clay, brown, mottled	transitional boundary
			2.5Y5/4	sandy mud, light olive brown	
			2.5Y4/4	very sandy mud, layered from 313-322 cm, grayish top, brownish base, coarsening upwards numerous sandy layers in 2-5 cm intervals, increasing in number upwards	
			2.5Y4/4	sandy mud, olive brown, coarsening upwards, layered	
5			2.5Y4/2	sandy mud, dark grayish brown, layered with some change in hue, IRD, 1-2 mm Ø, and mud clasts, clay layers at 400-397, 385-384 cm, sandy layer at 407-405 cm	mottled boundary
			2.5Y5/4	silty mud, light olive brown, homogeneous mottled	
			10YR3/3 2.5Y5/6	silty mud, dark brown, mottled layer of clay at 430-433 cm, grading downwards into light olive brown, sand lense at 443 cm	
			10YR3/3 2.5Y5/4	silty mud with IRD, grading into clay, dark brown, mottled	
			10YR3/3	clay, dark brown, mottled	

PS2177-5 (KAL)

Lomonosov Ridge

ARK VIII/3 (ARCTIC 91)

Recovery: 6.94 m

88° 2.1' N, 134° 36.7' E

Water depth: 1400 m

Lithology	Texture	Color	Description	Age
5		10YR3/3	clay, dark brown, mottled	
		2.5Y4/4	clayey mud, olive brown, mottled	
		2.5Y5/4	silty mud, light olive brown	
		10YR3/3	clay, dark brown, mottled	gradational color change
		2.5Y5/4	clayey mud, light olive brown, mottled	
		10Y3/3	clay, dark brown, mottled	mottled boundary
		10YR4/4	clay, dark yellowish brown, darker layer (1 cm) with slightly darker horizon down to 594 cm	
		2.5Y5/4	clay, light olive brown, cloudy dark areas, intensely mottled	
		10YR5/4	clay, yellowish brown	mottled boundary
		10YR4/3	clay, dark brown, mottled	
		10YR5/3	clay, brown, mottled	
		10YR4/3	clay, dark brown, mottled	
	10YR5/5	clay, yellowish brown		
	10YR4/3	clay, olive to dark brown, mottled, dark specks down to 685 cm		
	2.5Y4/4			
6				
7				

PS2177-1 (GKG)

Lomonosov Ridge

ARK VIII/3 (ARCTIC 91)

Recovery: 0.40 m

88° 02.2' N, 134° 55.1' E

Water depth: 1388 m

Lithology	Texture	Color	Description	Age
Surface silty clay, very dark grayish brown, smooth, few polychaets, few bivalves, rare planktonic foraminifers				
0		10YR4/2	silty clay, homogeneous, dark grayish brown	
		10YR3/2	clay, very dark grayish brown, abundant burrows	
		10YR4/2	silty clay, homogeneous, dark grayish brown, abundant burrows: 0.1-10 mm Ø	
		10YR4/3	silty clay, brown, homogeneous	
		10YR3/3	silty clay, dark brown, homogeneous	
		10YR4/3	silty clay, brown, tendency of brownish and olive brownish horizontal streaks	
10				
20				
30				
40				
50				

PS2177-6 (GPC)

Lomonosov Ridge

ARK VIII/3 (ARCTIC 91)

Recovery: 11.43 m

88° 2.3' N, 134° 19.6' E

Water depth: 1419 m

Lithology	Texture	Color	Description	Age
0		10YR3/3	clay, brown to dark brown, mottled mostly at 13-25 cm, upper 13 cm homogeneous	
		10YR4/3		
		10YR3/3	clay, brown to dark brown, gradational color change, mottled	
		10YR4/3		
		2.5Y4/4		
		2.5Y4/2	sandy mud, very dark grayish brown to dark grayish brown to olive brown, lighter colors from base to top, common mud clasts (< 2 cm Ø)	
		2.5Y3/2		
		2.5Y5/4		
1	▲	2.5Y4/2	sandy mud, dark grayish brown to light olive brown, fining slightly upwards	
		2.5Y4/4		
		10YR4/3	clay, olive brown at base and top, brown with olive brown specks in the middle, mottled	
		2.5Y4/4		
	▲	10YR4/3	clay, brown, mottled	
		2.5Y4/4		
		10YR3/3	clay, dark brown, lighter mottled, yellowish brown at 175-173 cm	
		2.5Y5/4		
2		2.5Y4/4	silty clay, light olive brown, yellowish brown clay at 197 cm	
		2.5Y4/4		
		10YR4/3	sandy clay, olive brown, dark brown and mottled at 199-200 cm	
		2.5Y4/4		
		10YR4/3	clay, brown, mottled, dark brown at 212-213 cm	
		2.5Y4/4		
		10YR4/3	clay, olive brown, mottled, gradational boundary to top unit	
		10YR4/3		
3	section 245-345 cm got stuck in the core barrel, bag sample			
		10YR3/3	clay, brown, mottled	
		2.5Y4/4		
		10YR3/3	clay, dark brown, lighter mottled, yellowish brown at 175-173 cm	
		2.5Y5/4		
		10YR3/3	silty clay, light olive brown, mottled	
		2.5Y4/4		
		10YR3/3	silty clay, dark brown, mottled	
		2.5Y5/4		
4		10YR3/3	silty clay, olive brown and light olive brown, mottled	
		2.5Y5/4		
		10YR3/3	silty clay, dark brown, mottled	
		2.5Y5/4		
		10YR4/3	silty clay, brown, mottled	
		10YR5/4		
		10YR3-4/3	silty clay, yellowish brown, mottled	
		10YR3-4/3		
		10YR3-4/3	silty clay, dark brown, mottled	
		2.5Y4/4		
		2.5Y4/4	silty clay, olive brown, mottled	
		10YR5/4		
5		10YR3/3	silty clay, yellowish brown, mottled	
		10YR3/3		
		10YR6/4	silty clay, light yellowish brown	
		10YR3/3	silty clay, dark brown, mottled	

coring disturbance

PS2177-6 (GPC)

Lomonosov Ridge

ARK VIII/3 (ARCTIC 91)

Recovery: 11.43 m

88° 2.3' N, 134° 19.6' E

Water depth: 1419 m

	Lithology	Texture	Color	Description	Age	
5			2.5Y4/4	silty clay, olive brown to light olive brown, mottled		
			2.5Y5/4	silty clay, dark brown, mottled, dark specks at 480-482 cm		
			10YR4/3	silty clay, brown, mottled		
			10YR3/3	silty clay, dark brown, mottled		
			2.5Y4/4	silty clay, olive brown, mottled		
			2.5Y4/2	silty clay, dark grayish brown, mottled, changing colors and lithology		
			10YR4/4			
			10YR4/3	silty clay, brown, mottled		
			2.5Y4/4	silty clay, olive brown, mottled, dark specks at base		
			2.5Y4/4	silty clay, olive brown, mottled, dark brown at top 2 cm		
6			10YR3/3	silty clay, dark brown, mottled		
			2.5Y4/4	silty clay, olive brown, mottled		
			10YR3/3	silty clay, dark brown, mottled		
			2.5Y5/4	silty clay, light olive brown, dark specks		
			10YR3/3	silty clay, dark brown, mottled		
			2.5Y4/4	silty clay, olive brown, mottled		
			10YR4/3	silty clay, brown, mottled		
			2.5Y4/4	silty clay, brown, mottled		
			2.5Y4/4	silty clay, brown, mottled		
			10YR3/3	silty clay, dark brown, mottled		
7			2.5Y4/4	silty clay, olive brown, mottled, dark specks, bands and clouds below 676 cm		
			10YR3/3	silty clay, dark brown, mottled, black bands/specks		
			2.5Y4/4	silty clay, olive brown, mottled, dark bands and spots		
			10YR4/3	silty clay, brown, mottled, dark bands and specks		
			2.5Y4/4	silty clay, olive brown, mottled, frequent dark specks and bands		
			2.5Y3/2	silty clay, very dark grayish brown, mottled, several dark spots and lenses		
			2.5Y4/4	silty clay, olive brown, mottled, dark spots above 760 cm		
			10YR4/3	silty clay, brown, mottled, small dark spots		
			2.5Y4/4	clay, olive brown, mottled, dark spots		
			10YR4/3	s.a.a.		
8			2.5Y4/4	s.a.a.		
			10YR4/3	s.a.a.		
			2.5Y4/4	sandy mud at 853-857 cm		
			10YR4/3	silty clay, brown, mottled		
			10YR5/4	silty clay, yellowish brown, mottled, some dark spots		
	9			2.5Y4/4	clay, olive brown, mottled, dark spots	
				10YR3/3	silty clay, dark brown, mottled	
				10YR5/3	silty clay, brown, mottled	
				2.5Y5/4	silty clay, light olive brown, mottled	
				10YR4/3	silty clay, brown, mottled	
10						

coring disturbance

dark bands does not follow layering in general

PS2177-6 (GPC)

Lomonosov Ridge

ARK VIII/3 (ARCTIC 91)

Recovery: 11.43 m

88° 2.3' N, 134° 19.6' E

Water depth: 1419 m

Depth in core (m)	Lithology	Texture	Color	Description	Age
10			2.5Y4/4	silty clay, olive brown, mottled	
			10YR4/3	silty clay, brown, mottled	
			10YR5/4	silty clay, olive brown grading upwards into yellowish brown, mottled, few dark specks at 1033-1050 cm	
			10YR3/3	silty clay, dark brown, mottled	
			2.5Y4/4	silty clay, olive brown, mottled	
			10YR4/3	silty clay, brown, mottled	
			2.5Y4/4	silty clay, olive brown, mottled	
			10YR4/3	s.a.a.	
			2.5Y4/4	s.a.a.	
			10YR4/3	s.a.a., dark brown uppermost layer	
11			10YR4/3	silty clay, brown, mottled	
			10YR5/4	silty clay, yellowish brown, mottled	
			10YR4/3	s.a.a.	
			10YR5/4	s.a.a.	

PS2177-6 (TWC)

Lomonosov Ridge

ARK VIII/3 (ARCTIC 91)

Recovery: 1.61 m

88° 2.3' N, 134° 19.6' E

Water depth: 1419 m

Depth in core (m)	Lithology	Texture	Color	Description	Age	
0			10YR3/2	clayey mud, to clay, olive brown grading into dark yellowish brown into very dark grayish brown, faint layering		
			10YR3/4			
			2.5Y4/4			
			10YR4/6			clayey mud, dark yellowish brown, mud clasts (frequent at 125-129 cm)
			10YR4/6			silty mud, dark yellowish brown, mottled grading downwards into sandy mud, dark gray
			10YR4/3			silty mud, brown, grading downwards into sandy mud, very dark grayish brown, clayey mud layer in dark yellowish brown at top
			10YR3/2			clayey mud layer in dark yellowish brown at top
			2.5Y4/4			silty mud, olive brown
			SS; 10YR3-4/2			clayey silt, dark grayish brown, grading downwards into very dark grayish brown, intensively mottled below 107 cm
			2.5Y4/4			silty mud, olive brown
1			2.5Y4/4	clayey mud, dark brown grading into olive brown, homogeneous		
			10YR3/3			
2				<i>presumably double penetration</i>		

PS2178-2 (GKG)

Makarov Basin

ARK VIII/3 (ARCTIC 91)

Recovery: 0.43 m

88° 0.2' N, 159° 14' E

Water depth: 4009 m

Lithology	Texture	Color	Description	Age
Surface				
silty clay, dark grayish brown, smooth, common planktonic foraminifers, scattered few light brown mud clasts				
		10YR4/2	silty clay, dark grayish brown, gradually becoming darker upwards, light brown streaks in the lower interval (8-14 cm)	
		10YR5/3	clay, brown, homogeneous	
	▲	5Y5/3	sand, olive, fining upwards (turbidite ?)	
		10YR5/3	clay, brown, homogeneous	
	10YR4/3	clay, dark brown, homogeneous		

PS2178-3 (TWC)

Makarov Basin

ARK VIII/3 (ARCTIC 91)

Recovery: 1.24 m

88° 0.3' N, 159° 10.1' E

Water depth: 4009 m

Lithology	Texture	Color	Description	Age
0				
		10YR3/3	clay, dark brown, soft, mottled	
		2.5Y4/4	clay, olive brown, mottled, well sorted sand at 17-21 cm	
		10YR4/3-5/4	clay, (yellowish) brown, mottled	
		10YR4/3	clay, brown, darker layers at 36, 42-43 cm	
		5Y4/3	clay, olive, laminated at 55-85 cm, darker specks at 53-85, 92-110 cm, gradational color change to upper unit at 56-51 cm	
	2.5Y4/2	clay, dark grayish brown, sand lense at 112-115 cm		

PS2178-3 (GPC)

Makarov Basin

ARK VIII/3 (ARCTIC 91)

Recovery: 13.72 m

88° 0.3' N, 159° 10.1' E

Water depth: 4009 m

	Lithology	Texture	Color	Description	Age
0			10YR3/3	clay, dark brown, soft, mottled	
			2.5Y4/4	clay, olive brown, mottled, gradational color change to top unit	
0			10YR4/3	clay, brown, mottled	
			10YR5/4	clay, yellowish brown, mottled in the upper part	
1			10YR4/3	clay, brown, soft, darker layers at 45, 50 cm	
			5Y4/3	clay, olive, well laminated at 70-112 cm, darker specks at 50-85, 95-157 cm	
2			5Y4/3	clay, olive, few black specks, two dark gray laminae at 199 cm	
			2.5Y4/4	clay, olive brown, mottled, clayey sand laminae at base, sand, olive brown at top	
3			2.5Y4/2	sandy mud, dark grayish brown, frequent mud clasts, clay, olive brown at 240-241, 243-245 cm	
			2.5Y5/4	clay, light olive brown, soft, slightly mottled in the upper part	
3			2.5Y4/2	clay, dark grayish brown, mottled	
			10YR4/3	clay, brown, mottled	
			5Y5/4	clay, olive, mottled	
			5Y4/3	clay, olive, mottled	
			2.5Y4/4	clay, olive brown	
			10YR3/3	clay, brown, mottled	
			5Y4/2	sandy mud, dark olive gray	
			10YR3/4	clay, dark yellowish brown, intensely mottled, grading downwards into brown	
			2.5Y4/4	clayey mud, olive brown, mottled	
			2.5Y4/4	sandy mud, olive brown, homogeneous, grading to top unit	
4			10-2.5Y4/4	clay, olive brown, grading upwards	
			10YR3/5	clay, dark yellowish brown	
			10YR3/3	silty mud, olive grading upwards into dark yellowish brown clay, mud clasts	
			10YR3/4	clay, dark yellowish brown, horizons of clay, olive at 376-378, 371-372 cm	
4			2.5Y4/2	clay, olive brown, mottled, dark specks, slightly darker horizons at 469, 475, 482, 500 cm	
			2.5Y4/4	very homogeneous	
5					

PS2178-3 (GPC)

Makarov Basin

ARK VIII/3 (ARCTIC 91)

Recovery: 13.72 m

88° 0.3' N, 159° 10.1' E

Water depth: 4009 m

	Lithology	Texture	Color	Description	Age
5			2.5Y4/4	clay, olive brown	
			2.5Y4/2	clay, dark yellowish brown	
			2.5Y4/4	clayey mud, olive brown	
			2.5Y4/4	clay, light olive brown, mottled down to 538 cm	
			2.5Y4/4		
			2.5Y5/4		
			2.5Y4/4	sandy clay, olive brown, common mud clasts, two clay layers at 542-545, 571-577 cm, weakly mottled	
			2.5Y5/4		
			2.5Y4/4		
			10YR4/3	clay, brown, mottled, few black spots	
6			2.5Y4/4	clay, olive, mottled, black spots at 590-595 cm	
7			5Y4/3	clay, olive, dark specks and streaks	
8					
9			5Y4/2	clay, olive gray, mottles at 863-877, 888-935 cm	
10			5Y3/2	clay, dark olive gray, homogeneous	
			5Y3/1	silt, very dark gray, laminated, fining upwards	
			5Y4/2	clay, olive gray, mottled	
			5Y5/4	clay, olive, mottled, darkening upwards	
			5Y4/2	clay, olive gray, intensely mottled	

PS2178-3 (GPC)

Makarov Basin

ARK VIII/3 (ARCTIC 91)

Recovery: 13.72 m

88° 0.3' N, 159° 10.1' E

Water depth: 4009 m

Depth in core (m)	Lithology	Texture	Color	Description	Age
10			10YR5/4	clay, yellowish brown, mottled	
			10YR5/4	sand, yellowish brown, layered, fining upwards	
			2.5Y5/6	clay, light olive, mottled with thin grayish laminae at 1031 cm	
			2.5Y4/4	sandy mud, olive brown, mottled	
11			2.5Y4/4	clay, olive brown, dark specks particular in layers at 1061, 1064-1065, 1074, 1083-1085, 1086-1087, 1096-1098, 1102-1104, 1115 cm	
			N4	silty laminae, dark gray	
			2.5Y4/2	clay, olive brown/dark grayish brown, dark specks/spots with cloudy appearance, dark gray lamina (0.3 cm) at base	
12			2.5Y4/2	sandy clay, dark grayish brown, mottled, olive brown at base	
			2.5Y4/4-2	sandy clay, dark grayish brown to olive brown, mottled	
			2.5Y4/2-4	sandy clay, dark grayish brown to olive brown at base, mottled	
			2.5Y4/2	sandy clay, dark grayish brown, mottled	
			10YR5/4	clay, yellowish brown, mottled	
			5Y4/4	sand, olive, graded	
			2.5Y4/2	sandy clay, dark grayish brown, mottled	
13			5Y4/3	clay, olive, sandy in the lower part, olive brown at top	
			2.5Y4/4	clay, olive brown, weakly laminated	
			2.5Y4/2	clay, dark grayish brown, homogeneous, gradational color boundary at top	
			5Y4/2	sandy mud, olive gray, gradational boundary to silty mud and clay	
14					
15					

PS2178-5 (KAL)

Makarov Basin

ARK VIII/3 (ARCTIC 91)

Recovery: 8.31 m

88° 1.5' N, 159° 42.2' E

Water depth: 4008 m

Lithology	Texture	Color	Description	Age
disturbed		10YR3/4	clay, dark yellowish brown, soft	
		2.5Y4/4	sandy mud, olive brown	
		10YR4/3-4/4	clay, dark brown grading to yellowish brown, soft, sharp lower boundary	
		10YR4/3	clay, dark brown, homogeneous, lamination at 40-48 cm gradual color change	
		5Y4/3	clay, olive, black spots (<1 mm) 56-63 cm, 75-97, 112-119, 135-136 cm lamination 64-68, 95-97, 116-118, 122-125, 129 cm	
		2.5Y4/2	at base: silty clay, dark grayish brown	
		2.5Y4/4	clayey mud, olive brown, sandy layers at 168-170 cm, mottled 170-180 cm	
		5Y4/3	gradual color change sandy mud, olive gray	
		2.5Y4/4	sandy mud, olive brown, with mud clasts (1 cm)	
		5Y4/3	sandy mud, olive gray, few mud clasts	
		2.5Y5/4	sandy mud to clay, olive brown to light olive brown, dropstone 5 cm Ø	
		2.5Y4/2	clay, dark grayish brown, mottled	
		2.5Y5/6	clay, light olive brown	
		2.5Y4/4	clay, olive brown, mottled, dropstone (7x3 cm) at 235-238 cm	
		10YR4/2	clay, dark grayish brown, sandy at base, dropstone (2 cm Ø) <- color change	
		2.5Y4/4	clay, olive brown, sandy laminae at top	
		10YR4/3	clay, dark brown, mottled, sandy mud with mud clasts, mottled, at base	
		10YR4-5/3	clay, dark brown, mottled, 1 cm thick brown layers at top and base	
		10YR3/4	clay, dark brown, mottled	
		10YR5/4	sandy mud, yellowish brown to olive brown, mottled, more sandy 276-286 cm	
		2.5Y4/4	clay, olive brown, dark spots	
		10YR3-5/3	clay, dark brown to brown, mottled, 1 cm sand at base	
		10YR3-5/3	clay, dark brown to brown, mottled	
		10YR3-5/3	clay, dark brown to brown, mottled	
		10YR3/3	clay, dark brown to brown, mottled, 1 cm sand at base <- color change	
		10YR5/3	gradual color change between 330 and 336 cm	
		2.5Y4/4	clay, olive brown, dark spots	
		2.5Y4/2	clay, dark grayish brown	
		2.5Y4/6	clay, light olive brown to olive brown, mottled	
		2.5Y4/4	sandy mud, olive brown to dark grayish brown, mottled	
		2.5Y5/4	clay, light olive brown, mottled	
		2.5Y4/4	sandy mud, olive brown, mud clasts, decreasing in number upwards	
		2.5Y5/4	clay, light olive brown, mottled, dark spots	
		2.5Y4/4	sandy mud, olive brown, mud clasts	
		10YR3/3	clay, dark brown, mottled, black disrupted layer at top	

PS2178-5 (KAL)

Makarov Basin

ARK VIII/3 (ARCTIC 91)

Recovery: 8.31 m

88° 1.5' N, 159° 42.2' E

Water depth: 4008 m

Lithology	Texture	Color	Description	Age
		5Y4/3	clay, olive, dark/black spots/lenses 647-499 cm, mottled 525-499 cm	
			faintly mottled 647-605 cm	
		5Y4/3	clay, olive, homogeneous 2 dark gray laminae 670, 672 cm at base	
		N4	clayey mud, dark gray	
		2.5Y4/4	clay, olive brown, mottled, spots of weak red (10R5/4) at top gradual color change	
		2.5Y3/2	clay, very dark grayish brown	
		2.5Y4/2	silty mud, dark grayish brown, mottled, upper part (1 cm) gray	
		2.5Y5/4	clay, light olive brown, mottled, sand layer at 742 cm sharp, mottled boundary gradual color change	
		2.5Y3/2	clay, very dark grayish brown, mottled down to 755 cm	
		2.5Y4/2	clay, dark grayish brown, mottled	
	5Y3/2	clay, dark olive gray, homogeneous		

PS2179-1 (GKG)

Lomonosov Ridge

ARK VIII/3 (ARCTIC 91)

Recovery: 0.37 m

87° 44.8' N, 138° 1.7' E

Water depth: 1230 m

Lithology	Texture	Color	Description	Age
Surface silty clay, dark grayish brown, smooth, abundant bivalves, few benthic and planktonic foraminifers				
			10YR4/2 silty clay, dark grayish brown, homogeneous	
			10YR3/3 silty clay, dark brown, homogeneous, laminae	
			10YR4/2 silty clay, dark grayish brown, patches of darker and lighter brown patches (burrows)	
			10YR3/3 silty clay, dark brown, streaks of lighter brown color	
			10YR4/3 silty clay, brown, silt streaks, gradually more silty downwards	

PS2180-1 (GKG)

Makarov Basin

ARK VIII/3 (ARCTIC 91)

Recovery: 0.48 m

87° 37.6' N, 156° 40.5' E

Water depth: 4005 m

Lithology	Texture Color	Description	Age
Surface	silty clay, dark grayish brown, smooth, one echinoid, one polychaete, common planktonic foraminifers, common small mud clasts		
	10YR4/2	silty clay, dark yellowish brown, homogeneous, common planktonic foraminifers	
	10YR4/3 to 10YR5/4	clay, yellowish brown to brown, grayish and brownish burrows and streaks increasing to top of section	
	2.5Y4/4	sandy clay, olive brown, stiff (turbidite?)	
	10YR4/3 to 10YR5/4	clay, yellowish brown to brown, with fine brownish horizontal streaks at top of section	
	10YR4/2	clay, dark yellowish brown, few dark brownish horizontal streaks	

PS2180-2 (TWC)

Makarov Basin

ARK VIII/3 (ARCTIC 91)

Recovery: 0.87 m

87° 38.6' N, 156° 58' E

Water depth: 3991 m

Lithology	Texture Color	Description	Age
	10YR5/4	clay, yellowish brown, soft, darker mottles	
	10YR4/3	clay, brown, soft, laminated from 15-28 cm, sharp upper boundary	
	5Y4/3	clay, olive, laminated, dark specks 28-49 cm, gradational color change to the above unit	
	2.5Y4/4	silty clay to clay, olive brown, homogeneous, dark specks, slight dark streaks indicating layering at 70 cm	

PS2180-2 (GPC)

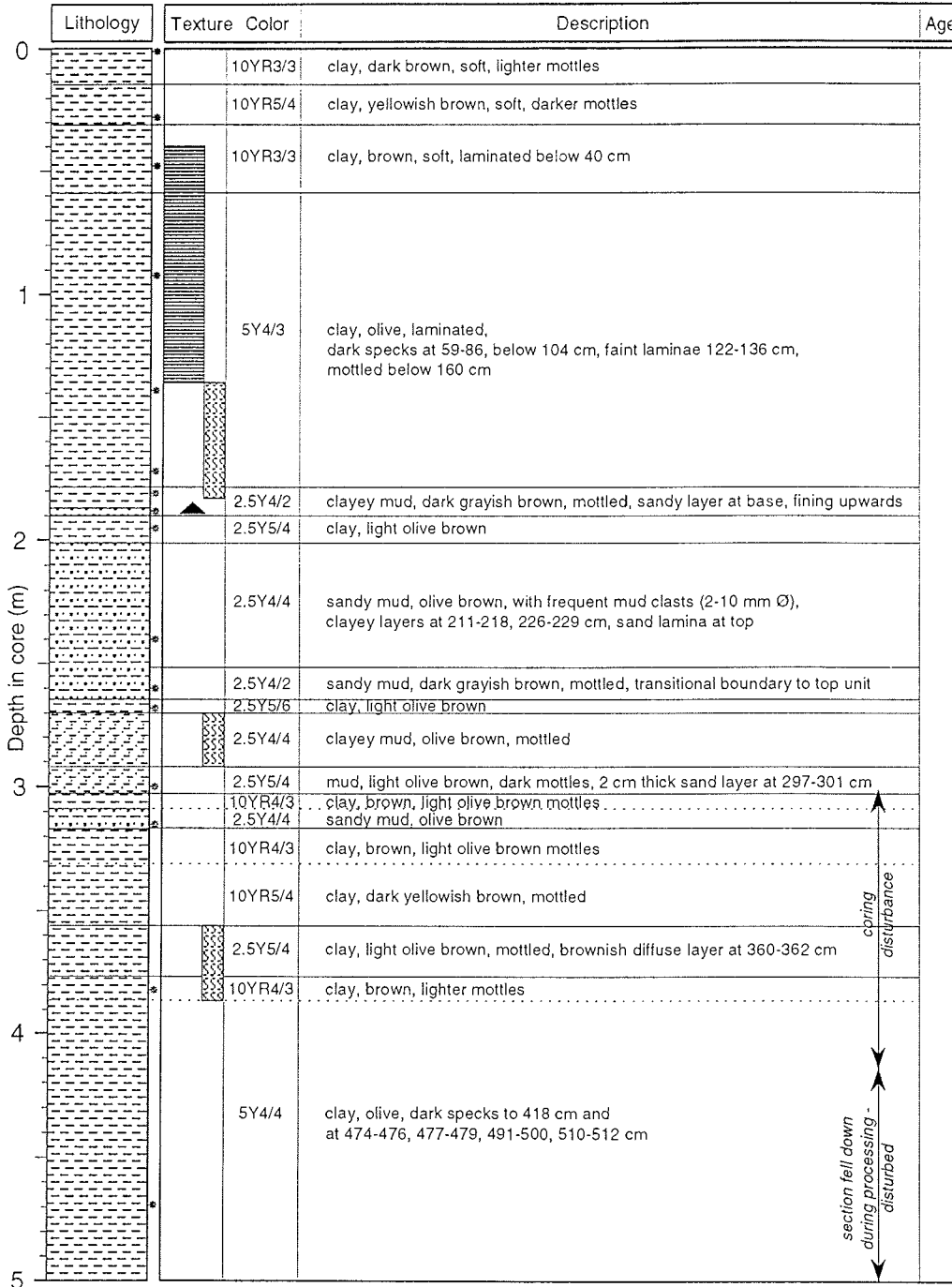
Makarov Basin

ARK VIII/3 (ARCTIC 91)

Recovery: 12.96 m

87° 38.6' N, 156° 58' E

Water depth: 3991 m



PS2180-2 (GPC)

Makarov Basin

ARK VIII/3 (ARCTIC 91)

Recovery: 12.96 m

87° 38.6' N, 156° 58' E

Water depth: 3991 m

	Lithology	Texture	Color	Description	Age
5			5Y4/4	clay, olive	
			5Y4/4	sandy clay, olive	
6			2.5Y5/4	clay, light olive brown, mottles of olive sandy clay at top 5 cm	
			2.5Y4/4	sand, olive brown, dark bands at boundaries	
			2.5Y4/4	sandy mud, olive brown, layered, clay layers at 515, 564, 571-573 cm, mud clasts throughout	
			10YR4/3	clay, brown, mottled, dark spots near the upper boundary	
7			5Y5/3	clay, olive, mottled, gradational color change to upper unit	
			5Y4/3		
			5Y4/3	clay, olive, homogeneous, except for black spots/clouds at 650-657 cm and small dark specks concentrated at 680, 705, 710, 670-683 cm	
			5Y4/2	clay, olive gray, black clouds/spots at 723-755 cm	
			5Y4/3(2)	clay, olive, homogeneous	
8			5Y5/4	clay, olive, darker mottles, boundary at top is marked by a very dark gray layer	
			5Y4/3	clay, olive, mottled, gradual color change to top unit	
			5Y4/3	clay, olive, mottled, upper boundary is marked by a lighter layer	
			2.5Y4/4	clay, olive brown, mottled, gray layer at 845-845.5 cm	
9			5Y4/3(2)	clay, olive, mottled 845-861, weakly mottled at 865-900 cm	
			5Y4/1	clay, dark gray, homogeneous, gradual color change to top unit at 930-920 cm	
			5Y4/2	clay, olive gray (olive at top), mottled	
10			2.5Y5/4	clay, light olive brown, homogeneous	
			5Y4/3	silty sand, olive, fining upwards	
			5Y5/4	clay, olive, mottled	

PS2180-2 (GPC)

Makarov Basin

ARK VIII/3 (ARCTIC 91)

Recovery: 12.96 m

87° 38.6' N, 156° 58' E

Water depth: 3991 m

Depth in core (m)	Lithology	Texture	Color	Description	Age
10			2.5Y5/4	clay, light olive	
			10YR5/4	clay, yellowish brown, mottled	
			5Y4/3	clay, olive, mottled, color changes are gradational	
			2.5Y5/4	clay, light olive brown	
			2.5Y4/4	clay, olive brown, dark small (< 1 mm) specks at 1062-1064 cm, gray layer (N4, 0.5 mm thick) at 1091 cm	
			2.5Y4/2	clay, dark grayish brown, dark specks, streaks between 1102 and 1124 cm, gradational color change to top unit between 1100 and 1090 cm	
			2.5Y4/4	clayey mud, olive brown, mottled, grayish layer at top boundary	
			2.5Y4/2	clayey mud, dark grayish brown, mottled	
			2.5Y4/4	clay, olive brown, mottled	
			2.5Y4/2	sandy mud, dark grayish brown, mottled	
			10YR5/4	clay, yellowish brown, mottled	
			2.5Y5/4	silty mud, light olive brown, laminated	
			2.5Y4/4	sand, olive brown, grayish in the upper part	
			2.5Y4/4	clay, light olive brown, mottled	
			2.5Y4/2	clay, dark grayish brown, lighter mottles	
10YR4/4	clayey mud, dark yellowish brown, mottled				
2.5Y4/2	clayey mud, dark grayish brown, mottled				
13			2.5Y4/4	mud, olive brown, black specks and streaks, faintly laminated	CC
			5Y4/3	sandy mud, olive	
			5Y4/3	clayey mud, olive, dark lenses, disturbed in the lower part, remains of laminae?	
14					
15					

PS2181-3 (GKG)

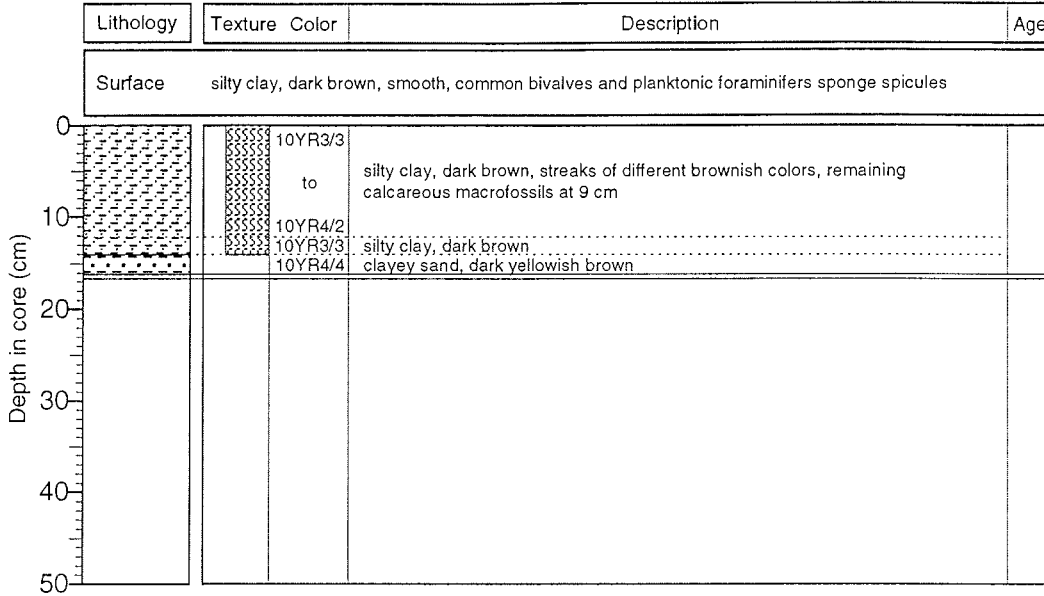
Lomonosov Ridge

ARK VIII/3 (ARCTIC 91)

Recovery: 0.16 m

87° 35.8' N, 153° 22.5' E

Water depth: 3331 m



PS2182-1 (GKG)

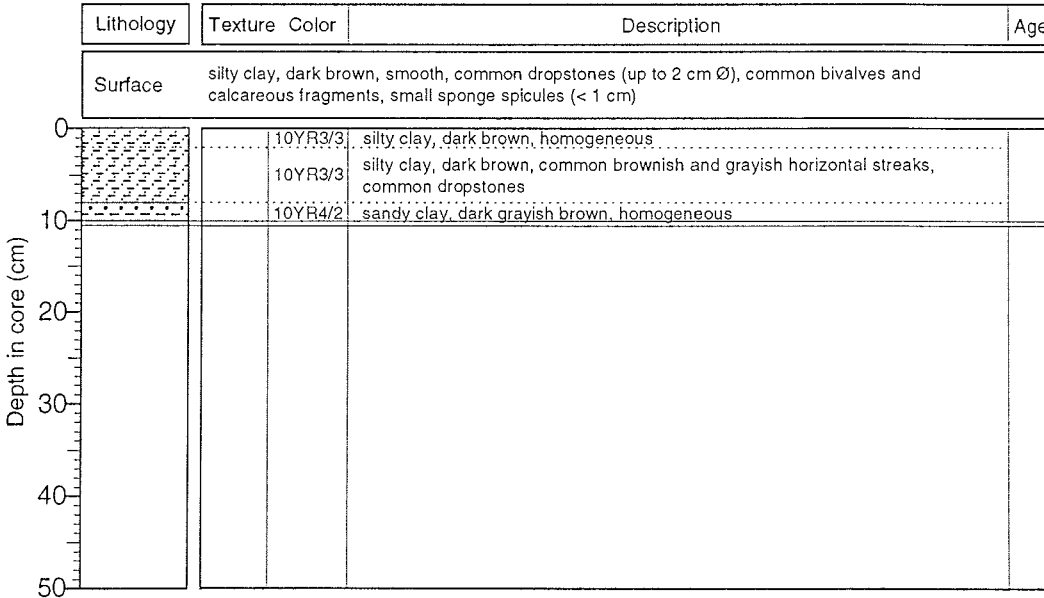
Lomonosov Ridge

ARK VIII/3 (ARCTIC 91)

Recovery: 0.10 m

87° 34.3' N, 151° 7.2' E

Water depth: 2489 m



PS2183-1 (GKG)

Lomonosov Ridge

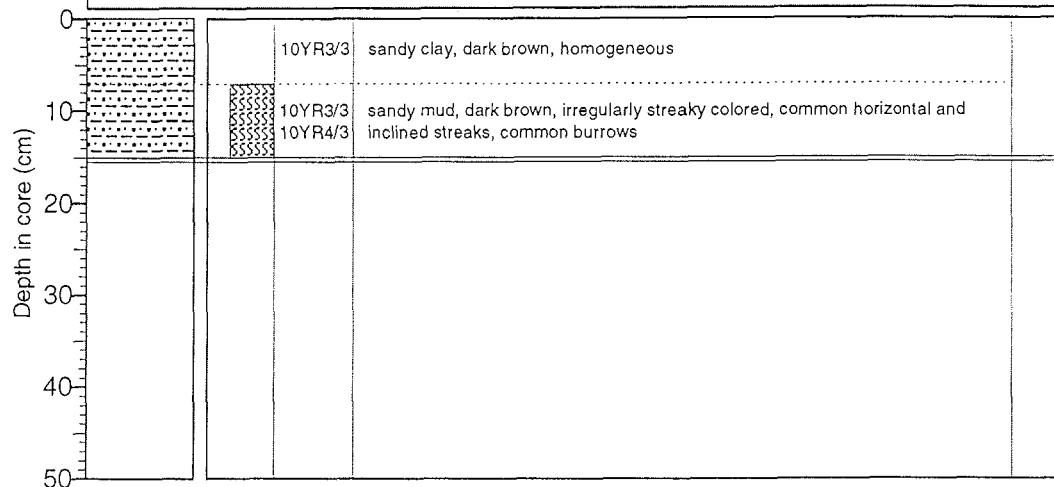
ARK VIII/3 (ARCTIC 91)

Recovery: 0.15 m

87° 36.1' N, 148° 49.8' E

Water depth: 2016 m

Lithology	Texture	Color	Description	Age
Surface			sandy mud, dark brown, abundant dropstones, (up to 8 mm Ø), single calcareous fragments of macrofossils, common planktonic foraminifers and sponge spicules	



PS2184-1 (GKG)

Lomonosov Ridge

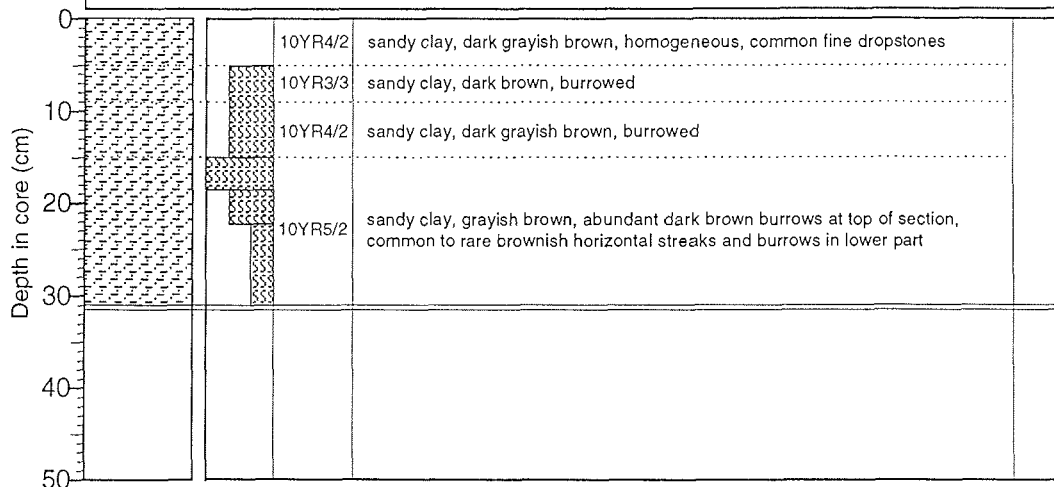
ARK VIII/3 (ARCTIC 91)

Recovery: 0.31 m

87° 36.7' N, 148° 8.4' E

Water depth: 1640 m

Lithology	Texture	Color	Description	Age
Surface			sandy clay, dark grayish brown, scattered small (< 5 mm) dropstones, fragments of calcareous macrofossils	



PS2185-7 (GPC)

Lomonosov Ridge

ARK VIII/3 (ARCTIC 91)

Recovery: 7.38 m

87° 32.3' N, 145° 25.1' E

Water depth: 1069 m

Lithology	Texture Color	Description	Age
0-3 missing			
	10YR3/3	clay, dark brown, mottled, soft	
	10YR3/4	sandy mud, dark yellowish brown, mottled	
	2.5Y4/4	sandy clay, olive brown, frequent mud clasts at 30-72 cm, dark grayish brown in the lower part, mottled at 60-81 cm, stratified at 48-54 cm, gradational color change at 60-70 cm	
	2.5Y4/2		
	2.5Y5/4	clay, light olive brown, mottled	
1	10YR4/3	clay, brown, lenses of olive brown clay, mottled, gradational color change at 103-98 cm, below sandy mud, olive brown, mottled	
	2.5Y4/4		
	10YR4/3	clay, brown to olive brown, lenses of olive brown clay, mottled	
	10YR4/3	clay, dark brown, mottled, upper cm is clay, light olive gray	
	2.5Y5/4	clay, light olive brown, partly laminated, gray lenses	
	10YR4/3	clay, dark brown, mottled	
	2.5Y5/4	sandy mud, light olive, dark brown laminae 159-162 cm, common mud clasts	
	2.5Y5/2	sandy mud, grayish brown, gray lenses in lower part	
	2.5Y5/4	sandy mud, light olive brown, fining upwards, mud clasts at the base	
	2.5Y5/4	mud, light olive brown, mud clasts, upper cm is clay, grayish brown	
2	10YR4/3	clay, dark brown, mottled	
	10YR4/3	clay, dark brown, mottled, upper 2 cm silty clay, light olive brown	
	2.5Y5/4	silty clay to sandy mud, light olive brown, dark spots	
	10YR4/3	clay, dark brown, mottled	
	2.5Y5/4	sandy mud, light olive brown, dark spots, mottled	
	10YR3/3	sandy mud/clay, dark brown, mottled	
	2.5Y5/4	sandy mud, light olive brown, some dark spots	
	10YR4/3	clay/sandy mud, brown, mottled, abundant lighter (2.5Y4/4) lenses and frequent small dark spots	
	2.5Y5/4	sandy mud, light olive brown, mottled	
3	10YR5/4	sandy mud, yellowish brown, mottled, abundant dark spots at 316-322 cm	
	10YR4/3	clay, brown, mottled, frequent dark spots	
	10Y5/5	clay, yellowish brown, mottled	
	10YR4/3	clay, brown, mottled, frequent dark spots	
	2.5Y5/4	sandy mud, light olive brown, dark spots in upper half, color grading to upper unit	
	10YR4/3	clay, brown, mottled, dark spots	
	2.5Y5/4	sandy mud, light olive brown, dark spots, mottled, color grading to upper unit	
4	2.5Y4/4	sandy mud, olive brown, dark spots at 400-402 cm,	
	2.5Y4/4	2 cm: sandy mud, yellowish brown, mottled at base	
	2.5Y4/4	sandy mud, olive brown	
	10YR4/3	clay, brown, mottled, frequent dark spots	
	10YR4/3	clay, brown, dark spots, upper 3 cm is clay, yellowish brown, mottled	
	2.5Y5/4	sandy mud, light olive brown, gradational color change to upper unit	
	10YR4/3	clay, brown, mottled, frequent dark spots at 477-482 cm	
	10YR5/4	sandy mud, yellowish brown, mottled	
5	2.5Y5/4	sandy mud, light olive brown, mottled	
	2.5Y4/4	sandy mud, olive brown, mottled, dark spots	

PS2185-7 (GPC)

Lomonosov Ridge

ARK VIII/3 (ARCTIC 91)

Recovery: 7.38 m

87° 32.3' N, 145° 25.1' E

Water depth: 1069 m

Lithology	Texture	Color	Description	Age
5		10YR4/4	clay, brown, mottled, dark spots	
	*	2.5Y4/4	sandy mud, olive brown, dark spots, mottled, gradational color change to upper unit	
6		10YR4/3	clay, brown, dark spots	
		2.5Y5/4	sandy mud, light olive brown, few dark spots (< 1 cm Ø)	
		10YR4/4		
		2.5Y4/4	sandy mud, olive brown, "clouds" of darker sediments	
	*	(10YR3/1)		<i>sequence between 550-710 cm may be disturbed</i>
7		10YR5/4	sandy mud, olive brown/yellowish brown, "clouds" of darker sediments, small dark spots	
		10YR4/3	clay, brown, mottled	
	*	2.5Y5/4	sandy mud, light olive brown, "clouds" of darker sediments, frequent dark spots	
		2.5Y4/4	sandy mud, light olive brown/olive brown, laminated, darker laminae at 711-715 cm	
		2.5Y5/4		
8				
9				
10				

PS2185-6 (KAL)

Lomonosov Ridge

ARK VIII/3 (ARCTIC 91)

Recovery: 8.20 m

87° 32.2' N, 144° 55.6' E

Water depth: 1052 m

	Lithology	Texture Color	Description	Age
0			10YR3/2-4/3 clayey mud, very dark brown, soft, grading to brown mottled clayey mud	
			10YR3/4 clay, dark yellowish brown, mottled	
			5Y4/3 sandy mud, olive, mottled	gradational color change
			5Y4/3	
			5Y4/2 sandy, silty mud, changing colors (olive to dark yellowish brown), layered,	
			5Y5/6 numerous mud clasts in particular 42-62, 73-106 cm,	
			10YR4/4 thin dark brownish horizons at 45, 82, 97 cm	mud clast
1			5Y4/2 sandy mud, olive gray, mottled	dropstone
			2.5Y4/4 silty mud, olive brown, mottled, homogeneous	
			10YR4/3 sandy mud, fining upwards to silty mud, brown, mottled, slightly lighter towards the base, sharp boundaries	
			10YR3/4 clay, dark yellowish brown, mottled, homogeneous	grading to
			5Y4/4 (silty) clay, olive, mottled, homogeneous	
2			10YR4/3 clay, brown, mottled, homogeneous	
			5Y5/4 silty mud, olive	
			2.5Y4/4 silty mud, olive brown, layered, numerous mud clasts	
			2.5Y5/2 clay bed at 273-280, 292-297 cm	
			2.5Y4/4 dark brownish thin layer at 256 cm	
3			10YR4/3 to 2.5Y4/4 clay, brown, mottled grading into clay, olive brown, mottled	sharp, mottled boundary
			10YR4/3 clay, brown, mottled, lighter horizon 145-150 cm	sandy lense
			2.5Y4/4 clay, olive brown, mottled	
			10YR4/3 clay, brown, mottled	
4			2.5Y4/4 clay, olive brown, mottled	
			10YR4/3 clay, brown, mottled, homogeneous	
			2.5Y4/4 clay, olive brown, mottled	
			10YR4/3 clay, brown, mottled	sharp, mottled boundary
			2.5Y4/4 clay, olive brown, mottled	sandy lense
5				

PS2185-6 (KAL)

Lomonosov Ridge

ARK VIII/3 (ARCTIC 91)

Recovery: 8.20 m

87° 32.2' N, 144° 55.6' E

Water depth: 1052 m

	Lithology	Texture	Color	Description	Age					
5			2.5Y4/4	clay, olive brown, mottled, 505-521 cm slightly darker with dark specks						
						sharp, mottled boundary				
			10YR4/3	clay, brown, mottled						
			2.5Y4/4	clay, olive brown, mottled		sharp, mottled boundary				
			10YR4/2	clay, brown, mottled, color boundary at 538 cm						
			2.5Y5/4	clay, light olive brown, mottled						
			2.5Y5/4	clay, light olive brown, mottled						
			2.5Y5/4	clay, light olive brown, mottled						
			10YR4/3	clay, brown, mottled						
			6				2.5Y4/4	clay, olive brown, mottled, dark specks at 588-598, 605-620, 630-634 cm		
										dark brown laminae
										sand lense
10YR4/3	clay, brown, mottled, slightly lighter horizon 646-649 cm									
10YR5/6	clay, yellowish brown, large darker mottles in upper 4 cm									
10YR4/3	clay, brown, mottled, dark specks 676-688 cm									
2.5Y4/4	clay, olive brown, mottled									
10YR4/3	clay, brown, mottled, dark specks 676-688 cm									
2.5Y4/4	clay, olive brown, mottled	thin dark layer at 742 cm								
10YR4/3	clay, brown, mottled, dark specks 676-688 cm	base of kastenlot								
7					2.5Y4/4		clay, olive brown, mottled			
										core catcher
					base of CC mütze					
8										
9										
10										

PS2186-5 (GKG)

Lomonosov Ridge

ARK VIII/3 (ARCTIC 91)

Recovery: 0.37 m

88° 30.9' N, 140° 29.4' E

Water depth: 2036 m

Lithology	Texture	Color	Description	Age
Surface silty clay, dark grayish brown, smooth, few bivalves and planktonic foraminifers				
		10YR4/2	silty clay, dark grayish brown, homogeneous, common planktonic foraminifers	
		10YR4/3	silty clay, brown, rare horizontal grayish streaks, burrows at top	
		10YR4/2	silty clay, dark grayish brown, homogeneous	
		2.5Y4/4	sandy silty clay, olive brown, burrowed at top	

PS2187-1 (GKG)

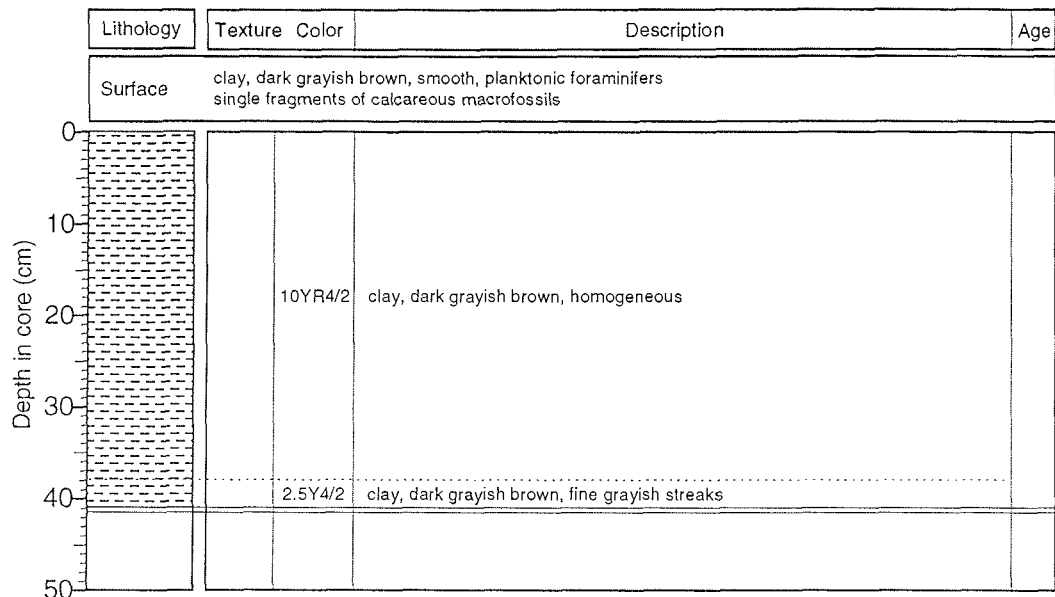
Lomonosov Ridge

ARK VIII/3 (ARCTIC 91)

Recovery: 0.41 m

88° 44.1' N, 126° 51.5' E

Water depth: 3813 m



PS2187-3 (TWC)

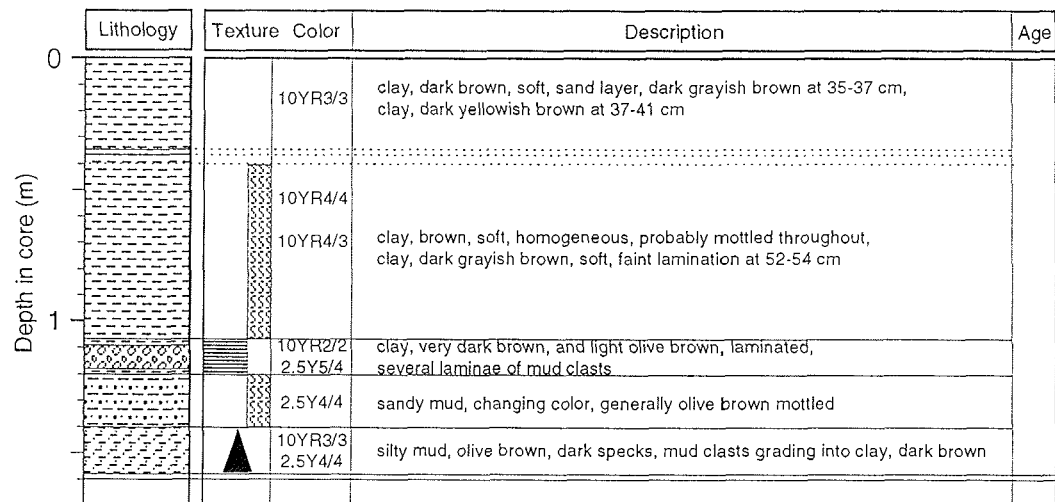
Lomonosov Ridge

ARK VIII/3 (ARCTIC 91)

Recovery: 1.58 m

88° 44.5' N, 126° 52' E

Water depth: 3819 m



PS2187-3 (GPC)

Lomonosov Ridge

ARK VIII/3 (ARCTIC 91)

Recovery: 9.07 m

88° 44.5' N, 126° 51.9' E

Water depth: 3820 m

Lithology	Texture	Color	Description	Age	
0		10YR3/3	clay, dark brown grading into dark grayish brown, homogeneous,		
		10YR4/2			
1		10YR3/2	clay, dark yellowish brown, very homogeneous		
		10YR3/4			
		10YR4/2			
		10YR3/6			
		10YR4/3			
		10YR3/4			
2		10YR4/2-2.5/2	clay, dark grayish brown grading to very dark brown		
		2.5Y4/4		sandy, silty mud, olive brown, homogeneous, slightly layered, numerous mud clasts, fining upwards to clayey mud, coal dropstone at 205 cm	
		2.5Y3/2			
		N3			
		2.5Y4/2			
		2.5Y4/2			
		2.5Y4/3			
		5Y4/3			
		5Y4/4			
		2.5Y4/4			
	2.5Y4/4				
3		2.5Y4/2-4	clay, dark grayish brown/olive brown, laminated		
		10YR5/4			
		10YR4/3			
		10YR5/4			
		10YR3/3			
		10YR3/3			
		10YR4/3			
		10YR4/3			
		10YR5/4			
		10YR3/3			
4		10YR3/3	clay, dark brown to brown to yellowish brown, mottled		
		10YR4/3			
		10YR5/4			
		2.5Y4/4			
		10YB5/4			
5		10YR4/3	clay, brown, mottled, sand lense at 462-465 cm, very dark grayish brown irregular layer at top		
		10YB5/4			
		10YR3/3			

PS2187-3 (GPC)

Lomonosov Ridge

ARK VIII/3 (ARCTIC 91)

Recovery: 9.07 m

88° 44.5' N, 126° 51.9' E

Water depth: 3820 m

Depth in core (m)	Lithology	Texture	Color	Description	Age
5			10YR3/3	clayey sand, dark brown, stratified, mottled, base and top lighter, darker layer at 505 cm, clay layer at 509 cm	
			10YR4/3 10YR3/1	clay and mud/silt, very dark gray, laminated, uppermost part is brown with dark specks, lowermost 2 cm clay and silt, olive gray, laminated	
			5Y4/1	clayey mud, dark gray	
			2.5Y4/4	clay, olive brown, mottled, silt layer at 555 cm	
6			2.5Y4/2		
			10YR5/4-3/3	clay, yellowish brown to dark brown, mud clasts in the upper part	
			10YR5/4	sandy mud, yellowish brown, darker towards base, layered, black lamina at 651 cm	
			2.5Y4/2	sandy mud, dark grayish brown	
			5Y3/1	sandy mud, very dark gray	
			5Y4/2		
			5Y4/3	clay, olive gray to olive, layered and slightly mottled	
7			2.5Y4-5/4	clay, light olive brown/olive brown, mottled, reddish mud clasts at 720-724 cm, varying hue throughout the unit, clay, dark grayish brown, abundant mud clasts at 734-736 cm, layered at 736-750 cm	
			10YR4/4	clay, dark yellowish brown, mottled	
8			2.5Y4/4	clay and sandy mud, olive brown, several mud clasts (1-2 mm Ø), sand lense at 785 cm	
			10YR4/3	clay, layered, varying colors: very dark brown-dark brown-brown-olive brown, mottled, lightest intervals at 818-826, 847-849, 859-867, 878-880, 889-890 cm, very dark interval at 838, 847 cm, sand lense at 853 cm, gradational color change from dark brown to olive brown at 902 cm	
			10YR2.5/2		
			2.5Y4/4		
			10YR3/3		
9					
10					

PS2187-4 (KAL)

Lomonosov Ridge

ARK VIII/3 (ARCTIC 91)

Recovery: 7.57 m

88° 45.3' N, 127° 2.4' E

Water depth: 3908 m

Depth in core (m)	Lithology	Texture Color		Description	Age
0			10YR3/3	clay, dark brown, soft, homogeneous, dark grayish brown at base (2 cm)	
			10YR3/3	clay, dark brown, mottled to 46 cm, dark brown at base (3 cm)	sharp boundary, marked by 2 mm thick laminae of dark yellowish brown
			10YR3/3	clay, dark brown, mottled, layered with grayish colors	
1			10YR4/4	clay, dark yellowish brown, slightly mottled, homogeneous	
			10YR3/3	clay, dark brown, homogeneous	color boundary
2			10YR5/3	clay, brown, mottled, darker specks	color boundary
			10YR2/2 and 2.5Y4/4	clay, very dark brown and olive brown, laminae and beds with sand and mud clasts in clayey matrix	
			2.5Y3/2	sandy mud, very dark grayish brown, mud clasts	transitional boundary
3			2.5Y3/1 N3	sandy mud, very dark gray, slightly layered, sand layer at 318-321 cm	
			5Y4/2	clay, olive gray to olive brown (below 380 cm), some layer of clayey sand with mud clasts at 354-361, 367-372, 388-397 cm	color boundary
4			2.5Y4/4		
			2.5Y3/2	sandy mud, very dark grayish brown, mud clasts	
			10YR4/3	clay, brown, mottled	
			10YR4/2	clay, dark grayish brown	
			2.5Y4/4	clay, olive brown, with reddish brown (5YR5/4) mud clasts (470-480 cm)	
5			10YR4/3	clay, brown, mottled	
			10YR5/4	clay, yellowish brown, frequent mud clasts at 494-497 cm	

PS2189-1 (GKG)

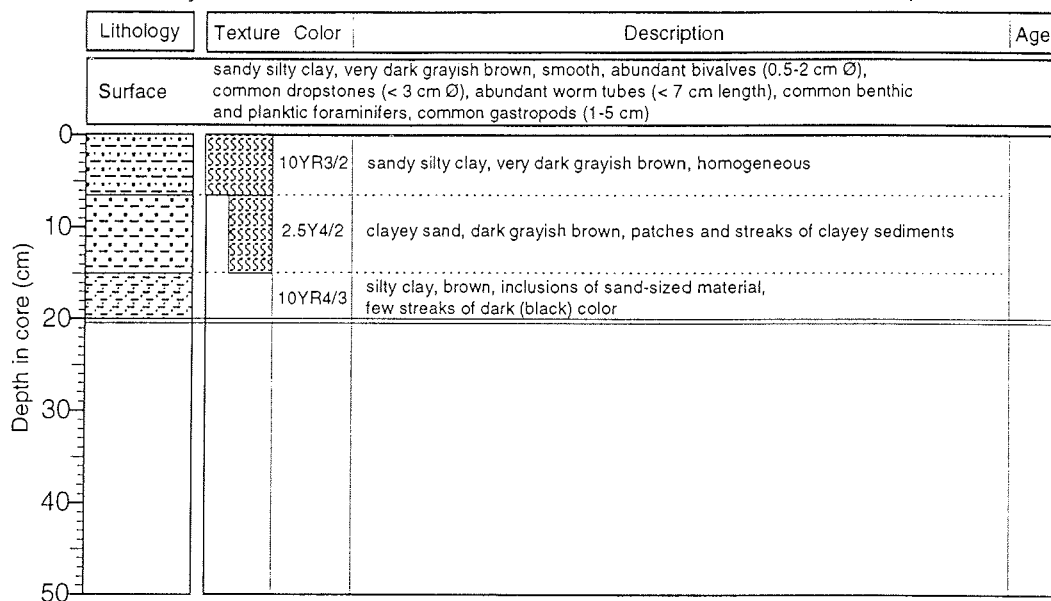
Lomonosov Ridge

ARK VIII/3 (ARCTIC 91)

Recovery: 0.20 m

88° 46.9' N, 144° 33' E

Water depth: 1018 m



PS2189-5 (TWC)

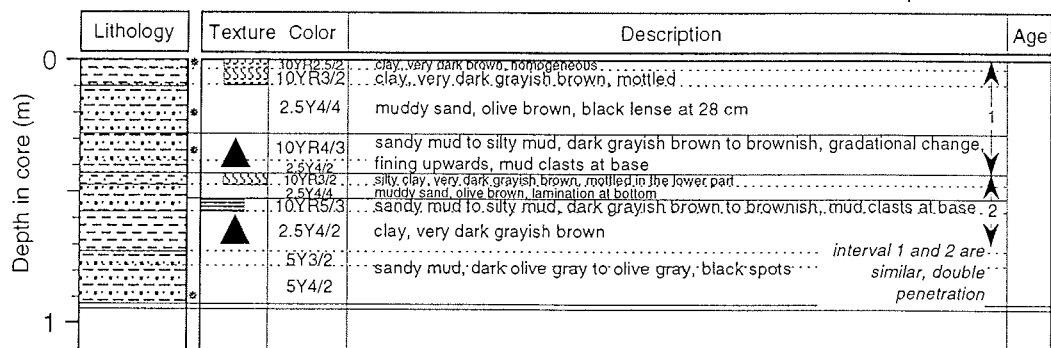
Lomonosov Ridge

ARK VIII/3 (ARCTIC 91)

Recovery: 0.93 m

88° 47.8' N, 144° 0.9' E

Water depth: 1001 m



PS2189-5 (GPC)

Lomonosov Ridge

ARK VIII/3 (ARCTIC 91)

Recovery: 10.35 m

88° 47.8' N, 144° 0.9' E

Water depth: 1001 m

Lithology	Texture	Color	Description	Age
			bag sample	
	▲	2.5Y4/2	sandy mud, dark grayish brown, 30-55 cm common mud clasts (dark grey), fining upwards	
		5Y3/2	muddy fine sand, dark olive gray, black lense at 66 cm, <i>totally disturbed by splitting procedure</i>	
	▲	5Y4/2	sandy mud, olive gray, mud clasts at base, fining upwards	
	▲	5Y4/3	sandy mud to silty mud, olive, fining upwards	
	▲	2.5Y4/4	sandy mud, olive brown, fining upwards, sand layer at base, silty mud at top	
1		10YR4/4	sandy mud, dark yellowish brown, dark brown layer at 102 cm, black layers at 111 and 125 cm, sand lense at 114 cm	
		2.5Y5/4	sandy mud, light olive brown	
	▼	10YR5/4	sandy mud, yellowish brown, several mud clasts (< 0.5 cm Ø), increasing to top and base few dark spots in lower 5 cm, dropstone at 155 cm	
	▲			
2		N3	sandy mud, very dark gray, grayish layer at the lower boundary	
		5Y4/2	sandy mud, olive gray, common mud clasts	
		5Y5/3	sandy mud, olive, sand lenses at upper boundary	
		2.5Y5/4	sandy mud, light olive brown	
		10YR4/4	clay (sandy mud), dark yellowish brown	
3		2.5Y5/4	sandy mud, light olive brown and olive	
		10YR3/3	clay (sandy mud), dark brown, dark spots, mottled	
		2.5Y5/4	sandy mud, light olive brown, mottled	
		10YR4/3	clay/sandy mud, brown	
		2.5Y5/4	sandy mud, light olive brown, few yellowish lenses at 360-364 cm, sandy layer at base	
		10YR4/4	sandy mud, brown, mottled, dark spots, sandy layer at 377 cm	
		2.5Y4/4	sandy mud, olive brown, mottled	
4		10YR4/2	clay, brown, mottled	
		2.5Y5/4	sandy mud, light olive brown, dark specks down to 420 cm, mottled, more brownish at 443-445 cm, irregular and transitional lower boundary	
		10YR4/4	sandy mud, dark yellowish brown	
		2.5Y5/4	sandy mud, light olive brown, dark spots at 467-490 cm, mottled	
5				

section disturbed by flow in!

PS2189-5 (GPC)

Lomonosov Ridge

ARK VIII/3 (ARCTIC 91)

Recovery: 10.35 m

88° 47.8' N, 144° 0.9' E

Water depth: 1001 m

Lithology	Texture	Color	Description	Age
5		2.5Y5/4	sandy mud, light olive brown, very dark layer (more sandy) at 539-540 cm	
		10YR4/4	silty mud, dark yellowish brown, mottled	
6		2.5Y5/4	silty mud, light olive brown, homogeneous, weakly laminated at 578-587 cm	
		10YR4/4	silty mud, dark yellowish brown, mottled	
		2.5Y5/4	silty mud, light olive brown, common small black dots (pyrite?)	
		10YR4/4	silty mud, dark yellowish brown, mottled	
7		2.5Y5/4	silty mud, light olive brown, common small black dots, weakly mottled, in the lower part (668-672 cm) more sandy, dropstone at 671 cm	
		10YR5/4	silty clay, yellowish brown, lower 2 cm light olive brown silty mud	
		10YR4/4	silty mud, dark yellowish brown, homogeneous, in the upper part mottled	
		2.5Y5/4	silty clay, light olive brown, common small black dots, mottled	
		10YR5/4	silty mud, light olive brown to dark yellowish brown, upper darker part mottled	
		2.5Y5/4	silty mud, light olive brown	
		10YR4/4	silty clay, dark yellowish brown, in the upper part strongly mottled	
		2.5Y5/4	silty mud, light olive brown, sandy at base	
		10YR4/4	silty clay, dark yellowish brown, mottled	
		2.5Y5/4	silty mud, light olive brown, few small black dots	
8		10YR5/4	silty clay, dark yellowish brown, mottled	
		2.5Y5/4	silty clay, light olive brown	
		10YR5/4	silty clay, yellowish brown	
		2.5Y5/4	silty mud, light olive brown, slightly mottled/bioturbated, sandy layer at top	
		10YR4/4	silty clay, dark yellowish brown, strongly mottled at top	
		2.5Y5/4	silty mud, light olive brown, slightly mottled, small black dots	
		10YR4/4	silty clay, dark yellowish brown, mottled	
		2.5Y5/4	silty mud, light olive brown	
		10YR4/6	clayey mud, dark yellowish brown, lenses (< 1 cm) of sand at base, dark specks	
		10YR3/3-4/6	clayey mud, dark brown to dark yellowish brown, mottled	
9		10YR4/6-3	clayey mud, dark yellowish to brown, small sand lenses at top	
		10YR4/6-4/9	clayey mud, dark yellowish brown to brown, dark specks	
		2.5Y4/4	sandy mud, olive brown, sandy horizon at 882, 885 cm, dark specks	
		10YR4/3	clayey mud, brown, dark specks, sand lense at 912, sand layer at 919 cm,	
		2.5Y4/4	sandy mud, olive brown at base	
		10YR4/3-4	clayey mud, brown, dark yellowish brown at base, dark specks	
		10YR3/3	clayey mud, brown, mottled	
		2.5Y4/4	clayey mud, sandy clay at top, olive brown, more clayey at 964-966 cm	
10.35		10YR3/3	sandy mud, brown, mottled at 965-970 cm, weakly mottled below, sand lenses at 985-1025 cm, very dark gray	

PS2190-1 (KAL)

Amundsen Basin/North Pole

ARK VIII/3 (ARCTIC 91)

Recovery: 4.27 m

90° N

Water depth: 4275 m

	Lithology	Texture Color	Description	Age
0		10YR4/2	silty clay, dark grayish brown, laminated	
		10YR4/1	silty sand, dark gray	
		2.5Y4/4 2.5Y5/4	erosional boundary silty clay, olive brown, fining upwards, bedded, thin sandy layer towards base clay, light olive brown, nonhomogeneous	
		10YR3/4	clay, dark yellowish brown, mottled, laminated sandy sequence, very dark grayish brown at base	
1		10YR5/4-3/2		
		10YR3/5	clayey mud, dark yellowish brown, laminated	
		10YR4/2	sand, dark grayish brown	
		10YR5/2	clay, dark yellowish brown	
		10YR4/3	sand layer with manganese crusts, dark grayish brown at 117 cm	
		10YR5/2	laminated brown sandy silt, grayish brown, fining upwards into clay	
		10YR5/2 10YR4/3 2.5Y3/2	laminated brown sandy silt, very dark grayish brown, fining upwards into clay, grayish brown	
		1		
		2		
		3		
2		5Y3/1	7 cycles of clay bed (top) and laminae of silty mud (base), very dark gray, silty mud laminae are cross-laminated in many places	
		4		
		5		
		6		
		7		
		2.5Y3/2		
3		5Y2.5/1	silty mud, black, frequent mud clasts (< 2 cm Ø, rounded), biggest mud clasts in the middle of the unit	
		1		
		2		
		3		
		5Y4/2	9 cycles of clay bed (top) and laminae of sandy silt (base), olive gray, very sharp lower boundaries of the individual cycles, internal boundaries are gradational	
		5Y4/3		
		5		
		6		
		7		
		8		
		9		
4		5Y4/3-4	sandy to silty mud, olive, mottled	
		5Y4/3	silty mud, olive, grading downwards into sandy layers	
5				

PS2190-3 (GKG)

Amundsen Basin/North Pole

ARK VIII/3 (ARCTIC 91)

Recovery: 0.35 m

89° 59' N, 84° 44.7' E

Water depth: 4240 m

Lithology	Texture	Color	Description	Age
Surface			clay, dark brown, soft, partly smooth, irregular surface, partly cracked	
		10YR3/3	clay, dark brown, homogeneous	
		5Y4/2	silty clay, olive gray, burrowed	
		5Y5/1	silty clay, gray, homogeneous	
		5Y5/2	clay, olive gray, homogeneous	

PS2190-4 (TWC)

Amundsen Basin/North Pole

ARK VIII/3 (ARCTIC 91)

Recovery: 0.58 m

89° 58.2' N, 96° 29.5' E

Water depth: 4237 m

Lithology	Texture	Color	Description	Age
		10YR3/3	clay, dark brown, very soft, mottled	
		5Y4/3	clay, silty in the lower part, olive, mottled	<i>core is probably repeated at the sharp boundary at 21 cm</i>
		10YR3/3	clay, dark brown, very soft, mottled	
		5Y4/3	clay, silty in the lower part, olive, mottled	
		2.5Y3/2	clayey sand, very dark grayish brown, 5 mm thick lamina at upper boundary	

PS2190-4 (GPC)

Amundsen Basin/North Pole

ARK VIII/3 (ARCTIC 91)

Recovery: 12.93 m

89° 58.2' N, 96° 29.5' E

Water depth: 4237 m

Depth in core (m)	Lithology	Texture Color		Description	Age
0		10YR3/3		clay, dark brown, soft, homogeneous	strongly disturbed
		5Y4/3		clay, olive, soft, mottled, upper boundary gradational	
	▲	2.5Y4/4		silty sand, olive brown, graded	
		2.5Y4/4		clay, olive brown, soft, dark brown layer at 62-65 cm, mottled in upper part	
	▲	2.5Y4/4		sand, olive brown, graded	
1		10YR4/3		clay, dark yellowish brown and brown mottled, olive brown at base, grading up	
		10YR4/3		clay, brown, soft, mottled	
		10YR4/4		clay, dark yellowish brown, grading upwards	
		10YR3/3		clay, dark brown, soft, mottled	
		2.5Y5/4		clay, light olive brown, soft, brown spots	
		10YR3/3		silty clay, dark brown, disturbed	
		10YR5/0		silty mud grading into clay, yellowish brown, mottled	
2	▲	2.5Y5/4		silt, laminated, grading into clay, light olive brown, mottled	
		2.5Y5/4		s.a.a.	
	▲	2.5Y5/4		s.a.a.	
		2.5Y5/4		s.a.a.	
	▲	2.5Y5/4		clay, light olive brown, brown specks	
		2.5Y5/4		s.a.a.	
	▲	2.5Y5/4		s.a.a.	
		2.5Y5/4		s.a.a.	
	▲	2.5Y4/4		s.a.a.	
		5Y3/2		s.a.a.	
3		5Y3/2		clay, dark olive gray, homogeneous	
	▲	5Y3/2		silty sand, fining upwards	
		5Y3/2		silt, dark olive gray, laminated	
	▲	2.5Y5/4		sandy mud, dark olive gray	
		5Y3/1		sandy mud, very dark gray, frequent mud clasts (< 3 cm Ø)	
4		5Y3/2		silty mud, dark olive gray, grading into clay, laminated at base	
	▲	5Y3/2		s.a.a.	
		5Y4/2		clay, dark grayish brown, mottled	
	▲	5Y3/2		silt, very dark grayish brown, grading upwards into	
		5Y4/2		s.a.a.	
	▲	5Y4/2		s.a.a.	
		5Y3/2		s.a.a.	
	▲	5Y4/2		s.a.a.	
		5Y3/2		s.a.a.	
5		5Y3/2		s.a.a.	

PS2190-4 (GPC)

Amundsen Basin/North Pole

ARK VIII/3 (ARCTIC 91)

Recovery: 12.93 m

89° 58.2' N, 96° 29.5' E

Water depth: 4237 m

Lithology	Texture	Color	Description	Age
5		5Y3/2	s.a.a.	
		5Y3/2	sandy mud, very dark grayish, clay layers at 521-520, 525-526, 523-524 cm	
		2.5Y4/4	clay, olive brown, mottled	
		2.5Y4/2	sandy mud, very dark grayish, mottled in the upper part	
6		2.5Y4/2-4	silt, dark grayish brown, grading upwards into clay, olive brown, mottled	
				sequence of turbidites as described above
7		5Y4/1		
8		5Y4/1	sandy mud, dark gray	
		5Y4/2	silt, very dark gray, grading upwards into clay, olive gray	
		5Y3/1		
		N4	silt, olive brown, grading into clay, dark grayish brown and dark gray, mottled clay on top	
		2.5Y4/4	sandy mud, olive brown	
		2.5Y4/2	clay, dark grayish brown, laminated	
		10YR4/6	silt, dark yellowish, laminated	
9		2.5Y4/2	clay, dark grayish brown, laminated	
		2.5Y4/4	silt/clay, olive brown, laminated	
		2.5Y4/2	silt, dark grayish brown, grading upwards into mottled clay	
				sequence of turbidites
10		2.5Y4/4		
		2.5Y4/2		
		2.5Y4/4	sandy mud, olive brown, 1 cm thick black layer at 972 cm	
		10YR4/3	sandy mud, brown, several black layers/bands	

PS2190-4 (GPC)

Amundsen Basin/North Pole

ARK VIII/3 (ARCTIC 91)

Recovery: 12.93 m

89° 58.2' N, 96° 29.5' E

Water depth: 4237 m

Depth in core (m)	Lithology	Texture	Color	Description	Age
10		▲	2.5Y4/2	silt, dark grayish brown, grading upwards into mottled clay	
		▲			
		▲	2.5Y4/4	sequence of turbidites	
		▲	2.5Y4/2		
		▲	2.5Y4/2		
11		▲	5Y4/2		
		▲	2.5Y4/2	clay, dark grayish brown, mottled, pinkish 1-2 mm large clasts	
		▲	2.5Y4/4	turbidite, s.a.a.	
		▲	2.5Y4/2	clay, dark grayish brown, mottled	
		▲	2.5Y4/4-2	clay/silt, olive brown and dark grayish brown, laminated	
		▲	10YR4/4	turbidite	
		▲	10YR4/4	turbidite	
		▲	5Y4/3		
12		▲	2.5Y4/2	turbidite	
		▲	2.5Y4/2	silty mud, dark grayish brown	
		▲	10YR4/4	turbidite	
		▲	10YR3/3	sandy mud, dark brown, mottled	
		▲	10YR4/4	sandy mud, brown	
		▲	10YR4/4	sandy mud, olive brown, mud clasts, grading upwards into brown clay with mud clasts	
		▲	2.5Y4/4	clay, olive brown, some black specks	
		▲	2.5Y4/4	sandy mud, olive brown, mud clasts	
		▲	10YR4/4	sand, olive brown, grading upwards into dark yellowish brown mottled clay	
		▲	2.5Y4/4		
		▲			
		▲		sequence of turbidites as described above	
		▲			
13					
14					
15					

PS2192-1 (GKG)

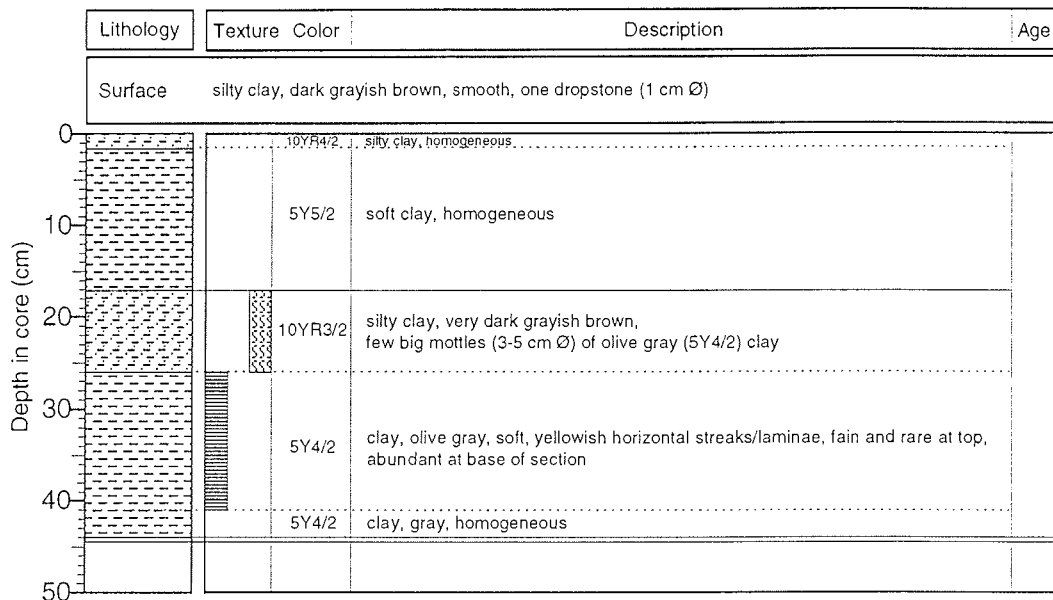
Amundsen Basin

ARK VIII/3 (ARCTIC 91)

Recovery: 0.44 m

88° 15.7' N, 9° 52.7' E

Water depth: 4375 m



PS2193-2 (GKG)

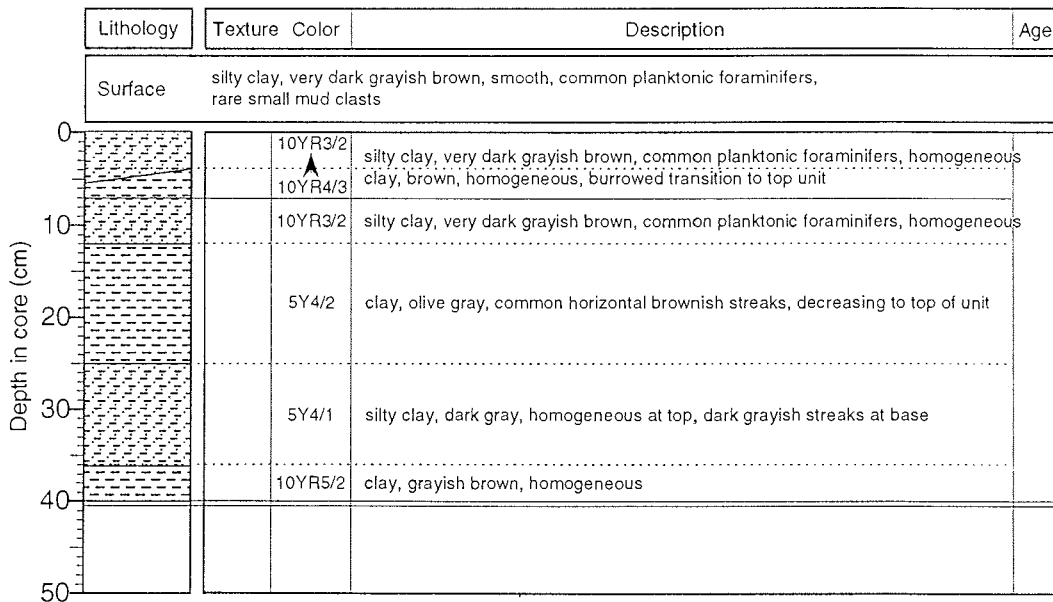
Amundsen Basin

ARK VIII/3 (ARCTIC 91)

Recovery: 0.40 m

87° 31.1' N, 11° 15.5' E

Water depth: 4337 m



PS2194-1 (GKG)


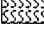
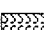
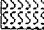
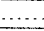
Amundsen Basin

ARK VIII/3 (ARCTIC 91)

Recovery: 0.20 m

86° 35.6' N, 7° 29.3' E

Water depth: 4326 m

Lithology	Texture Color	Description	Age	
Surface silty clay, dark grayish brown, smooth, soft, common planktonic foraminifers, few small dropstones and mud clasts, <i>core partly cracked by coring</i>				
Depth in core (cm) 0 10 20 30 40 50		10YR4/2	silty clay, dark grayish brown, homogeneous,	
		10YR4/3	clay, brown, homogeneous, burrowed transition to top unit	
		10YR4/2	silty clay, dark grayish brown, homogeneous,	
		10YR4/3	clay, brown, homogeneous,	
		5Y4/2	silty clay, dark grayish brown, homogeneous,	

PS2195-4 (GKG)

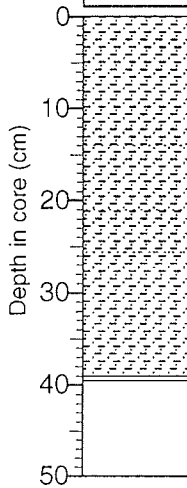
Amundsen Basin

ARK VIII/3 (ARCTIC 91)

Recovery: 0.39 m

86° 13.7' N, 9° 35.6' E

Water depth: 3873 m

Lithology	Texture	Color	Description	Age
Surface silty clay, dark brown, smooth, common bivalves and planktonic foraminifers				
	10YR3/3		silty clay, dark brown, homogeneous, common faint horizontal gray streaks in lower part	
	5Y4/2		silty clay, olive gray, faint brownish horizontal streaks	
	10YR4/4		silty clay, dark yellowish brown, homogeneous	
	10YR4/2		silty clay, dark grayish brown, homogeneous	

PS2195-3 (TWC)

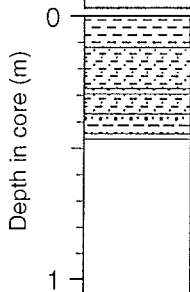
Amundsen Basin

ARK VIII/3 (ARCTIC 91)

Recovery: 0.45 m

86° 14.2' N, 9° 41' E

Water depth: 3966 m

Lithology	Texture	Color	Description	Age
	10YR3/3		clay, dark brown, slightly mottled	
	2.5Y4/2		clayey mud, dark grayish brown	
	10YR4/2		clayey mud, dark grayish brown	
	2.5YR4/2		silty sand, dark grayish brown	
	10YR3/6		clayey mud, dark grayish brown	
			2.5Y4/2 sandy mud, dark grayish brown, mud clasts	

PS2195-3 (GPC)

Amundsen Basin

ARK VIII/3 (ARCTIC 91)

Recovery: 9.59 m

86° 14.2' N, 9° 41' E

Water depth: 3966 m

Lithology	Texture	Color	Description	Age
		10YR3/3	clay, dark brown, slightly mottled	
		2.5Y4/2 10YR4/2	clayey mud, dark grayish brown grading upwards into lighter color	
		10YR3/6	clayey-sandy mud, dark grayish-yellowish brown	
		10YR4/3	silty mud, brown	
		10YR4/4	sandy mud, dark yellowish brown	
		10YR4/4	sandy and silty mud, dark yellowish brown, slight changes of grain size, numerous mud clasts	
		10YR3/3	silty mud, dark brown	
		10YR3/1	clayey mud, very dark gray, mud clasts, brownish laminae at top, 2 sand lenses at 132-140 cm	
		2.5Y4/2	sandy and silty mud, dark grayish brown, grading upwards into clayey mud, slightly layered due to textural changes	core disturbed
		2.5Y4/3	sandy mud, very dark gray	
		2.5Y3/2	sandy to silty mud, very dark grayish brown, mud clasts, mottled, slight color changes suggest faint layering, brown lamina at 304 cm	
		2.5Y3/2 2.5Y1/3	silty mud, brown, mud clasts silty mud, very dark gray, grading upwards into	
		2.5Y4/2	clayey to silty mud, dark grayish brown, homogeneous	
		10YR4/2	silty mud, dark grayish brown, slightly layered, in parts mottled, few mud clasts	
		10YR4/3 10YR4/2	sand, dark grayish brown, clayey mud, brown on top	
	10YR4/3	sandy to silty mud, brown to dark brown, mud clasts, thin sand layer at 429 cm		
	10YR4/6	silty mud, dark yellowish brown		
	10YR3/4	silty mud, dark yellowish brown, sandy layers at 495-465 cm, speck of coaly material (1 cm Ø) at 469 cm		
	2.5Y4/4	clayey mud, olive brown		

PS2195-3 (GPC)

Amundsen Basin

ARK VIII/3 (ARCTIC 91)

Recovery: 9.59 m

86° 14.2' N, 9° 41' E

Water depth: 3966 m

	Lithology	Texture	Color	Description	Age
5			2.5Y4/4	clayey mud, olive brown, layering indicated by slight color changes, thin sandy layer at 506 cm, overlain by 2-3 cm mud, grayish	↑ core disturbed ↓
			10YR3-4/3	sandy-silty mud. (dark) brown	
6			10YR3/2	silty mud, very dark grayish brown, some sandy layers, dark speck at 569 cm	
			10YR3/4	silty mud, sand layers (11x at 610-593), dark yellowish brown, grading upwards in finer material	
			10YR2.5/2	silty mud, very dark brown, thin sandy mud horizons	
			10YR4/2	silty mud, dark grayish brown, slight color changes indicate layering, sand layer at 628-629 cm	
			2.5Y4/2	silty mud, dark grayish, silty mud and sand lenses at 650-570 cm	↑ core disturbed ↓
	2.5Y4/2	silty mud, dark grayish brown, sand layer at 685-684, 677-679 cm			
7			2.5Y4/2	silty mud, dark grayish brown, homogeneous, uppermost part slightly layered due to color changes	
			2.5Y4/2	sand grading into silty and clayey mud, gradual color change	
			10YR4/4		
			saa		
			saa		
			saa		
			saa		sequence of turbidites
	saa				
8			2.5Y4/2	sandy to silty mud, very dark grayish brown, sand layers, color changes indicate layering	
			2.5Y3/2		
			10YR2.5/2		
			10YR2.5/2		sandy mud, very dark brown to very dark gray, sand layers (15x, 3-5 mm thick)
			10YR3/2		
			N3		
	2.5Y4-3/2	silty mud, very dark grayish brown, grading into dark grayish brown clayey mud			
	2.5Y4/2	silty mud, dark grayish brown, mud clasts (pinkish gray, 7.5YR6/2), slightly layering of color changes			
9					
10					

PS2196-2 (GKG)

Amundsen Basin

ARK VIII/3 (ARCTIC 91)

Recovery: 0.28 m

85° 57.1' N, 0° 6.9' E

Water depth: 3958 m

Lithology	Texture	Color	Description	Age
Surface silty clay, dark grayish brown, soft, smooth, common planktonic foraminifers				
	10YR4/2		silty clay, dark grayish brown, homogeneous,	
	5Y4/3		silty clay, olive, homogeneous,	
	10YR4/2		silty clay, dark grayish brown, homogeneous,	

PS2197-1 (KAL)

Amundsen Basin

ARK VIII/3 (ARCTIC 91)

Recovery: 8.96 m

85° 46' N, 4° 8.5' W

Water depth: 4154 m

	Lithology	Texture	Color	Description	Age
0	[Pattern]	[Pattern]	10YR4/4 10YR3/3	clay, separated in layers by thin laminae of silty mud, dark yellowish brown grading upwards to dark brown	
			10YR4/4	clay, dark yellowish brown, stratified, each layer is 3-10 cm thick, underlain by a sand layer, olive brown, (39-40, 63-65, 83, 90 cm)	
1	[Pattern]	[Pattern]	10YR4/2-4	clay, dark yellowish brown and dark grayish brown	
			10YR4/3	clay, brown, layer (1-10 cm thick) separated by silt laminae (0.5-1 cm thick)	
	[Pattern]	[Pattern]	5Y4/3 10YR4/3	clay, olive and brown layers, mottled, silt laminae at 159, 160 cm	
2			10YR4/3	clay, brown, with silt layers (0.1-1 cm thick), silt layers at: 171, 178-179, 180-181, 183-183.5, 199, 204, 208, 211, 217, 219, 231-232, 238, 242, 243, 246, 256 cm, several thin clay layers of grayish color	
	[Pattern]	[Pattern]	10YR3/4 10YR4/4	clay, dark yellowish brown (top), reddish (base), silt laminae at 258, 280-281 cm, slightly mottled	
3			10YR4/4 2.5Y4/2 10YR3/2 2.5Y4/2	dark yellowish brown dark grayish brown very dark grayish brown dark grayish brown	clay, layered with silt laminae at 283, 284, 286, 296, 306, 308 cm, slightly mottled at 297-305, 310-323 cm
	[Pattern]	[Pattern]	10YR4/3	clay, brown, 2-3 cm thick, separated by silt laminae	
	[Pattern]	[Pattern]	10YR5/4	clay, yellowish brown, 2-5 cm thick, separated by silt layers 0.5-1 cm thick	
	[Pattern]	[Pattern]	2.5Y5/2	sandy mud, grayish brown, black laminae on top	
	[Pattern]	[Pattern]	10YR5/4	clay, yellowish brown, silt layer at 364-364.5 cm, sharp boundaries	
	[Pattern]	[Pattern]	10YR4/2	silty mud, dark grayish brown, mottled, clay layers at 383-383.5, 384-384.5, 386-388, 389-390, 394-395, 395.5-396 cm, color of clay layers is 10YR5/4	
4	[Pattern]	[Pattern]	10YR3/2	silty mud, very dark grayish brown, clay layers, dark grayish brown at 414-415, 416-418, 418-419 cm	
	[Pattern]	[Pattern]	10YR4/4	clay, dark grayish brown, silt layers at 423-424, 441-442, 455, 458, 492, 498-499, numerous small color changes with sharp upper boundaries, slightly mottled 440-450, 460-483 cm, dark grayish brown silty layer at 498-500 cm	
5	[Pattern]	[Pattern]			

PS2197-1 (KAL)

Amundsen Basin

ARK VIII/3 (ARCTIC 91)

Recovery: 8.96 m

85° 46' N, 4° 8.5' W

Water depth: 4154 m

	Lithology	Texture	Color	Description	Age
5			s.a.a.		
			2.5Y4/2	sandy mud, dark grayish brown	
			10YR3/2	sandy mud, very dark grayish brown, few mud clasts, gradational color change	
			2.5Y4/2	clay, dark grayish brown	
			2.5Y4/4	clay, olive brown, silty mud layer at 545-547 cm, gradational color change to top	
			2.5Y4/4	silty mud, olive brown, common mud clasts at 562-575 cm	
			2.5Y3/2	silty mud, very dark grayish brown	
6					
7			10YR4/2	clay, dark grayish brown, 5-20 cm thick with thin silt layers mostly at: 611-612, 621-622, 625, 635-636, 644-647, 676-677, 684-685, 701-703, 732, 736, 756-757, 765-772, 778, 787-789, 809-810, 816 cm, mottled at 724-726, 737-748 cm	
8			2.5Y4/4	sandy mud, olive brown	
			10YR5/3	clay, brown	sandstone, red, rounded, striated
			5Y5/2	clay, olive gray	
			2.5Y5/4	clay, light olive brown, silt layer at 851-852 cm	
9			10YR5/4	clay, yellowish brown, nearly homogeneous, silt layers at 880, 885, 888, 893 cm	
10					

PS2197-4 (GPC)

Amundsen Basin

ARK VIII/3 (ARCTIC 91)

Recovery: 10.11 m

85° 44.8' N, 4° 22.7' W

Water depth: 4115 m

Lithology	Texture	Color	Description	Age
		2.5Y4/2	clay, dark grayish brown, soft	
		10YR3/3		
		10YR4/4		
		10YR4/4		
		10YR4/4		clay, dark yellowish brown, dark brown at 7-13, 29-33 cm, grayish brown at 80-83 cm, silty layers at 59-69, 79, 89, 92 cm
		10YR5/3		silt, brown
		10YR4/4		clay, dark yellowish brown, soft, darker laminae at 142, 143.5 cm, silt lamina at 139 cm
		10YR3/3		clay, brown, soft, silt lamina at 169, grayish brown at 169-171 cm
		10YR4/4		clay, dark yellowish brown (reddish hue), olive brown at 232-235 cm, soft, silt laminae at 187, 190, 194, 257, 273, 279, 283 cm, stratified, slight color change grading upwards to olive brown
		10YR4/4		clay, dark yellowish brown, slight changes in color to olive brown, dark grayish brown at 372-377 cm, stratified, slightly mottled, silt layers at 324, 331, 356, 365, 367, 370, 372, 377, 386, 396 cm
		10YR4/3		clay, dark grayish brown to brown, mottled
		10YR4/4		clay, dark yellowish brown, stratified, thin silt laminae, mottled
	2.5Y4/2		clay, dark grayish brown, mottled, silt layers at 451, 456 cm	
	10YR3/3-4		clay, brown and dark yellowish brown, stratified, mottled, silt layer at 467-469 cm	
	2.5Y4/4		clay, olive brown	
	10YR4/4		clay, dark yellowish brown, silt laminae, mottled, <i>see below</i>	

PS2197-4 (GPC)

Amundsen Basin

ARK VIII/3 (ARCTIC 91)

Recovery: 10.11 m

85° 44.8' N, 4° 22.7' W

Water depth: 4115 m

	Lithology	Texture	Color	Description	Age									
5				10YR4/4	clay, dark yellowish brown (reddish hue), stratified, separated by thin beds/laminae of silt at 491, 496, 501, 504, 506, 515, 517, 525, 529 cm, mottled									
				2.5Y4/4	clayey mud, olive brown, mud clasts									
				10YR4/4	clay, dark yellowish brown, stratified									
				2.5Y4/4	clayey mud, olive brown, mud clasts, clay layers at 553, 559, 561 cm									
				10YR3/1	silty mud, very dark gray									
				6				10YR4/2	clay, dark grayish brown, stratified, mottled in the upper part, very dark laminae to silty mud at 502-504 cm, silt laminae at 604, 625, 627, 660 cm, dark grayish brown laminae at 600 cm					
								2.5Y4/2	sandy mud, dark grayish brown, mud clasts in the lower part					
								10YR3/1	silty mud, very dark gray					
								5-10YR4/2	clay, dark grayish brown, grading upwards to olive, mottled					
								2.5Y4/2	silty mud, dark grayish brown, mud clasts					
7								10YR3/1	silty mud, very dark gray, mud clasts					
								10YR4/2	clay, stratified, dark grayish brown, silt layers at 751, 758, 761, 765, 769, 774, 775, 787 cm					
								10YR4/4 and 2.5Y4/4	clay, dark yellowish brown and olive brown, silt laminae, sand layer at 847-857 cm, mottled weakly					
								5Y4/2	silty mud, olive gray					
								8				10YR4/4	clay, dark yellowish brown, stratified, layers 2-5 cm thick, weakly mottled	
				5Y4/1	clay, dark gray, mottled									
				10YR4/3	clay, brown, silty at base, laminated									
				10YR4/4	1000-1011 cm: clay, dark yellowish brown, silty layer									
				9										
10.11														

PS2198-1 (GKG)

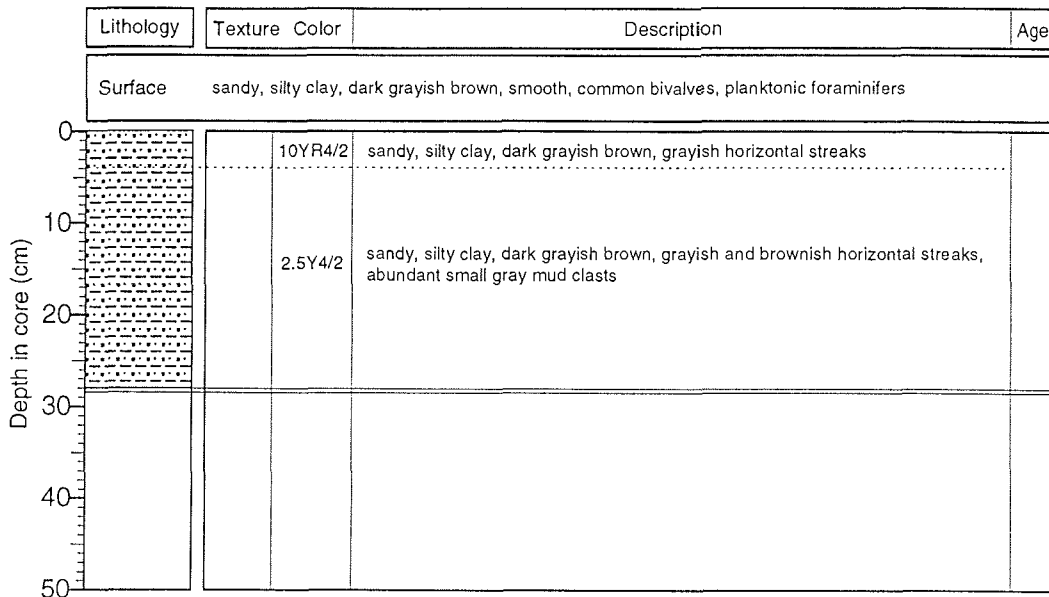
Morris Jesup Rise

ARK VIII/3 (ARCTIC 91)

Recovery: 0.28 m

85° 33.9' N, 9° 3.5' W

Water depth: 3767 m



PS2199-4 (GKG)

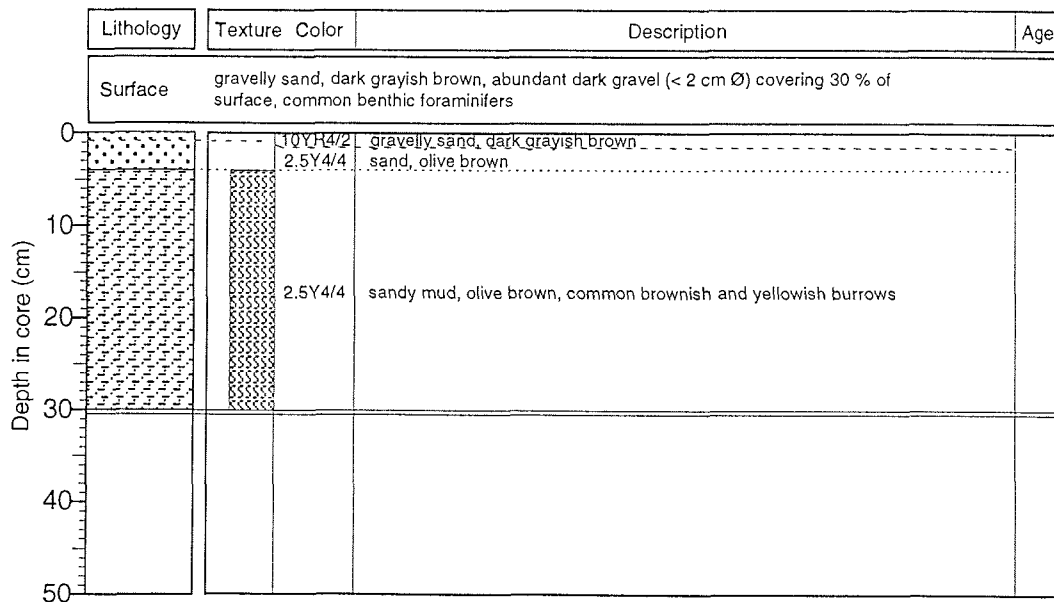
Morris Jesup Rise

ARK VIII/3 (ARCTIC 91)

Recovery: 0.30 m

85° 25.9' N, 11° 56.3' W

Water depth: 1614 m



PS2200-5 (KAL)

Morris Jesup Rise

ARK VIII/3 (ARCTIC 91)

Recovery: 7.70 m

85° 19.4' N, 14° W

Water depth: 1073 m

Lithology	Texture	Color	Description	Age
0	*	10YR3/3	silty clay, dark brown, mottled	
				sand lense at 7-10 cm
1	*	2.5Y4/4	silty mud, olive brown, frequent mud clasts, abundant at 26-28, 35-36, 46 cm, mottled at top and at 40-55 cm	
		2.5Y3/2	sandy mud, very dark grayish brown, laminated	
		2.5Y4/2	clayey mud, dark grayish brown	
		2.5Y4/4	sandy mud, olive brown, dark specks at 70-88 cm, weakly mottled, gradational color changes to upper and lower unit	black dropstone at 80 cm
		2.5Y3/2	silty mud, very dark grayish brown	
		2.5Y4/2	clayey mud, dark grayish brown	
		2.5Y4/4	clayey mud, olive brown, mottled	
		5Y4/3	clayey mud, olive, mottled	
		5Y4/4	clayey mud, olive	calcareous concretions at 137-139 cm
		2.5Y4/4	sandy mud, olive brown, fining upwards, mottled	
2	*	10YR5/3	clay, brown, mottled	
		10YR4/3	gradational color changes	
		10YR5/3	sandy mud, brown, mud clasts at 196-233 cm	
		10YR5/2	clay, grayish brown	dropstone at 233 cm
		2.5Y4/4	sandy mud, olive brown, frequent mud clasts at 245-259 cm	
		10YR5/2	silty mud, grayish brown	
		2.5Y4/4	sandy mud, olive brown, mud clasts	
		10YR5/2	silty mud, grayish brown	
		2.5Y5/4	silty mud, light olive brown, calcareous silt, diagenetically consolidated, light brownish gray (2.5Y6/2) at 310 cm	
		2.5Y4/4	sandy mud, olive brown, mud clasts	
3	*	2.5Y5/4	sandy mud, light olive brown	
		2.5Y5/4	sandy mud, light olive brown	
		2.5Y4/2	silty mud, dark grayish brown	
		2.5Y5/2	silty mud, grayish brown	
		2.5Y4/4	clayey mud, olive brown, mottled	
		2.5Y5/4	clayey mud, light olive brown, mottled	
		2.5Y4/4	clayey mud, olive brown, mottled	
		2.5Y5/4	sandy mud, light olive brown, fining upwards, dropstones and mud clasts at 413-420 cm	
		10YR3/3	silty mud, dark brown	
		2.5Y4/4	silty mud, olive brown	
4	*	10YR5/2	clay, grayish brown	
		2.5Y5/4	sandy mud, light olive brown, sandy layer at 462-458 cm	
		10YR5/3	clay, brown, mottled	dropstone at 492 cm
5				

PS2200-5 (KAL)
Recovery: 7.70 m

Morris Jesup Rise
85° 19.4' N, 14° W

ARK VIII/3 (ARCTIC 91)
Water depth: 1073 m

Lithology	Texture	Color	Description	Age
5		2.5Y5/4	clay, light olive brown, mud clasts at 513-515, 517-520 cm	
		2.5Y5/4	clay, light olive brown	
		2.5Y5/4	clay, light olive brown, dark specks at 540-552 cm, sand lense at 538 cm	
		10YR4/3	clay, brown, mottled	
6		2.5Y5/4	silty mud, light olive brown, more brownish at 586-605 cm, mud clasts and ice rafted debris at 629-632 cm, dark specks throughout, sand layer at 630 cm	
		2.5Y5/4	silty mud, light olive brown	
7		2.5Y5/4	silty mud, light olive brown	CC: 698-749 cm
		2.5Y5/4	silty mud, light olive brown	mütze: 749-770 cm
8				
9				
10				

PS2200-6 (GPC)

Morris Jesup Rise

ARK VIII/3 (ARCTIC 91)

Recovery: 5.85 m

85° 19.2' N, 13° 52.3' E

Water depth: 1087 m

	Lithology	Texture Color	Description	Age
0		10YR3/3	clay, dark brown	
		2.5Y4/4	silty mud, olive brown grading upwards into brown, frequent mud clasts, mottled at top silty mud, very dark grayish brown at 38-36 cm	
		2.5Y4/4	sandy mud, olive brown, dark specks at 52-64 cm, clay, grayish brown at 39-38 cm, silty mud, very dark grayish brown at 63-64 cm	
		5Y5/3	clayey mud, olive, mottled, clay, gray, with foraminifers at 66-64 cm	
		2.5Y4/4	sandy clay, olive brown, bioturbated with infill of sediments of the overlying unit	
1		2.5Y5/4	clay, light olive brown, sandy mud mottles	
		2.5Y4/4	sandy clay, olive brown, mottled	
		2.5Y5/4	clay, light olive brown, mottled	
		2.5Y4/4	sandy mud, olive brown, mottled, calcareous concretion at 135-131 cm	
		10YR5/4	clay, yellowish brown, mottled	
		2.5Y4/4	sandy mud, olive brown, mottled	
		10YR5/4	sandy clay, yellowish brown/ clay, light olive brown, forams at 170-172 cm	
2		2.5Y4/4	sandy mud, olive brown	
		2.5Y5/4	clay, light olive brown, mottled, dark specks throughout	
		10YR4/3	silty clay, brown, mottled	
		2.5Y4/4	sandy mud, olive brown	
		2.5Y4/4	silty clay, olive brown/ silty clay, brown, mottled at 238-236 cm	
		10YR4/3	silty clay, brown, mottled	
3		2.5Y4/4	silty clay/sandy mud, olive brown, brown layer at 312-313, 322-323 cm	
		2.5Y4/4	sandy mud, olive brown	
		2.5Y4/4	clay, olive brown, dark specks, grayish layer at top	
		10YR4/3	clay, brown, mottled	
		2.5Y4/4	clay, olive, mottled?	
4		10YR4/3	sandy clay, brown, dark and olive brown specks, mottled	
		5YR4/4	sandy mud, reddish brown	
		10YR4/3	clay, brown, dark olive brown specks, mottled	
		2.5Y5/4	clay, light olive brown	
		2.5Y4/4	clay, olive brown, dark specks /clay, brown at top 1 cm	
		10YR4/3	clay, brown, dark specks, lighter spots, mottled	
5		2.5Y4/4	silty clay, olive brown, dark specks, dropstone at 469 cm	

PS2200-6 (GPC)

Morris Jesup Rise

ARK VIII/3 (ARCTIC 91)

Recovery: 5.85 m

85° 19.2' N, 13° 52.3' E

Water depth: 1087 m

Lithology	Texture	Color	Description	Age
		2.5Y4/4	silty clay, olive brown, dark specks	
		10YR4/3 2.5Y4/4	clayey mud, brown and olive brown (base), some dark specks, weakly mottled, gradual color change	
		s.a.a.		
		s.a.a.		
		s.a.a.		

PS2200-6 (TWC)

Amundsen Basin

ARK VIII/3 (ARCTIC 91)

Recovery: 0.93 m

85° 19.2' N, 13° 52.3' W

Water depth: 1087 m

Lithology	Texture	Color	Description	Age
		10YR3/3 10YR4/3	silty clay, dark brown, mottled <i>compared to KAL, the top is missing</i>	
		2.5Y4/4	silty mud, olive brown, frequent mud clasts, high concentration at 18-30, 42-44 cm, mottled at the top, color grading upwards	
		2.5Y4/4	sandy mud, olive brown, dark specks in lower 8 cm, grayish layer (3 mm) at top	
		2.5Y3/2	sandy mud, very dark grayish brown	
		5Y5/3	clayey mud, olive, mottled, gray clay with foraminifers at 82-80 cm	

PS2200-2 (GKG)

Morris Jesup Rise

ARK VIII/3 (ARCTIC 91)

Recovery: 0.30 m

85° 19.6' N, 14°

Water depth: 1074 m

Lithology	Texture	Color	Description	Age
Surface	sandy, silty clay, dark grayish brown, smooth, common polychaete-tubes, bivalves, some gastropods, one echinoid, common planktonic and benthic foraminifers, common small dropstones			
		10YR4/2	silty clay, dark grayish brown, common small dropstones	
		10YR5/2 to 2.5Y4/4	silty clay, grayish brown to olive brown, patches and streaks of brown to grayish brown silty clay, coal fragments at 27 cm	

PS2202-7 (GPC)

Morris Jesup Rise

ARK VIII/3 (ARCTIC 91)

Recovery: 10.43 m

85° 6' N, 14° 25.2' W

Water depth: 1081 m

	Lithology	Texture	Color	Description	Age
0			10YR4/3	silty clay, brown, mottled	
			2.5Y4/4	silty clay, olive brown, dark grayish brown at base, mud clasts at 18-24 cm, mottled, brown laminae at 37.5 cm gradational color change to upper unit	
1			2.5Y4/2	s.a.a.	
			2.5Y4/4	s.a.a.	
			2.5Y5/4	silty clay, light olive brown, calcareous	
			10YR6/3	sandy clay, pale brown, calcareous, mottled	
2			2.5Y4/4	silty clay, light olive brown to olive brown, dark layer at 98 cm	
			2.5Y4/4	clay, olive brown, mottled	
			10YR5/4	sandy clay, yellowish brown, mottled, sand lense at 149 cm	
3			2.5Y5/4	clay/sandy clay, light olive brown, dropstones at 200-210 cm, calcareous, grayish calcareous layer at top	
			10YR4/4	silty clay, dark yellowish brown, mottled, pale brown layer of sandy clay at top	
			2.5Y5/4	silty clay, light olive brown, few dark specks	
			10YR4/4	silty clay, light olive brown, mottled	
			10YR4/4	silty clay, olive brown	
			10YR4/4	s.a.a.	
			2.5Y4/4	sand grading into sandy mud, brown	
			10YR4/3	sand/silt, dark yellowish brown, grading into silty mud	
			10YR4/4	slight gradational coarsening upwards	
			10YR5/2	silty clay, yellowish brown, fining upwards, coarser horizon at bottom with mud clasts,	
4			10YR4/4	dark yellowish brown	
			10YR5/2	silty mud, grayish brown to brown	
			10YR5/4	silty mud, yellowish brown, sand layer at 355-357 cm, few mud clasts, slightly pinkish at 363-365 cm, small dark specks at 370-375 cm, layer of dark specks at 378-398 cm	
			2.5Y5/4	silty clay, light olive brown, dark specks, weakly mottled	
5			10YR5/4	silty clay, yellowish brown, dark specks, mottled	
			2.5Y5/4	silty clay, light olive brown, dark specks, particularly at 480-482 cm, weakly mottled, layer with several dropstones at bottom	

PS2202-7 (GPC)

Morris Jesup Rise

ARK VIII/3 (ARCTIC 91)

Recovery: 10.43 m

85° 6' N, 14° 25.2' W

Water depth: 1081 m

	Lithology	Texture	Color	Description	Age
5			2.5Y4/4	silty clay, olive brown, grading lighter downwards to light olive brown, dark specks throughout, weakly mottled	
			2.5Y5/4		
6			10YR4/4	silty clay, dark yellowish brown, mottled	
			2.5Y5/4	silty clay, light olive brown, dark specks, mud clasts (< 2 mm) in the lower part	
			10YR4/3	silty clay, brown, few small mud clasts	
			5Y5/3		
			2.5Y5/4	silty clay, light olive brown, dark specks throughout, mottled, olive layer at 567-568 cm, dropstone at 608 cm	
			10YR5/4	silty clay, yellowish brown, mottled, sandy clay with dropstones at 638-640 cm	
2.5Y4/4	silty mud, olive brown, gravel fragments at 647 cm				
7			2.5Y4/4	silty clay, olive brown, dark specks and "clouds", sand lense at 691 cm, mottled	
			2.5Y4-5/4	silty clay, olive brown/light olive brown, dark specks and clouds to 712 cm	
8			2.5Y4/4	sandy mud, olive brown, dark spots, coarsening upwards	
			2.5Y4/4		
			2.5Y5/4	silty clay, olive brown, dark spots and clouds at 734-767, 775-795, 810-820 cm, grayish brown laminae at 774 cm, sandy mud at 775-778, 785-789 cm	
			2.5Y4/4		
9			2.5Y4/4	sandy mud, olive brown, coarsening upwards	
			2.5Y5/4	sandy mud, olive brown, pebbles at base	
			2.5Y5/4	silty mud, light olive brown, mottled at 889-880 cm, olive brown sandy mud with pebbles at base, fining upwards	
			2.5Y5/4	silty mud, light olive brown, mottled throughout	
			2.5Y4/4	sandy mud, olive brown, mud clasts and sand lenses	
10.43			2.5Y5/4	silty mud, light olive brown, more brownish and sandy downwards	
			2.5Y4/4	sand lense at 930-933 cm	
			2.5Y4/4	silty clay, olive brown, few dark specks	
			2.5Y5/4	clay, yellowish brown, mottled, grading upwards into light olive brown	
			10YR5/4		
			2.5Y5/4	s.a.a.	
			2.5Y5/4	silty clay, light olive brown and olive brown, dark spots, mottled throughout,	
			2.5Y4/4		

sections 836-851, 937-945 were removed for tests at AGC, Canada

PS2202-2 (GKG)

Morris Jesup Rise

ARK VIII/3 (ARCTIC 91)

Recovery: 0.30 m

85° 6.4' N, 14° 22.7' W

Water depth: 1083 m

Lithology	Texture	Color	Description	Age
Surface			sandy silty clay, dark grayish brown, common gastropods, bivalves, polychaetes, small dropstones (< 4 cm Ø), few echinoderms, common planktonic and benthic foraminifers	
		10YR4/2	sandy silty clay, dark grayish brown, homogeneous	
		2.5Y4/2	sandy silty clay, dark grayish brown, strongly burrowed in upper part, common small dropstones (coal clasts and others), burrowed in lower part with grayish and brownish horizontal streaks	

Depth in core (cm)

PS2202-7 (TWC)

Morris Jesup Rise

ARK VIII/3 (ARCTIC 91)

Recovery: 1.10 m

85° 6' N, 14° 25.2' W

Water depth: 1081 m

Lithology	Texture	Color	Description	Age
		10YR4/3	silty clay, brown, lighter mottles, coarsening upwards	
		2.5Y4/4	silty clay, olive brown, dark grayish brown at base, brown lamina at 39 cm	
		2.5Y4/2		
		2.5Y4/4-2	silty clay, olive brown, dark grayish brown at base	
		2.5Y4/4-2	s.a.a.	
		2.5Y5/4	silty clay, light olive brown, more brownish at base, calcareous	
		10YR6/3	sandy clay, pale brown, calcareous	
		2.5Y5/4	silty clay, light olive brown/olive brown, dark yellowish brown at 84-80 cm, dark layer at 95 cm	
		2.5Y4/4		
<i>presumably double penetration</i>				

Depth in core (m)

PS2206-1 (KAL)

Amundsen Basin

ARK VIII/3 (ARCTIC 91)

Recovery: 1.58 m

84° 15.8' N, 2° 33.4' W

Water depth: 3020 m

Lithology	Texture Color	Description	Age
0	10YR3/4	silty clay, dark yellowish brown, mottled, foraminifera (Pyrgo)	
	10YR4/4	(silty) clay, dark yellowish brown, darker mottles	
	10YR4/4	clayey sand, laminated, fining upwards	
	10YR4/4 5YR4/2 10YR4/3 2.5Y5/2 10YR5/4	clay, varying color, few small mud clasts	
	10YR4/4	sandy mud, dark yellowish brown	
	10YR4/4	clay, dark yellowish brown	
	2.5Y4/4	silty mud, olive brown (slump?), light olive brown, laminated at 101-108 cm	
	2.5Y4/4	sandy mud clasts, dark grayish brown and dark brown at 130-137, 152 cm	

PS2208-2 (GPC)

Nansen Basin

ARK VIII/3 (ARCTIC 91)

Recovery: 6.85 m

83° 38.6' N, 4° 39.5' E

Water depth: 3682 m

	Lithology	Texture	Color	Description	Age
0			10YR3/3	clay, dark brown, soft, mottled, mud clasts at 10 cm	
			10YR4/3	clay, brown, soft, mottled, layer with black mud clasts at 38-41 cm	
1			2.5Y4/4	clay, olive brown, soft, mottled in the upper part, sand layers at 59, 66 cm	
			10YR4/3	clay, brown, soft, lighter mottles	
			2.5Y4/2	clay, dark grayish brown, soft, mottled	
			10YR4/3	clay, brown, soft, mottled	
			2.5Y4/2	clay, dark grayish brown, soft, mottled	
			10YR4/3	clay, brown, soft, mottled	
2			2.5Y4/4	clay, olive brown, soft, mottled in the upper part, two lenses of reddish brown clay at 123, 127 cm, darker laminae at 141 cm, dark specks (< 1 mm) below 141 cm	
			2.5Y4/4		
			2.5Y4/2	clay, olive brown, dark grayish brown in the lower part, small black specks (< 1 mm), black layering and spots at 197-252 cm	
3			2.5Y4/2	clay, dark grayish brown, soft, homogeneous (upper part of turbidite)	
			2.5Y4/2	sand/silt, dark grayish brown, graded, layered, fining upwards from coarse/medium sand to silt/clay, laminated in the upper part (turbidite)	
4			2.5Y4/2	sandy mud, dark grayish brown, pebbles, dark gray mud clasts (1-2 cm Ø), one brown clay clasts, one clast of light olive brown silty clay, well consolidated, (slump deposit ?)	
			2.5Y4/2		
5			2.5Y4/2	clay, dark grayish brown, soft, homogeneous	
			2.5Y3/2		
			2.5Y4/2	clay, olive brown, dark grayish brown to very dark grayish brown, mottled throughout, sand lense at 403-410 cm	
			2.5Y4/4		
			10YR4/3	clay, brown, mottled	
			2.5Y4/4	sand fining upwards into silt and clay, olive brown, weak lamination at 450-456 cm (turbidite)	
			2.5Y4/4	sand fining upwards into clay, olive brown, mottled in the upper part	
	2.5Y4/4				
	2.5Y4/2				

PS2208-2 (GPC)

Nansen Basin

ARK VIII/3 (ARCTIC 91)

Recovery: 6.85 m

83° 38.6' N, 4° 39.5' E

Water depth: 3682 m

Depth in core (m)	Lithology	Texture Color		Description	Age
5			2.5Y4/2	sandy mud, dark grayish brown, grading upwards into sandy mud, olive brown	
		▼	5Y3/1	sandy mud, very dark gray, clay at 530-535 cm	
		▲	5Y4/2	clay, olive/olive gray, weakly mottled in the lower part,	
			5Y4/3	sand laminae at 552, 547 cm	
			2.5Y4/2	sandy mud, dark grayish brown, laminated at 571-582 cm	
			N3	sandy mud, very dark gray, sand lamina at 589 cm	
6			2.5Y4/2	sandy mud, dark grayish brown, more brownish towards 608 cm	
		▲	N3	clayey silt, very dark gray	
			5Y4/1	clay, dark gray	
			2.5Y4/2	clay, dark grayish brown	
		▲	2.5Y4/2	sand, fining upwards into silt, dark grayish brown	
			2.5Y4/2	sandy mud, dark grayish brown	
			2.5Y4/2	clay/sandy mud, dark grayish, different colors, mixed	
		▲	2.5Y4/2		
			mix		
		▲	2.5Y4/4	sand fining upwards into silt, olive brown	
7					

coring disturbance

PS2208-2 (TWC)

Nansen Basin

ARK VIII/3 (ARCTIC 91)

Recovery: 1.32 m

83° 38.6' N, 4° 39.5' E

Water depth: 3682 m

Depth in core (m)	Lithology	Texture Color		Description	Age
0			10YR3/3	clay, dark brown, soft, mottled, mud clasts (< 1 cm) at 5 cm	
			10YR3/3	clay, brown, soft, mottled, olive brown at 10-5 cm, layer with black mud clasts at 27-28 cm	
			2.5Y4/4	clay, olive brown, soft, mottled in the upper part, sand layers at 41, 47 cm	
			10YR4/3	clay, brown, soft, mottled	
			2.5Y4/2	clay, dark grayish brown, soft, mottled	
			10YR4/3	s.a.a.	
			10YR4/3	clay, brown, soft, mottled	
1			2.5Y4/4	clay, olive brown, soft, mottled in the upper part, lenses of reddish brown clay at 85 cm, dark weakly developed laminae at 102 cm, dark specks (< 1 mm) below 102 cm	

presumably double penetration

PS2209-1 (GKG)

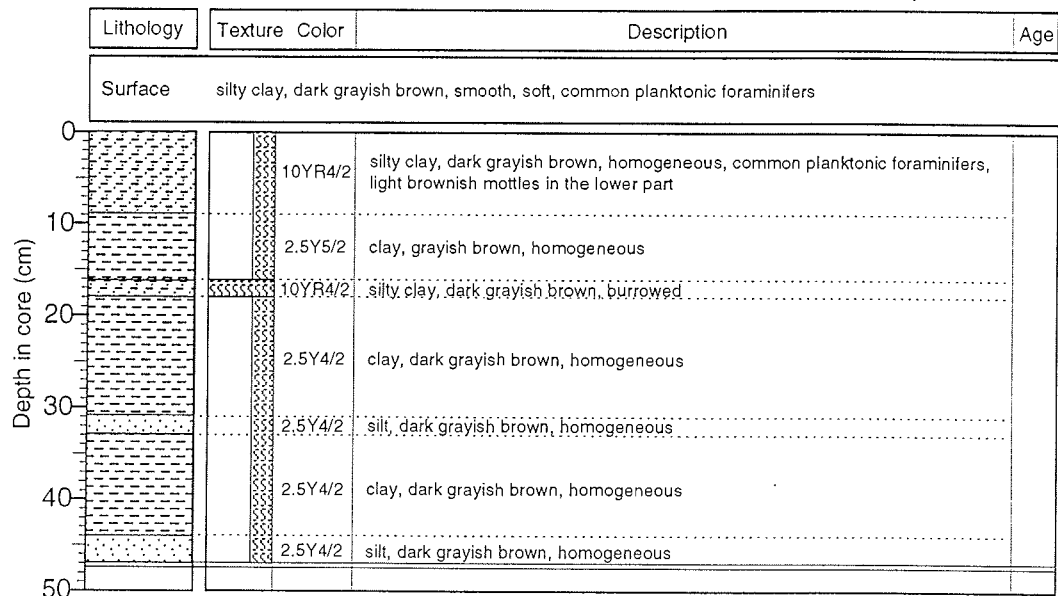
Nansen Basin

ARK VIII/3 (ARCTIC 91)

Recovery: 0.47 m

83° 13.5' N, 8° 34.4' E

Water depth: 4046 m



PS2210-1 (GKG)

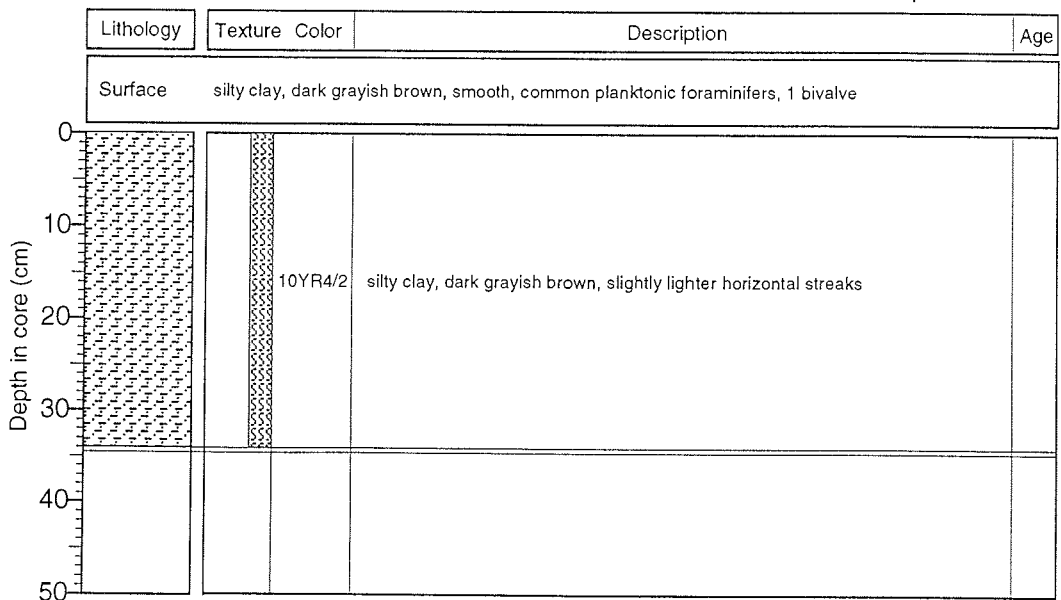
Nansen Basin

ARK VIII/3 (ARCTIC 91)

Recovery: 0.34 m

83° 2.7' N, 10° 7.5' E

Water depth: 3949 m



PS2212-3 (KAL)

Yermak Plateau

ARK VIII/3 (ARCTIC 91)

Recovery: 7.70 m

82° 4.2' N, 15° 51.2' E

Water depth: 2550 m

	Lithology	Texture	Color	Description	Age
0	[Lithology pattern]		10YR4/4	silty mud, dark grayish brown grading upwards into dark yellowish brown, homogeneous, common benthic foraminifers (Pyrgo)	
			2.5Y4/2		
			2.5Y4/4	sandy mud, olive brown, mud clasts	
			10YR3/4	clay, dark yellowish brown, laminated	
			10YR3/4+4/3	clay, dark yellowish brown and brown, laminated, iron crust at top (10YR3/6)	
			5Y4/2	clay, dark grayish brown and olive gray, small mud clasts (< 2 mm)	
1			5Y5/3	clay, olive, small mud clasts and foraminifers at 80-77 cm, dropstone at 100 cm	
			5Y4/2	sandy mud, olive gray, mud clasts	
			5Y3/2	clay, olive gray, mud clasts at 132-135 cm, laminated at 118-115.5, brownish	
			5Y4/2	sandy mud, olive gray, mud clasts	
			2.5Y4/4	clay, olive brown, homogeneous	
2			10YR4/4	clay, dark yellowish brown, mottled, small mud clasts at 202-208 cm	
			10YR3/3	sandy mud, dark brown, mud clasts	
			10YR4/4	clay, dark yellowish brown, mottled, few mud clasts, enriched at 219-221 cm	
			2.5Y4/2	sandy mud, dark grayish brown, mud clasts	
			2.5Y4/4	clay, olive brown, mottled, few mud clasts	
			2.5Y4/1	sandy mud, olive brown, mud clasts	
			2.5Y4/4	clay, dark grayish brown grading upwards into olive brown, laminated, mud clasts at 250-256 cm	
			5Y4/2	clay, olive gray, homogeneous, weak color changes indicating layering	
3			5Y4/3	clay, olive, mottled at 266-279 cm, dark layer at 278 cm	
			5Y5/3		
			2.5Y4/4	clay, olive brown	
			5Y5/3	clay, olive, grading upwards into olive brown, mottled	
4			2.5Y5/4	sandy mud, light olive brown, mud clasts and dropstones, stratified	
			2.5Y5/4	silty clay, light olive brown, fining upwards to clay	
			2.5Y4/2	sandy mud, dark grayish brown, mud clasts, fining upwards to silty mud with few mud clasts	
			5Y3/2	silty clay, dark olive gray	
			5Y4/2	clay, olive gray, weakly mottled, faint color changes indicating stratification	
5			2.5Y3/2	sandy mud, very dark grayish brown, frequent clay clasts	
			5Y4/2	clay, olive gray, homogeneous	

PS2212-3 (KAL)

Yermak Plateau

ARK VIII/3 (ARCTIC 91)

Recovery: 7.70 m

82° 4.2' N, 15° 51.2' E

Water depth: 2550 m

Lithology	Texture	Color	Description	Age	
5	▲	5Y4/3	sandy mud, very dark gray grading into dark olive gray silty mud grading into olive mottled clay		
		5Y3/2			
		5Y3/1			
			5Y3/2	clay, dark olive gray	
			2.5Y4/2	silty mud, very grayish brown, mud clasts, grading into dark grayish brown clayey mud with scattered mud clasts	
			2.5Y3/2		
			5Y4/1	clay, dark gray, homogeneous	
			2.5Y4/1	sandy mud, olive gray, grading into dark gray, mud clasts, mottled	
			5Y4/3	clay, olive, mottled	
	6		5Y3/2	sandy mud, dark olive gray, mud clasts	
			5Y4/2	clay, olive gray, weakly mottled	
			2.5Y3/2	silty mud, very dark grayish brown, mud clasts, dropstones	
			5Y3/2	clay, dark olive gray, weakly mottled	
			2.5Y4/2	sandy mud, dark grayish brown, mud clasts	
				5Y4/2	clay, olive gray, mottled, silty layer at 637 cm
7		5Y3/2	silty mud, dark olive gray		
		5Y3/1	silty mud, very dark gray/black, mud clasts, homogeneous		
		5Y4/1	clay, dark gray, silty mud clasts at 706.5 cm, finely dispersed monosulfides (5Y3/1), very dark gray at 727-736 cm		
		5Y4/1	s.a.a.	CC and mütze	

PS2212-5 (GKG)

Yermak Plateau

ARK VIII/3 (ARCTIC 91)

Recovery: 0.39 m

82° 4' N, 15° 46' E

Water depth: 2485 m

Lithology	Texture	Color	Description	Age
Surface			silty clay, dark grayish brown, smooth, common planktonic and benthic foraminifers, single bivalve shells, 2 small sponges (1 cm Ø)	
0		10YR4/2	silty clay, dark grayish brown, homogeneous, common planktonic and benthic foraminifers in upper half	
40		2.5Y4/4	sandy, silty clay, olive brown, brownish mud clasts	same layer as in PS2212-3KAL at 41-43 cm

PS2213-6 (GPC)

Yermak Plateau

ARK VIII/3 (ARCTIC 91)

Recovery: 13.09 m

80° 27.6' N, 8° 2.6' E

Water depth: 853 m

Lithology	Texture Color	Description	Age
	10YR3/3	silty clay, dark brown and very dark brown, mottled	
	10YR3/2	silty mud, dark grayish brown, mud clasts	
	2.5Y4/2	silty mud, dark olive gray	
	5Y3/2	silty mud, dark olive gray	
	5Y4/1	silty mud, dark gray, layer of frequent mud clasts at 46-51 cm, brownish colors, calcareous tube at 55 cm	
	5Y5/2	silty clay, gray, grading upwards into olive gray, brownish streaks and spots at 79, 86 cm, mud clasts (< 2 mm), mottled in the upper part, dark mottles	
	5Y5/1	silty clay, gray, grading upwards into olive gray, brownish streaks and spots at 79, 86 cm, mud clasts (< 2 mm), mottled in the upper part, dark mottles	
	5Y4/1	sandy mud, dark gray, mud clasts	
	5Y3/2	clay, black, mud clasts, grading into dark olive gray	
	5Y4/2	clay, dark grayish brown, grading into olive gray	
	2.5Y4/2	clay, dark grayish brown, grading into olive gray	
	2.5Y3/2	clay, very dark grayish brown, brownish zones	
	5Y3/2	clay, dark olive gray, very weak color changes indicate layering	
5Y4/2	clay, dark olive gray, grading upwards into olive with brownish streaks		
5Y3/2	clay, dark olive gray, very homogeneous		
10YR3/2	clay, very dark grayish brown single dark specks at 420-425 cm		
5Y3/1	clay, very dark gray		

disturbed

PS2213-6 (GPC)

Yermak Plateau

ARK VIII/3 (ARCTIC 91)

Recovery: 13.09 m

80° 27.6' N, 8° 2.6' E

Water depth: 853 m

	Lithology	Texture	Color	Description	Age
5			5Y3/1	clay, very dark gray, very homogeneous black specks at 525-535 cm	
			2.5Y3/2	clay, very dark grayish brown, grading into very dark gray	
6			5Y4/2	clay, very dark grayish brown, grading into olive gray	
			2.5Y3/2		
			2.5Y3/2	thin olive bands at 599-601 cm few mud clasts at 633-696 cm clayey mud, dark olive gray grading into very dark gray	
			5Y4/2 2.5Y4/2 2.5Y3/2	clay, very dark grayish brown, grading into dark grayish brown, into olive gray	
7			5Y3/2	clay, dark olive gray, homogeneous, very dark grayish brown at base	
			2.5Y3/2		
8			5Y3/1 5Y3/2	clay, very dark gray, grading into very dark olive gray silty mud	
			5Y3/2	very dark gray layer at 728 cm, weakly brownish layer at 743-745 cm, black layer at 752 cm clay, dark olive gray, homogeneous, dark specks, weak color changes indicate layering	
			5Y3/1 5Y3/2 5Y3/3	black specks at 780-810 cm, weak color changes suggest layering clay, dark olive grading into dark olive gray grading into very dark gray	
9			5Y3/2	sandy silt, olive gray, grading into clay, dark olive gray	
			5Y4/2		
10			5Y3/2 5Y4/3 5Y2.5/2	clayey mud, dark olive gray, grading into black clay with few mud clasts, grading into olive clay, grading into dark olive gray	
			5Y3/2	clay, dark olive gray, dark specks at 966-973 cm, dropstone at 977 cm, weakly brownish layer at 950 cm, small mud clasts at 945-955 cm, olive gray, weakly brownish at 937-939 cm	
			5Y4/2		
			5Y3/2		
			5Y4/1	sandy mud, dark gray, black specks	
	5Y4/1	clay, dark gray, black specks at 998-1009 cm			

PS2213-6 (GPC)

Yermak Plateau

ARK VIII/3 (ARCTIC 91)

Recovery: 13.09 m

80° 27.6' N, 8° 2.6' E

Water depth: 853 m

Depth in core (m)	Lithology	Texture	Color	Description	Age
	10			5Y4/1	clay, dark gray, black specks at 998-1009 cm
			5Y4/1	sandy mud, dark gray, faint layering in the upper part	
			5Y4/1	clay, dark gray	
			5Y4/1	sandy mud, dark gray, black specks	
			5Y4/1	clay, dark gray, layer of dark olive gray sandy mud at 1055-1057 cm, black specks at 1061-1067 cm	
			5Y2.5/2	clayey mud, black	
11			5Y3/4	clay, dark olive gray, homogeneous, weak color changes indicate layering	
			2.5Y3/2 5Y3/2	clay, dark olive gray, few mud clasts and dark specks, grading to very dark grayish brown	
			5Y3/1	silty clay, very dark gray, mud clasts	
12			5Y3/2	clay, dark olive gray, weakly mottled	
			2.5Y3/2	sandy mud, very dark brown, grading upwards into very dark grayish brown, mud clasts in the upper part	
			5Y2.5/1	sandy mud, black, homogeneous	
			5Y5/1- 5Y4/1	clay, gray/dark gray, few dropstones	
13			5Y3/2	clay, dark olive gray, few dark specks at 1289-1294 cm	
14					
15					

PS2214-1 (GKG)

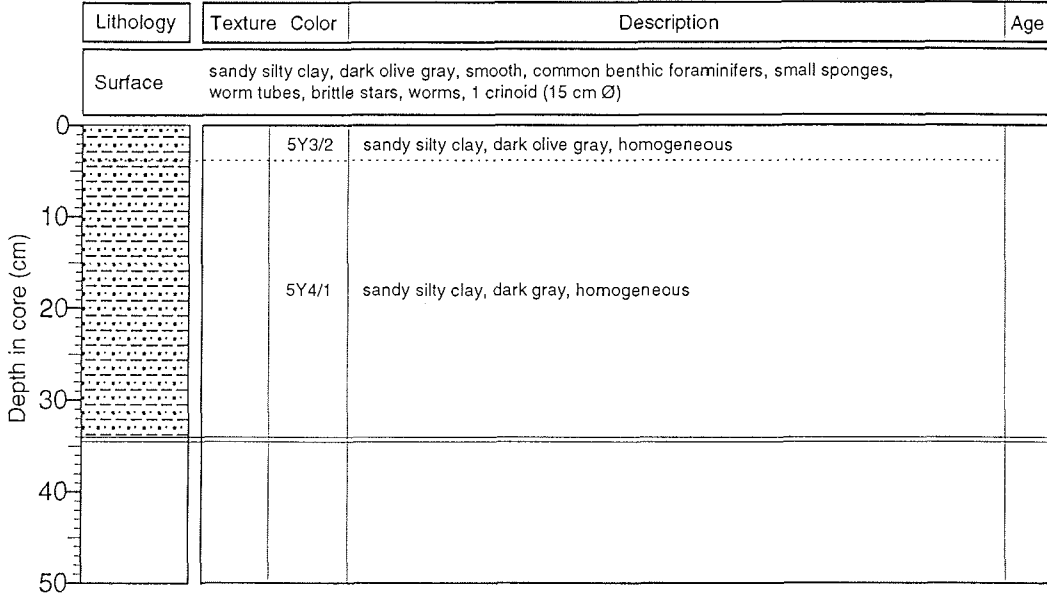
Yermak Plateau

ARK VIII/3 (ARCTIC 91)

Recovery: 0.34 m

80° 16.1' N, 6° 37.6' E

Water depth: 552 m



PS2215-2 (GKG)

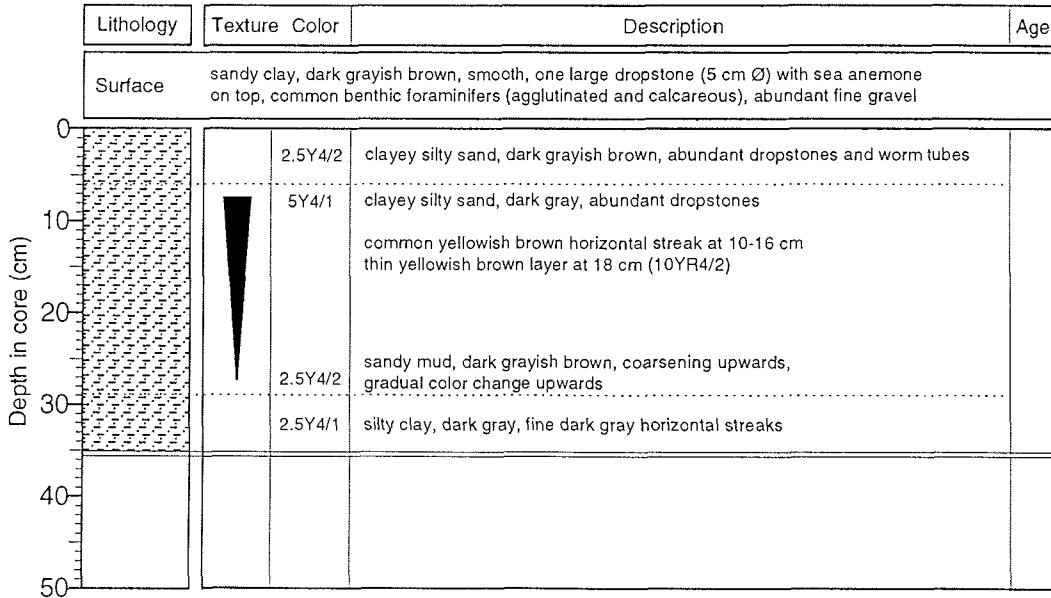
Yermak Plateau

ARK VIII/3 (ARCTIC 91)

Recovery: 0.35 m

79° 42.4' N, 5° 15.6' E

Water depth: 2019 m



9.3 Sample Distribution

9.3.1 Sediment Sample Distribution Policy Statement (as of December 28-1990)

The sample distribution policy for ARCTIC-91 is designed to provide guidelines for the distribution of samples collected on ARCTIC-91 in a manner that will guarantee a fair distribution of material, minimize the duplication of scientific effort, and maximize the scientific return from these most valuable samples.

1. The Alfred-Wegener-Institut shall serve as the core repository for all ARCTIC-91 sediment samples. AWI will be responsible for the distribution of samples to shipboard and shorebased investigators following the recommendations of the Sample Distribution Committee (see below). AWI will maintain a record of all samples that have been distributed and the nature of the investigations being undertaken. This information will be available to investigators on request.

2. All cores collected on the expedition will be labelled and recorded according to the AWI and POLARSTERN standard scheme. Samples distributed from these cores will be labelled with a standard identifier which will include a core identifier and the interval from which the sample was removed. This standard identifier should be associated with all data reported; residues of samples should remain labelled so that they can be related to earlier data.

3. Any investigator wishing to request samples from the expedition shall submit, in writing, a sample request to AWI at least TWO MONTHS prior to the departure of the cruise (departure presently scheduled for 1 August, 1991). The request should contain a statement of the nature of the proposed research, the size and approximate number of samples required to complete the study. In addition any special sampling techniques required should be specified. These sample requests will be reviewed by the Sample Distribution Committee.

4. The Sample Distribution Committee shall consist of one representative from each of the nations participating in the geological program of the expedition. Suggested members of this committee are:

CANADA -- Kate Moran
GERMANY -- Dieter K. Fütterer
SWEDEN -- Kurt Boström
U.S.A. -- William B. Curry

This committee will evaluate the sample requests to ensure that there will be no duplication of efforts, unless such duplication is determined to be in the interest of the overall scientific program.

5. Costs associated with the taking and/or receiving samples from the AWI repository shall be accounted for by the requesting party.

6. For twelve months following the expedition, sampling shall be limited to shipboard participants and shorebased investigators agreed upon by the geoscience participants in advance of the expedition. Recognizing the tremendous investment in time and energy expended by members of the expedition's scientific party, in general preference shall be given to sample requests from shipboard participants.

9.3.2 Shipboard Sampling and Sample Distribution

Type of Sample	Shipboard Scientist(s)
1 smear slides (core description)	Brass/Stein/Thiede
2 smear slides (nanno plankton)	Gard/Backmann
3 x-ray slabs	Grobe/Kassens/Tarasov/Vorren
4 resistivity/density/porosity	Bergmann
5 p-wave velocity	Mosher
6 shear strength	Kassens/Moran
7 susceptibility	Fredrichs/Nowaczyk
8 paleomagnetic	Nowaczyk/Fredrichs
9 water content/density/porosity	Kassens/Moran
10 clay minerals/sand:silt:clay	Brass/Stein
11 TOC, carbonate	Stein
12 organic geochemistry	Stein/Schubert
13 benthic foraminifera	Bergsten
14 pollen	Mudie
15 methane gas in sediments	Cranston
16 salinity	Moran

Core No.:	Gear	Length	1	2	3	4	5	6	7	8	9	10	11	12	13	14	15	16
PS 2157-5	TWC	77	X	X		X			X	X								
PS 2157-6	TWC	78	X	X		X	X	X			X	X	X					X
PS 2157-6	GPC	376	X	X		X	X	X	X	X	X	X	X			X	X	X
PS 2159-6	TWC	0	no recovery															
PS 2159-6	GPC	218	X	X		X	X	X	X	X	X	X	X			X	X	X
PS 2161-3	TWC	92	X	X		X	X		X	X								
PS 2161-3	GPC	70	X	X		X	X		X									
PS 2163-3	TWC	72	X	X		X	X	X			X	X	X					X
PS 2163-3	GPC	582	X	X		X	X	X	X	X	X	X	X	X		X	X	X
PS 2163-4	KAL	30	not processed															
PS 2164-6	TWC	57		X		X	X	X			X	X	X					X
PS 2164-6	GPC	238	X	X		X	X	X	X	X	X	X	X	X		X	X	X
PS 2165-1	TWC	67		X		X	X											
PS 2165-1	GPC	567	X	X		X	X	X	X	X	X	X	X			X	X	X
PS 2165-4	KAL	227	X	X	X	X												
PS 2166-3	TWC	47		X		X	X											
PS 2166-3	GPC	215	X	X		X	X		X				X	X		X	X	
PS 2167-1	TWC	187		X		X	X											
PS 2167-1	GPC	640	X	X		X	X	X	X	X	X	X	X	X		X	X	X
PS 2168-2	TWC	34		X		X	X											
PS 2168-2	GPC	417		X		X	X		X							X	X	
PS 2169-1	TWC	113		X		X	X	X										
PS 2169-1	GPC	611		X		X	X		X			X	X			X	X	
PS 2170-3	TWC	76		X		X	X	X			X	X	X					X
PS 2170-3	GPC	1151	X	X		X	X	X	X	X	X	X	X	X		X	X	X
PS 2171-4	KAL	325	X	X	X	X	X	X	X	X								X
PS 2171-5	TWC	182	not processed															
PS 2171-5	GPC	986	not sampled						X									
PS 2172-4	TWC	174		X		X	X											
PS 2172-4	GPC	958		X		X	X		X	X				X		X	X	
PS 2173-1	KAL	550				X			X	X								
PS 2174-3	TWC	110		X		X	X	X			X	X	X					
PS 2174-3	GPC	1300	X	X		X	X	X			X	X	X	X		X	X	
PS 2174-5	KAL	960	X	X	X	X	X	X	X	X	X	X	X	X	X	X	X	X
PS 2175-1	TWC	61	not processed															
PS 2175-1	GPC	1124	not processed															
PS 2175-5	TWC	102		X		X	X	X			X	X	X					X
PS 2175-5	GPC	1692	X	X		X	X	X	X	X	X	X	X	X		X	X	X
PS 2176-1	TWC	80		X		X	X	X			X	X	X					X
PS 2176-1	GPC	1421	X	X		X	X	X	X	X	X	X	X	X		X	X	X
PS 2176-3	KAL	976	X	X	X	X		X	X	X	X	X	X	X	X	X	X	
PS 2176-6	TWC	86	not processed															
PS 2176-6	GPC	863	not processed															
PS 2177-4	KAL	575	penetration of weight											X				
PS 2177-5	KAL	780	X	X	X	X	X	X	X	X	X	X	X	X		X	X	

9.4 List of Participating Institutions / Beteiligte Institutionen

<u>Country and Institution</u>	<u>No of Participants</u>
<u>Germany</u>	
AWI Alfred Wegener Institute for Polar and Marine Research P.O.Box 12 01 61 D-W-2850 Bremerhaven	19
FGB Department of Geosciences University of Bremen P.O.Box 33 04 40 D-W-2800 Bremen	3
GEOMAR GEOMAR- Research Centre Wischhofsstraße 1-3 D-W-2300 Kiel 14	4
SFB-313 Sonderforschungsbereich 313 University of Kiel Olshausenstraße 40-60 D-W-2300 Kiel	1
HSW Helikopter Service Wasserthal GmbH Kärtnerweg 43 D-W-2000 Hamburg 65	4
IUH Institute for Environmental Physics University of Heidelberg Im Neuenheimer Feld 366 D-W-6900 Heidelberg	
SWA Seewetteramt Hamburg Deutscher Wetterdienst Bernhard-Nocht-Straße 76 D-2000 Hamburg 76	2
<u>Canada</u>	
AGC Atlantic Geoscience Centre Geological Survey of Canada Dartmouth, NS B2Y 4A2	4
<u>GUS</u>	
MMBI Murmansk Marine Biology Institute Dalnye Zelentzy Murmanskaya obl., Kamshilova 1 183023 Murmansk	1

NGM Niimorgeophysica 1
Department of Methods and Technique for
Arctic Geophysics
183023 Murmansk

Norwegen

DGT Department of Geology 1
University of Tromsø
P.O.Box 3985, GULENG
N-9001 Tromsø

SOB Institute for Solid Earth Physics 2
University of Bergen
N-5000 Bergen

Sweden

CUG University of Gothenburg 1
Department of Geology
S-412 96 Gothenburg

GIS Department of Geology and Geochemistry 3
University of Stockholm
S-106 91 Stockholm

GUU Section of Solid Earth Physics 2
University of Uppsala
P.O. Box 556
S-75722 Uppsala

Switzerland

PIB Institute of Physics 1
Department of Environmental Physics
Siedlerstraße 5
CH-3012 Bern

U.S.A

LDGO Lamont Doherty Geological Observatory 1
Columbia University
Palisades, NY-10962

RSMAS Rosenstiel School of Marine and 1
Atmospheric Sciences, University of Miami
4600 Rickenbacker Causeway
Miami, FL 33149

9.5 List of Participants / Teilnehmerliste

<u>name / Name</u>		<u>institution / Institut</u>
Alvers	Michael	AWI
Backman	Jan Erik (Scientific Adviser)	GIS
Bergmann	Uwe	FGB
Bergsten	Eva Helene	CUG
Bouravtsev	Vadim	NGM
Brass	Garret W.	RSMAS
Dierking	Wolfgang	AWI
Doescher	Torsten	AWI
Eicken	Hajo	AWI
Fjellanger	Jan Petter	SOB
Frederichs	Thomas	FGB
Fütterer	Dieter Karl (Chief Scientist)	AWI
Gard	Ingrid Gunilla	GIS
Gradinger	Rolf	AWI
Grobe	Hannes	AWI
Haas	Christian	AWI
Haertling	Stefan	AWI
Heesemann	Bernd	AWI
Heitmüller	Karl-Heinz	HSW
Jodrey	Frederik	AGC
Jokat	Wilfried	AWI
Kassens	Heidemarie	GEOMAR
Köhler	Herbert F.H.	SWH
Kristoffersen	Yngwe	SOB
Kröncke	Ingrid	AWI
Kromer	Bernd	IUH
Lemke	Peter	AWI
Lif	Nils Arne	GSU
Lindgren	Per Jonas	GUU
Ludin	Andrea	PIB
Manchester	Keith	AGC
Meder	Matthias	IUH
Michel	Andreas	AWI
Möhrke	Holger	HSW
Moran	Kathryn	AGC
Mosher	David C.	AGC
Nowaczyk	Norbert	FGB
Nürnberg	Dirk	GEOMAR
Rasmussen	Thorkild	GUU
Richter	Bernd K.	SWH
Riewesell	Christian	HSW
Schlosser	Peter	LDGO
Schöne	Tilo	AWI
Scholten	Jan Christian	SFB-313
Schrank	Wolfgang	HSW
Schubert	Carsten	AWI
Spielhagen	Robert	GEOMAR
Stein	Rüdiger	AWI
Tarasov	Guennadii	MMBI
Thiede	Jörn	GEOMAR
Uenzelmann-Neben	Gabriele	AWI
Vorren	Tore	DGT
Wieschollek	Ursula	AWI

Ships Crew / Schiffspersonal ARK-VIII/3

Master	Greve	Ernst-Peter
Chief Mate	Gerber	Klaus-Dieter
1st Officer	Rodewald	Martin
2nd Officer	Bürger	Manfred
3rd Officer	Schwarze	Stefan
Doctor	Schroeder	Andreas
Radio Officer	Müller	Eberhard
Radio Officer	Butz	Johann
Chief Engineer	Schulz	Volker
1st Engineer	Delff	Wolfgang
2nd Engineer	Simon	Wolfgang
3rd Engineer	Schulz	Christian H.
Electronician	Hoops	Klaus-Jürgen
Electronician	Kampen	Michael
Electronician	Humm	Harald
Electrician	Piskorzynski	Andreas
Boatswain	Erdmann	Reinhard
SBM	Schwarz	Reinhold
SBM	Zulauf	Reinhard
Carpenter	Junge	Heinz-Dieter
A.B.	Kassubek	Peter
A.B.	Winkler	Michael
A.B.	Suarez Paisal	Antonio
A.B.	Meis Torres	Manuel
A.B.	Novo Loveira	Jose
A.B.	Pereira Portela	Bernardo
A.B.	Prof Otero	Antonio
Storekeeper	Barth	Bernhard
Motorman	Heurich	Erwin
Motorman	Jordan	Gerd
Motorman	Buchas	Ferdinand
Motorman	Reimann	Siegmar
Motorman	Fritz	Günter
Cook	Köwing	Walter H.K.
Butcher	Roggatz	Friedhelm
Cook Mate	Kästner	Mario
1st Steward	Peschke	Dieter
Stewardess/Nurse	Meier	Gaby
Stewardess	Mund	Kati
2nd Steward	Neves	Alexandre
2nd Steward	Mui	Kee Fung
2nd Steward	Tu	Jian-Min
2nd Steward	Yu	Chung-Leung
2nd Steward	Yang	Chien-Chang